Max-Planck-Institut
für Plasmaphysik

Fusion

FORSCHUNG & FORSCHUNGS-MANAGEMENT

FESTSCHRIFT FÜR KLAUS PINKAU

INHALT

1.1
IN MEMORIAM KLAUS PINKAU
SIBYLLE GÜNTER
SEITE 4

2.1
EINLEITUNG TOKAMAKS
KARL LACKNER
SEITE 8

3.1
EINLEITUNG STELLARATOREN
FRIEDRICH WAGNER
SEITE 184

1

VORWORT

1.1 IN MEMORIAM KLAUS PINKAU

Von der Kernphysik über die Astronomie und Fusionsforschung bis hin zu Wissenschaftsmanagement und Politikberatung sowie zu grundsätzlichen Fragen zum Verhältnis von Gesellschaft und Wissenschaft spannte sich das Themen- und Tätigkeitsfeld von Professor Dr. Drs. h.c. Klaus Pinkau, der das Max-Planck-Institut für Plasmaphysik (IPP) von 1981 bis 1999 als Wissenschaftlicher Direktor leitete. Diese Festschrift, die seinen 90. Geburtstag feiern sollte, muss nun – nachdem er am 15. Oktober 2021 in München verstorben ist – in Memoriam erscheinen.

Der Werdegang Klaus Pinkaus, geboren am 3. April 1931 in Leipzig, begann nach dem Abitur mit einer handwerklichen Ausbildung als Reproduktionsfotograf. Es folgte das Studium der Physik in Tübingen, Hamburg und Bristol/England. Seine hier entwickelte kernphysikalische Methode, die Energie von Gammastrahlen zu messen, nutzte er später – zur Astrophysik umschwenkend – um die energiereiche Strahlung aus dem Kosmos zu untersuchen. Am Max-Planck-Institut für Extraterrestrische Physik in Garching, das er von 1972 bis 1977 als Direktor leitete, etablierte er den in der Bundesrepublik neuen Forschungszweig der Hochenergie-Astronomie. Der hier betreute Satellit COS-B wurde einer der erfolgreichsten Satelliten des europäischen Raumfahrtprogramms und fertigte die erste Himmelskarte der Milchstraße im Licht der kosmischen Gammastrahlung an.

Was für uns im IPP besonders wichtig ist: 1981 wandte sich Klaus Pinkau abermals einem neuen Wissenschaftsgebiet zu. Von den Plasmen im Weltraum wechselte er zu den Fusionsplasmen des IPP in Garching, dessen rund tausend Mitarbeiter die Grundlagen für ein Kernfusionskraftwerk entwickeln. Es sei für ihn wichtiger, Forschung möglich zu machen als selbst Forschung zu treiben, wird er in seinem alten Institut zur Erklärung dieses Wechsels zitiert. Achtzehn Jahre, von 1981 bis 1999, war Klaus Pinkau der Wissenschaftliche Direktor des IPP, zugleich der Vorsitzende des Direktoriums und der Wissenschaftlichen Leitung.

Begonnen hat er seine Arbeit im IPP im Februar 1981 mit einer Programmdiskussion. Das Ergebnis dieser institutsweit organisierten Überlegungen waren die „Aims of IPP“, die bereits Mitte April 1981 bei den Aufsichtsgremien des Europäischen Fusionsforschungsprogramms eingereicht werden konnten.

Als „Ziele des IPP“ wurden damals formuliert: Eingebettet in das europäische und internationale Forschungsumfeld war beabsichtigt, die Tokamak-Forschung fortzusetzen. Aufbauen wollte man auf den wertvollen Erkenntnissen, die mit dem seit 1980 betriebenen

Divertor-Tokamak ASDEX zu Plasma-Wand-Wechselwirkung, Verunreinigungskontrolle und Langpuls-Entladungen gewonnen worden waren. Die Arbeiten an ASDEX sollten mit erweiterter Ausrüstung weitergeführt werden. An den Forschungen mit der großen europäischen Gemeinschaftsanlage JET, dem „Joint European Torus“, der damals im Bau war, wollte man sich beteiligen. Im IPP in Garching war der Bau eines ASDEX-Nachfolgers geplant: ASDEX Upgrade. Mit diesem Divertor-Tokamak wollte man – kraftwerksnäher als mit ASDEX möglich – einen kalten Plasmarand erreichen, um die Gefäßwand zu schützen, die Energie- und Teilchenabfuhr aus dem Plasma verbessern und die Anforderungen an einen Kraftwerks-Divertor definieren – allesamt Fragen, zu denen man von dem ohne Divertor geplanten JET keine Antworten erwarten konnte. Zur Definition eines JET-Nachfolgers, der Testreaktor-Studie zu einem „Next European Torus“ NET, wollte man beitragen und das IPP als Standort für das europäische Planungsteam anbieten. Diese Arbeiten sollten zugleich in die Studienarbeiten für den Internationalen Tokamak-Reaktor INTOR einfließen, an denen seit 1979 in einer ersten Zusammenarbeit von USA, Sowjetunion, Japan und Europa gearbeitet wurde.

Ebenso wollte man im IPP das Stellarator-Programm weiterführen. Man plante, die seit 1975 laufenden Experimente an dem erfolgreichen Wendelstein 7-A fortzusetzen und dabei insbesondere den stellarator-typischen Betrieb ohne Plasmastrom zu untersuchen. Ein nach Vorgaben der Theorie optimierter „Advanced Stellarator“ – Wendelstein 7-AS – sollte geplant und gebaut werden. Die Ziele: verbesserter Plasmaeinschluss durch maßgeschneiderte Magnetfelder und modulare Magnetspulen anstelle der spiralförmigen Magnetwicklungen des Vorgängers. Das Kraftwerkspotential der Stellaratoren sollte dann die darauffolgende Anlage Wendelstein 7-X demonstrieren.

Und so kam es. Wie die nachfolgenden Kapitel zeigen, blieb das 1981 in den „Zielen“ aufgestellte Forschungsprogramm bis heute bestimmend für die Arbeit des IPP und war die Richtschnur für vierzig Jahre überaus erfolgreicher Forschung – „über Wechselfälle der Bundespolitik, über europäische Klippen und Schwellen, über weltweite Einigungsprozesse, über Sparzwänge und Stelleneinzugsprogramme, über Emeritierungen und Neuberufungen hinweg“, wie es Professor Dr. Hans Zacher, ehemaliger Präsident der Max-Planck-Gesellschaft, 1999 in seiner Laudatio[1)] auf dem Abschiedskolloquium für Klaus Pinkau formulierte. Das 1981 aufgestellte Forschungsprogramm ist bis heute in den Arbeiten an ASDEX Upgrade und Wendelstein 7-X wirksam und bestimmte darüber hinaus auch die Entwicklungen am europäischen Gemeinschaftsexperiment JET, an dem internationalen Experimentalreaktor ITER und sogar die Pläne für ein Demonstrationskraftwerk DEMO.

Abgesehen von der Forschungsplanung gab Klaus Pinkau dem IPP wesentliche neue Impulse auch bei der Nachwuchsförderung, für die er Stellen aus der Infrastruktur umwandelte. Er setzte sich für die Frauenförderung ein – da es leichtfertig sei, die Hälfte der Intelligenz brachliegen zu lassen – und sorgte für verbesserte Verbindungen zu Universitäten, beginnend 1985 mit parallelen Berufungen an das IPP und die Universität Bayreuth.

Obwohl der Schwerpunkt dieser Festschrift auf dem Wirken Klaus Pinkaus im IPP und für die deutsche und internationale Fusionsforschung liegt, wäre dieser Überblick unvollständig, wenn sein großer, über Astrophysik und Fusionsforschung hinausgehender Einsatz für Aufgaben der Forschungssteuerung und Politikberatung unerwähnt bliebe: Unter anderem war er Mitglied des Wissenschaftsrates, Vorsitzender des Beratungskomitees der Europäischen Raumfahrtbehörde ESA und leitete 1980 den Gutachterausschuss „Großprojekte der Grundlagenforschung“, der das Bundesforschungsministerium bei der Einrichtung neuer Großprojekte unterstützte.

Groß war Klaus Pinkaus Interesse an der Frage nach dem Verhältnis von Gesellschaft und Wissenschaft. Aus seinem vielfältigen und tiefgehenden Engagement in diesem Bereich seien drei Projekte herausgegriffen: Die Frage, ob und wie die moderne Wissenschaft zur Lösung der Zukunftsschwierigkeiten beitragen und helfen kann, die von ihr ausgelösten Entwicklungen zu beurteilen, setzte er als Vorsitzender des Gründungsausschusses der Berliner Akademie der Wissenschaften in ein interdisziplinäres organisatorisches Konzept um. Anstelle der üblichen Akademie-Einteilung in permanente Klassen sah es die Aufteilung in Arbeitsgruppen vor. Für spezifische Aufgaben zeitlich

befristet eingerichtet, brachten diese Gruppen Fachleute verschiedener Disziplinen zusammen. Die Akademie sollte, so Klaus Pinkau 1985 bei der Übergabe der Gründungs-Denkschrift, „die Probleme der technischen, wirtschaftlichen und gesellschaftlichen Entwicklung in neuen Organisationsformen wissenschaftlich bearbeiten. Sie ist sicherlich nicht die erste und nicht die einzige Institution, die sich dieses Ziel vornimmt. Sie soll aber nach unserer Überzeugung ein neuer Ansatz sein. Sie soll die Wissenschaft vereinen, sie zu gemeinsamer Arbeit an den Themen zusammenführen, die die Wissenschaft und unsere Gesellschaft uns stellen[2)]".

Die Akademie wurde 1987 im Westteil Berlins mit Klaus Pinkau als Vorstandsmitglied gegründet, nach der deutschen Einigung jedoch bereits zum Ende des Jahres 1990 durch einen Beschluss des Berliner Abgeordnetenhauses wieder aufgelöst. An ihre Stelle – und zugleich an die Stelle der Ostberliner Akademie der Wissenschaften der DDR – trat 1992 die Berlin-Brandenburgische Akademie der Wissenschaften, deren Mitglied Klaus Pinkau wurde.

Einzelne Vorhaben der aufgelösten Berliner Akademie der Wissenschaften allerdings konnten bis 1993 fortgeführt werden. So wurde Ende 1990 der Bericht der Arbeitsgruppe „Umweltstandards", fertiggestellt, deren Sprecher Klaus Pinkau war[3)]. Am Beispiel des Strahlenschutzes widmet sich die umfangreiche Studie der Funktion von Umweltstandards, ihrer wissenschaftlichen Fundierung und den Problemen bei Entscheidungsprozessen, in denen unterschiedliche Zielvorstellungen miteinander in Konflikt liegen.

1995 konnte die Karl Heinz Beckurts-Stiftung Klaus Pinkau zum Vorsitzenden (bis 1999) gewinnen. Die von der Helmholtz-Gemeinschaft Deutscher Forschungszentren getragene Stiftung will die Partnerschaft von Wissenschaft und Wirtschaft fördern und unterstützt wissenschaftliche Arbeiten, die Brücken zwischen Natur-, Technik- und Geisteswissenschaften bauen können. Die unter Klaus Pinkaus Ägide veranstalteten interdisziplinären Symposien setzten sich mit so unterschiedlichen Themen auseinander wie „Bedingungen langfristig orientierter Technologiepolitik in demokratischen Gesellschaften", „Deutsche Naturphilosophie und Technikfeindlichkeit" oder „Die Zukunft der Aufklärung".

> Forscher,
> Lehrer,
> Vermittler,
> Erklärer

Dem in Akademie und Beckurts-Stiftung verfolgten interdisziplinären Ansatz blieb Klaus Pinkau auch nach seiner Emeritierung treu. 2004 wurde er als Wissenschaftlicher Direktor an das „Alfried Krupp Wissenschaftskolleg Greifswald" berufen. Das Kolleg bringt Wissenschaftlerinnen und Wissenschaftler unterschiedlicher Disziplinen zu gemeinsamer Arbeit zusammen und unterstützt fächerübergreifende Forschungsvorhaben. Nach Ende seiner Amtszeit 2008 blieb er für viele Jahre Mitglied im Wissenschaftlichen Beirat des Kollegs.

Auf allen diesen Feldern inner- und außerhalb des IPP hat Klaus Pinkau prägend gewirkt, „als Forscher, auch als Lehrer, Vermittler, Erklärer", um nochmals Hans Zacher zu zitieren[4)], „als Politiker, nicht als Parteipolitiker, aber auch nicht nur als Forschungspolitiker, sondern als ein homo politicus, der Menschen und Organisationen auf Ziele hin zu orientieren weiß, die es wert sind, und kreativ und sensibel die Strategien findet, die nötig sind, um die Ziele auch zu erreichen, ein homo politicus, der weiß, daß die Ziele zu den Menschen und die Menschen zu den Zielen passen müssen; als eine Autorität, die nicht nur wegen ihrer Rationalität überzeugt, sondern auch wegen ihrer Moralität, wegen ihres Wissens um Verantwortung, wegen ihrer Bereitschaft zur Verantwortung, wegen ihrer Redlichkeit. Im letzten aber wegen seiner Menschlichkeit, wegen seiner Unmittelbarkeit zu einem jeden, wegen seiner Offenheit, wegen seiner Herzlichkeit."

Sibylle Günter,
Wissenschaftliche Direktorin des Max-Planck-Instituts für Plasmaphysik

[1] Hans Zacher: Laudatio, in: Wissenschaft, Gesellschaft und Wissenschaftspolitik. Festkolloquium am 20. April 1999 anlässlich der Emeritierung von Prof. Dr. Drs. h. c. Klaus Pinkau. Hrsg: Max-Planck-Institut für Plasmaphysik, 1999

[2] Klaus Pinkau, Ansprache anlässlich der Übergabe der Denkschrift für die Gründung einer Akademie der Wissenschaften zu Berlin, In: Jahrbuch 1987, Hrsg.: Akademie der Wissenschaften zu Berlin, 1988, Seite 194 ff

[3] K. Pinkau, K. Decker, C.F. Gethmann, H.W. Levi, J. Mittelstraß, S. Peyerimhoff, G. zu Putlitz, A. Randelzhofer, O. Renn, C. Streffer, F.E. Weinert: Umweltstandards – Grundlagen, Tatsachen und Bewertungen am Beispiel des Strahlenrisikos. Akademie der Wissenschaften zu Berlin, Forschungsbericht 2, 1992

[4] Hans Zacher: Laudatio, in: Wissenschaft, Gesellschaft und Wissenschaftspolitik, Seite 10

2

TOKAMAKS

2.1 EINLEITUNG

Energie in einem Brennvorgang durch Verschmelzen von Atomkernen zweier Wasserstoffisotope – Deuterium und Tritium – zu gewinnen, ist eine außerordentlich attraktive Idee: Der Brennzyklus beginnt mit relativ häufig vorkommenden Ausgangsstoffen, Lithium und Deuterium, und endet mit einem chemisch und nuklear inerten Material, Helium. Ein radioaktives Isotop – Tritium – taucht nur als Zwischenprodukt auf. Außerordentlich sind allerdings auch die physikalischen Anforderungen: Bei ausreichend hoher Dichte muss ein Plasma von 100 Millionen Grad thermisch isoliert werden, wobei die Wärmedämmung hundertmal besser sein muss als die von Styropor. Diese Forderungen kann man am besten durch das sogenannte Tripelprodukt $nT\tau$ aus der Teilchendichte n, der Temperatur T und der Einschlusszeit τ beschreiben. Die erreichten Werte dieses Produkts waren stets der Maßstab für den Fortschritt der Fusionsforschung.

Dabei bestimmt die Energieeinschlusszeit die Stärke der Plasmaheizung, die nötig ist, um den Zielwert für den Energieinhalt des Plasmas zu erreichen. Je besser die Wärmeisolation ist, umso weniger Heizung ist nötig, um die Betriebsbedingungen für ein Fusionskraftwerk zu erreichen und zu halten. Dabei muss das Plasma bis zur Zündung von außen geheizt werden, nach der Zündung dann von innen durch die bei der Fusion entstehenden schnellen Helium-Ionen.

Erreicht werden soll diese Wärmeisolation durch Einschluss des Plasmas in einem passenden Magnetkäfig. Während der 1950er und 1960er Jahre erwiesen sich jedoch die meisten der vorgeschlagenen Käfigkonstruktionen als durchlässig oder bogen sich auf, sobald sie mit Plasma gefüllt wurden. Einen Durchbruch brachte Ende der 1960er Jahre das Experiment T-3 in Russland, ein sogenannter Tokamak. In einem passenden, stabilen Plasmazustand erzielte T-3 Rekordwerte für das Tripelprodukt. Vor allem die erreichten Temperaturen erschienen so sensationell, dass sie erst dann allgemein akzeptiert wurden, als sie von Gastwissenschaftlern aus England mit einer neuartigen Messmethode bestätigt worden waren.

Diese Ergebnisse verursachten eine Revolution in der Fusionsforschung. Alle größeren Institute starteten mit dem Bau neuer, größerer Tokamaks. Mit wenigen Ausnahmen wurde weltweit die Arbeit an anderen Konzepten eingestellt oder zumindest drastisch reduziert.

Allerdings ist eine gute thermische Isolation des Plasmas zwar notwendig, jedoch alleine zum Brennen des Plasmas nicht ausreichend. Beim Kontakt des heißen Plasmas mit den Gefäßwänden lösen sich dort Materialien ab, die als Verunreinigung in das Plasma eindringen und dort hohe Abstrahlungsverluste verursachen und das Plasma stark abkühlen können. Das IPP beschloss daher Anfang der 1970er Jahre, diesem Aspekt bei dem geplanten mittelgroßen Tokamak – dem Axialsymmetrischen Divertor-Experiment ASDEX – besondere Aufmerksamkeit zu widmen und ein innovatives Konzept zur Kontrolle der Plasma-Wand-Wechselwirkung zu erproben: den Divertor. Dabei werden die Magnetfeldlinien am Plasmarand in eine separate Kammer abgelenkt. Erst dort hat das Plasma Wandkontakt. Die entstehenden Verunreinigungen werden so von dem heißen Zentralplasma ferngehalten. Beim Entwurf von ASDEX wurde vor allem auch auf die gute Vergleichbarkeit mit klassischen Tokamaks Wert gelegt, bei denen der Kontakt des Plasmas mit der Wand an verschieden geformten Limitern in der Hauptkammer stattfindet.

Die erste Nachfolge-Generation des russischen T-3-Tokamak war sehr erfolgreich. Auf ihrer Basis entschloss man sich in Europa, gemeinsam einen Tokamak zu planen, der in den Wertebereich – vor allem den Temperaturbereich – künftiger Fusionskraftwerke vordringen sollte. Dieser „Joint European Torus" JET sollte mit einem Deuterium-Tritium-Gemisch betrieben werden und unter günstigen Vorhersagen Break-even erreichen können, d.h. Gleichstand zwischen der in das Plasma von außen eingespeisten Heizleistung mit der erzeugten Fusionsleistung. Für die Plasmabegrenzung war ein konventioneller Limiter vorgesehen, da ein Divertor im ASDEX-Stil dem Hauptplasma zu viel Magnetfeldvolumen geraubt hätte. Mutiger als die US-Kollegen mit dem Parallelexperiment TFTR, dem „Tokamak Fusion Test Reactor" in Princeton, setzte man hingegen auf einen D-förmigen Plasmaquerschnitt, der der Theorie nach große Vorteile besitzen sollte, was aber bis dahin an keinem Tokamak verifiziert worden war. Das IPP bemühte sich damals intensiv, Standort dieser wichtigen Anlage zu werden, verlor aber in der Endausscheidung gegen das Plasmalabor in Culham in Großbritannien.

Diese erste Filialgeneration des T3-Tokamak litt allerdings unter einer folgenschweren Einschränkung: Das Plasma wurde ausschließlich durch die Joule'sche Wärme aufgeheizt, die der Plasmastrom im Plasma erzeugt, der zur Erzeugung der Feldlinienkonfiguration notwendig ist. Da der elektrische Widerstand des Plasmas mit zunehmender Temperatur stark absinkt, kann diese Form der Heizung allein jedoch nicht zu Temperaturen führen, bei denen das Plasma zündet und die Fusionsreaktionen schließlich selbst die nötige Wärme liefern. Experimente, die lediglich mit dieser sogenannten „Ohm'schen" Heizung durch den Plasmastrom ausgerüstet waren, gaben daher ein sehr einseitiges Bild des Energieeinschlusses. Denn man konnte das Plasma nur dann stärker heizen, wenn man zugleich den Strom und damit das Magnetfeld erhöhte. Man wusste daher nicht, ob eine Änderung in τ eine Folge des geänderten Magnetfeldes oder der Temperatur wäre. Eindeutig folgte aus diesen ersten Experimenten jedoch, dass die Energieeinschlusszeit mit der Dichte und der Querschnittsfläche des Plasmas anwuchs und die erreichbare Dichte mit der Stärke des Magnetfelds bzw. der Plasmastromdichte stieg. Diese Skalierung, genannt Alcator-Intor-Skalierung, ergab sehr günstige Vorhersagen. Insbesondere sollten relativ „kleine" Hochfeld-Anlagen durch Kompression des Plasmas in den Zustand thermonuklearen Brennens vordringen können. Auch das IPP verfolgte diese Option mit der Konzept-Planung für den Tokamak Zephyr, das „Zündexperiment für die Physik im Reaktor". Das zugehörige Personal wurde nach Aufgabe anderer Forschungslinien – der toroidalen und helikalen Pinche – frei bzw. war ursprünglich für die Standortunterstützung von JET vorgesehen.

Tokamak-Anlagen mit zusätzlicher Plasmaheizung durch Radio- oder Mikrowellenheizung und Neutralinjektion – d.h. Einschießen energiereicher Wasserstoffatome, die im Plasma ionisiert werden und dort ihre Energie abgeben – begannen in großem Stile Ende der 1970er Jahre. Anfang der 1980er waren die aus den Experimenten zu ziehenden Schlussfolgerungen deprimierend, aber unausweichlich: Der Energieeinschluss verschlechterte sich stark mit steigender Plasmaheizung. „Alcator-Intor" und ähnliche, auf nur stromgeheizten Anlagen fußende Skalierungen waren ein Artefakt, produziert durch die oben beschriebene Entartung der Datenbasis. Kompakten Hochfeld-Zündexperimenten wie Zephyr war damit die Grundlage entzogen. Aber auch die Hoffnung auf Break-even an JET und die Perspektive für ein Fusionskraftwerk erlitten einen ernsten Rückschlag.

Diese fatale Verschlechterung des Energieeinschlusses bei Zusatzheizung wurde anfangs auch an ASDEX gefunden. Dagegen waren bereits die frühen Experimente an ASDEX sehr erfolgreich, soweit sie die Plasma-Wand-Wechselwirkung und die Physik des Divertors betrafen. Da ASDEX – mit Ausnahme der äußersten Randzone – bezüglich Form und Lagestabilität des Plasmas einem konventionellen Limiter-Tokamak sehr ähnlich war, konnte man die Vorteile des Divertor-Konzeptes in direkten, sauberen Vergleichsexperimenten beweisen[1)]. Vor allem ließ sich die weitgehende Entkopplung der Zustände in der Divertor- und der Hauptkammer demonstrieren sowie die vorteilhaften Folgen für die Verunreinigungskontrolle. Die Vorteile des Divertor-Konzeptes wurden daher von großen Teilen der Wissenschaft akzeptiert. Grundlegende Skepsis herrschte jedoch bezüglich der Realisierbarkeit in einem Fusionskraftwerk.

[1)] siehe Seite 25 ff.: Y. Shimomura et al.: Characteristics of the Divertor Plasma in Neutral-Beam-Heated ASDEX Discharges, in: Nucl. Fusion 23, Seite 869-879 (1983)

Das IPP-Tokamak-Programm von 1981 bis 1999

Der Tokamak hatte Ende der 1960er Jahre das Konzept des magnetischen Plasmaeinschlusses aus einer ersten Krise herausgerissen, aber die allgemein beobachtete Verschlechterung des Energieeinschlusses drohte ihn jetzt selbst in eine Krise zu stürzen. In dieser Situation übernahm im Februar 1981 Klaus Pinkau die Leitung des IPP.

Bereits vier Monate später konnte er dem European Fusion Review Panel in Vorbereitung des nächsten Fünf-Jahres-Programmes von EURATOM ein „White Paper“ vorlegen – „The Aims of IPP“. Sie bestimmen in großen Zügen das Institutsprogramm bis in die heutigen Tage. Bis dahin einmalig am IPP war der Prozess, der zu ihrem Entstehen führte. Für acht Sitzungen während zweier Monate wurde die Wissenschaftliche Leitung von einem permanenten Beraterkreis begleitet, dem außer den Mitgliedern des Wissenschaftlerrates auch rund ein Dutzend Wissenschaftler angehörten, die sich vor allem bei der Ausarbeitung von Programmvorschlägen engagiert hatten. Nach einer allgemeinen Bestandsaufnahme magnetischer Einschlusskonzepte sollten dabei Optionen für künftige Anlagen in Garching und für die Rolle des IPP in internationalen Kooperationen erarbeitet werden.

Vor allem nach den vielversprechenden ersten Ergebnissen zum Divertor-Betrieb stand mit ASDEX eine der Säulen dieses Programmes fest, da die Plasma-Wand-Wechselwirkung immer einer der kritischen Aspekte eines Fusionskraftwerks bleiben würde. Diese Ergebnisse zeigten aber auch nötige Erweiterungen der Anlage auf:

- Zunächst war es wichtig, die Heizleistung zu steigern, um Aussagen auch bei kraftwerksähnlicheren Plasmatemperaturen, bei höherer Wandbelastung und bei höherem Plasmadruck (im Verhältnis zum Magnetfelddruck) machen zu können.
- Für einen schlüssigen Vergleich von Divertor- und Limiter-Betrieb sollte auch für letzteren eine toroidal gleichmäßige Leistungsbeaufschlagung sichergestellt werden. Dazu wurde der untere der beiden Divertoren durch einen toroidal umlaufenden, ebenfalls axial-symmetrischen Limiter ersetzt.
- Eine mögliche Verunreinigungsquelle waren die Heizsysteme selbst, die entweder in Antennennähe oder durch im Plasmainneren erzeugte schnelle Teilchen Wandmaterial zerstäuben konnten. Daher wurden an ASDEX im Laufe der Jahre drei unterschiedliche Zusatzheizsysteme – Neutralteilchenheizung sowie Wellenheizung im hohen Mega- bzw. Gigahertz-Bereich – eingerichtet und sowohl im Vergleich als auch in ihrem Zusammenwirken getestet.
- Saubere Plasmen ermöglichen eine lange Pulsdauer, die aber umgekehrt auch erforderlich ist, um die Effizienz der Verunreinigungskontrolle überzeugend nachzuweisen. Auch ohne Induktion über einen Transformator lässt sich mit Hilfe von Neutralteilchen-Heizung, vor allem aber durch die Einkopplung von Wellen im Gigahertz-Frequenzbereich der sogenannten Lower-Hybrid-Resonanz der im Tokamak nötige toroidale Plasmastrom aufrecht erhalten. Entsprechend wurden die Aufgaben erweitert um lange Entladungszeiten und Heizmethoden mit Stromtrieb-Potential.
- Schließlich ging es auch um die Plasmadichte. Sie muss durch Nachfüllung aufrechterhalten werden, um die Verluste durch Ausströmen auszugleichen und im Kraftwerk den Tritium-Abbrand zu kompensieren. Das einfache Einblasen von Gas vom Rande des Plasmagefäßes her funktioniert zwar, ist aber vergleichsweise ineffektiv, da ein großer Teil der dabei entstehenden Ionen schnell wieder auf den Limiter oder in die Divertorkammer abgeleitet werden. Kügelchen aus gefrorenem Wasserstoff, die mit einem Blasrohr oder mit einer Zentrifugen-Schleuder eingeschossen werden, dringen tiefer ins Plasma ein und füllen das Plasma daher effizienter nach. In den folgenden zehn Jahren wurde dieses Ausbauprogramm, das in Grundzügen in den „Aims of IPP“ formuliert worden war, ausgeführt – mit außerordentlichen wissenschaftlichen Erfolgen.

ASDEX war ein wunderbares Instrument der Grundlagenforschung, da seine kompromisslose Auslegung mit klarer Trennung von Hauptplasma und Divertorkammer sehr schlüssige Vergleiche zuließ. Kritik am Divertor-Konzept betraf daher nicht die Ergebnisse, sondern die Schwierigkeiten, sie auch unter Kraftwerksbedingungen zu realisieren. Ein Problem ergab sich aus der Anordnung der Spu-

len: Das stärkste Magnetfeld im Tokamak verläuft in toroidaler Richtung und wird von einem Satz poloidal geschlossener Spulen gebildet. Die Divertor-Spulen und die Divertorkammern verbrauchen wertvolles Volumen in dem vom Toroidalfeld erfüllten Gebiet, das damit für das Hauptplasma und die Fusionsreaktionen nicht zur Verfügung steht. Außerdem wäre die Verknüpfung der beiden Spulensätze in der bei ASDEX gewählten Anordnung mit Supraleitern nicht zu verwirklichen.

Parallel dazu zeichnete sich zu diesem Zeitpunkt auch ein Verständniswechsel in der Rolle der Plasma-Wand-Wechselwirkung ab. Dominierendes Thema in der frühen Phase der Fusionsforschung war der Schutz des Plasmas vor den von den Wänden kommenden Verunreinigungen. Neuere Experimente mit zunehmend längerer Pulsdauer und stärkerer Zusatzheizung sowie realistischere Kraftwerksstudien rückten jetzt jedoch den Schutz der Wand vor den hohen Leistungsflüssen aus der Plasmarandschicht in den Fokus. Es genügte nicht, den Energiefluss des Plasmas in einen fernen Divertor abzulenken – man musste ihn darüber hinaus stark reduzieren. Dieser Gedanke war zunächst an Limiter-Tokamaks aufgekommen, vor allem an JET und in der Zephyr-Studie des IPP, wo die Idee einer selbstregulierenden „Photosphäre“ zur Absenkung dieser Energieflüsse rechnerisch untersucht wurde.

Ein radialer Energiefluss, getrieben durch externe Heizung oder Fusionsreaktionen, ist nötig, um im Inneren des Plasmas den radialen Temperaturgradienten aufrecht zu erhalten. Im Gebiet von Feldlinien mit Wandkontakt angekommen, strömt dieser Energiefluss jedoch in einer sehr dünnen Schicht auf die Divertor- oder Limiter-Platten und führt dort zu einer hohen Belastung: In einem Kraftwerk wären Leistungsflussdichten zu erwarten, die höher sind als die auf der Sonnenoberfläche. Ideal wäre es, diesen Energiefluss kurz vor dem Plasmarand in elektromagnetische Strahlung, d.h. Lichtstrahlung umzuwandeln, die – gleichmäßig auf die ganze Gefäßwand verteilt – tolerable Belastungen ergäbe. Möglich würde dies durch gezielte Verunreinigung des Plasmas mit einem Material, das dank der Temperaturabhängigkeit seiner Strahlungscharakteristik vor allem in den kälteren, d.h. den äußersten Plasmazonen strahlt. Die Konzentration dieser Verunreinigung muss dabei sehr genau kontrolliert werden, um einen Strahlungskollaps der Entladung wegen zu hoher Verluste zu vermeiden. Eine relativ hohe Plasmadichte ist ebenfalls nötig, da – bei gegebener Verunreinigungskonzentration – die Strahlung mit dem Quadrat der Dichte steigt. Im Tokamak ist die erreichbare Dichte jedoch durch das sogenannte „Greenwald-Limit“ begrenzt und hängt von Stromdichte und Plasmaform ab.

Hauptsächlich aus diesen beiden Forderungen nach einer für ein Kraftwerk relevanten Divertor-Konfiguration und besseren Voraussetzungen für eine Photosphäre entstand der Projektvorschlag für ein Nachfolgeexperiment von ASDEX: ASDEX Upgrade. Diese Forderungen passten auch zu einem D-förmigen Plasmaquerschnitt, der ein höheres – kraftwerksrelevantes – Verhältnis von Plasmadruck zum Magnetfelddruck versprach.

Daneben sollte das Institut laut den „Aims of IPP“ auch weiterhin maßgeblich an gesamteuropäischen und internationalen Tokamak-Projekten teilnehmen. An JET sollte dies vor allem durch die Entwicklung passender Diagnostiken geschehen; in die Studien für ein Nachfolgeexperiment wollte man möglichst früh eigene programmatische Vorstellungen einbringen. Unter der Schirmherrschaft der Internationalen Atomenergie-Agentur IAEA hatten sich Euratom, Japan, die Sowjetunion und die USA bereits 1979 zu gemeinsamen Konzeptstudien für den nächsten Schritt hin zum Fusionskraftwerk zusammengeschlossen. Einigkeit herrschte unter den vier Partnern, dass diese Anlage – der Internationale Torus INTOR – neben der Physik des zumindest beinahe gezündeten Betriebes auch technische Komponenten testen sollte, die für den Brennstoffkreislauf und die Energieauskopplung in einem Kraftwerk notwendig sind[2) 3)]. In den Details des Anforderungsprofils – etwa der Nähe zur vollständigen Zündung, dem Grad der Selbstversorgung der Anlage mit Tritium und der geforderten Pulsdauer –, aber auch im Optimismus der zugrunde gelegten physikalischen Annahmen unterschieden sich die Vorstellungen der Partner jedoch so stark, dass eigentlich vier unterschiedliche Projekte ausgearbeitet wurden. Das IPP bewarb sich erfolgreich um den Sitz der europäischen Projektstudiengruppe für den „Next European Torus“, kurz NET. Diese geographische Nähe hatte

auch starke symbiotische Effekte: So wurden die Divertor- und Plasma-Konfigurationen von NET[4] und ASDEX Upgrade weitgehend parallel und unter Nutzung derselben Codes erarbeitet.

Diese Ideen und Projektvorschläge wurden in den acht Sitzungen des Beratungsteams gemeinsam mit den Vorschlägen aus dem Stellarator-Kreis kritisch verfeinert und in ihren wesentlichen Forderungen in den „Aims of IPP“ formuliert. Der iterative Prozess und die breite Beteiligung der IPP-Wissenschaftler an den Beratungen führte nicht nur zu einem Programm, das auf äußere Kritik gut vorbereitet war, sondern einte auch die IPP-Forschung. In Zukunft wurde jeder wissenschaftliche Erfolg als einer des gesamten Institutes und somit als Rechtfertigung für das Gesamtprogramm gewertet.

Die „Aims of IPP“ beeindrucken heute durch ihre Weitsicht und die Breite der darin erhobenen Ansprüche. Das IPP wollte nicht nur neue Anlagen mit den beiden zukunftsträchtigen Einschlusskonzepten Tokamak und Stellarator bauen, sondern auch die Physik aller Heiz- und Stromtriebsysteme, Nachfüllmethoden und Energieabfuhrsysteme in breitem Rahmen untersuchen und ebenso auf dem Gebiet der Plasmasteuerung eine Spitzenstellung besetzen.

Die Formulierung dieser Ansprüche war die eine Sache, ihre Akzeptanz und das Einwerben ihrer Finanzierung in Deutschland und Europa jedoch eine andere. Der allgemeine wissenschaftliche Ruf des IPP, politisches Geschick der Spitze und die bereits erwähnte Einigkeit der IPP-Wissenschaftler waren dabei zentrale Elemente, wurden aber auch unterstützt durch eine Prise wohlverdienten Glücks.

Die oben erwähnte fatale Verschlechterung des Energieeinschlusses bei Zusatzheizung wurde anfangs auch an ASDEX gefunden. Sein direktes Konkurrenzexperiment PDX, das „Poloidal Divertor Experiment“ in den USA, verfügte sogar über mehr Heizleistung, besaß jedoch eine schwieriger zu steuernde Divertor-Konfiguration, so dass Hochleistungsexperimente hier zunächst überwiegend in Limiter-Konfiguration liefen. Bei ASDEX hingegen war der Divertor-Betrieb bei allen experimentellen Fragestellungen die Standard-Betriebsweise.

1982, bald nach Einbau eines zweiten Neutralteilcheninjektors, machte man an ASDEX eine aufregende Beobachtung, nämlich eine Bifurkation des Einschlussverhaltens: Ab einer bestimmten Heizleistung konnte es zu einem plötzlichen Übergang in einen Plasmazustand mit etwa doppelter Energieeinschlusszeit kommen, in das sogenannte „High-Confinement Regime“, oder kurz H-Regime[5] [6]. Bei ausreichend hoher Heizleistung war dieser Zustand sogar dominant!

Der Einfluss dieser Entdeckung auf das weltweite Fusionsprogramm kann kaum überbewertet werden[7] [8]. Auf dieser Basis war der gezündete Betrieb eines Fusionskraftwerks im gewünschten Leistungsbereich wieder denkbar und alle Kraftwerksstudien akzeptierten das H-Regime als Grundlage der Auslegung. Innerhalb Jahresfrist wurde das H-Regime auch an zwei Divertor-Tokamaks in den USA gefunden, vorhandene Limiter-Tokamaks wurden umgebaut und keiner der nach 1983 entworfenen Tokamaks sollte ohne Divertor auskommen. Für den Weg des Programmvorschlages[9] zu ASDEX Upgrade durch die Europäischen Institutionen brachte diese Entdeckung entscheidenden Rückenwind.

Die Entdeckung des H-Regimes und die Versuche seiner Erklärung veränderten auch das theoretische Verständnis des Energietransportes grundlegend. Elegante Experimente an ASDEX zur Aus-

---

[2] siehe Seite 126 ff.: G. Grieger: INTOR - A European View, in Fusion Technology, 8 (1985)

[3] siehe Seite 135 ff.: G. Grieger & INTOR-Group: INTOR: Critical Analysis of INTOR-Like Designs, in: Plasma Physics and Controlled Nuclear Fusion Research, Vol. 3

[4] siehe Seite 147 ff.: F. Engelmann (1993). NET Predesign Overview, in: Plasma Physics and Controlled Nuclear Fusion Research, 1992

[5] siehe Seite 20 ff.: F. Wagner, Regime of Improved Confinement and High Beta in Neutral-Beam-Heated Divertor Discharges of the ASDEX Tokamak, in: Phys. Rev. Letters 49, Nr. 19, 1982

[6] ASDEX Team: The H-Mode of ASDEX, in: Nucl. Fusion 29, Seite 1959-2040 (1989)

[7] siehe Seite 36 ff.: F. Wagner, The history of research into improved confinement regimes, in: The European Physical Journal H, Volume 43 (2018)

[8] Auch dem Betrieb eines Demonstrationskraftwerks wird das H-Regime zugrunde liegen: siehe Seite 173 ff.: G. Federici et al., DEMO design activity in Europe: Progress and updates, in: Fusion Engineering and Design 136, Seite 729-741 (2018)

[9] siehe Seite 64 ff.: ASDEX-Upgrade Design Team and Tokamak Theory Group: ASDEX-Upgrade. Definition of a tokamak experiment with a reactor compatible poloidal divertor, IPP 1/197, März 1982 (Ausschnitt)

breitung von Wärmepulsen im Übergangsbereich zwischen den beiden Plasmazuständen – dem bisherigen schlechten „Low-Confinement Regime“ (L-Regime) und dem H-Regime – zeigten, dass die Veränderungen vom Plasmarand ausgingen. Dies passte gut zur offensichtlichen Verbindung des H-Regimes mit der Divertor-Geometrie. Trotzdem betraf die Verbesserung des Einschlusses auch das Plasmainnere – wegen einer Steifheit der logarithmischen Temperaturprofile. Dies erklärt sich so, dass turbulente Verluste erst jenseits eines bestimmten Temperaturgradienten dramatisch ansteigen. Sie führen damit zu ähnlichen Vorgängen wie beim Entstehen des Schüttwinkels einer Aufschüttung. Die Randbarriere der H-Mode hingegen wurde durch eine verscherte Rotation des Plasmas erklärt, die turbulente Wirbel zerstört, aber selbst durch diese getrieben wird. Dieses Wechselspiel und die damit verbundene Möglichkeit zur Bifurkation wurde zuerst von US-Theoretikern erkannt und erklärte später auch andere Aspekte des turbulenten Transportes.

Natürlich hatte die Entdeckung des H-Regimes starken Einfluss auf das weitere Programm von ASDEX, wobei sich weiterhin viele Synergien mit dem Divertor-Programm ergaben. So konnte man dank der Oben-Unten-Symmetrie des Magnetfeldes und der absoluten Lagestabilität des Plasmas schlüssig zeigen, dass vertikale Teilchendriften einen starken Einfluss auf den Transport in der Randschicht und auf den Übergang vom L- in das H-Regime besitzen, und dass sich Turbulenz und turbulente Energieverluste vor allem an der Außenseite des Plasmas einstellen. Das robuste Divertor-Konzept und die erfolgreiche Entkopplung der Vorgänge im Hauptplasma von denen am Kontakt von Plasma und Wand zeigte sich eindrucksvoll auch darin, dass ASDEX mit drei unterschiedlichen Materialien für die Prallplatten des Divertors – Edelstahl, Titan und Kupfer – vergleichbar gute Ergebnisse erzielte, während Limiter-Tokamaks bei starker Plasmaheizung nur mit Graphit oder Kohlefasern ausreichend niedrige Verunreinigungskonzentrationen erreichen konnten.

Die Frage, ob das H-Regime auch mit weniger aufwändigen Magnetfeldkonfigurationen oder sogar – bei reduziertem Plasmastrom – durch geänderte Strombeschickung der übrigen Spulen erzielt werden könnte, wurde im Prinzip schon im Jahr seiner Entdeckung an dem US-Tokamak Doublet III positiv beantwortet. Auch an JET, wo man dem Divertorprinzip anfänglich sehr skeptisch gegenüberstand, gelangen ein paar Jahre später solche Versuche. Schließlich wurde auch JET durch Einbau zusätzlicher, plasmanaher Spulen zu einem Divertor-Tokamak umgerüstet[10)].

Der Übergang von ASDEX zu ASDEX Upgrade war motiviert durch die Notwendigkeiten der Kraftwerksrelevanz und hatte inzwischen durch die Planung des internationalen Projektes ITER[11)] einen neuen Fokus erhalten. Im Gegensatz zur INTOR-Studie stand hinter der Planung von ITER – mit zunächst den gleichen Partnern – auch eine konkrete Bauabsicht in absehbarer Zeit. Das internationale Tokamak-Programm wandelte sich damit zu einem zielgerichteten Entwicklungsprogramm, in dem keine Frage unbeachtet oder unbeantwortet bleiben durfte. Es war ein weiterer politischer Erfolg, dass das IPP während der ersten Planungsphase Gastgeber des ITER-Teams wurde, später einer von drei Standorten des internationalen ITER-Teams. Neben der Anerkennung für das Institut bedeutete dies vor allem, dass der Informationsaustausch über Probleme und Lösungsansätze zwischen den Teams von ITER und ASDEX Upgrade nicht allein auf offizielle Berichte und Workshops angewiesen war, sondern auch bei täglichen Begegnungen auf kleinem Dienstweg stattfinden konnte.

Sichtbarste Konsequenz dieser geänderten Ausrichtung war die oben erwähnte neue Einschätzung der Plasma-Wand-Wechselwirkung. Der Schutz der Wand rückte nun in den Vordergrund. Zahlreiche Beobachtungen erhielten damit neue Bedeutung, zum Beispiel ein Nebenprodukt des H-Regimes, die sogenannten „Edge-Localised Modes“ oder ELMs: Diese periodisch auftretenden Fluktuationen am Plasmarand waren anfänglich willkommen, da sie Verunreinigungen aus dem Plasma warfen. In ITER und einem Kraftwerk würden sie jedoch zu starke Wärmepulse auf den Divertor-Platten abladen. Ihre Vermeidung bzw. Kontrolle wurde daher zu einem der wesentlichen Programmpunkte von ASDEX Upgrade.

Neben den mit der Divertor-Konfiguration verbundenen Fragen und der gezielten Absenkung der Leistungsflüsse traten allgemeine Fragen der Entladungssteuerung in den Vordergrund. Seit ASDEX

waren die Möglichkeiten zur Datenverarbeitung in Realzeit gewaltig gestiegen. Die Plasmalage und -form von ASDEX Upgrade wurde von Anfang an mit Hilfe einer frühen Generation von Parallelrechnern geregelt. Optimierte Langpuls-Entladungen benötigten darüber hinaus jedoch weitere Regelsysteme, die ein breiteres Spektrum an Diagnostiken und komplexere Regelalgorithmen nutzten. Fast jeder Einsatz eines neuen Regelsystems endete in einem Aha-Erlebnis angesichts der plötzlich geglätteten Ergebniskurven. Retrospektiv wurde zum Beispiel klar, dass die Ablösung bzw. das „Detachment“ des Plasmas bereits an ASDEX beobachtet, aber mangels Kontrollmöglichkeiten falsch, nämlich als Vorstufe eines Entladungszusammenbruches gedeutet wurde. Bei diesem Detachment löst sich das Plasma von den Divertorplatten, weil bei sehr hoher Dichte und geringem Energiefluss die Plasma-Ionen und Elektronen vor den Prallplatten rekombinieren und fast nur noch ein Polster aus Neutralgas Wandkontakt hat. Auch die Erzeugung einer Photosphäre durch gezielten Verunreinigungszufluss war bei ASDEX an mangelnden Regelungsmöglichkeiten gescheitert.

Die „Aims of IPP“ schickten ASDEX Upgrade auf den richtigen Weg, um die kritischen physikalischen Fragen für ITER zu erkunden: Integrierte Betriebsszenarien mussten gefunden werden, welche die scheinbar widersprüchliche Forderung nach einem möglichst heißen Plasmazentrum und einem möglichst kalten Plasmarand erfüllen konnten. Neben den richtigen konzeptuellen Entscheidungen zu Divertor-Geometrie, Wandmaterial und Heizmethoden war hierfür vor allem nötig, die Einflussmöglichkeiten, ihre Zusammenhänge und ihre Umsetzung in vernetzten Regelsystemen zu verstehen.

Der Schlüssel dazu war klar: Die Leistungsflüsse mussten in elektromagnetische Strahlung von Verunreinigungen umgewandelt werden und dies sollte möglichst am Plasmarand geschehen, bevor das Plasma in Kontakt mit den Prallplatten des Divertors kommt. Mit Prallplatten aus Graphit oder Kohlefasern geschah dies mehr oder weniger automatisch und selbstregulierend, da deren Abtragung bereits für eine Verunreinigungsquelle sorgte. Diese Lösung passte aber nur in einem bestimmten Leistungsbereich. Vor allem war sie ungeeignet für den Langzeitbetrieb, in dem die Prallplatten viel zu schnell erodiert würden. Das robuste Metall Wolfram dagegen konnte kraftwerksrelevante Standzeiten garantieren – aber nur dann, wenn man zugleich mit der Energieumwandlung in Strahlung erfolgreich war und ausreichend niedrige Temperaturen im Divertor garantieren konnte. Es war also eine risikoreiche Entscheidung, ASDEX Upgrade schrittweise mit Wolfram auszukleiden – sie wurde aber wegweisend für die Fusionsforschung[12)]. Untrennbar damit verbunden war die Technik, dem Plasma einen Cocktail von Verunreinigungen zu verabreichen, der in gezielter, rückkopplungsgesteuerter Zusammensetzung die Energieabstrahlung am passenden Ort stattfinden ließ.

Auch die Dichte des Wasserstoffplasmas erfordert maßgeschneiderte Kontrolle. Anblasen der Entladung mit Gas in der Hauptkammer oder im Divertor oder eingeschossene Eiskügelchen sind unterschiedlich effektiv und können in passender Kombination unterschiedliche Anforderungen erfüllen. Das relativ einfache Gasblasen erhöht die Dichte in Plasmarand und Divertor und wäre im Kraftwerk mit einem hohen Umsatz von Tritium verbunden. Eiskügelchen erhöhen die Dichte im Plasmainneren, wo in einem Kraftwerk die Kernverschmelzung hauptsächlich ablaufen würde. Eine hohe Randdichte ist nützlich, da sie die Strahlungskühlung fördert und die Prallplatten schützt; zentrales Nachfüllen erlaubt höhere Plasmadichten und wird in einem Kraftwerk für den effektiveren Abbrand des Tritiums sorgen. Über Rückkopplung gesteuert, kann ein kombiniertes System den optimalen Kompromiss ermöglichen.

Um das Hauptplasma zu optimieren, sind vor allem stabile Entladungszustände zu identifizieren und robuste Zugangswege zu finden. Kontrolle der Plasmaprofile und aktives Stabilisieren von Störungen kann diesen Bereich wesentlich ausweiten und damit vor allem den Betrieb bei höherem Plasmadruck ermöglichen bzw. in einem Kraftwerk bei höherer Fusionsleistung. Möglichkeiten zur Steuerung bieten vor allem die verschiedenen Methoden für Heizung und Stromtrieb, mit denen ASDEX Upgrade gut ausgestattet ist. Heizung und Stromtrieb durch Mikrowellen im Frequenzbereich der Zyklotron-Resonanz der Elektronen war inzwischen ebenfalls technisch möglich geworden. Mit ihrer Hilfe konnte man Plasmen sehr lokal und mit „chirurgischer“ Präzision beeinflussen. Da Instabilitäten

meist eng lokalisiert um „empfindliche“ Flussflächen auftreten, an denen sich Magnetfeldlinien nach wenigen Umläufen schließen, konnte damit ein druckbegrenzender, aber nur langsam wachsender Störungstyp sogar aktiv kontrolliert werden. Auch gezielte kleine Änderungen im Stromprofil rund um diese „empfindlichen“ Flussflächen konnten die Stabilität effektiv beeinflussen.

Da unterschiedliche Heizmethoden an ASDEX Upgrade verfügbar sind, konnte man synergetische Effekte bei ihrem gleichzeitigen Einsatz entdecken, aber auch auf Zustände vorgreifen, wie sie in ITER und einem Kraftwerk herrschen werden. Dort wird das Wasserstoff-Plasma durch die Abbremsung der geladenen, energiereichen Helium-Ionen geheizt werden, die bei der Fusionsreaktion entstehen. Neutralinjektion und die Welleneinstrahlung im Ionenzyklotron-Frequenzbereich heizen das Plasma ebenfalls über suprathermische Ionen. Sie gestatten somit einen ersten Blick auf neue physikalische Effekte und erlauben es vor allem, Codes zu testen, die zu ihrer Beschreibung in Hinblick auf ITER entwickelt wurden. Bei der Entwicklung von Heizmethoden setzte das IPP stark auf Zusammenarbeit mit auswärtigen Institutionen und förderte dabei auch zahlreiche Pionierleistungen. Als wegweisend erwies sich vor allem, Hochfrequenzentladungen als Ionenquelle für die Neutralteilcheninjektion einzusetzen, ein Verfahren, das später für das ITER-Heizsystem essentiell wurde.

Parallel zu diesen experimentellen Entwicklungen begann in den 1990er Jahren auch ein neuer Höhenflug der Theorie, angetrieben durch immer leistungsfähigere Großrechner. Traditionell waren am IPP Theoretiker stets maßgeblich an der Planung neuer Experimente beteiligt. Wichtiger noch als bei den axialsymmetrischen Tokamaks war dies bei den komplex strukturierten Stellaratoren. Hier konnten nur sehr aufwändig zu berechnende Magnetfeld-Konfigurationen die Anforderungen erfüllen, die beim Tokamak bereits durch die Symmetrie sichergestellt sind, wie geschlossene Flussflächen, guter Einschluss der durch Fusion produzierten schnellen Helium-Ionen und ein geringer durch Stöße verursachter Teilchen- und Energietransport.

Die tatsächlich an Tokamaks gefundenen Verluste wurden jedoch weniger durch Stöße als durch turbulente Fluktuationen erzeugt und waren wesentlich höher als die klassischen Stoßeffekte erwarten ließen. Mit neu entwickelten Plasma-Modellen und neuen Großrechenanlagen wurde jetzt die direkte Ab-Initio-Simulation dieser turbulenten Fluktuationen möglich. Die Modelle nutzten aus, dass Turbulenzphänomene langsamer und auf einer größeren Skala ablaufen als die schnelle Kreisbewegung der Plasmateilchen um die Feldlinien. Die unter Klaus Pinkau intensivierte Nachwuchsförderung des IPP führte in den 1990er Jahren praktisch zu einer „Schule“ für die Entwicklung einschlägiger Code-Familien, die heute internationale Spitzenstellungen einnehmen. Gefördert wurde diese Entwicklung auch durch die Politik des IPP, stets Zugang zu Rechnern der obersten Leistungsklasse bereitzuhalten. Auch auf anderen Theoriefeldern wie der Analyse von Wellenausbreitung und -absorbtion, der Wechselwirkung schneller Teilchen mit Fluktuationen im Plasma, der nichtlinearen Entwicklung makroskopischer Instabilitäten und der Simulation der komplexen Wechselwirkungen im Divertor sicherte sich das IPP damals eine Spitzenstellung.

Das Tokamak-Konzept ist mit einer Erbsünde geboren: dem toroidal umlaufenden Plasmastrom. Er sorgt zwar für die gewünschten, geschlossenen magnetischen Flussflächen bei einer im Prinzip rigorosen Axialsymmetrie, die – siehe oben – auch weitere Vorteile birgt. Reißt dieser starke Strom jedoch ab, wird die Energie des von ihm erzeugten Magnetfeldes frei und kann im Gefäß thermische und mechanische Schäden verursachen. Derartige „Disruptionen“ zu vermeiden oder abzumildern steht daher obenan im Pflichtenheft für ITER und ein Tokamak-Kraftwerk. Zwar wird der Betriebsbereich eines Kraftwerks in ein weitgehend disruptionsfestes Gebiet gelegt werden, jedoch können Störfälle nicht vollkommen ausgeschlossen werden. Daher ist eine mehrschichtige Strategie angesagt, die auf Früherkennung abnormalen Verhaltens und kontrolliertes Herunterfahren der Entladung baut. Darüber hinaus entwickelte ASDEX Upgrade Methoden, um auch nicht mehr kontrollierbare Entladungen durch schnelle Zufuhr von zusätzlichem Wasserstoff oder Verunreinigungen schadensfrei zu beenden.

Der Tokamak ASDEX Upgrade während des Aufbaus

Foto: IPP

Bilanz des IPP-Tokamak-Programms der Jahre 1981 bis 1999

Am Anfang dieser beiden Jahrzehnte stand das Tokamak-Konzept vor einer ernsten Krise, am Ende stand die physikalische Basis für die konkrete Bauplanung von ITER zur Verfügung. Zwar war noch keine Einigung darüber erzielt, wo genau ITER in dem Parameterraum zwischen JET und einem Demonstrationskraftwerk angesiedelt werden sollte, aber die Instrumente und Informationen für das detaillierte Design standen bereit.

Einigen musste man sich vor allem auf den Zielwert für den Leistungsfaktor Q – das Verhältnis der Fusionsleistung zu der im Plasma deponierten, von außen zugeführten Heizleistung – sowie auf die angestrebte Pulsdauer und den vorgesehenen Brennstoffverbrauch, der eng mit der integrierten Wandbelastung durch Neutronen korreliert und bestimmt, wieviel Tritium in der Anlage erbrütet werden muss. Auch viele wichtige politische Entscheidungen über Partner, Standort, Finanzierung und Governance waren noch zu treffen. Dass jedoch die wissenschaftliche Basis für ein attraktives Projekt existierte, wurde am besten dadurch dokumentiert, dass es den Partnern Europa, Japan und Russland gelang, nicht nur den zwischenzeitlich abgesprungenen Partner USA, sondern auch drei weitere große Wirtschaftsmächte – China, die Koreanische Republik und Indien – mit an Bord zu holen.

Die Planung von ITER identifizierte einen Katalog kritischer physikalischer Fragen, die vor einem Baubeschluss ausreichend abgeklärt werden mussten[13]: Entwicklung robuster Entladungsszenarien mit gutem Energieeinschluss, eine Lösung für die Plasma-Wand-Wechselwirkung, die lange Plasmapulse und lange Betriebsphasen ermöglicht und makroskopische Instabilitäten vermeidet, welche frühzeitige Entladungsabbrüche erzwingen würden.

Zur Klärung all dieser Punkte hatte das Tokamak-Programm des IPP unter der Leitung von Klaus Pinkau wesentliche Beiträge geleistet – zu einigen der wichtigsten sogar die entscheidenden.

3.1
EINLEITUNG STELLARATOREN
FRIEDRICH WAGNER
SEITE 184

Karl Lackner,
emeritiertes Wissenschaftliches Mitglied des Max-Planck-Instituts für Plasmaphysik

[10] siehe Seite 113 ff.: JET Joint Undertaking: Annual Report 1992, Seite 85-99 (Future Programme), Mai 1993

[11] siehe Seite 161 ff.: B. Bigot: Progress toward ITER's First Plasma, in: Nucl. Fusion 59 (2019)

[12] Einen Überblick über aktuelle Arbeiten an ASDEX Upgrade gibt: H. Meyer et al.: Overview of physics studies on ASDEX Upgrade, in: Nucl. Fusion 59, 2019 (siehe Seite 191 ff.)

[13] M. Rosenbluth: Physics fundamentals for ITER, in: Plasma Phys. Control. Fusion 41 (1999) Seite A99-A113

ASDEX

Im Plasmagefäß des
Tokamaks ASDEX
(1980 - 1990)

Foto: IPP

2.2 ASDEX

Regime of Improved Confinement and High Beta in Neutral-Beam–Heated Divertor Discharges of the ASDEX Tokamak

F. Wagner, G. Becker, K. Behringer, D. Campbell, A. Eberhagen, W. Engelhardt, G. Fussmann, O. Gehre, J. Gernhardt, G. v. Gierke, G. Haas, M. Huang,[a] F. Karger, M. Keilhacker, O. Klüber, M. Kornherr, K. Lackner, G. Lisitano, G. G. Lister, H. M. Mayer, D. Meisel, E. R. Müller, H. Murmann, H. Niedermeyer, W. Poschenrieder, H. Rapp, H. Röhr, F. Schneider, G. Siller, E. Speth, A. Stäbler, K. H. Steuer, G. Venus, O. Vollmer, and Z. Yü[a]

Max-Planck-Institut für Plasmaphysik, EURATOM-Association, D-8046 Garching, München, Germany

(Received 6 August 1982; revised manuscript received 1 October 1982)

A new operational regime has been observed in neutral-injection–heated ASDEX divertor discharges. This regime is characterized by high β_p values comparable to the aspect ratio A ($\beta_p \leq 0.65A$) and by confinement times close to those of Ohmic discharges. The high-β_p regime develops at an injection power ≥ 1.9 MW, a mean density $\bar{n}_e \geq 3\times 10^{13}$ cm^{-3}, and a $q(a)$ value ≥ 2.6. Beyond these limits or in discharges with material limiter, low β_p values and reduced particle and energy confinement times are obtained compared to the Ohmic heating phase.

PACS numbers: 52.55.Gb, 52.50.Gj

One of the main goals in fusion-oriented tokamak research is the production and investigation of high-temperature, high-β plasmas. The stimulation for these efforts is the requirement of high β values for a fusion reactor device in order to achieve high fusion power output at low investments of magnetic field energy. A significant portion of the research program of all major tokamaks is devoted to the investigation of the confinement properties of auxiliary-heated high-β tokamak plasmas.[1] ASDEX ($R = 165$ cm, $a = 40$ cm, toroidal field $B_T \leq 2.8$ T, plasma current $I_p \leq 0.5$ MA) is a divertor tokamak with neutral-beam injection (NI) presently capable of delivering 3.1 MW to the plasma for 200 msec at a source voltage of 40 kV. The power is delivered by two beam lines both oriented tangentially in the direction of the plasma current. Hydrogen

is injected into deuterium plasmas. The technical details of the ASDEX tokamak and the NI system are described by Keilhacker *et al.*[2] and Stäbler *et al.*[3] With NI an increase is seen in both the ion and electron temperatures T_i and T_e. The increase in total energy content, however, is reduced by a decrease in global energy confinement time τ_E and in particle confinement time τ_p.[4] Two different types of discharges, however, can develop.[5] In one case the reduction in confinement lasts throughout the NI pulse. Because of the low values of β_p achieved during these discharges they are called L-type discharges. In the other case, particle and energy confinement suddenly improve during the NI pulse. As a higher value of β_p is obtained, this discharge type is called H type.

The two types of discharges are compared in Fig. 1 (left column, L type; right column, H type) The only difference in the externally controlled parameters is an increase in injection power P_{NI} into the plasma vessel from 1.6 MW (L type) to 1.9 MW (H type).

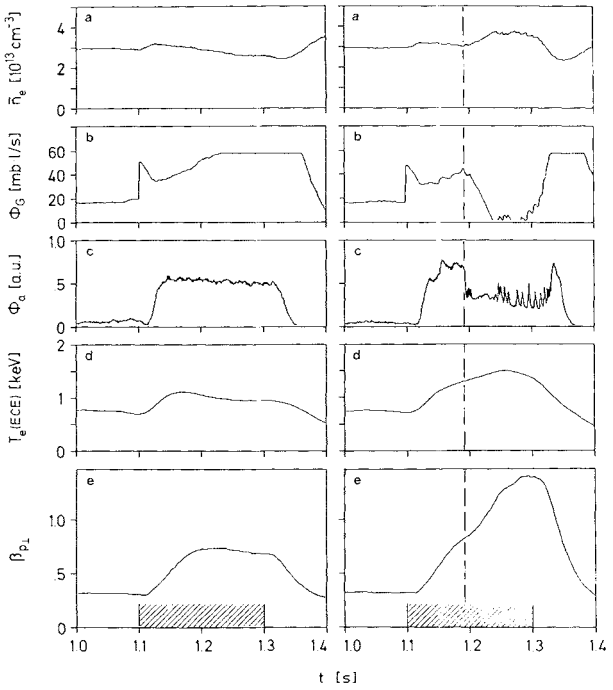

FIG. 1. Time dependence of various plasma parameters of L-type (left column) and H-type (right column) discharges: (a) line averaged density $\bar{n}_e$, (b) external gas flux φ_G, (c) atom flux φ_a (E = 273 eV) reflected from the divertor neutralizer plate, (d) central electron temperature, and (e) beta poloidal. The neutral injection phase is indicated by the hatched time interval. The dashed vertical line indicates the transition from the L to the H regime (see text).

L-type discharge.—The left-hand column of Fig. 1 shows the line-averaged density during the NI pulse (indicated by the hatched time interval) as it develops during a discharge with feedback-controlled density. The density tends to decrease although the external gas flux φ_G, plotted in Fig. 1(b) (left column), increases up to the maximum, and an additional 5 mb • L/s • MW are deposited by the beams. From the total ionization rate (deduced from toroidal H_α-D_α measurements), which rises while the density decreases, it is concluded that τ_p deteriorates during NI. Another indication of the change in particle confinement is the outflux of plasma ions measured at energies $\geq$ 100 eV as a flux φ_a of back-reflected atoms from the divertor neutralizer plates by a charge exchange analyzer. φ_a increases during NI as shown in Fig. 1(c) (left column). The increase in atom flux is caused by a reduction in particle confinement and to a lesser extent by an increase in the plasma-edge ion temperature. Another indication of a degradation in confinement is an increase in hard x-ray radiation caused by an enhanced outflux of runaway electrons produced during the initial phase of the discharge. The deterioration in τ_p is accompanied by a decrease in energy confinement time τ_E during NI into L-type discharges which is a common feature of NI-heated tokamak plasmas.[1] The value of τ_E during an Ohmically heated deuterium discharge with $\bar{n}_e = 3 \times 10^{13}$ cm^{-3} and I_p = 0.3 MA is between 50 and 70 msec. Figure 2 shows τ_E (deduced from temperature and density profiles) and $\tau_E{}^+$ (deduced from the diamagnetically measured $\beta_{p\perp}$) during NI versus $\bar{n}_e$ at I_p = 0.3 MA and for $P_{NI} \geq 2$ MW. τ_E and $\tau_E{}^+$ are determined from the absorbed power (shine-through, orbit, and primary charge-exchange losses are subtracted). There is good agreement between thermally and magnetically measured energy confinement times. In L-type discharges τ_E and $\tau_E{}^+$ decrease to 20–30 msec. A beam power of 2 times the power input during the Ohmic phase is sufficient to affect the confinement deleteriously.[5] In addition to the observed decrease in global energy confinement, the favorable $\tau_E \propto \bar{n}_e$ scaling of Ohmically heated plasmas is not seen with NI into L-type discharges. A numerical transport-code analysis of this discharge type[6] shows that the degradation of confinement with NI results from enhanced electron heat conduction and particle diffusion. The ion heat conduction continues to be approximately neoclassical.

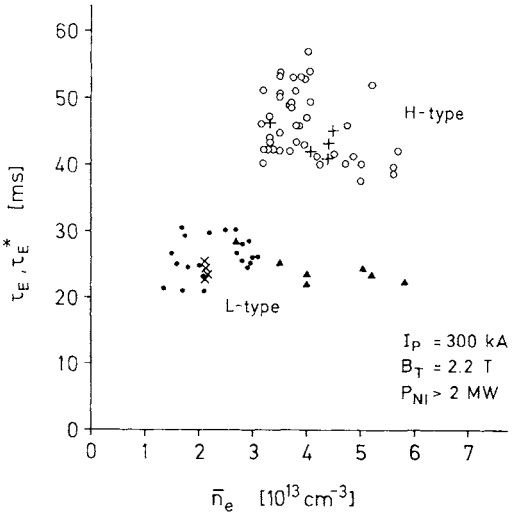

FIG. 2. Global energy confinement time vs average line density for toroidal limiter (triangles) and divertor discharges (other symbols). τ_E (plusses and crosses) is deduced from thermal profiles and τ_E^+ (open circles, solid circles, and triangles) is determined from the diamagnetically measured $\beta_{p\perp}$.

H-type discharge.—Some of the discharge characteristics are plotted in the right-hand column of Fig. 1. The discharge begins as L type. The line density tends to decrease with the beginning of NI [Fig. 1(a) (right column)], and the external gas valve counteracts by increasing its throughput [Fig. 1(b) (right column)]. At $t = 1.18$ sec, however, as indicated by the dotted line, the density suddenly increases without modifications from the external controls. The gas valve closes, but nevertheless the density continues to rise and exceeds the value obtained during the plateau of the Ohmic phase. From bolometric measurements and from the intensity of O VI and Fe XVI radiation (O and Fe are intrinsic impurities), it can be excluded that the density rise is caused by an enhanced impurity influx. All three signals, normalized with respect to the plasma density, decrease at the transition into the H regime.

The increase in density is caused by a sudden improvement in particle confinement. This can be seen from the variation of the back-reflected atom flux from the neutralizer plates [see Fig. 1(c) (right column)]. At the transition into the H regime the back-reflected flux drops suddenly as a consequence of a corresponding reduction in plasma ion outflux. The improvement in particle confinement is also indicated by H_α-D_α and hard x-ray radiation measurements. At the transition both signals decrease approximately to the values obtained during the Ohmic phase.

The improvement in particle confinement in H-type discharges is accompanied by an improvement in global energy confinement. In Fig. 1(d) (both columns) the time variation of the central electron temperature T_e (measured by electron cyclotron emission) of the two discharge types is compared. In the H regime T_e increases to a value 540 eV above T_e of the L-type discharge despite the increase in electron density. The overall improvement in plasma energy content and confinement time is illustrated in Fig. 1(e) (right column), which shows $\beta_{p\perp}$ (with tangential injection, this signal contains only a minor beam contribution). Compared to the L-type discharge [Fig. 1(e) (left column)], $\beta_{p\perp}$ increases by a factor of 2, although the injection power is only 18% larger. The energy confinement time of the H type is 40–50 msec at $I_p = 0.3$ MA (see Fig. 2) and increases linearly with plasma current. At $I_p = 0.38$ MA, τ_E^+ is between 50 and 70 msec. In the H regime the values of τ_E and τ_p attained during Ohmic discharges are approximately recovered. This result holds up to the highest injection power of 3.1 MW.

$\Delta[\beta_p + \frac{1}{2} l_i]$, the increase in the measured signal $\beta_p + \frac{1}{2} l_i$ due to NI, is plotted in Fig. 3 versus the power, P_{NI}, injected into the vessel, both for L-type (solid symbols) and H-type (open symbols) discharges. The plasma current is 0.3 MA. There are experimental indications that the internal inductance l_i does not change much during NI (a slight reduction cannot be excluded). $\beta_p + \frac{1}{2} l_i$ is deduced from the plasma equilibrium by use of either the applied vertical field or measurements of the poloidal magnetic flux and field near the plasma boundary. The values for $\beta_p + \frac{1}{2} l_i$ obtained from the two measurements agree within 10%. $\Delta[\beta_p + \frac{1}{2} l_i]$ of L-type discharges increases linearly with injection power. No saturation or β_p limit is observed. Above 1.9 MW the $\Delta[\beta_p + \frac{1}{2} l_i]$ curve of the H-type discharge branches off. Although there is a larger scatter in the data points, there seems to be no saturation in $\beta_p + \frac{1}{2} l_i$ of the H-type discharges either.

So far, the highest β_p value measured at a plasma current of 0.2 MA is 2.65 (~0.3 is the beam contribution). This value corresponds to 65% of the aspect ratio A ($A = 4.1$). The highest observed value of the volume-averaged toroidal beta is $\langle\beta\rangle = 1.06\%$ at a $q(a)$ value of 2.8.

In the following, the experimental conditions and the range of plasma parameters which allow

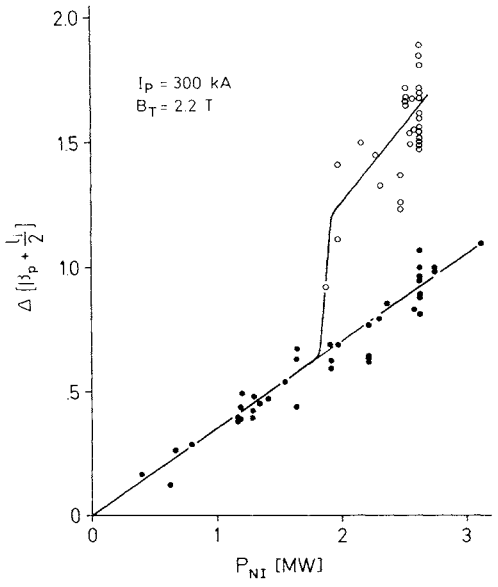

FIG. 3. Increase in $\beta_p + \frac{1}{2}l_i$ with respect to the Ohmic phase vs the power P_{NI} injected into the vessel in the L regime (solid symbols) and the H regime (open symbols).

the development of the H regime are described. Figure 3 reveals that there are only L-type discharges at an injection-power level $P_{NI} < 1.9$ MW. Above this power level both discharge types are encountered depending on $\bar{n}_e$ and B_T. Figure 2 reveals that the H phase develops above $\bar{n}_e = 3 \times 10^{13}$ cm^{-3}. In the density range $(3-3.5) \times 10^{13}$ cm^{-3} there is a transition region where either an L-type or an H-type discharge can develop without external modifications. At high density at $I_p = 0.38$ MA the achieved β_p values of the H regime decrease again, possibly because of the limitation in available injection power or deposition depth, and L-type discharges can develop.

H-type discharges have been obtained at plasma currents between 0.2 and 0.4 MA. A decrease of the toroidal magnetic field resulting in a lower $q(a)$ value can lead to a transition into the L regime. H-type discharges have not been observed for cylindrical values of $q(a) < 2.6$ [$q(a) \equiv 2\pi a^2 B_T / \mu_0 R I_p$].

The H regime is characteristic of divertor discharges in ASDEX. It has never been obtained in ASDEX limiter discharges. $\tau_E{}^+$ values of toroidal limiter discharges are plotted in Fig. 2. Given a limited number of shots with material limiters, the accuracy of this statement is mainly based on the observation that the H regime disappears at the transition from divertor to limiter discharges. In sequential discharges, both divertor and limiter behavior could be compared. The H-type characteristics of the divertor discharges with NI always disappeared in the limiter discharge which followed.

The observation that the H type does not develop in limiter discharges may be the result of the higher impurity content of these discharges. The role of impurities in the formation of the H-type discharges was empirically studied by puffing small amounts of low-Z (CH_4) and high-Z (Kr) gases into the discharges. The addition of impurities deteriorates an H-type discharge or prevents its formation. As a result of radiation, particularly from the plasma edge, added impurities or those released from the limiter may suppress the formation of very broad, nearly circular, temperature and density profiles, which are characteristic of H-type discharges.

The achieved β_p values and confinement times in H-type discharges are affected by short bursts, detected by Mirnov coils and soft-x-ray diodes, which lead to periodic density and temperature reductions in the outer plasma zones. The gross plasma parameters remain unaffected in the plasma center. In particular, these discharges show no sawtooth activity. Bursts are also observed in the back-reflected flux from the neutralizer plate [see Fig. 1(c) (right column)] as thermal particles are expelled from the main plasma into the boundary layer. There are indications that these bursts can cause the transition back into the low confinement regime which, however, is not maintained as long as enough beam power is available. Figure 1(c) (right column) shows that the H regime is sustained until 20 msec after termination of the beams. Then the discharge changes to an L-type discharge as indicated by a sudden increase in flux, φ_a. The transition back into the L regime occurs simultaneously with, or is triggered by, a burst. Possibly as a result of the decaying beam, the plasma does not return to the H regime, but transforms into the Ohmic heating phase as an L-type discharge.

In summary, a new operational regime in neutral-injection-heated discharges of ASDEX is discovered with high β_p values. It is documented that NI-heated discharges can have confinement properties close to those of Ohmic discharges. The new regime extends over a wide range of q values, plasma currents, and densities, but—so far—has only been obtained in divertor discharges.

Thanks are due to the operational teams of

ASDEX and the NI group and to F. Dylla for critically reading the manuscript.

[a]On leave from Academia Sinica, Peking, People's Republic of China.

[1]Proceedings of the International Atomic Energy Agency Workshop on Finite-Beta Limits and Transport Phenomena in Thermonuclear Plasmas, Varenna, 1982 (to be published).

[2]M. Keilhacker *et al.*, in *Proceedings of the Eighth International Conference on Plasma Physics and Controlled Nuclear Fusion Research, Brussels, 1980* (International Atomic Energy Agency, Vienna, 1981), Vol. II, p. 351.

[3]A. Stäbler *et al.*, in *Proceedings of the Ninth International Symposium on Engineering Problems of Fusion Research, Chicago, 1981*, edited by C. K. Choi (IEEE, New York, 1981), Vol. I, p. 767.

[4]F. Wagner *et al.*, Max-Planck-Institut für Plasmaphysik Report No. III/78, 1982 (unpublished).

[5]F. Wagner *et al.*, in Proceedings of the Ninth International Conference on Plasma Physics and Controlled Nuclear Fusion Research, Baltimore, 1982 (to be published), Paper No. IAEA-CN-41/A-3.

[6]G. Becker *et al.*, to be published.

CHARACTERISTICS OF THE DIVERTOR PLASMA IN NEUTRAL-BEAM-HEATED ASDEX DISCHARGES

Y. SHIMOMURA*, M. KEILHACKER, K. LACKNER,
H. MURMANN
Max-Planck-Institut für Plasmaphysik,
EURATOM-Association,
Garching,
Federal Republic of Germany

ABSTRACT. Scrape-off plasma parameters have been measured in ASDEX both in the divertor chamber and in the mid-plane, for neutral-injection powers of up to 2.5 MW. Measurements demonstrate the existence of strong inhomogeneities parallel to the field lines and show the dependence of divertor density and temperature on bulk plasma density, heating power and mode of divertor operation (gettered/ungettered, different divertor slit widths, additional gas puffing in the divertor). Three recycling regimes, characterized by different dependences of the divertor density on the bulk plasma density, are identified in agreement with a numerical fluid model of the scrape-off plasma. In the particularly attractive high-recycling regime, divertor temperatures could be kept around 7 eV for the whole range of heating powers tested.

1. INTRODUCTION

ASDEX [1] is a large tokamak ($R = 1.65$ m, $a = 0.4$ m, $B_t \leqslant 2.8$ T, $I_p < 500$ kA) combining a double-null poloidal divertor with a near-circular cross-section of the interior flux surfaces. In a divertor tokamak, the charged particles lost from the bulk plasma flow in a narrow scrape-off layer along field lines into a separate chamber. The major plasma-wall interaction is thus restricted to the divertor region.

Successful impurity control by this means has been demonstrated for Ohmically heated discharges in DIVA [2], PDX [3] and ASDEX [1] and for neutral-injection-heated discharges with heating powers of up to 3 MW in ASDEX [4]. Neutral-beam injection into diverted ASDEX discharges has also revealed the existence of a new operational regime of high β_p and good confinement [5, 6] so far not found in limiter experiments. These results underline the attractiveness of the poloidal-divertor concept.

To apply a poloidal divertor to a reactor-grade device, two major problems have to be overcome: the divertor configuration has to be modified to become compatible with the large plasma-coil distances imposed by the shielding and breeding structures [7], and the temperature of the diverted plasma near the neutralizer plates has to be controlled [8]. The latter problem is studied in this paper.

Cooling of the diverted plasma is essential to avoid serious erosion of the neutralizer plates and may also – if associated with significant radiation or charge-exchange power losses – reduce the high heat flux densities. To effectively suppress both hydrogen- and impurity-ion sputtering, the electron temperature near the neutralizer plate T_{ed} has to be very low, typically 10 eV or less. The global energy and particle balance, together with the restrictions on energy transmission through the electrostatic sheath in front of the target plates, yields the following simple expression for T_{ed} [2]:

$$T_{ed} = \frac{\bar{\tau}_p}{\tau_E} \frac{3}{\gamma} \frac{P_{in} - P_r}{P_{in}} \bar{T} \qquad (1)$$

Here P_{in}, P_r, $\bar{T}$ and τ_E are, respectively, the heating power, the radiative loss power including charge-exchange losses, the mean temperature in the plasma, and the energy confinement time. The heat transmission rate γ is the ratio of energy to ion flux onto the target plates; the global particle confinement time $\bar{\tau}_p$ is defined by

$$\bar{\tau}_p = \bar{N}_e / F_w \qquad (2)$$

* Permanent address: Japan Atomic Energy Research Institute, 311–02 Nakamaki, Naka-gun, Ibaraki-ken, Japan.

in terms of the total number of electrons $\bar{N}_e$ and the total ion flux F_w onto material surfaces (target plates and vessel walls). In a divertor device, for a particle exhaust efficiency of 100%, F_w is the ion flux onto the neutralizer plates.

In the small tokamak DIVA [2], $\bar{\tau}_p$ was almost equal to the particle confinement time of the bulk plasma, τ_p, defined by the ion loss flux through the separatrix, F_s, and approximately equal to τ_E, and P_r originated only from the main plasma. Together with $\gamma \leqslant 10$ (as obtained from sheath models and experiments) and $P_r < 0.5\ P_{in}$, this yielded $T_{ed} > 0.15\ \bar{T}$, which, if simply applied also to large devices, would cause very high values of T_{ed} and serious erosion problems [8].

In large (or very high-density) devices, we have the possibility of strong recycling localized in the target plate vicinity or the divertor chamber resulting in substantial variations of the plasma parameters along the magnetic field lines in the scrape-off region [9, 10]. In this case, $\bar{\tau}_p$ will be strongly decreased with respect to τ_p, and even significant contributions to P_r may arise in the divertor chamber: both effects contributing to a strong reduction in T_{ed}.

These possibilities were already suggested by previous experimental results of relatively high-density, Ohmically heated discharges in ASDEX [1, 11, 12] and Doublet III [13–15], which showed significant enhancement of neutral-gas pressure and scrape-off layer plasma density in the divertor and also substantial radiation losses (more than 50% of the input power) emanating from this region. In these investigations, no localized measurements of plasma parameters in the scrape-off (in particular of T_{ed}) were made, and active control of the divertor plasma was not studied.

For the present paper, these studies were extended to examine experimentally the predicted inhomogeneities along field lines, to investigate the effect of active control measures on scrape-off parameters, and to pursue these investigations into the regime of strong additional heating. For this purpose, characteristics of the scrape-off and divertor plasmas were investigated in recent ASDEX experiments with neutral-beam heating ($0 < P_{NI} < 2.5$ MW) [16]. The following section describes typical plasma parameters in the scrape-off layer, proving also the existence of large temperature and density gradients along magnetic field lines by comparing parameters at the torus mid-plane to those near the divertor plate. In Section 3, successful control of the divertor plasma at low temperatures with $0.0 < P_{NI} < 2.5$ MW is described, and the lower limit of electron temperature and the upper limit of plasma density in the divertor are studied. Section 4 gives a discussion of the divertor plasma characteristics including comparison with model estimates, and Section 5 summarizes the most significant results.

2. TYPICAL PLASMA PARAMETERS IN THE SCRAPE-OFF LAYER

Electron temperature and density profiles of the divertor plasma in ASDEX are measured by scanning Langmuir probes near the divertor plate. The location of these probes and of microwave horns are shown in Fig.1 in a schematic figure of the divertor region including the flux surfaces resulting from MHD equilibrium calculations. Scrape-off plasma characteristics in the main chamber are measured by a Thomson scattering system giving electron temperature and density profiles in the torus mid-plane.

The measurements were carried out for a wide range of discharge conditions, both with Ohmic and with neutral-beam heating. The neutral-injection system consisted of two beam lines, both oriented tangentially

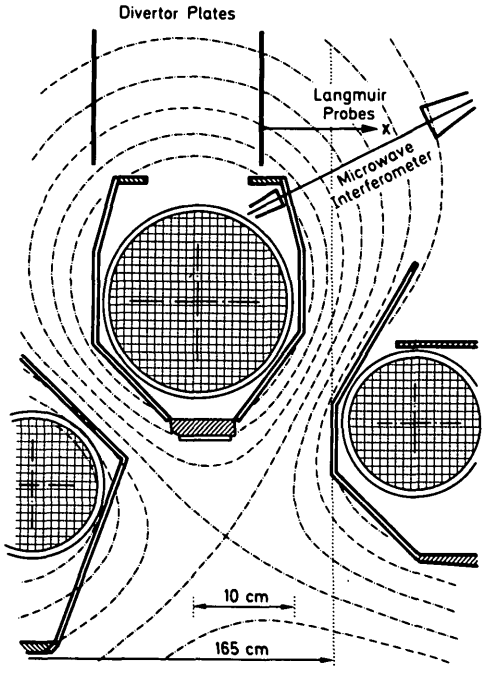

FIG.1. Schematic drawing of divertor region indicating location of Langmuir probes and microwave horns.

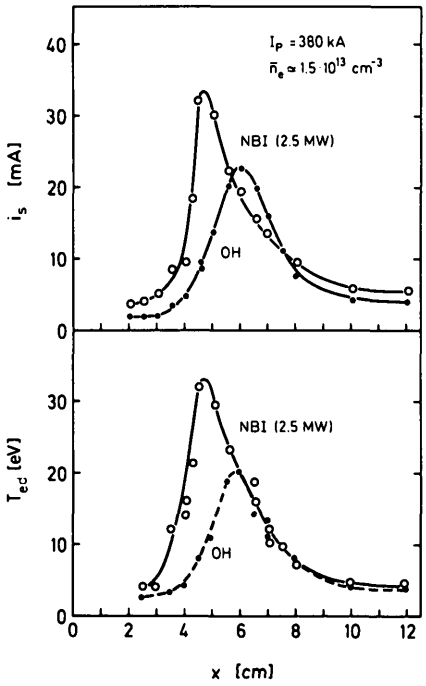

FIG.2. Typical profiles of ion saturation current i_s and electron temperature T_{ed} in divertor for rather low-density discharges ($\bar{n}_e \approx 1.5 \times 10^{13}$ cm^{-3}) with Ohmic heating (OH) and 2.5-MW neutral-beam injection (NBI), respectively. Distance x is counted from collector plate.

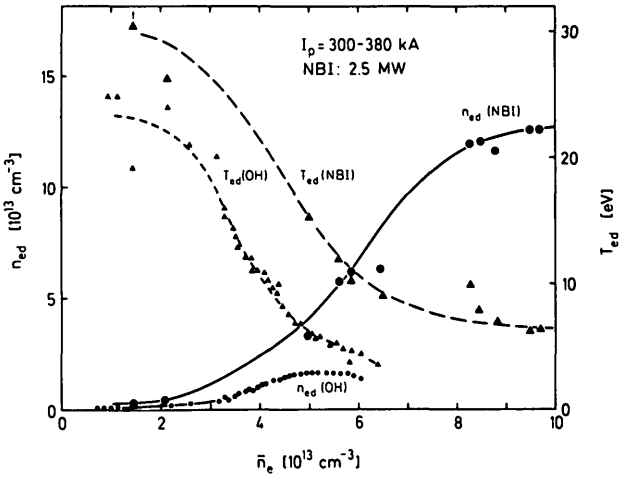

FIG.3. Peak values of electron density n_{ed} and temperature T_{ed} near divertor plate as functions of bulk plasma density $\bar{n}_e$ for discharges with Ohmic heating (OH) and 2.5-MW neutral-beam injection (NBI), respectively.

in the direction of the plasma current, and delivering a power of $P_{NI} \leqslant 2.5$ MW (H^0 beam, 40 kV, 0.2 s) into the torus. If not stated differently, the filling gas was D_2, the toroidal field was set at 2.17 T, and a double-null divertor configuration with a minimum divertor slit width of 6.5 cm and no divertor pumping (D operation) was employed.

In Fig.2, typical profiles of ion saturation current i_s and electron temperature T_{ed} in the divertor are shown for rather low-density discharges with 2.5 MW neutral injection and Ohmic heating, respectively. Both temperature and ion saturation current are larger with neutral-beam injection. The peaks of the profiles are located near the calculated separatrix surfaces, with their shift in position during neutral-beam injection being mainly caused by the change in the magnetic configuration due to the increase in β_p. The relative variation of electron density n_{ed} is calculated from i_s and T_{ed}, and its absolute value is calibrated by using the cut-off density of 3.3-mm micro-waves.

The peak density n_{ed} and the peak temperature T_{ed} of these profiles with and without neutral-beam injection are shown in Fig.3 for a set of experiments in which only the (line-average) bulk plasma density $\bar{n}_e$ was scanned, while the other discharge parameters were kept constant. The following three regions are observed both in discharges with and without neutral-beam injection:

At lower plasma densities ($\bar{n}_e < 3 \times 10^{13}$ cm^{-3} for $P_{NI} = 0$ and $\bar{n}_e < 5 \times 10^{13}$ cm^{-3} for $P_{NI} = 2.5$ MW) the density n_{ed} increases slowly with increasing bulk plasma density $\bar{n}_e$.

In an intermediate density regime (3.5×10^{13} cm$^{-3} < \bar{n}_e < 4.5 \times 10^{13}$ cm^{-3} with $P_{NI} = 0$ and 5×10^{13} cm$^{-3} < \bar{n}_e < 8 \times 10^{13}$ cm^{-3} with $P_{NI} = 2.5$ MW), n_{ed} increases steeply with increasing bulk plasma density $\bar{n}_e$.

In the highest density range ($\bar{n}_e > 5 \times 10^{13}$ cm^{-3} for $P_{NI} = 0$ and $\bar{n}_e > 8 \times 10^{13}$ cm^{-3} for $P_{NI} = 2.5$ MW), n_{ed} saturates or even decreases.

The absolute values $\bar{n}_e$ for the limits of each region change with changing discharge conditions – especially the heating and recycling conditions – as discussed later. The characteristics of the three regions, however, do not change, and agree qualitatively with the results of recent numerical calculations [9].

In purely Ohmically heated discharges, the first region was previously observed in DIVA [2] and the first and second regions in ASDEX [11] and Doublet-III [14, 15]. The third regime, where n_{ed} saturates or decreases with increasing $\bar{n}_e$, shows the

limit on divertor density. In the experimental sequence shown in Fig.3 the maximum value of n_{ed} is 1.7×10^{13} cm^{-3} for $P_{NI} = 0$ reached at $\bar{n}_e = 5 \times 10^{13}$ cm^{-3} and 1.3×10^{14} cm^{-3} for $P_{NI} = 2.5$ MW at $\bar{n}_e = 9 \times 10^{13}$ cm^{-3}. Thus, particularly with strong additional heating, very high divertor densities in excess of the bulk plasma density can be obtained. The divertor electron temperatures T_{ed}, also shown in Fig.3, are in the range 5–30 eV and are found to decrease with increasing $\bar{n}_e$ and n_{ed}.

To understand the characteristics of the scrape-off layer plasma along the magnetic field lines, the electron density, n_{eb}, and temperature, T_{eb}, profiles in the torus mid-plane as obtained by the Thomson scattering system are compared with the corresponding profiles in the divertor. As the radial temperature fall-off length at the mid-plane λ_{Te} is very short ($\lambda_{Te} \lesssim 1$ cm), the identification of identical flux surfaces in the mid-plane and the divertor chamber with sufficient accuracy to discriminate between variations along and across the scrape-off layer cannot be made purely on the basis of magnetic measurements and computed flux patterns. In this paper, we assume $n_e T_e$ = const along a magnetic surface (justified for low-Mach-number flow and either $T_i \approx T_e$ or $T_i \ll T_e$) and adjust the two electron pressure profiles by moving the assumed position of the separatrix magnetic surface at the torus mid-plane.

Results are shown in Figs 4 and 5 for four typical cases:

(1) a high-current, high-density discharge with $P_{NI} = 2.5$ MW;
(2) a high-current discharge with $P_{NI} = 0$;
(3) a low-current discharge with $P_{NI} = 2.5$ MW; and
(4) a low-current discharge with $P_{NI} = 0$.

Temperature and density inhomogeneities along the magnetic field lines are observed in all cases, particularly in the high-density discharge with $P_{NI} = 2.5$ MW, where the electron temperature in the divertor chamber is reduced and the density increased by a factor of ten compared to the corresponding mid-plane values.

The observed strong inhomogeneities along magnetic field lines are expected from the recent numerical study of Ref.[9] and are considered to be caused mainly by the finite electron conductivity parallel to the field. The inhomogeneity is predicted to be stronger with neutral injection, because of the higher heat flux. Electron temperatures on the separatrix at the mid-plane, calculated on the basis of a simplified model taking into account only electron heat conduction

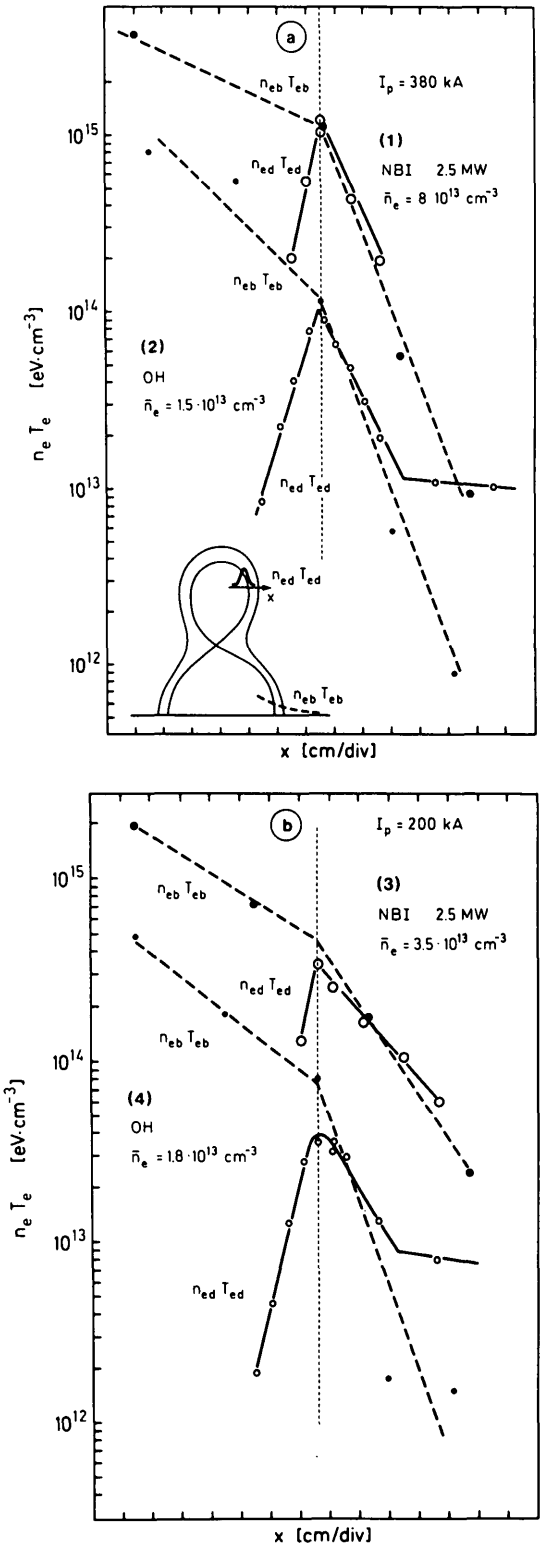

FIG.4. Radial profiles of electron pressure at torus mid-plane ($n_{eb}T_{eb}$) and near divertor plate ($n_{ed}T_{ed}$) for four typical cases: (a, 1) high-current, high-density discharge with $P_{NI} = 2.5$ MW; (a, 2) high-current discharge with $P_{NI} = 0$; (b, 3) low-current discharge with $P_{NI} = 2.5$ MW; (b, 4) low-current discharge with $P_{NI} = 0$. Abscissa gives horizontal distance in the divertor. For torus mid-plane, distance is around 0.5 cm/div.

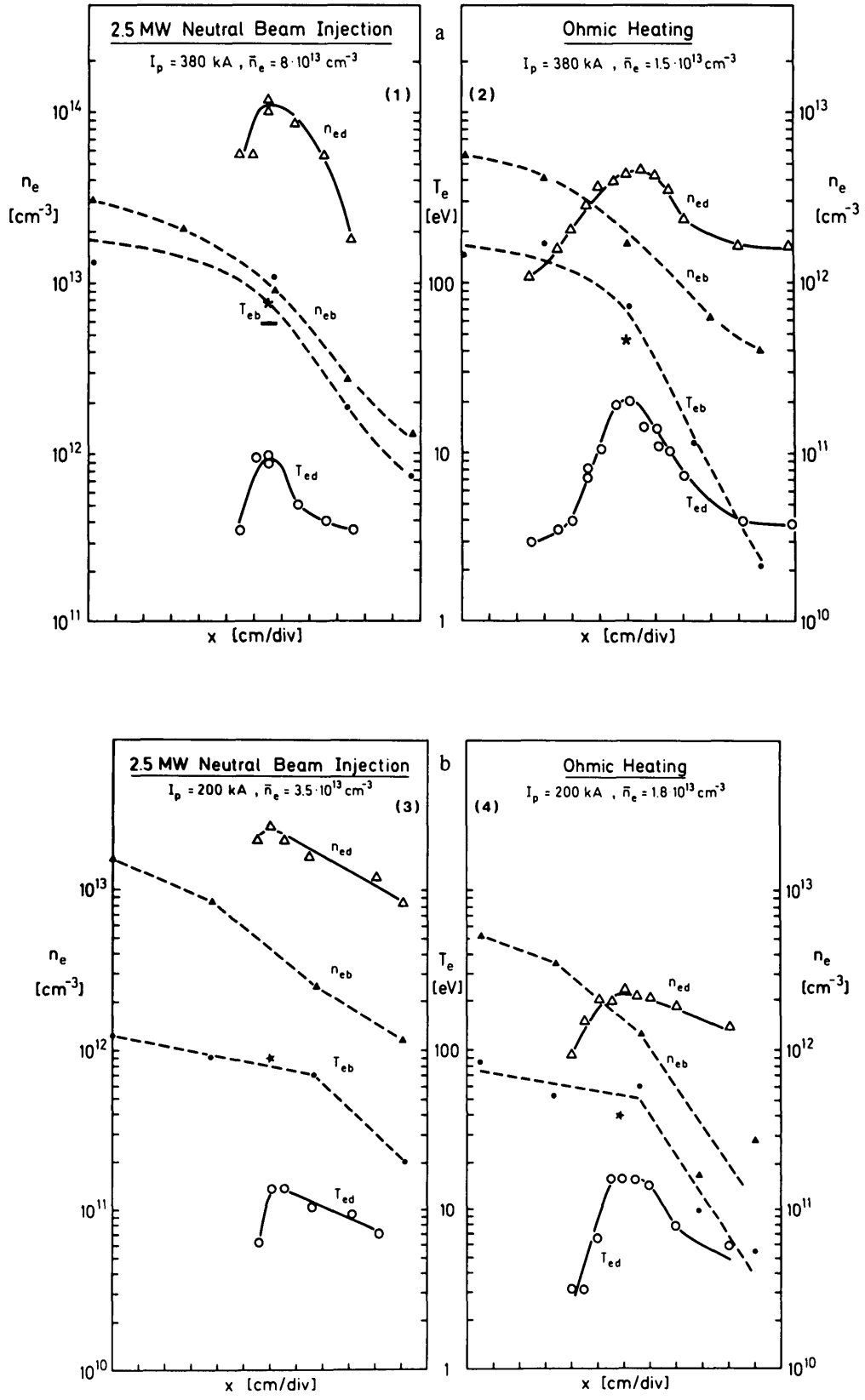

FIG.5. Radial profiles of electron density and temperature at torus mid-plane (n_{eb}, T_{eb}) and near divertor plate (n_{ed}, T_{ed}) for the four cases of Fig.4: (a) cases 1 and 2; (b) cases 3 and 4.

parallel and perpendicular to flux surfaces [17], are also given in Fig.5 (points indicated by *), showing good agreement with the observed values.

3. CONTROL OF DIVERTOR PLASMA

The strong inhomogeneities along the plasma flow direction in the scrape-off layer offer the possibility of controlling the divertor plasma without changing the bulk plasma parameters. The most effective method for this consists in controlling the particle recycling conditions in the divertor chamber. The following modes of divertor operation have been studied in ASDEX:

pumping (Ti gettering) in the divertor (DP operation),
no pumping in the divertor (D operation),
gas puffing in the divertor (DG operation),
narrowing the divertor throat (DN operation).

In a purely Ohmically heated DP discharge (Fig.8), T_{ed} becomes sufficiently low (5 eV) at a certain, rather high bulk plasma density ($\bar{n}_e = 7 \times 10^{13}\,cm^{-3}$). Addition of 2.5 MW neutral-injection power at the same value of $\bar{n}_e$ leads to an increase of T_{ed} to 17 eV (see points indicated by ○ in Fig.6). Addition of more heating power would further increase the divertor electron temperature, leading finally to intolerable values. T_{ed} can be reduced by increasing the particle source in the divertor through enhancement of the neutral density. This can be realized by stopping titanium gettering (D mode of operation), leading to a reduction in T_{ed} to 10 eV or less (● in Fig.6). If a still lower divertor temperature is required at the same bulk plasma density and heating power, an additional particle source can be created by puffing gas into the divertor chamber (DG operation, ⊙ in Fig.6). The effect of divertor recycling conditions on T_{ed} and n_{ed} is qualitatively similar in both discharge regimes (H- and L-type) observed in injection-heated ASDEX experiments [5, 6].

Applying these methods we can maintain the electron temperature T_{ed} at a low value even if the heating power is increased and the bulk plasma density kept fixed. This is illustrated in Fig.7 for $\bar{n}_e \approx 7 \times 10^{13}\,cm^{-3}$ and a heating power varied between 0.3–2.5 MW. T_{ed} stays at around 7 eV while n_{ed} increases from $1 \times 10^{13}\,cm^{-3}$ to $1.3 \times 10^{14}\,cm^{-3}$. With $P_{NI} = 2.5$ MW, the electron density n_{ed} is almost twice higher than the line-average bulk plasma density $\bar{n}_e$. It is the increased charged-particle flux onto the divertor plates, associated with this high density, that cools the plasma to a sufficiently low value of T_{ed}.

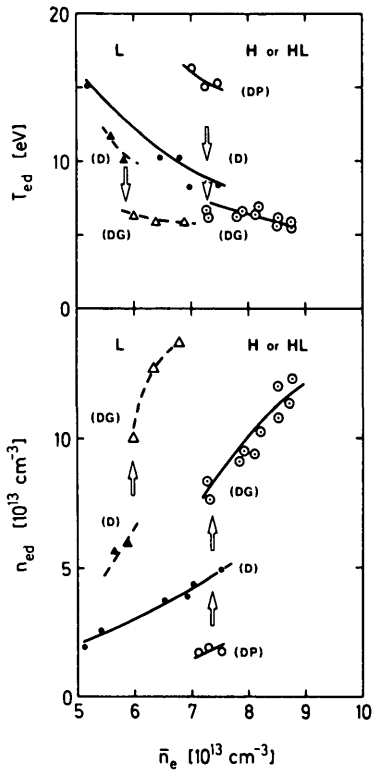

FIG.6. Variation of electron temperature T_{ed} and density n_{ed} near divertor plate for various recycling conditions in divertor: pumping (DP), no pumping (D) or gas puffing (DG) in divertor chamber. L and H denote L- and H-type discharges. Discharges at $I_p = 300 - 380$ kA with 2.5-MW neutral-beam injection.

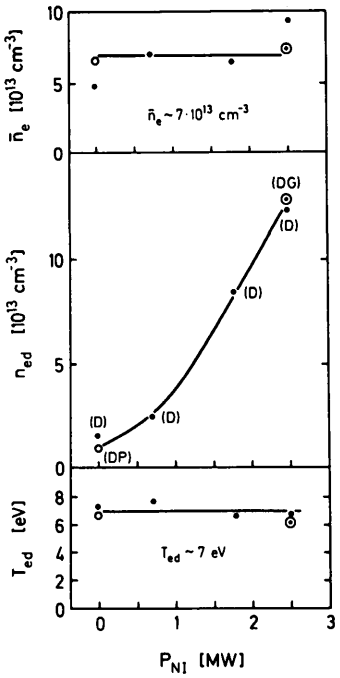

FIG.7. Control of electron temperature near divertor plate T_{ed} at low value ($T_{ed} \approx 7$ eV) even for high neutral-injection powers ($P_{NI} \leqslant 2.5$ MW) by changing recycling conditions in divertor (for fixed bulk plasma density, $\bar{n}_e \approx 7 \times 10^{13}\,cm^{-3}$). $I_p = 380$ kA.

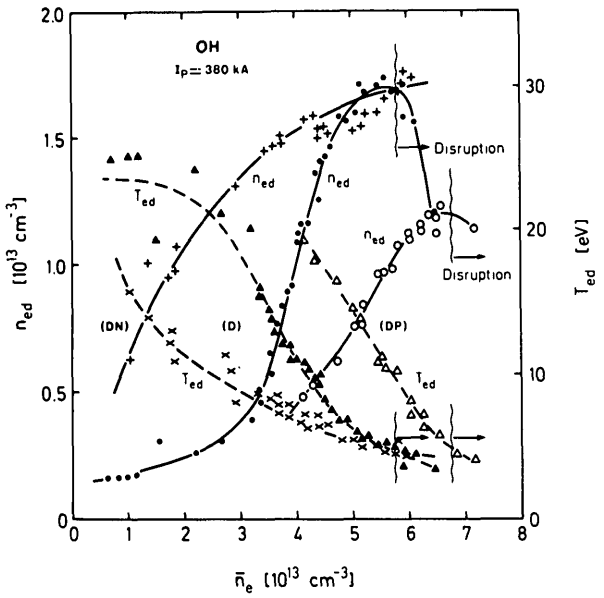

FIG.8. Electron temperature T_{ed} and density n_{ed} near divertor plate as functions of bulk plasma density $\bar{n}_e$ for various recycling conditions in divertor chamber: pumping (DP), no pumping (D) and narrowing divertor slit width from 6.5 to 3.7 cm (DN). Ohmically heated discharges with $I_p \approx 380$ kA. For DN discharges, filling gas is hydrogen.

Figure 7 also shows that, for a fixed mode of divertor operation, n_{ed} and T_{ed} can, of course, also be controlled by adjusting the bulk plasma density.

It is important to establish the minimum value of T_{ed} and the maximum of n_{ed} which can be obtained, and in particular, also to assess the feasibility of the gaseous-neutralizer concept [18]. For this investigation, n_{ed} was varied by monotonically increasing the bulk plasma density $\bar{n}_e$. This experiment was performed for a variety of discharge conditions such as gas influx rate, recycling condition, and heating power. Some results for Ohmically heated plasmas are summarized in Fig.8. The observed minimum temperature for a stable discharge is around 5 eV. At this value of T_{ed}, n_{ed} saturates, and in some cases starts even to decrease with increasing $\bar{n}_e$. Beyond this point, the discharge tends to go into a disruptive phase. For electron temperatures of about 5 eV, the probability for further ionization of the neutral gas in the divertor becomes very small.

The observed minimum divertor temperatures in stable discharges are not sufficiently low for a gaseous-neutralizer scheme as proposed in Ref.[18], which would require values of $T_{ed} \approx 1$ eV. Only in this range would recombination processes become dominant, and divertor plates – and the associated thermal-load problems – could be eliminated. To approach this regime, a further reduction in the gas backflow from the divertor would be needed. This could be accomplished, e.g. by either elongating the divertor plasma layer or by reducing the divertor throat width. In ASDEX, this was tested by reducing the divertor throat width from 6.5 to 3.7 cm, resulting in the expected enhancement of n_{ed} (Fig.8) at low and intermediate plasma densities (although the quantitative significance of this comparison is clouded by the fact that the data for the narrow divertor throat case were obtained in hydrogen). In contrast, no significant changes were observed in the minimum T_{ed} and maximum n_{ed} values achieved, showing that a much deeper and narrower divertor would be required for the gaseous-neutralizer concept. Such a divertor would however not be compatible with a reactor due to the resulting complexity and the stringent control requirements on the magnetic configuration.

These results show that the minimum electron temperature in the divertor for stable discharges is clamped to the regime where the ionization rate drops drastically, and remains fairly constant when varying the heating power. The maximum divertor plasma density is associated with the attainment of the minimum T_{ed} and is therefore linked to the energy flow into the scrape-off. As – at least in the relatively high density regime discussed at this point – the major part of the heating power flows into the divertor, a linear dependence of the maximum divertor density on the input power is expected and also found from the experimental results (Fig.9).

The mean plasma density in the divertor chamber has already previously been found to be a strong function of the density in the main chamber [11, 14]; the present results show it to be also strongly affected by the recycling conditions (Figs 6 and 8). Therefore, no universal relation between n_{ed} and $\bar{n}_e$ can be observed. Figure 10 shows that a strong relation, independent of the discharge mode, does exist between n_{ed} and T_{ed} at constant heating power, although it does not follow the simple $n_{ed} T_{ed}^{3/2} \propto (P_{OH} + P_{NI})$ law expected from the plasma sheath conditions [19]. (Possible reasons for this deviation will be discussed in the next section.)

This result and Fig.9 suggest that the most essential relation between bulk plasma and divertor plasma is through the power flow maintaining the latter. Variations in other bulk plasma characteristics can, within limits, be compensated for by measures controlling the divertor recycling (see Figs 6 to 8).

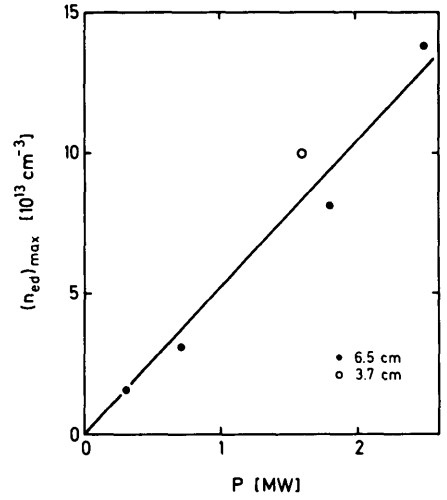

FIG.9. Observed maximum electron density near the divertor plate $(n_{ed})_{max}$ as function of the heating power $P = P_{OH} + P_{NI}$ for a divertor slit width of 6.5 cm (●) and 3.7 cm (○), respectively.

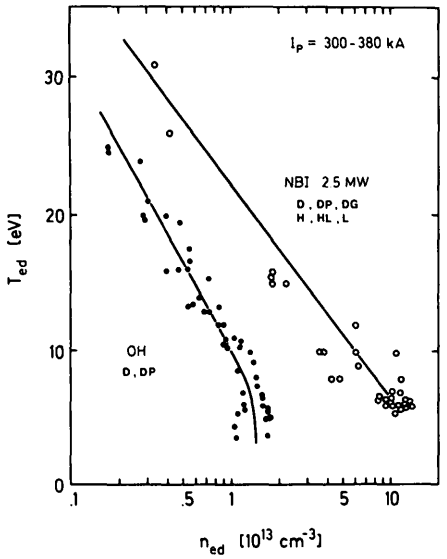

FIG.10. Electron temperature in divertor T_{ed} versus density n_{ed} at constant heating power (OH: 0.3–0.4 MW, NBI: 2.5 MW) for various discharge modes: pumping (DP), no pumping (D) or gas puffing (DG) in divertor; L- and H-type discharges.

There is a strong observed correlation between the saturation of divertor density (concomitant with reaching $T_{ed} \cong 5$ eV) with increasing bulk plasma density and the occurrence of disruptive instabilities. This could be indication of a connection between the universally observed bulk plasma density limit and the energy flux limitation on the recycling in the divertor chamber or the limiter vicinity. Observations related to this point have also been reported from Doublet III [20] and DITE [21].

4. DISCUSSION

The characteristics of the divertor plasma have been studied in ASDEX over a wide range of discharge conditions, and it is important to compare these measurements with the predictions of theoretical analysis. Global characteristics of the scrape-off layer can be compared with the results of the two-fluid model described in Ref.[9] and plasma characteristics near the neutralizer plate with the relations yielded by electrostatic sheath models (see Section 1 and Refs [19, 22]).

Good agreement between experimental results and the two-fluid scrape-off model is observed in the following points:

The variation of divertor density with bulk plasma density exhibits three regimes: i.e. small variation at low densities in the main chamber, a steep dependence at medium densities and a saturation at high density.
The saturation density in the divertor is proportional to the heating power.
A strong inhomogeneity exists in the plasma parameters along the flow direction for high energy fluxes.

This agreement in principal features supports the physics assumptions employed in Ref.[9], although a quantitative prediction of the boundaries of the different recycling regimes will require inclusion of an advanced model for the neutral-particle dynamics. Calculations also predict a strong relation between T_{ed} and n_{ed} as is shown in Fig.10, but disagree quantitatively with the measured values, particularly for low divertor densities and high divertor temperatures. The latter disagreement is linked to the difficulty encountered in this regime to account for the total power input using measured divertor parameters and the conventional sheath relations.

According to the latter, the total particle loss F_w and the total heat loss P_w onto the neutralizer plates are given by [19]:

$$F_w = \frac{1}{e}\int \vec{i} \cdot d\vec{f} \qquad (3)$$

$$P_w = \int \gamma \vec{i}\, kT_e \cdot d\vec{f} \qquad (4)$$

where $\vec{i}$ is the ion current density and $d\vec{f}$ the surface element of the neutralizer plate.

Theoretical values for the heat transmission coefficient γ have originally been derived for the field-free case or the case of $\vec{B}$ perpendicular to the target plates; recent numerical calculations for the realistic case of oblique field line incidence [22] have – although showing significant changes in the spatial structure of the sheath region – confirmed these predictions for γ. The ion saturation current density i_s and T_{ed} are measured near the divertor plates, where $|\vec{i}| \cong i_s$ and $T_e \approx T_{ed}$ can be expected. In this case, and on the assumption of $T_i = T_e$, the total particle and the total heat loss to the divertor plates can be derived directly from the measurements.

The total ion loss F_w obtained like that can be used to compute the global particle confinement time $\bar{\tau}_p$ of Eqs (1) and (2), with the results given in Fig.11. The figure shows an increase in $\bar{\tau}_p$ with increasing bulk plasma density for $\bar{n}_e$ up to $2 \times 10^{13}\,cm^{-3}$ and a decrease beyond this point. At low densities, few ionizations should occur in the divertor chamber, and the global particle confinement time $\bar{\tau}_p$ is expected to be approximately equal to the particle confinement time of the bulk plasma:

$$\tau_p = N_e/F_s \qquad (5)$$

defined in terms of the total electron number in the bulk plasma and the net ion flow out of it. In high-density discharges, ionization in the divertor becomes dominant, and $\bar{\tau}_p$ drops to very small values.

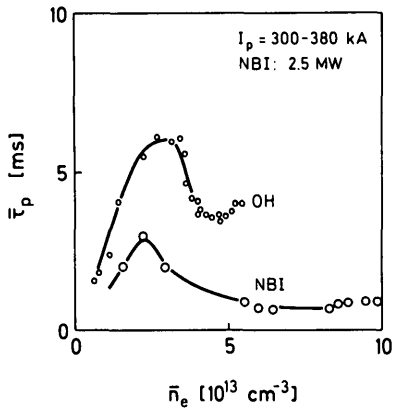

FIG.11. Global particle confinement time $\bar{\tau}_p$ as function of bulk plasma density $\bar{n}_e$ for Ohmically (OH) and neutral-beam-(NBI)-heated discharges.

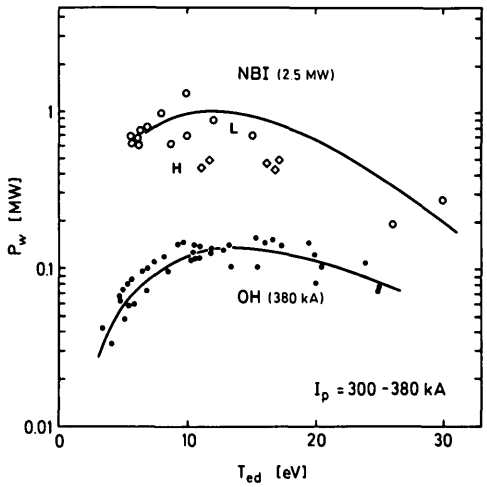

FIG.12. Total power loss onto divertor plates $P_w = \int \gamma i_s T_{ed} df$ as calculated from ion saturation current i_s and electron temperature T_{ed} for discharges with Ohmic heating (OH) and 2.5-MW neutral-beam injection (NBI, L-type and H-type), respectively. Heat transmission rate is assumed to be $\gamma = 7$.

In the latter regime, T_{ed} and the values of $\bar{\tau}_p$ derived from Eqs(1) and (2) are consistent with the power input and the radiative losses. In purely Ohmically heated, ungettered discharges (D-mode) with $\bar{n}_e = 5 \times 10^{13}\,cm^{-3}$, $\bar{\tau}_p/\tau_E$ is approximately 0.1, and Eq. (1), for $\gamma = 7$, gives $T_{ed} \approx 0.04\,\bar{T}(P_{in} - P_r)/P_{in}$. Together with the rather large radiative losses observed mainly in the divertor chamber [12], this yields a reasonable value for T_{ed}. In high-bulk-density, neutral-beam-heated discharges, much higher densities are observed in the divertor, and $\bar{\tau}_p$ becomes very small (Fig.11). In this case, $\bar{\tau}_p/\tau_E$ is smaller than or equal to 0.03, and Eq.(1) gives $T_{ed} \lesssim 0.015\,\bar{T}\,(P_{in} - P_r)/P_{in}$, again consistent with measured values of T_{ed}. The same situation can be realized at lower bulk plasma densities by puffing additional gas into the divertor chamber (Fig.6).

The total energy flow onto the neutralizer plates can be calculated from the measured values of i_s and T_{ed}, using Eq.(4). In these calculations, we assume up-down symmetry between the two divertors, a distribution of power losses with 20% onto the inner and 80% onto the outer plates, $T_{id} = T_{ed}$, and $\gamma = 7$. For purely Ohmically heated discharges, these calculations yield $P_w \approx 150$ kW or 50% of the input power for $n_{ed} \lesssim 10^{13}\,cm^{-3}$ and $T_{ed} \gtrsim 10$ eV (Fig.12), decreasing further down to 50 kW for higher values of n_{ed}. Combined with measurements of the radiative losses from the bulk and, in particular, the divertor plasma [12],

these calculated energy flows are consistent with the global power balance. Obviously, under these conditions, the conventional sheath model gives the correct relation between heat transfer and divertor plasma parameters, as previously found on DIVA [19].

In experiments with neutral-beam heating, a similar consistency is observed only for divertor plasmas with low T_{ed} or high n_{ed} ($T_{ed} < 15$ eV or $n_{ed} > 3 \times 10^{13}\,cm^{-3}$). At high values of T_{ed} or low n_{ed}, power losses computed from the measured data of i_s and n_{ed} account only for a small fraction of the total input power (Fig.12). For an injection power of 2.5 MW, at a divertor density of $n_{ed} = 5 \times 10^{12}\,cm^{-3}$, probe measurements yield $T_{ed} = 25$–30 eV and predict only a total charged-particle power flow of $P_w = 0.2$–0.3 MW onto the target plates.

Uncertainties in the use of Langmuir probe data for the computation of power losses derive from the unknown ion temperature, fluctuations in the divertor parameters, and the possibility of non-Maxwellian electron distributions.

In the low-n_{ed}/high-T_{ed} regime, it is not reasonable to assume $T_{id} = T_{ed}$, as the temperature equipartition time becomes longer than the particle flow time in the scrape-off layer. A higher ion temperature – expected especially in this situation with intense neutral-beam injection – would give higher power losses than are shown in Fig.12.

In H-type discharges, bursts are observed in the energy losses from the bulk plasma and in the divertor plasma parameters [6]. During these bursts, the divertor electron temperature is estimated to be significantly higher ($\gtrsim 30$ eV) than during the intermittent quiescent phases with $T_{ed} \approx 10$ eV, enhancing thereby the time-averaged loss flow.

The most basic limitation of the conventional sheath model arises from the assumed Maxwellian distribution of the electrons entering the sheath. The strong inhomogeneity of plasma parameters along the field lines could supply suprathermal electrons to the divertor plasma: for densities $n_{ed} < 10^{13}\,cm^{-3}$, the mean-free path of an electron with an energy equal to the mid-plane temperature in the scrape-off (~ 100 eV) is longer than the length of the field line to the target plate. Near the divertor plate, this situation could give rise to an electron energy distribution with a high-energy tail, yielding a higher heat flux and $\gamma > 7$ [19]. In this regime, obviously, also the use of the two-fluid model with a purely collisional expression for the electron heat conductivity [9] ceases being valid.

The deficit in the global power balance for discharges in this regime might, however, also be due to incompletely taking account of the other loss channels. Further experimental and theoretical studies are, therefore, required to clarify the divertor plasma characteristics at low densities or high temperatures.

5. CONCLUSIONS

The studies of the divertor plasma in ASDEX reported in this paper have demonstrated the existence of large gradients of plasma parameters along the field lines of the scrape-off layer, obviously caused by recycling localized in the divertor chamber and by the reduced parallel heat conductivity at low electron temperatures. This allows a partial decoupling of bulk and divertor plasma characteristics, with the latter determined by bulk plasma density, recycling conditions and input power.

It was, in particular, possible to realize in these experiments a divertor regime with high plasma density and low electron temperature ($T_{ed} \approx 7$ eV) for all tested values of heating power ($P_{NI} \leqslant 2.5$ MW) by a proper choice of the bulk plasma density or by manipulation of the recycling conditions in the divertor chamber.

This regime is obviously extremely attractive for reactor operation, and the present results are encouraging for the development of future large devices with poloidal divertor like JT-60, ASDEX-Upgrade and INTOR.

ACKNOWLEDGEMENTS

The authors wish to thank Dr. G. Siller for developing the Langmuir probe system which was used for measuring the divertor plasma characteristics and Mr. R. Komen for technical help with these probes. They are grateful to their colleagues from the ASDEX team, particularly to Drs H. Niedermeyer and E.R. Müller, for many fruitful discussions.

REFERENCES

[1] KEILHACKER, M., ALBERT, D.B., BEHRINGER, K., BEHRISCH, R., ENGELHARDT, W., et al., in Plasma Physics and Controlled Nuclear Fusion Research (Proc. 8th Int. Conf. Brussels, 1980) Vol.2, IAEA, Vienna (1981) 351.

[2] DIVA GROUP, Nucl. Fusion 18 (1978) 1619.

[3] MEADE, D., ARUNASALAM, V., BARNES, C., BELL, M., BITTER, M., et al., in Plasma Physics and Controlled Nuclear Fusion Research (Proc. 8th Int. Conf. Brussels, 1980) Vol.1, IAEA, Vienna (1981) 665.
[4] KEILHACKER, M., BECKER, G., BEHRINGER, K., CAMPBELL, D., EBERHAGEN, A., et al., in Plasma Physics and Controlled Nuclear Fusion Research (Proc. 9th Int. Conf. Baltimore, 1982) Vol.3, IAEA, Vienna (1983) to appear.
[5] WAGNER, F., BECKER, G., BEHRINGER, K., CAMPBELL, D., EBERHAGEN, A., et al., Phys. Rev. Lett. **49** (1982) 1408.
[6] WAGNER, F., BECKER, G., BEHRINGER, K., CAMPBELL, D., EBERHAGEN, A., et al., in Plasma Physics and Controlled Nuclear Fusion Research (Proc. 9th Int. Conf. Baltimore, 1982) Vol.1, IAEA, Vienna (1983) 43.
[7] SHIMOMURA, Y., et al., Some Consideration of Ash Enrichment and Ash Exhaust by a Simple Divertor, Japan Atomic Energy Research Institute Rep. JAERI-M 8294 (1979).
[8] SHIMOMURA, Y., MAEDA, H., J. Nucl. Mater. **76 & 77** (1978) 45.
[9] CHODURA, R., LACKNER, K., NEUHAUSER, J., SCHNEIDER, W., WUNDERLICH, R., in Plasma Physics and Controlled Nuclear Fusion Research (Proc. 9th Int. Conf. Baltimore, 1982) Vol.1, IAEA, Vienna (1983) 313.
[10] PETRAVIC, M., POST, D., HEIFETZ, D., SCHMIDT, J., Phys. Rev. Lett. **48** (1982) 326.
[11] ASDEX TEAM, presented by M. Keilhacker, Proceedings of IAEA Technical Committee Meeting on Divertors and Impurity Control, Garching 1981 (Keilhacker, M., Daybelge, U., Eds) 23.
[12] MÜLLER, E.R., BEHRINGER, K., NIEDERMEYER, H., Nucl. Fusion **22** (1982) 1651.
[13] NAGAMI, M., FUJISAWA, N., IOKI, K., KITSUNEZAKI, A., KONOSHIMA, S., et al., in Plasma Physics and Controlled Nuclear Fusion Research (Proc. 8th Int. Conf. Brussels, 1980) Vol.2, IAEA, Vienna (1981) 367.
[14] SHIMADA, M., NAGAMI, M., IOKI, K., IZUMI, S., MAENO, M., et al., Phys. Rev. Lett. **47** (1981) 796.
[15] MAENO, M., IOKI, K., IZUMI, S., KITSUNEZAKI, A., NAGAMI, M., SHIMADA, M., et al., Nucl. Fusion **21** (1981) 1474.
[16] SHIMOMURA, Y., KEILHACKER, M., LACKNER, K., MURMANN, H., SILLER, G., Characteristics of Divertor Plasma in Neutral-Beam-Heated ASDEX Discharges, Max-Planck-Institut Rep. IPP III/80 (1982).
[17] KEILHACKER, M., LACKNER, K., BEHRINGER, K., MURMANN, H., NIEDERMEYER, H., Phys. Scr. **T2** (1982) 443.
[18] MILLS, R.G. (Ed.), Fusion Power Plant, Princeton Plasma Physics Laboratory Rep. MATT-1050 (1974).
[19] KIMURA, H., MAEDA, H., UEDA, N., SEKI, M., KAWAMURA, H., et al., Nucl. Fusion **18** (1978) 1195.
[20] OHYABU, N., et al., General Atomic Rep. GA-A16484 (1982).
[21] PROUDFOOT, G., HARBOUR, P.J., J. Nucl. Mater **111 & 112** (1982) 44.
[22] CHODURA, R., Phys. Fluids **25** (1982) 1628.

(Manuscript received 15 February 1983)

➜ F. Wagner: The history of research into improved confinement regimes, in: The European Physical Journal H, 2018

ASDEX UPGRADE

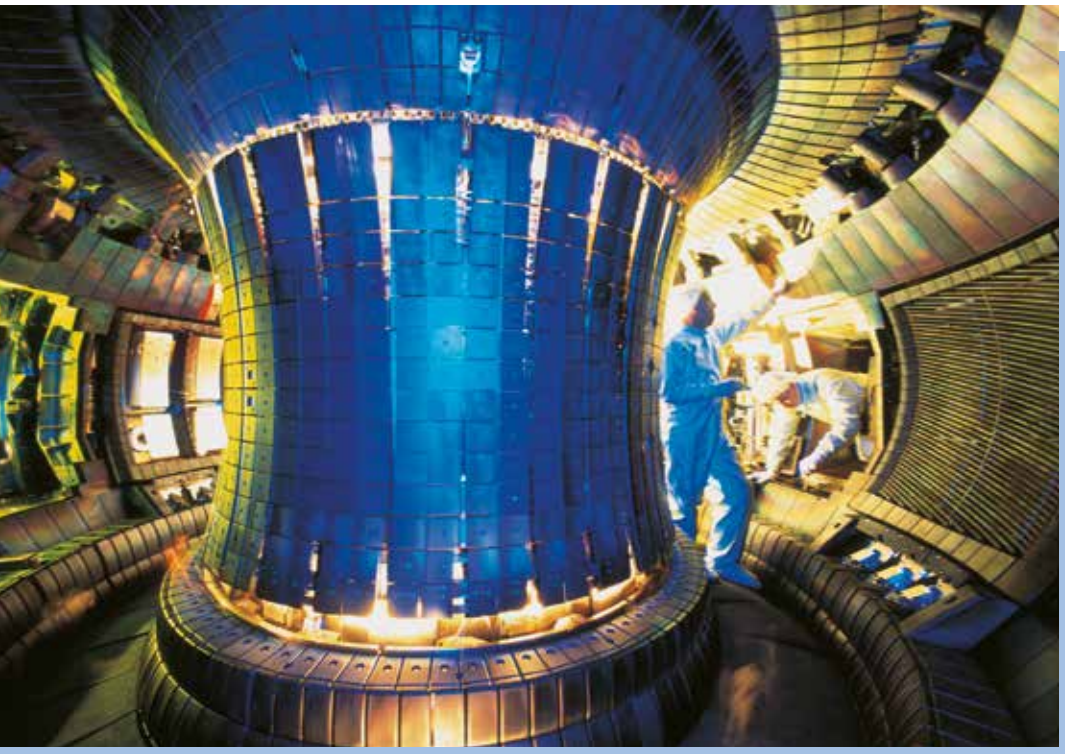

Blick in das Plasmagefäß des Tokamaks ASDEX Upgrade, der 1991 den Betrieb aufnahm.

Foto: IPP, Peter Ginter

2.3 ASDEX UPGRADE

ASDEX Upgrade
Definition of a tokamak experiment with a reactor compatible poloidal divertor

ASDEX-Upgrade Design Team and Tokamak Theory Group
Max-Planck-Institut für Plasmaphysik, EURATOM Association
8046 Garching

IPP 1/197, März 1982

This report was prepared by the tokamak theory and the tokamak design group, supported by other project groups and guest scientists of IPP and by other institutions.

IPP:
G. Becker, M. Blaumoser, K. Borrass, M. Brambilla, R. Chodura, U. Daybelge, W. Feneberg, J. Gruber, O. Gruber, U. Jandl, A. Kaleck*, M. Kaufmann, W. Kerner, W. Köppendörfer, H. Kollotzek, H. Kotzlowski, K. Lackner, L. Lengyel, J. Neuhauser, M. Pillsticker, H. Preis, W. Schneider, U. Seidel, B. Streibl, M. Tendler*, H. Vernickel, F. Werner, R. Wunderlich, H.-P. Zehrfeld

Kernforschungszentrum Karlsruhe:
F. Arendt

(* Guest scientist)

Abstract
ASDEX Upgrade is intended as the next experimental step after ASDEX. It is designed to investigate the physics of a divertor tokamak as closely as possible to fusion reactor requirements, without thermonuclear heating. It is characterized by a poloidal divertor configuration with divertor coils located outside the toroidal field coils, by machine parameters which allow a line density within the plasma boundary sufficient to screen fast CX particles from the plasma core, by a scrape-off layer essentially opaque to neutrals produced at the target plates, and, finally, by an auxiliary heating power high enough for producing a reactor-like power flux density through the plasma boundary. Design considerations on the basis of physical and technical constraints yielded the tokamak system optimized with respect to effort and costs as described in the following. It uses normal-conducting coil systems, is the size of ASDEX, and has a field of 3.9 T, a plasma current of up to 1.5 MA, and a pulse duration of 10 s. To provide the required power flux density, an ICRH power of 10 MW is needed. For comparison, a superconducting version is under investigation.

I. Introduction

The European fusion programme aims at solving by the end of this decade all physical questions which constitute conditions for the concept, the design and the decision to build NET[1] /1 - 3a/.

In this respect JET plays a central role since the aim of this experiment is to get as close as possible to a fusion plasma of a tokamak reactor. The investigations at JET, however, have to be backed up by an additional “basic tokamak programme” within the Community to prepare, on the physical side, the ground for NET. The work in progress for defining NET has revealed well defined critical questions which have to be solved in time, and which cannot be tackled by existing devices. ASDEX Upgrade – as described in the following, is devoted to solving an essential part of these questions.

The ASDEX Upgrade concept evolved from the experiments conducted in ASDEX and their interpretation. In its two years of operation ASDEX has made a major contribution to our understanding of the divertor concept. Besides these experimental results, however, studies and prognostic calculations for future experiments such as ZEPHYR, JET and INTOR carried out by IPP and elsewhere have added to the basis for ASDEX Upgrade.

[1] For the following it is assumed that NET is provisionally defined as being identical with INTOR.

The object underlying ASDEX Upgrade is to investigate the plasma boundary and plasma wall interaction problems sufficiently well such that an optimal solution for power flux and particle flux control can be found for NET and INTOR. An experiment being capable of tackling this aim has to meet essentially three requirements: It has to be equipped with a reactor-compatible divertor, it has to provide a sufficiently high particle density in the plasma boundary and scrape-off region, and the power flux from the plasma core into the plasma boundary has to equal reactor values. The parameters of the plasma boundary – defined by the range of fast charge exchange particles – determine, in particular, whether it is possible to achieve sufficient limitation of wall erosion and hence of impurities in the plasma when the large power flux from the plasma is continuously transferred to the walls. Besides meeting these requirements, the boundary region must also allow sufficiently fast helium pumping.

The increasing understanding of the divertor concept has shown in the meantime that the solution of the energy extraction problem and the solution for helium pumping, too, are closely linked with the divertor and the limiter concepts and the densities attainable in scrape-off and divertor regions. Analysis has demonstrated that the divertor concept is a much more likely solution for NET. For this reason, the study concluded the necessity of providing this machine with a divertor and a sufficient line density margin.

If a divertor is needed for NET and if its concept is to be understood sufficiently well for the design, the question is whether experiments on existing machines, such as ASDEX, can adequately investigate the divertor for NET. The investigations in ASDEX will not, however, suffice since for technological reasons the superconducting divertor coils in NET have to be installed outside the main field coils. Even if based on the same principles as the poloidal divertor, the divertor for NET has to be changed considerably and will hence raise additional questions. These problems specific to NET will have to be studied in a separate experiment. This experiment has to prove that the principles of a poloidal divertor will finally work under the NET constraints and will have to provide us with the data base to design NET.

An investigation of the NET divertor in a separate experiment has to work close to the final NET parameters, especially in the following three respects:

- the magnetic field configuration has to be close to NET in all critical regions;
- the power flux density through the boundary has to be close to NET values;
- the minor plasma radius and the magnetic field have to allow a sufficiently large $\bar{n}\cdot a$ to make a sufficiently thick cold plasma mantle feasible.

Besides the need to change the divertor itself, ASDEX with its limited magnetic field fails to meet especially the last condition. Since NET can only achieve its objective with a reasonable degree of risk if a divertor is used, and since ASDEX – although it has yielded important know-how on the divertor concept – cannot sufficiently guarantee the proper functioning of the NET divertor, it is necessary to build ASDEX Upgrade to investigate these questions.

2. The Physics Basis of the ASDEX Upgrade Proposal

In this chapter we describe the physics arguments for the construction of ASDEX Upgrade. The first section discusses the potential of the poloidal divertor based on the impurity-control needs of a reactor, the operational experience of ASDEX, a description of the differences inherent in the plasma-wall interaction between limiter and divertor discharges and the resulting divertor-specific scenarios for the power transfer and the impurity-handling problem. Competing with this are scenarios also feasible with a (pump)-limiter which are assessed in the last part of this first section.

The second one describes the consequences of the obvious need to place poloidal field coils in a reactor at a large distance from the plasma, leading to topological differences to the ASDEX divertor with expected large consequences on the mode of operation. The final section derives the parameters which determine the plasma-wall interaction and which should therefore be chosen identical – or in the case of $\bar{n}\cdot a$ larger than a given minimum value – to ensure similarity in these processes between an experimental device and a reactor.

2.1 The potential of the poloidal divertor

2.1.1 The dimensions of the impurity problem in a reactor

A reactor will operate under rather narrowly defined conditions for total particle content and average power flow through the walls. The crucial question will therefore be, how to transfer the fraction of fusion energy deposited by α-particles in the plasma to the wall without causing an intolerable impurity production.

A rather simple argument, first given in /4a,b/ and summarized in fig. 1 (rescaling data from /4c/) shows that if this energy transfer were to proceed via charged particle motion, hydrogen ion sputtering alone would cause a production of impurities tolerable only for very small values of their effective confinement time. Total sputtering rates given in this figure refer to a 3 GW thermal (total) device and are computed assuming an energy transfer of 4 kT per hydrogen impact on the wall. T was varied parametrically, illustrating the influence of the recycling rate. Over a large range of plasma boundary temperatures the impurity production remains fairly constant; the values, related to their tolerable concentrations, require, however, effective impurity particle confinement times of the order of only 1 - 2 msec for iron and ≲ 30 msec for carbon /5/.

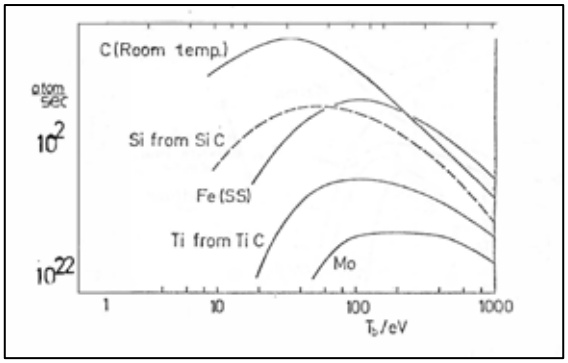

Fig. 1 Sputtering rate for a 3 GW thermal reactor in case of energy transfer to the walls via particle motion. Every ion impact is assumed to be accompanied by a total energy transfer (electron + ion) of 4 kT_b; the acceleration in the potential sheath is not taken into account.

These numbers are two to three orders of magnitude less than the required energy confinement times, and can only be realized if most of the impurity atoms are prevented from entering the bulk plasma. They are based on actually even optimistic estimates, obtained by neglecting other, additive, impurity production processes like self-sputtering or arcing. It, therefore, seems improbable that the power-transfer and impurity-balance problem can be solved merely by optimizing the material properties of target plates and walls; engineering of the boundary-zone plasma physics will certainly also be required to make the major contribution.

For the above considerations, the limiting carbon concentration was given by the fusion power reduction due to fuel dilution at given plasma pressure. This is no concern for devices aiming only at the demonstration of reactor relevant ß-values or energy confinement times; these aims could conceivably be achieved also at Z_{eff} values between 2 - 3 using wall-interaction control techniques not sufficient in a reactor. For such experimental devices with a very small duty factor, also the wall erosion, which for the above example of a reactor would be > 250 tons of carbon or > 40 tons of iron/year, would be no dominating concern.

For a reactor, however, more controlled means of power transfer to the wall have to be found and the intrinsic reactor impurities – helium – have to be pumped efficiently enough to keep their fraction below ≃ 5%.

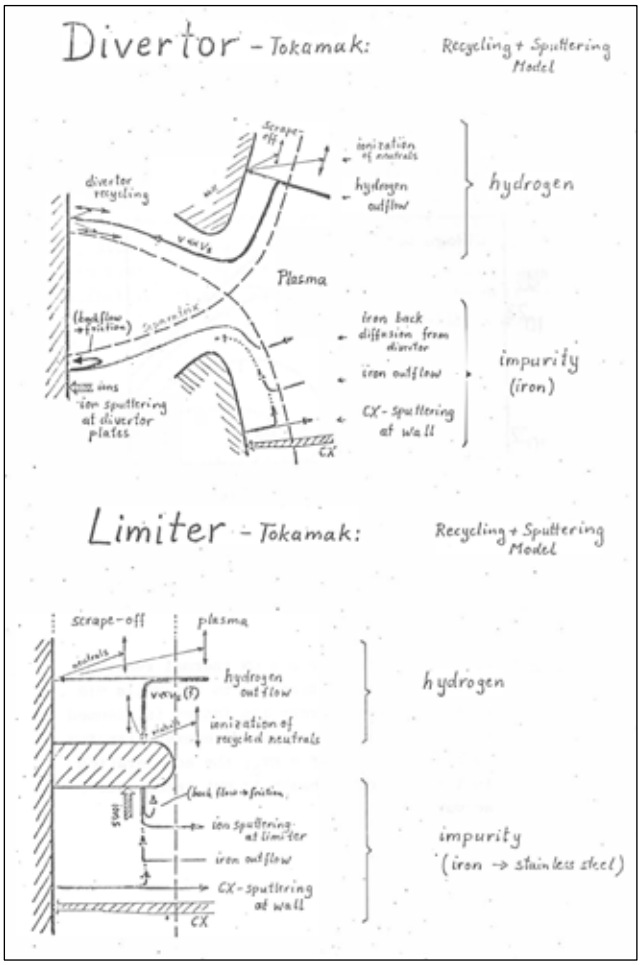

Fig. 2 Schematic representation of the processes contributing to the hydrogen and impurity household (here: iron) in a divertor and limiter tokamak.

2.1.2 The operational experience with ASDEX

Divertor experiments with ohmic and neutral-injection heating (up to 2.7 MW) in ASDEX have consistently shown very small impurity concentration ($Z_{eff} \lesssim 1.2$) over a large density regime ($10^{12} < \bar{n}_e < 8 \times 10^{13}$ cm^{-3}), and radiation losses from the bulk plasma amounting to less than 10% of the total input power (see ref. /6/). The low loop-voltage and the stationarity of the discharges allowed also to realize record pulse-lengths of 3 - 10 sec. The achievement of these performance parameters was accompanied by a high reproducibility, and no need for particular conditioning procedures or discharge build-up scenarios.

This ease of operation was only fully appreciated after a continuous toroidal limiter was inserted blocking the lower divertor entrances. Shifting the plasma column in vertical direction, either separatrix or limiter-bounded discharges could thus be studied. Not only did limiter experiments – in comparison to divertor discharges – result in much increased Z_{eff} values ($\gtrsim 4$) and fractional radiated power losses (only about 10% of the input power was deposited on the limiter surface), but also extraordinary care had to be taken to produce disruption-free discharges, with a poor record for their reproducibility.

These findings do not exclude the possibility of considerable improvement – in fact already demonstrated elsewhere – of the limiter discharges by special conditioning or gettering procedures, different limiter materials or special discharge build-up scenarios; they do, however, prove that the favourable performance of the ASDEX divertor is not merely a consequence of the small specific power load or its toroidally homogeneous distribution, but is rather associated with the separatrix-bound nature of the plasma. The ultimately most important result of this comparison, however, is the ease with which clean, reproducible discharges can be produced in a poloidal divertor configuration.

2.1.3 Expected differences in limiter and divertor plasma wall interaction

Figs. 2a and 2b give a schematic view of the processes determining the hydrogen and impurity (for the example taken, iron) household in a limiter or divertor tokamak. In the divertor case the major interaction between plasma and material walls is proceeding in a separate chamber; from this fact one expects a number of basic differences in the behaviour:

Probability for impurities produced by ion sputtering at the target plates to reach the bulk plasma
In the case of a divertor, these impurities have to diffuse up-stream along field lines against a net plasma flow over a distance comparable to the major circumference of the torus, before being able to reach closed flux surfaces of the bulk plasma via cross-field diffusion. In a limiter tokamak, impurities created at the exposed edge can reach closed flux surfaces by direct flight as neutral particles, and also all others born at the limiter and ionized in the scrape-off are immediately susceptible to cross diffusion into the bulk plasma.

Possibility of forming a protective cold plasma layer in the vicinity of the target plates
Such effects depend on the formation of inhomogeneities along field lines, and the possibility of a strongly enhanced neutral gas density in the target plate vicinity. They will in principle exist in both divertor and limiter geometries, but will be much weaker in the latter, as the immediate vicinity of the closed flux surfaces of the bulk plasma tends to erase inhomogeneities, and acts as a strong pump for the neutral particles originating at the limiter within one mean free path from the plasma edge.

Hydrogen recycling into the bulk plasma
In an ideal divertor geometry, neutral particles originating at the divertor plates can reach the bulk plasma only after a complicated path, having typically Frank-Condon energy upon arrival at the bulk plasma edge. In the limiter case energetic neutrals created at the limiter will contribute to the refuelling, enhancing the average penetration depth. As a consequence, the divertor scrape-off may be expected to be thicker.

Hydrogen or gaseous impurity (helium) pumping
For the control of density, fusion devices require a capability to pump hydrogen. Helium pumping is obviously needed to avoid fuel dilution in a reactor, and a finite, but controlled content of gaseous impurities might be desirable to create a radiation layer in the periphery of the bulk plasma.

Whereas pumping of gaseous impurities can naturally be incorporated into a divertor, it requires modification of the conventional limiter to a pump limiter. In the latter case, however, basic topological reasons – and quantitatively probably dominating, considerations of tolerable power flux – imply that only flux surfaces a certain distance away from the plasma edge can be led into the pumped region, so that the plasma flow building up the neutral gas pressure is expected to be smaller than in the divertor case, where also the high plasma pressure region in the immediate vicinity of the discharge edge is linked to the chamber. This should result in higher neutral gas densities in the case of the divertor, obviously facilitating helium pumping.

Stability of plasma wall interaction with respect to non-axisymmetric magnetic perturbation
In the divertor, the plasma wall interaction zone is separated from the bulk plasma by a separatrix, which corresponds to a zone of extremely high shear. As a consequence, unsymmetries originating in the bulk plasma are expected to be mixed out before reaching the target plate. A divertor should therefore be less susceptible to changes in the plasma-wall interaction due to MHD-activity.

2.1.4 Divertor scenarios for controlled power transfer to the walls

From the above differences a number of scenarios for power transfer to the walls arise which are feasible only in a divertor tokamak.

The probably most obvious divertor effect is the reduction in the fraction of impurities originating at the target plate that can ultimately enter the bulk plasma. Whereas the estimates given in section 2.1.1 for the amount produced still hold, only the fraction entering the main chamber is relevant for the plasma contamination. Theoretical predictions for this impurity backflow effect are difficult and require codes for the plasma dynamics along the field lines currently under development. It is, however, possible to study the effect of parametrically varying this “impurity backflow fraction” in a one-dimensional

transport code using a scrape-off model including impurity production by ion sputtering and self-sputtering at the target plates and by CX sputtering at the walls. In this model (described in appendix A) the impurity balance tends to come to a stationary state when the radiated power fraction is large enough to reduce the particle energy flow to walls and target plates to a low enough level. The residual impurity production then will be just compensated by their unloading.

A characterizing result is therefore – for a given total power flow – the fraction of power radiated as given in Fig. 3. The reduction in the impurity backflow into the main chamber in case of an efficient divertor will allow the device to operate with a smaller fraction of radiated power in the main chamber, with positive consequences expected for the thermal stability of the discharge.

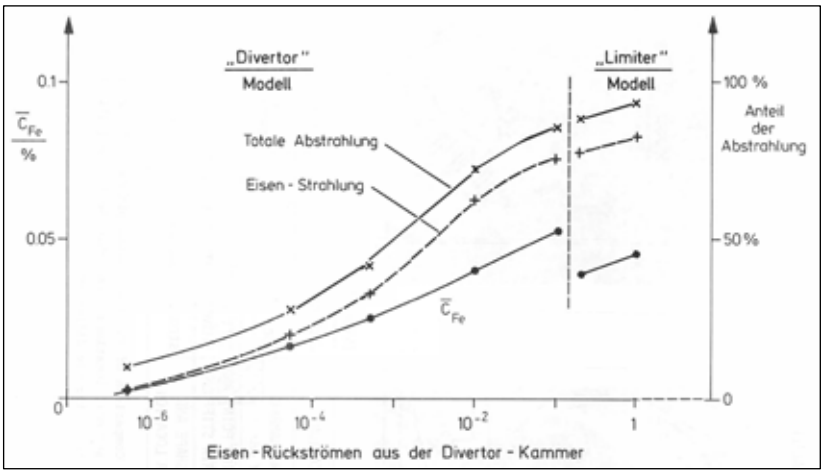

Fig. 3 Dependence of Iron-concentration and radiative power losses on the impurity backflow fraction from the divertor chamber or the limiter, for a device with JET dimensions and power fluxes.

Sweeping back the impurities produced at the target plate gives rise to a stationary scrape-off obviously only if the effective self-sputtering coefficient – including the effect of the acceleration of the multiple charged ions in the potential sheath – will be less than one. This, depending on the choice of material, implies a limit on the divertor electron temperature which in the high density divertor regime experimentally found in ASDEX and presently considered the favoured option for INTOR will be established by enhanced recycling or radiation losses in the divertor. Although presently considered less likely, it had been previously also suggested that even in a low-density, high-temperature regime this condition could be realized in a divertor by cross-diffusion (or free flight in the neutral state) of the impurities out of the narrow, high temperature region of the scrape-off /7/.

A more consistent discussion of the diffusion processes in the scrape-off layer and experimental observations have shown, on the other hand, that there is no significant difference in the capability of limiters and divertors to shield against vessel-wall-produced impurities. This implies that CX-produced impurities will ultimately determine the limit on discharge cleanliness for a divertor tokamak, a consideration important in selecting minimum dimensions for an experiment reactor-similar in this respect. The rate of CX production of impurities is expected, however, to be different in divertor and limiter tokamaks, as in the latter a large amount of hydrogen neutrals will originate from its exposed edge, penetrating into higher temperature regions of the discharge and enhancing thereby the primary CX sputtering.

A milestone in the assessment of the potential of the poloidal field divertor has been the discovery of the major role of inhomogeneities along the scrape-off field lines. Determining for this on the one hand were measurements in ASDEX /8/ and partly also Doublet III /9/ showing largely enhanced neutral gas pressure and strong bolometrically detectable power losses in the divertor chamber and low Mach number flow (an indication of strong back-pressure) in the scrape-off. The second important contribution came from the INTOR studies which suggest radiation losses from the divertor chamber as a means of power unloading /10/, and modelled the effect of recycling at the target plates in a high-density scrape-off regime /11/.

In a divertor chamber whose exit to the main discharge vessel is well blocked by the plasma scrape-off, neutral particles produced by the impact of ions on the target plate have a high probability to be re-ionized in the scrape-off, thus

participating many times in the process of energy convection into the wall. Enhancement of the recycling at given power flow will lower the temperature T_b bringing it below the threshold for self-sputtering and possibly into the region where even the hydrogen sputtering yield in fig. 1 decreases drastically.

Such enhanced recycling has been at several occasions suggested also as a means of solving the power transfer problem in conventional tokamaks, but requires boundary plasma densities in excess of the desired peak density in the center. As empirical findings suggest cross-field particle flow to be of density-gradient driven type or even to have an additional inward component /12/, there seems no hope to realize such profiles in the main plasma chamber.

The dynamics along field lines, however, in the low Mach number case is determined by the requirement of nearly constant pressure, and any kind of energy sink or cold particle source in the divertor chamber will lead to a corresponding density increase there. This is quantitatively underlined by the results of a parallel flow model described in appendix B. The main energy flow channel into the divertor will then be heat conduction, as has been shown in ASDEX simulation calculations for the electron channel in ohmically heated discharges /13/, and will become true also for ions of higher input powers (appendix B).

The power unloading could be considerably facilitated by radiative losses in the divertor chamber. Apart from type and concentration of the impurities, the radiated power will strongly depend on their spatial distribution: in a regime of strong coupling between electron and ion temperatures the constant pressure requirement along field lines leads to a very favourable tendency. A reduction in temperature in the target plate vicinity will lead to a density increase, and both effects will tend to enhance radiative losses. This will particularly be the case if the impurity content were also peaked there, as may be expected from the impurities produced at the plates and swept back by the plasma flow. A purely indicative estimate might be gained using the Coronal model and a constant impurity fraction f_z, suggesting that the whole a-particle power of the before-mentioned 3 GW reactor could be radiated by 1% oxygen impurities for a mid-plane value of the scrape-off electron pressure integral $\int n_e T_e dx = 1.8 \times 10^{16}$ cm^{-2} eV.

2.1.5 Non-Divertor Solution to the Power Unloading and Impurity Balance Problem

Proposals along these lines can be subdivided into two types:

- power transfer via radiation from a narrow zone in the outer region of the bulk plasma (“photosphere”), reducing the energy flow associated with particle motion and possibly resulting also in a cool plasma mantle blocking CX sputtering (combined with a pump limiter to eliminate the helium ash);
- attempts to obtain divertor-type benefits by possibly simpler technical means (“ergodic limiter”).

The formation of a radiation layer, first demonstrated in 1-d transport calculations by Gibson and Watkins /14/, would seem a technically attractive solution which should certainly be studied also in the proposed ASDEX experiment as a competing option. The relevant computational models have since that time been considerably refined by adding more self-consistent descriptions of the plasma-wall-interaction processes (see review in /5/ and appendix A); recently we have started to add also a non-corona description of the impurity effects /15/ to the BALDUR code, with first results now available. The crucial questions to this approach are:

- Thermal and MHD stability of the resulting profiles?
  The temperature characteristics of the radiation efficiency at constant impurity concentration indicate a potential for thermal instability, as a reduction in temperature would lead to an enhancement in the radiated power. This argument was born out by analytical studies indicating instability for inward peaked electron or impurity density profiles /16/ if the radiated power fraction were to exceed a certain percentage (≈ 50%); it was confirmed also by numerical calculations using a simplified impurity balance model /17/.

  Computations carried out with a more consistent plasma-wall interaction model indicate that this instability (found analytically under the assumption of an impurity concentration constant in time) might under certain conditions be compensated by a simultaneous variation in the impurity content. In this and several other features, results depend on the assumed impurity transport model.

Limiter scenarios involving such radiation layers rely on the self-limiting nature of the impurity content. An increased flexibility could be obtained by using gaseous impurities, artificially introduced and feedback-controlled in their concentration: such scenarios obviously require a possibility for also pumping them, making a divertor ideal for their study or practical application.

Photosphere-type situations have been observed experimentally in ohmically heated discharges with strong oxygen contamination. Situations of this type tended to be rather prone to disruption; in fact, the current profiles resulting from established radiation layers in computations with low $\underline{q}$ at the boundary make their resistive MHD stability suspect;

- Feasibility with inward peaked density profiles?
  Energy transfer via a radiation layer in an ignited tokamak requires that the increased radiation efficiency of impurities at low temperatures compensates the effect of the volume ratio between the plasma core and a narrow boundary zone: otherwise radiation from the center would dominate, making self-sustained thermonuclear burn impossible. Theoretical computations usually involve a gradient-driven diffusion model for the plasma density, which produces very flat profiles. Accepting strong experimental evidence for an additional inward drift term /12/ would suggest peaked n_e profiles also in reactor-size devices, resulting in an increased central radiation efficiency even for a flat impurity concentration.

The so-called ergodic limiter relies on the action of modest helical perturbation fields resonant with $\underline{q}$ surfaces close to the plasma boundary /18/. Their combined action leads to a random walk of field lines in a near-edge zone with an enhancement in the effective “radial” electron heat conduction, and the possibility of an average radial flow of hydrogen and impurity ions. Presently available theoretical models for these effects are quite poor; they tend to predict, however, promising performance in the role to reduce impurities. There exists no relevant experimental evidence.

- Production of a predictable and controlled degree of ergodicity is considerably more difficult in a non-circular high-ß (or low aspect ratio) tokamak, as these effects tend to lead to additional coupling between the helical field perturbations. First experiments of this type should therefore be carried out – as soon as possible – on a circular tokamak (TEXTOR). If such results were positive and would promise a favourable scaling to reactor conditions, corresponding windings could later be installed also in ASDEX-Upgrade to study their effect under the much more complex conditions of a non-circular tokamak.

Summarizing, the non-divertor options to the power unloading and impurity control problem should certainly continue to be studied because of the obvious technical facilitations. At present, however, they cannot be considered a high-probability solution to the reactor problems, as demonstrated by the INTOR decision to use a poloidal divertor as basis option. Considering this decision, and the fact that the three approved European devices of the next generation (JET, TORUS-2, FTU) rely on non-divertor concepts, a further study of the divertor option seems mandatory.

2.2 Reactor-like poloidal divertor configurations

As has been underlined by the results of the INTOR study, a poloidal divertor will have to rely on poloidal field coils outside the blanket and – for maintenance reasons – most probably also outside the main field coils. This has immediate important consequences on the possible plasma shape and divertor configurations as illustrated in fig. 4, where the plasma-limiting separatrix, some structural elements, and the divertor coils are drawn for INTOR and ASDEX in scales giving approximately the same minor plasma diameter in the equatorial plane. The principal configurational differences are summarized in the table immediately below the figure.

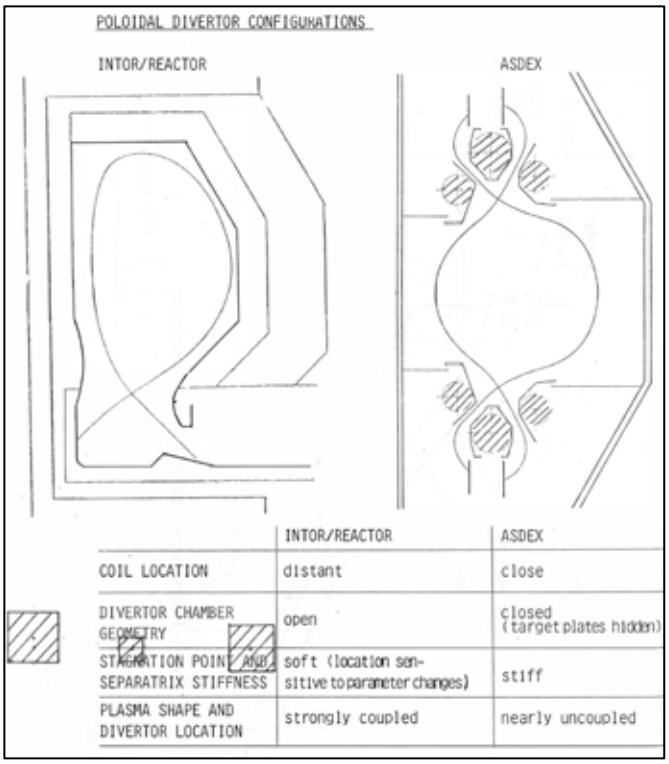

	INTOR/REACTOR	ASDEX
COIL LOCATION	distant	close
DIVERTOR CHAMBER GEOMETRY	open	closed (target plates hidden)
STAGNATION POINT AND SEPARATRIX STIFFNESS	soft (location sensitive to parameter changes)	stiff
PLASMA SHAPE AND DIVERTOR LOCATION	strongly coupled	nearly uncoupled

Fig. 4 Comparison of INTOR and ASDEX plasma configurations and coil locations. The table describes qualitatively the principle differences.

As most of the principal divertor advantages depend critically on inhomogeneities in density, temperature (and impurity concentration) along the field lines to the target plates, and the possibility of sustaining a significantly enhanced neutral pressure gradient between the divertor chamber and the main plasma vessel, different behaviour has to be expected in the two cases. Whereas the blocking of neutral gas in an ASDEX-type configuration is helped by an arrangement of separating plates and the central multipole itself, it has to rely in an open configuration completely on the transverse impenetrability of the scrape-off to neutral particles. (The central role of the divertor slits for the gas back-flow and the recycling is illustrated by a picture of an ASDEX discharge in H_α light, fig. 5).

This requires a minimum line-integral density across the scrape-off of the value given by Lehnert's impenetrability condition ($\approx 10^{14}$ cm^{-2}) or actually even larger, as also neutrals originating at the target plates should have a high probability to be immediately reionized before leaving the scrape-off. These very large scrape-off line densities have also to be reached in an experiment simulating the behaviour of such an open divertor in the reactor.

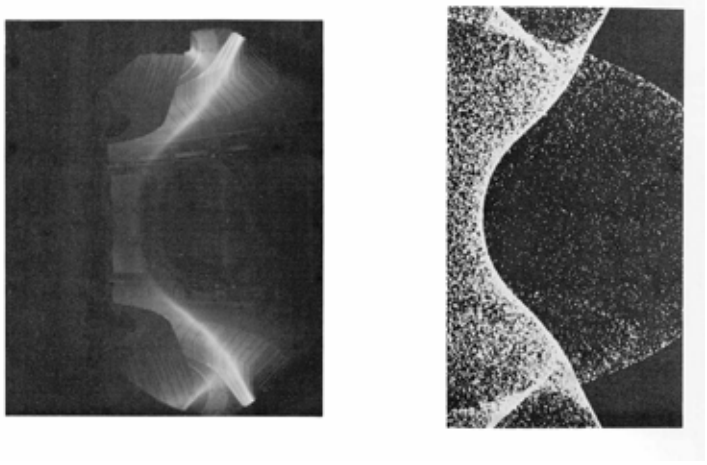

Fig. 5 Photography of ASDEX in H_α-light, illustrating the role of the divertor slits in the recycling. The picture at the right is a computer simulation based on calculated MHD equilibria clarifying the topology of the radiating zone.

This necessity will be facilitated somewhat by the expansion of the flux surfaces towards the target plates which in a configuration produced by distant coils is necessarily larger than in an ASDEX-type one (assuming constant density along a field line, the $\int n \cdot dx$ across the scrape-off varies along it like the inverse of the poloidal field).

In a configuration with coils close to the plasma column their fields can be designed to produce a very steep gradient in magnitude: this gives a large stiffness to the location of the stagnation point and to the separatrix during its passage through the divertor slits against motion or parameter changes of the plasma column. In contrast to this, in a configuration like INTOR, a vertical plasma displacement, for example, causes a vertical shift of the stagnation point by a nearly equal amount, unless additional control measures are undertaken.

Finally, close coils allow virtually to decouple the shape of interior flux surfaces from the existence and position of the divertor whereas distant coils determine both of them simultaneously. This requires consideration of MHD stability against interior modes to be taken into account when determining the divertor lay-out. According to the present understanding of ideal MHD stability this calls for divertors on top and/or bottom, leading to a vertically elongated plasma cross-section unstable to axisymmetric displacement modes in the absence of passively and actively stabilizing elements. Passive conductors will only stabilize on their respective time constant and will have to be augmented by actively controlled fields. Depending on the displacement-sensing diagnostic, the strength of the instability, the position of the control field coils and the feedback circuity, this will result in residual oscillations of a certain amplitude, which of course interact with the divertor efficiency.

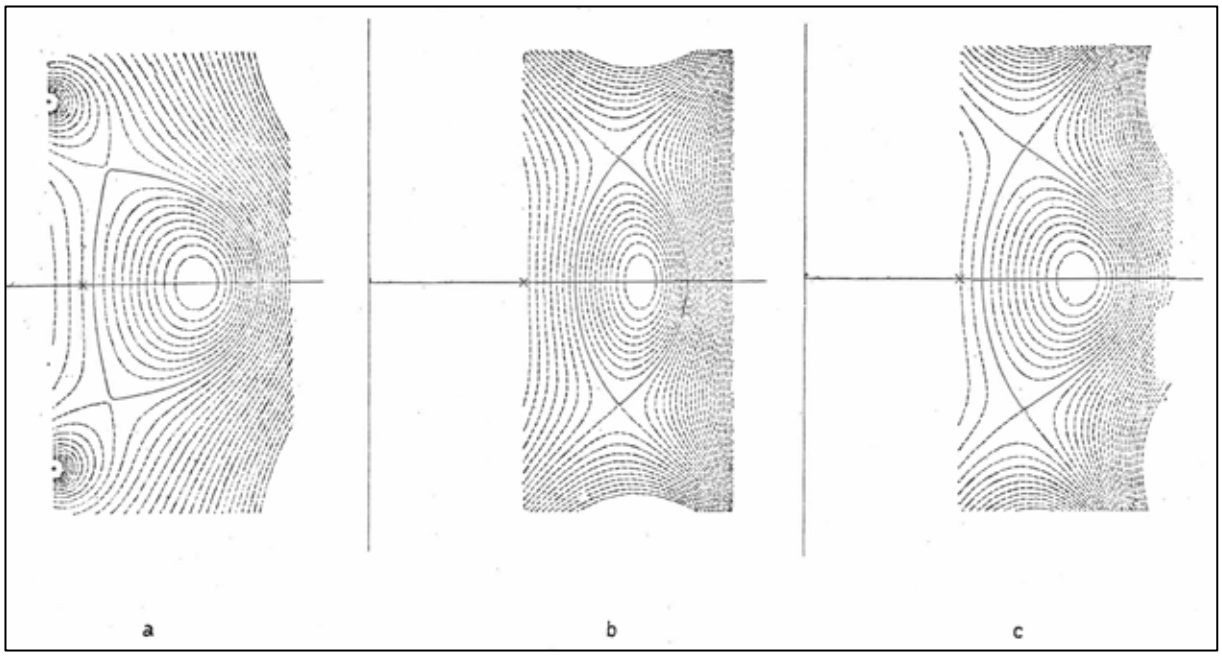

Fig. 6 Illustration of the effects contributing to the formation of a separatrix at hand of the results of equilibrium calculations. Case a) corresponds to a high $ß_p/A$ situation, where to a large part the toroidal high-ß effects contribute to the stagnation-point formation. Case b) uses a nearly pure quadrupole configuration, whereas for case c) a large hexapole moment is superposed to shift the stagnation point and to control the b/a ratio and the axisymmetric stability behaviour.

A separatrix in the poloidal field pattern using distant coils can be produced in different ways distinguishing themselves in magnetic field energy, flexibility and the required effort for positional control. Three extreme configurations are illustrated in Fig. 6 a - c.

At high $ß_{pol}$ values, toroidal effects alone tend to produce stagnation points on the torus inside, close to the plasma boundary. Utilizing this effect, a poloidal divertor configuration can be constructed with relatively modest additional coil currents (case a), operational, however, only during the high $ß_{pol}$ phase and with a scrape-off layer shape which allows at best to utilize the outside branch for pumping. The feasibility of such a scheme hinges on the possibility of operation at

high $ß_{pol}$ /A (A: aspect ratio, defined using the small plasma diameter in the midplane), and of dispensing of the divertor in the heating-up phase.

Poloidal multipole fields increase from their nominal center like $r^{m/2 - 1}$ (with m = 4 for a quadrupole, = 6 for a hexapole field). As a consequence, quadrupole fields are the least sensitive to the distance between stagnation point and coil location (Fig. 6 b). They do produce, however, an elliptic plasma cross-section (with a ratio b/a determined by the plasma current distribution) known to be strongly unstable against vertical displacements (time constant ~ 1 μsec).

The vertical instability growth rate together with the ellipticity b/a can be reduced (and controlled against variations in the current distribution) by superposing an additional hexapole field, which rapidly tends to dominate, however, the magnetic field effort. Figure 6 c shows such a configuration as foreseen as a limiting case for the ASDEX-Upgrade device. A corresponding single null configuration (INTOR-similar) can be obtained by different feeding of the coils. Clearly, to reduce the magnetic field effort it is desirable to move as much as possible in the direction of a lower hexapole component, or to utilize as much as possible the natural tendency towards a high $ß_p$ separatrix.

Two of the principal aims of the ASDEX-Upgrade device are therefore

- to study the physics of INTOR (reactor)-like poloidal field divertor defined as configurations feasible with distant coils;
- to find among the various configurations possible the one combining acceptable divertor performance (power unloading, impurity control, helium pumping) and controllability of the separatrix shape and position with the minimum required poloidal field effort.

2.3 Parameter requirements of a reactor-similar divertor experiment

2.3.1 Heating power requirements

ASDEX Upgrade aims at simulating the plasma conditions of a reactor in the layer determining the plasma-wall interaction. In particular this requires similar temperature values in the region of interest. The desired situation is illustrated in fig. 7 giving the solution of the radial energy flow equation for three devices of different size: ASDEX Upgrade, INTOR and a power producing reactor.

The profiles correspond to equal power flux densities at the plasma border, and hold under the assumption of $n \cdot \chi = f(T)$ and, peaked, similar heat deposition profiles but arbitrary plasma density distributions. They are plotted against distance from the plasma boundary, illustrating thereby the similarity over the first 10 cm from the walls, in spite of the vastly different temperatures reached at the center. If also equal neutral gas boundary density and particle diffusion behaviour are postulated, also the radiative power losses for equal impurity concentration conserve this similarity.

The important similarity parameter derived from these considerations is therefore the power flux density through the plasma boundary: as reference, INTOR values, based on an additional heating power of 75 MW give about 0.23 MW/m^2, increasing to ~ 0.3 MW/m^2 during the thermonuclear burn phase.

An additional critical requirement on plasma heating is a power deposition profile with little input into the boundary zone. This will be the dominating criterium in the selection of the additional heating method. The presently favoured scheme is ICRH at the second harmonic, for which theoretical calculations (ray tracing) have given promising results. In particular they have shown

- Ray tracing can be used for ASDEX Upgrade at f ≈ 100 MHz.
- At low temperature power deposition is concentrated near $\omega = 2\,\Omega_{ci}$ in the cross-section of the beam (which is small in circular geometry, but somewhat larger in the real, elongated geometry). Whether a single transit is enough to complete absorption or not cannot be told by ray tracing alone.
- At high temperature, in addition to localized absorption near $\omega = 2\,\Omega_{ci}$ as before, strong absorption by the electrons (transit time pumping, not electron Landau damping!) also sets in and can account for a large fraction of total absorption over something like the internal half of the cross-section (from r = 0 to r = a/2).

At the same time magnetic field values actually chosen for our design are in a regime not definitely ruling out the availability of gyrotrons at the time required, so that also ECRH could be considered.

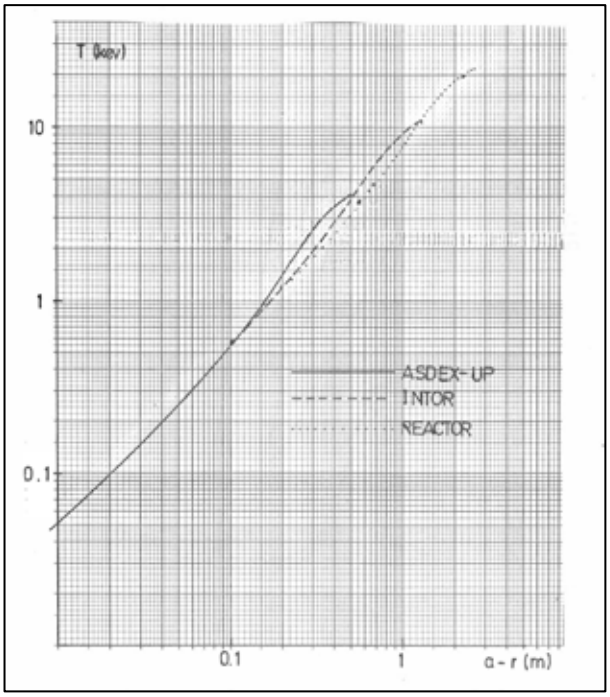

Fig. 7 Temperature profiles for identical heat flux through the boundary, for experiments of different size (obtained under the assumption of peaked, similar heat deposition profiles and a heat conduction law of the form $n \cdot \chi = f(T)$).

2.3.2 Requirements on the plasma line density $\bar{n}a$

Crucial in determining the minimum size of an experiment expected to simulate the reactor-type wall interaction is the dimension of the boundary region determining it. Among the processes affecting power transfer or impurity production, radiation and charge exchange are volumetric ones, originating under reactor conditions from a near boundary zone.

The impurity production via charge exchange depends on neutral gas density and temperature at the boundary and the plasma temperature profile as a function of the line integrated density from the walls $\int_r^a n\, dr$.

Several effects interact in a complicated manner:

- the penetration of neutrals into the interior (as determined by charge exchange and ionization);
- the probability of fast neutrals, produced by charge exchange in the hotter regions to reach the wall. This is a function of their energy and the $\int n \cdot dr$ they have to traverse;
- the sputtering efficiency of these hot neutrals, which again increases strongly with their energy.

All these effects are included in the Monte Carlo treatment of the hydrogen neutral dynamics and the evaluation of their sputtering yield incorporated in the BALDUR transport code. Fig. 8 summarizes the results of fairly extensive calculations for ZEPHYR and JET in terms of the dependence of the resulting iron production rate per cm^2 vessel surface, on the density line integral from the boundary to three selected temperature isotherms. (A given plasma profile corresponds on this graph to a point on each line; this redundant information is given as the output of the code does not identify in a simple way the plasma region responsible for most of the impurity production). These curves illustrate that the required $\int n \cdot dr$ for sputtering suppression is actually only a rather weak function of the impurity production considered tolerable, suggesting a line density of about 2×10^{15} cm^{-2} between the walls and the 300 eV isotherm necessary for sufficient shielding.

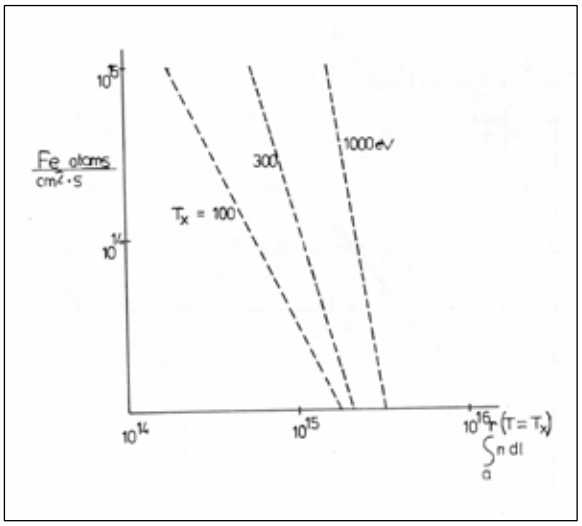

Fig. 8 Iron sputtering by CX neutrals as a function of the density line integral between wall and different isotherms. The lines shown are a composite result of various JET and ZEPHYR simulation runs. A sputtering rate of 3 x 10^{14} Fe-atoms/cm^2 · s corresponds to a yearly wall ablation of 1 mm.

Although including results for two devices supposed to operate in rather different density regimes, these calculations are still limited in validity by the use of a particular transport model with all variations resulting essentially only from different heating power fluxes and radiation losses. The form of presentation in fig. 8 was chosen to minimize the dependence on model variations, as for example a change in the boundary neutral gas density would only logarithmically modify the value of $\int_{r\,(T=Tx)}^{\infty}$ n dr needed to give a fixed CX sputtering yield. Uncertainties in the particle confinement model, dependences on details of the refuelling (e.g. whether a limiter is present, enhancing fast neutral penetration – see discussion in 2. 1.3), and more detailed changes in the temperature profiles have been shown however to change (generally reduce) the above quoted $\int$ n· dr value by perhaps up to a factor of three. The criterium cited above – a boundary zone width of $\int_{r\,(T=300\,eV)}^{a}$ n dr > 2 x 10^{15} cm^2 should therefore be considered primarily only a dimensioning requirement for an experiment aimed at studying wall interaction under all reasonable diffusion assumptions.

An experiment with the aims of ASDEX Upgrade should also be large enough to accommodate a photosphere to radiate, if desired, a large fraction of the total power flux. The plasma region required for this depends on the impurity species and the heat conduction law; for the Alcator-Intor transport model and iron as impurity, INTOR calculations suggest a dimension of the radiation layer of about 10 - 20 cm. The same values would hold for a simulation experiment operating at the same power fluxes and at the same boundary densities, again combining to a requirement of $\int$ n· dr ~ 1 - 2 x 10^{15} cm^2 for the boundary simulation zone.

The lay-out of ASDEX Upgrade should, therefore, guarantee achievement of a value of $\bar{n}$a large enough to allow considering a layer with a line density of 2 x 10^{15} cm^2 as a boundary zone. As a lower limit for this the remaining core of the plasma should certainly at least contain again as many particles as the so-called boundary zone, giving for flat profiles $\bar{n}$a $\gtrsim$ 3.5 x 2 x 10^{15} cm^2. This indeed seems a minimum requirement for ASDEX Upgrade; on the other hand, we will demand that it should be achievable even respecting the Murakhami-limit on the possible plasma densities.

Since the original suggestions of the existence of a limit on density $\bar{n} \lesssim \alpha \cdot B_t/R$, considerable improvements have been made in the actual value of the proportionality constant α, and an additional dependence on the safety factor (as expressed by the so-called Hugill diagram) has been established. In some experiments in ISX-B and PDX the possibility of exceeding this limit in the presence of strong additional heating – an absolute requirement for the achievement of INTOR's goals and the feasibility of a reactor – have also been demonstrated. The parameter B_t/R does remain, however, a valid figure of the merit for comparing different devices.

A requirement on $\bar{n}$a then corresponds, because of $\bar{n}a \lesssim \alpha \cdot B_t/R \cdot a = \alpha \cdot B_t/A$ to a lower limit on B_t/A. Inserting values from the highest density discharges in ASDEX ($\bar{n}$ = 8 x 10^{13} cm^2, a = 40 cm, R_0 = 165 cm at B_t = 2.2 T), and a postulated $\bar{n}a \gtrsim 7 \times 10^{15}$ cm^{-2}, suggests an ASDEX Upgrade requirement of $B_t/A \gtrsim 1.2$ Tesla.

This value corresponds also very closely to INTOR parameters (B_t = 5.5, R/a = 4.4), implying that both devices will reach during the ohmic heating phase the same value of $\bar{n}a$. ASDEX Upgrade will thus also give information about the INTOR density build-up process during additional heating, starting out from very similar penetrability conditions.

The above criterium does not specify absolute dimensions or densities; strong arguments exist, however, for operating ASDEX Upgrade in a density (particularly boundary-density)-regime close to that of INTOR or a reactor:

- Under Alcator-Intor scaling, temperature profiles, at given power flux, are similar as a function of distance from the boundary, independently of density. To have them similar at the same time also as a function of $\int_r^a$ n dr (for equal CX sputtering behaviour) requires therefore identical densities.
- Some of the processes in the boundary layer, like radiation losses or collisional power transfer between ions and electrons depend quadratically on density, requiring comparable values of n_e for their simultaneous simulation.
- The refuelling flux should be a strong function of the density in the boundary layers. Changing the latter considerably between ASDEX Upgrade and INTOR would change the particle to energy flux ratio, which is expected to be important for the physics of the plasma to wall power transfer.

2.3.3 Pulse length requirements

The pulse lengths for all systems should be chosen large enough to allow the physical effects of interest to come into stationary equilibrium. For the experiment in question, the longest time constants are given by the establishment of a stationary plasma current distribution, and by plasma-wall interaction processes.

The characteristic time for the adjustment of current distributions (which is shorter than the L/R time by approximately the ratio of internal to total inductance of the discharge) depends on electron temperature, Z_{eff} and dimensions. For the proposed design, with Z_{eff} = 1 and T_{e0} = 4 keV, it would amount approximately to 5 sec.

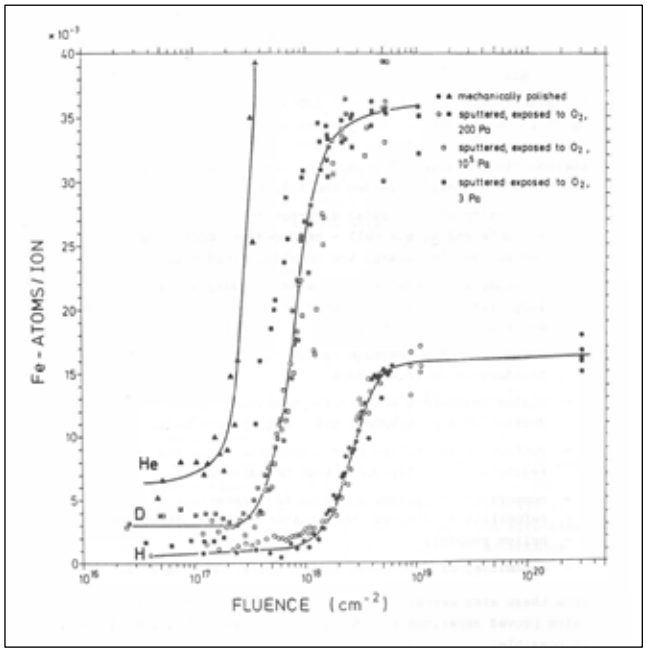

Fig. 9 Effect of wall conditioning and ion fluence on the sputtering yield from steel surfaces (from /19/).

Among the wall interaction processes, particularly the dependence of the sputtering yield on the fluence of hydrogen atoms hitting sample walls shown in fig. 9 seems to be important in determining necessary discharge lengths. The time required to reach the asymptotic regime of large (clean metal) sputtering rates depends on the refuelling fluxes required to maintain the desired density regime of $n \gtrsim 1.5 \times 10^{14}$ cm^{-3}; it is, however, typically to be expected 10 sec or larger.

3. The Aims of ASDEX Upgrade

The general reasoning behind an ASDEX successor or an upgraded ASDEX is to investigate the physics of a divertor tokamak as close as possible to fusion reactor requirements without thermonuclear heating. The physical considerations discussed in the preceding section yielded the following aims:

- production of a poloidal divertor tokamak configuration - double and single null - produced and controlled by coils located mainly outside the toroidal field coils;
- a plasma line density and plasma boundary density sufficiently large for screening energetic CX neutrals from the plasma in order to reduce sputtering from the walls;
- production of an average energy flux through the plasma boundary of up to 0.3 MW/m^2;
- plasma parameters and heating scenarios suited to the production of a photosphere and a cold plasma mantle;
- control of impurities by divertor operation and/or by self-regulating impurity production mechanisms;
- comparison of limiter and divertor operation; refuelling in divertor and limiter operated discharges helium pumping;
- capability of lang-pulse plasma operation $t_p \approx 10$ s.

From these aims certain conditions and requirements were derived using proved experimental tokamak physics and technology as far as possible.

(gekürzt um Kapitel 4 bis 5.7)

5.8 Summary of ASDEX Upgrade design data (reference system)

According to the above described considerations the following data were selected as basis for a detailed ASDEX Upgrade design.

The TF magnet consists of N = 16 double pan cake coils.

	mode I	mode II
magnetic field on axis	$B_0 = 3.2$ T	3.9 T
radius of inner coil leg	$R_i = 0.68$ m	
radius of outer coil leg	$R_a = 2.92$ m	
thickness of coil	d = 0.37 m	
maximum conductor width	w = 0.202	
major plasma radius	$R_0 = 1.625$	
plasma aspect ratio	A = 3.25 m	
density parameter	$c = B_0/A = 1.0$	c = 1.2
TF current density in throat	$j_{TF} = 16.4$ MA/m^2	20 MA/m^2
filling factor (TF)	f = 0.7	
TF magnetic energy	$W_m = 280$ MJ	415 MJ
TF ohmic power loss	P = 81 MW	120 MW
TF-excitation time	$t_A = 7$ sec	10 sec
<u>Plasma current</u> (for q = 1 at R = R_0)		
design value	$J_p = 1.2$ MA	1.5 MA

<u>Divertor coil, equilibrium field coil and plasma shaping coil for $J_p = 1.0$ MA plasma current</u>

divertor coil:	$R = 1.6$ m; $Z = \pm 2.2$ m; $J_1 = 2.0$ MA
equilibrium field coil:	$R_2 = 2.3$ m; $Z_2 = \pm 1$ m; $J_2 = -0{,}6$ MA
plasma shaping coil:	$R_3 = 2.45$ m; $Z_3 = \pm 0.6$ m; $J_3 = -0.3$ MA

<u>OH Transformer (central coil)</u>	
OH coil current density, design value	$j_{OH} = 40$ MA/m^2
OH coil outer radius	$R_{OH} = 0.49$ m
OH coil thickness	$\Delta R_{OH} = 0.315$ m
OH flux swing	$2\,\varnothing_{OH} = 12.5$ Vsec
For comparison:	
calculated required value for $J_p = 1.2$ MA	$2\,\varnothing_{OH\,requ.} \simeq 10$ Vsec
<u>Vacuum Vessel</u>	
Critical distance plasma - TF coil, radially	$\Delta = 0.25$ m
Available for vessel	$\Delta_{vessel} = 0.25$ m
Height of stagnation point	$h_p = 0.85$ m
Clearance between TF coil and torus midplane	$h_{TF} = 1.5$ m
Power load on vessel walls (average)	$P_v \lesssim 0.3$ MW/m^2

(Ende des Auszugs)

References

/1/ Research and Training Programme (1982-86) for the European Atomic Energy Community in the Field of Controlled Thermonuclear Fusion, EUR FU BRU/XII/627/81

/1a/ Report of the European Fusion Review Panel, June 81, EUR FU BRU/XII-715/81

/2/ "Tokamak Physics for NET", D. Düchs, F. Engelmann, Internal Working Paper of the NET/INTOR Steering Committee, Nov. 81

/3/ INTOR Phase I Conceptual Design, Vols. I and II, July 81, EUR FU BRU/XII 2/8l/EDV-50, IAEA-Vienna

/3a/ INTOR Phase IIA, Conclusions from the Third Workshop Meeting, December 81, EUR FU BRU/XII-2/81/EDV 80, IAEA-Vienna

/4a/ H. Vernickel, Nucl. Fus. 12 (1972), 386

/4b/ R. Behrisch, Nucl. Fus. 12 (1972), 695

/4c/ H. Kotzlowski, F. Mast, H. Vernickel, J. Nucl. Mat. 93+94 (1980) 442

/5/ K. Lackner, J. Neuhauser, Proc. of IAEA Meeting on Divertors and Impurity Control, Garching (1981), p. 58

/6/ ASDEX contributions to IPP Jahresbericht 1981

/7/ S. Sengoku, M. Azumi, V. Matsumoto, H. Maeda, Y. Shimomura, Nucl. Fusion 19 (1979) 1327

/8/ ASDEX-Team (presented by M. Keilhacker), Proc. of IAEA Meeting on Divertors and Impurity Control, Garching (1981), p. 23

/9/ J.C. Wesley et al., ibid., p. 32

/10/ P.J. Harbour, M.F.A. Harrison, private communication (1979)

/11/ M. Petravic et al., PPPL-1924 and D.E. Post et al., PPPL-1935

/12/ K. Behringer, W. Engelhardt, G. Fussmann and ASDEX team, ibid., p. 42

/13/ G. Becker, C.E. Singer, ibid. p. 63

/14/ A. Gibson, M.L. Watkins in Controlled Fusion and Plasma Physics (Proc. 9th Europ. Conf., Prague) 1 (1977) 31

/15/ K. Lackner, K. Behringer, W. Engelhardt, R. Wunderlich, IPP 1/195 (1981)

/16/ J. Neuhauser, IPP 1/182 (1980)

/17/ D.E.T.F. Ashby, M.H. Hughes, INTOR report, EURFUBRU/XII-2/81/EDV70 (1981) B.5 - 2 - Phys.

/18/ W. Feneberg, G.H. Wolf, Nucl. Fusion 21 (1981) 669

/19/ R. Behrisch et al., J. Nucl. Mat. 93:& 94 (1980) 645

CHAPTER 1: ASDEX UPGRADE—INTRODUCTION AND OVERVIEW

ALBRECHT HERRMANN* and OTTO GRUBER
Max-Planck-Institut für Plasmaphysik, 85748 Garching, Germany

Received February 27, 2003
Accepted for Publication April 15, 2003

This special issue of Fusion Science and Technology is a comprehensive review of the main physical and technological results achieved with the Axial Symmetric Divertor EXperiment (ASDEX) Upgrade located at the Max-Planck-Institut für Plasmaphysik in Garching, Germany. It includes special chapters presenting details of machine operation and control as well as results from the main topics of scientific investigations. This introductory chapter gives a survey of the aims of ASDEX Upgrade and the evolution of the scientific goals, which were accompanied by technical modifications during the more than 10 yr of operation. It presents a short overview on hardware modifications and on the scientific program. This chapter is also a summary of major scientific results, which are then described in more detail in the following chapters.

KEYWORDS: *ASDEX Upgrade, tokamak, overview*

I. THE ASDEX UPGRADE PROJECT

The tokamak fusion experiment ASDEX Upgrade is operated by the Max-Planck-Institut für Plasmaphysik in Garching, Germany. It is the largest fusion experiment in Germany and one of the leading fusion experiments worldwide. The first plasma was produced on March 21, 1991, after nearly 10 yr of planning, design, and construction. During the following years, ASDEX Upgrade was equipped with up to 30 MW of additional heating and additional diagnostic systems. Figure 1 shows a three-dimensional overview of ASDEX Upgrade together with both neutral beam injector boxes and the wave heating systems.

The ASDEX Upgrade design is based on the successful operation of the Axial Symmetric Divertor Experiment (ASDEX) and conceptual studies for a next-step fusion reactor, in particular the need for an elongated plasma shape. The purely physical divertor concept of ASDEX, with divertor coils inside the vacuum vessel close to the plasma, was adapted with ASDEX Upgrade to meet the technical requirements of a fusion reactor. The poloidal magnetic field coils, which are a prerequisite to form the elongated plasma shape with an X-point, have to be outside the vacuum vessel and outside the toroidal magnetic field coils in a fusion reactor (see Fig. 2). As a consequence, the divertor chambers are no longer separated from the plasma vessel by narrow slits but are wider open. The benefit is an increased plasma volume. Even though the major plasma radius of ASDEX and ASDEX Upgrade as well as the geometry of the toroidal magnetic field coils are the same, the plasma volume and in turn the plasma current could be increased by a factor of 3 (see Table I in Chap. 2 for the main machine parameters).

The reactor-relevant plasma shape of ASDEX Upgrade is an essential prerequisite for the contribution of ASDEX Upgrade to the discussion of physical issues arising during the design of ITER. ASDEX Upgrade is close to ITER in the magnetic geometry and in particular the relative length of both divertor legs compared with the plasma dimensions. It comes close to a geometrically scaled-down version of the ITER configuration by a factor of 4, as shown in Fig. 2.

ASDEX Upgrade was designed to tackle most of the plasma boundary and first-wall problems, which can be investigated by discharges without thermonuclear heating, in particular the transfer of energy to the first wall, the control of impurities, and helium pumping. Furthermore, the improved impurity and plasma density control due to the poloidal divertor configuration allows the confinement properties of clean plasmas to be investigated. Essential plasma properties, primarily the plasma density and the wall load have been adapted to conditions that are expected in a fusion reactor. The installed heating power of up to 30 MW ensures that the energy fluxes through the plasma boundary are equivalent to those in ITER. This similarity is expressed in heating power P normalized to major plasma radius R. The ASDEX Upgrade value of $P/R = 17$ MW/m is close to the ITER design value of 24 MW/m.

*E-mail: albrecht.herrmann@ipp.mpg.de

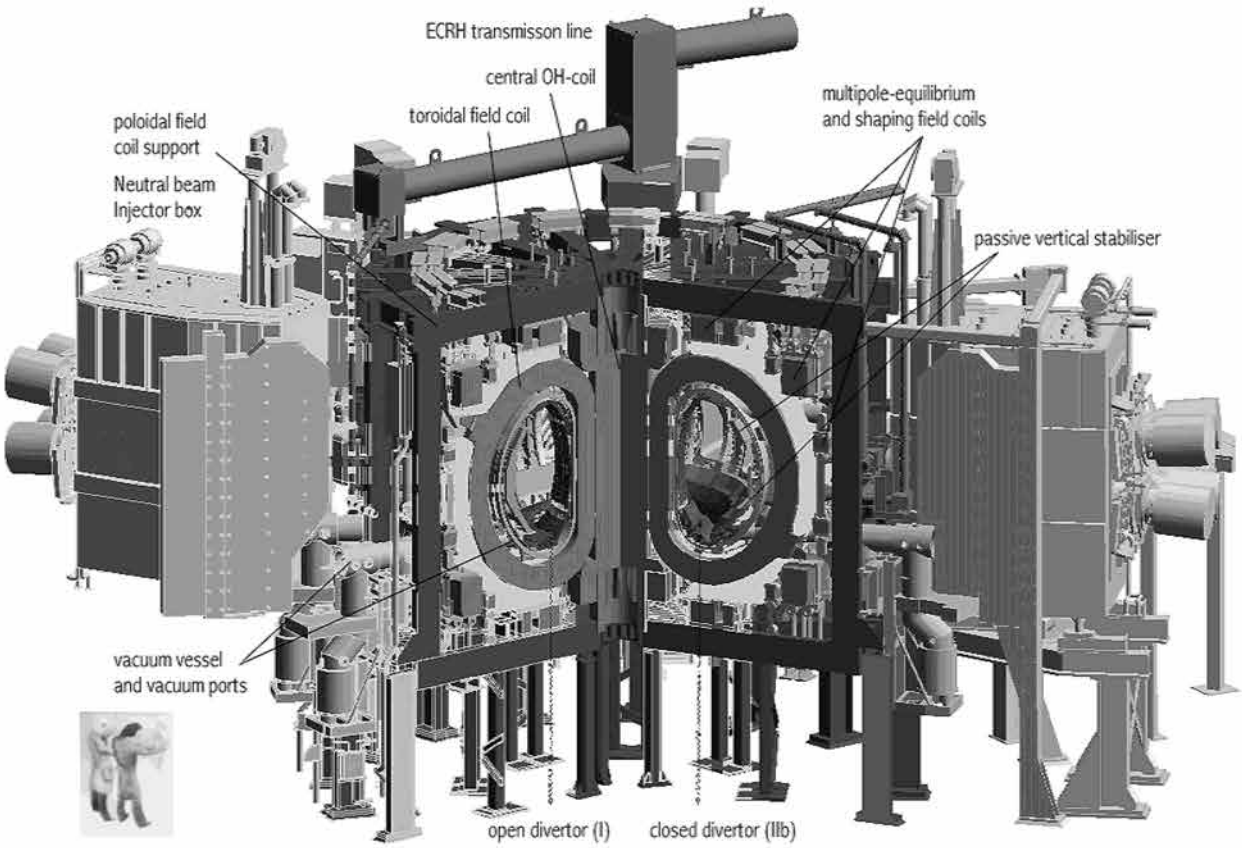

Fig. 1. Three-dimensional cutaway view of ASDEX Upgrade with heating systems and two different divertor configurations. Left: the open divertor I; right: the closed divertor IIb configuration.

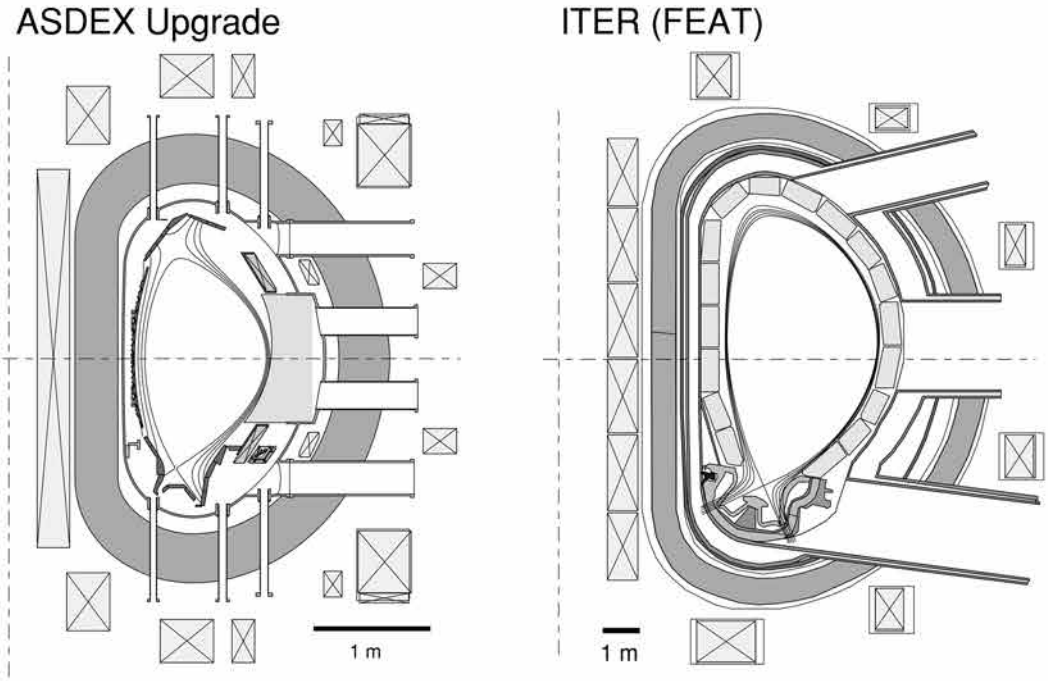

Fig. 2. Cross section of ASDEX Upgrade and ITER.

During the years of operation, the scientific program has expanded according to the needs of the ITER design, as discussed in detail in Sec. II. Thereby, a significant part of the scientific program, e.g., the investigation of the relation between core physics and plasma edge, was only possible due to the high degree of flexibility for plasma heating scenarios. The scientific progress during the years of ASDEX Upgrade operation as well as the hardware evolution is summarized in Fig. 3.

The ASDEX Upgrade Program has strong international links, both within the EURATOM associations (see Appendix B) and the United States, Japan, Russia, and Korea. With the increasing number of experiments proposed by collaborators, a formal structure was needed in order to allow the associates to be involved in the decision-making process for the ASDEX Upgrade Program. This was started in 2001 by opening the ASDEX Upgrade Program Committee to the European associates.

II. HARDWARE ENHANCEMENTS

Major modifications were performed during the operation of ASDEX Upgrade to expand the experimental possibilities and to contribute to the discussion of the ITER design. The main steps are shown in Fig. 3.

The replacement of carbon by tungsten-coated divertor plates in 1996 was the first step in the tungsten program to investigate tungsten erosion, deposition, and transport in divertor configurations. After 2 yr of tungsten divertor operation, the open flexible divertor with flat divertor plates was replaced by a closed optimized divertor in 1997, Div II. The design of the new divertor was based on experimental experience with the open divertor configuration and on results from code calculations. It was aimed at the investigation of pumping and radiation capability, as well as the heat flux handling of closed divertor structures and as an experimental basis for the ITER divertor design. In parallel with the change of the divertor geometry, the available heating power was nearly doubled by installing a second neutral beam injector box with four 100 kV beams and 10 MW total heating power (first box 58 kV, 10 MW). Together with the wave heating systems [8 MW ion cyclotron resonance heating (ICRH), 2 MW electron cyclotron resonance heating (ECRH)] a heating power of 30 MW is available for experiments with reactor-relevant heat fluxes in the scrape-off layer. The surplus of heating power

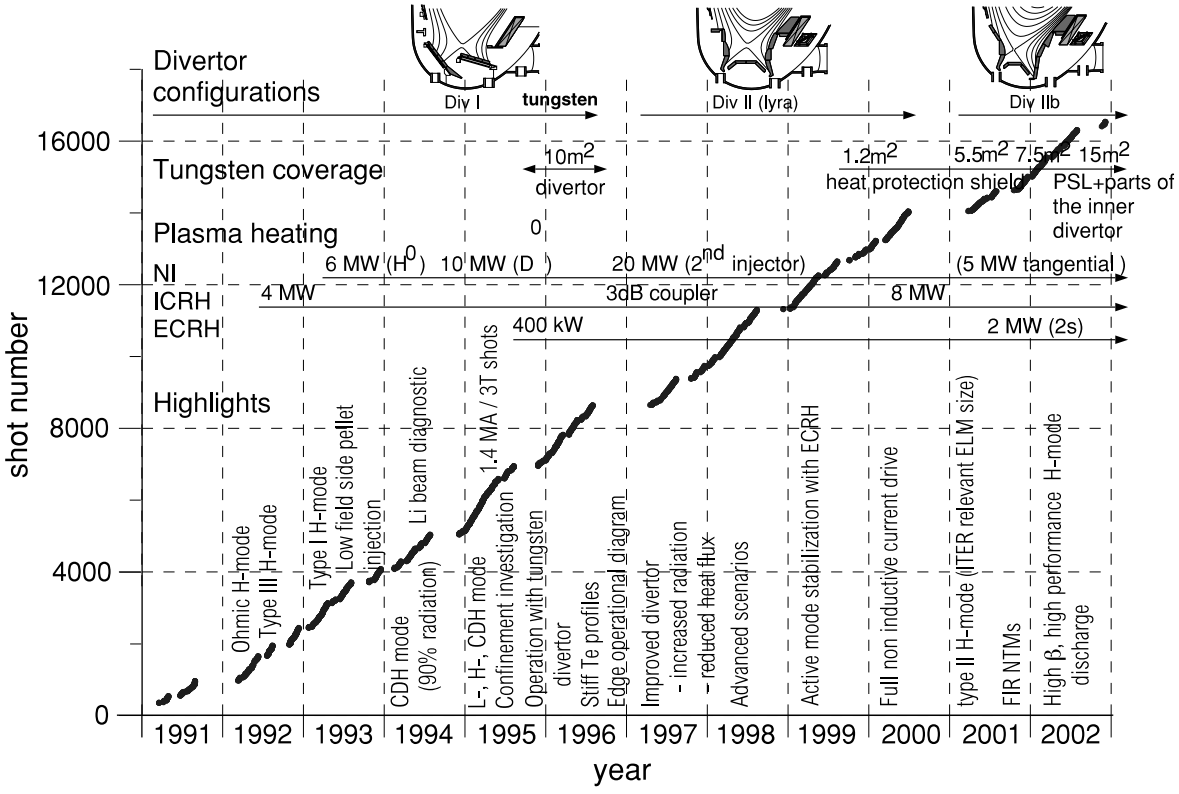

Fig. 3. Overview of ASDEX Upgrade operation. The gaps in the line for the accumulated number of shots mark shutdown periods. Major hardware changes, such as increased heating power and divertor modifications, are indicated. The main physical results and the start of program topics are mentioned in the lower part of the figure.

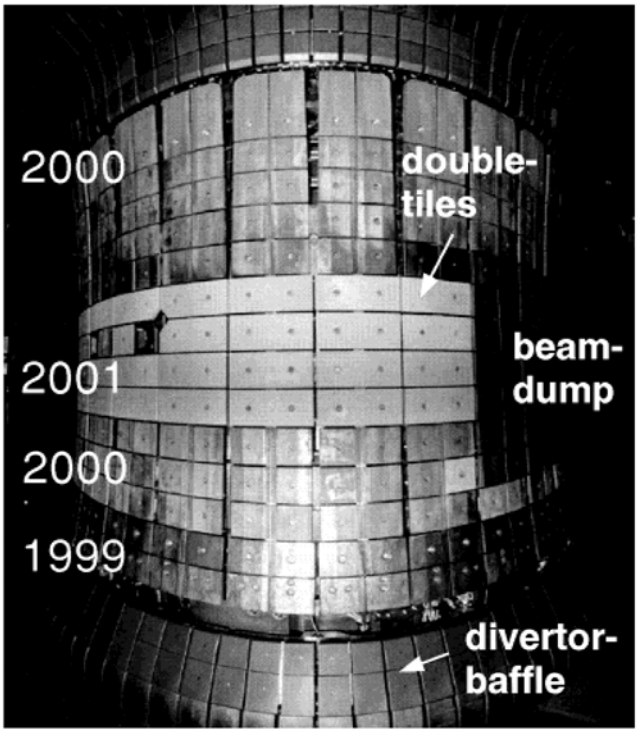

Fig. 4. The central column of ASDEX Upgrade with tungsten-coated tiles.

compared to the H-mode threshold of a few megawatts gives a high degree of flexibility to investigate the effect of heating methods and heat deposition on plasma performance and current drive—especially the investigation of density peaking and heat transport, which was only possible because of this flexibility.

Starting in 1999, inner-wall components were stepwise covered by tungsten to investigate the tungsten migration in dependence on plasma conditions (Fig. 4). The tungsten coverage of the inner heat protection shield was increased to 100%, or 7.5 m^2, during the opening in 2002. In addition, parts of the retention region of the inner divertor and the protection elements of the passive stabilizing loop at the low-field side were covered with tungsten, resulting in a total of 15 m^2 tungsten surface.

In preparation of the tungsten program, coated carbon tiles manufactured with different technologies were evaluated according to their adhesive properties under thermal load, their impurity content, and the surface coverage. It turned out that coatings deposited by plasma arc deposition with a few micrometres of thickness fulfill the requirements of ASDEX Upgrade.

The second neutral beam injector box was turned by a few degrees for tangential injection and pulled back from the plasma for off-axis current drive experiments in 2001. During this opening, the outer leg of the optimized lyre-shaped divertor was redesigned to accommodate a larger variety of plasma shapes with bottom triangularities up to 0.5 (Div IIb; see Fig. 2).

Part of the scientific program is the development and installation of diagnostics optimized for the physics problem under investigation. Approximately 70 raw data diagnostics measure different core and edge plasma parameters as well as magnetic fields, vessel temperatures, and forces. Further physical information is stored in ~200 high-level diagnostics after postprocessing of the raw data. In particular, a diagnostic using the motional stark effect to measure the q profile in the plasma core and a fast high-resolution Thomson scattering diagnostic able to measure density and temperature fluctuations on a microsecond timescale were recently installed.

III. THE SCIENTIFIC PROGRAM AND MAJOR RESULTS

The ASDEX Upgrade scientific program gives priority to the preparation of the ITER design, physics, and discharge scenarios. It consists of the study of the following:

1. confinement and performance of the ITER baseline scenario, the ELMy H-mode near operational limits, including edge-localized mode (ELM) mitigation
2. investigation of scenarios and physics of advanced tokamak plasma concepts with both internal transport barriers and improved H-mode scenarios leading to enhanced performance, long hybrid operation, and possibly steady-state operation
3. magnetohydrodynamic (MHD) stability and active stabilization of beta-limiting instabilities as well as avoidance and mitigation of disruptions
4. edge and divertor physics in high-power, high-confinement regimes to optimize power exhaust and particle control (ash removal)
5. testing of alternative first-wall materials, especially tungsten.

An overview of the achievements in these areas is given in Secs. III.A through III.G.

III.A. Confinement and Transport Studies

Confinement studies of conventional L- and H-modes indicate that the ion and electron temperature profiles are generally limited by a critical value of the temperature gradient length $(\nabla T/T)^{-1}$. The resulting stiffness of the profiles is reflected by a proportionality between core and pedestal temperatures (Fig. 5). Clearly, for stiff profiles, the edge temperature is an essential parameter for the profile behavior and, consequently, for confinement. The physical mechanism causing such a profile (self-organization phenomenon) is attributed to plasma turbulence driven by ion temperature gradient modes, trapped

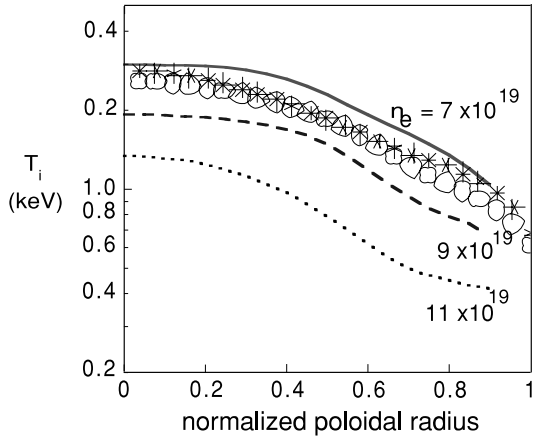

Fig. 5. H-mode ion temperature profiles measured during a density scan (lines) and for on- and off-axis heat deposition (symbols) are stiff with a constant temperature gradient length $T/\nabla T$ in the confinement region between 0.3 and 0.8 of normalized poloidal radius.

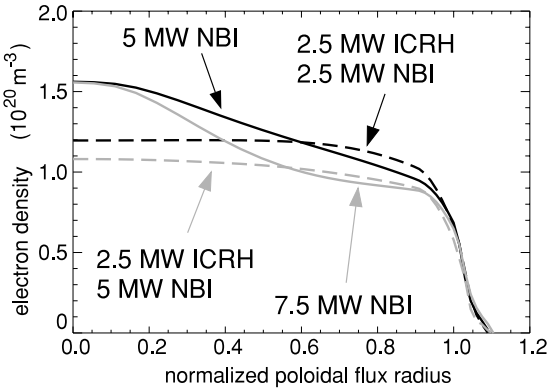

Fig. 6. Central heating (in this experiment by ICRH) results in flat profiles. The profiles taken from deconvolution of interferometry and lithium beam.

electron modes, and possibly electron temperature gradient modes, which cause a strong increase of the heat transport for temperature gradient lengths below the critical value.

III.B. Particle Transport, Fueling, and Density Profiles

Density control by strong gas puffing from the plasma edge is accompanied by a reduction of the edge temperature and, through profile stiffness, by confinement degradation. Peaking of the density profiles due to anomalous transport or due to central plasma refueling by pellets can avoid this degradation. Plasma refueling with pellets is more effective with high-field-side pellet injection because drift effects accelerate the ablated pellet material radially toward the outside of the torus.

Investigation of discharges with density peaking reveals that the equilibration time for peaked profiles can be much longer than the energy confinement time. The shape of the density profiles depends on the heat deposition profile (Fig. 6). At high density, these findings are described well by an empirical model coupling the particle diffusivity to the anomalous heat diffusivity and taking into account an inward pinch comparable to the neoclassical one. In this picture, density peaking is strongly reduced by central heating due to the increase of turbulent transport, which also causes an increase of particle transport. At low density, however, a turbulent inward pinch is needed to explain the density peaking, consistent with theoretical modeling.

III.C. Advanced Scenarios

Advanced scenarios seek to improve the confinement and stability of plasmas over the standard H-mode plasmas with stiff temperature profiles. Such an improvement of plasma performance can be achieved by tailoring the q profile, either in combination with density peaking and suppression of confinement degradation at high density (advanced H-mode) or suppressing the turbulent radial transport, i.e., breaking the temperature profile stiffness in an internal transport barrier. A further goal is the development of noninductive-driven discharges by current profile optimization.

Steady-state advanced H-mode plasmas combine improved core confinement through density peaking with an ELMy H-mode edge and stiff temperature profiles. At moderate densities ($\bar{n}/n_{GW} \approx 0.3$) and low triangularities, the pulse length can be up to 6 s or 40 energy confinement times, only limited by the duration of the neutral beam injection (NBI). The highest fusion product obtained in such discharges is $n_0 T_0 \tau_E = 1.1 \times 10^{20}$ m$^{-3}\cdot$keV$\cdot$s. A further performance increase is prevented by neoclassical tearing modes, which are the limiting instability for monotonic q profiles.

These discharge scenarios were extended to densities above 85% of the Greenwald density limit and a good confinement with $H_{ITER98\text{-}P} = 1.2$ in steady state. The plasma configuration in these experiments is shaped with high triangularity ($\delta = 0.45$) and a nearly double-null configuration. In addition, the ELM characteristic changes significantly from type I to favorable type II ELMs (Fig. 7). This could be a favorable ITER scenario for a 5000-s-long hybrid operation with a large fraction of noninductive current drive.

Internal transport barriers are usually obtained through strong additional heating in the current rampup phase with an L- or H-mode edge. The magnetic shear is transiently reversed in the center, and internal transport barriers form with central ion temperatures above 20 keV and high global performance of $H_{ITER89\text{-}P} = 3.0$ and $\beta_N = 4$. However, this internal transport barrier regime is limited by continuous evolution of the current profile, which, without an off-axis current drive method, could

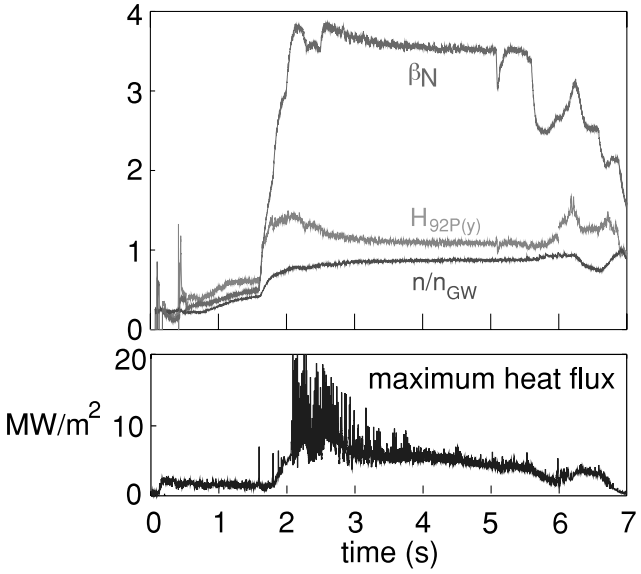

Fig. 7. High β_N discharge with reduced ELM activity as seen in a reduction of the maximum heat flux.

not be prevented and finally leads to a termination of the barrier by MHD instabilities in the core or edge.

The fraction of inductively driven current can be reduced by increasing the fraction of bootstrap current, generated by the pressure gradient. To achieve this, the poloidal β was maximized by operation at low plasma current (400 kA) and sufficiently high heating power. The fraction of noninductive-driven current from the combination of a large fraction of bootstrap current (~50%) and neutral-beam-driven current is nearly 100%.

III.D. MHD Stability

The MHD instabilities pose a severe limit on the accessible operational space and, in particular, on the confined plasma pressure. The instability with the most impact on plasma performance in standard H-mode discharges is the neoclassical tearing mode (NTM). The onset β of these modes scales dominantly with the normalized ion gyro radius and may result in a severe limit for ITER. Therefore, adequate tools for avoiding or stabilizing such modes are essential.

In discharges with high heating power and, hence, high β_N values, a regime was observed in which NTMs never reach their saturated size because of a repeated abrupt reduction of the mode amplitude due to the coupling between a fast-growing ideal $(m + 1, n + 1)$ mode with the (m,n) NTM in the presence of the (1,1) mode. This frequently interrupted mode regime (FIR) results in a confinement recovery.

Active stabilization of NTMs can be achieved with electron cyclotron current drive replacing the missing bootstrap current in the magnetic islands. At β_N near 2.5, a (3,2) mode could be completely stabilized by applying electron cyclotron current drive power of ~10% of the total heating power. Once the mode is stabilized, the normalized beta can be raised above the onset value if the total heating power is increased and the electron cyclotron current drive is on (Fig. 8).

III.E. Plasma-Edge-Related Operation Boundaries

It has been shown that various operation boundaries have their cause at the plasma edge and can be summarized by combining the edge parameter dependence of various operational regimes in a single diagram (edge operation diagram, Fig. 9). The operational space in this diagram is limited at high edge pressure gradients by ideal instabilities. A lower temperature limit is given by the onset of a MARFE thermal instability below $T_e \approx$ 90 eV, which occurs at sufficiently high edge density. The L-H threshold in terms of local parameters is

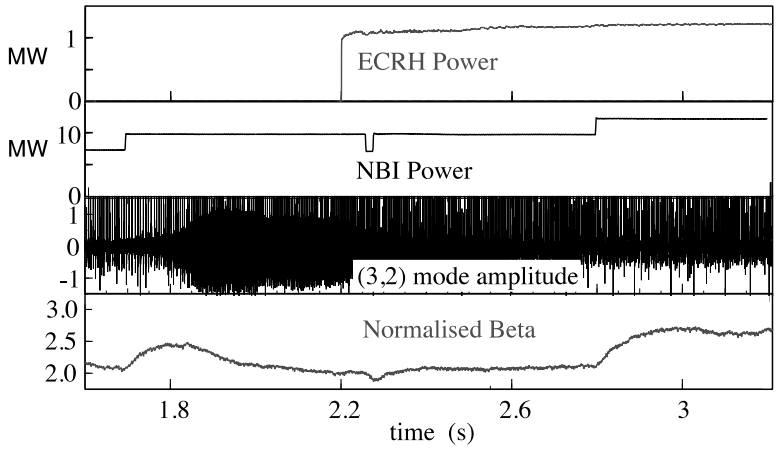

Fig. 8. Stabilization of neoclassical tearing modes with electron cyclotron current drive as indicated by the amplitude of the $m = 3$, $n = 2$ magnetic perturbations. Value $\beta_N = 2.6$ was achieved in steady state without these modes by raising the neutral beam power.

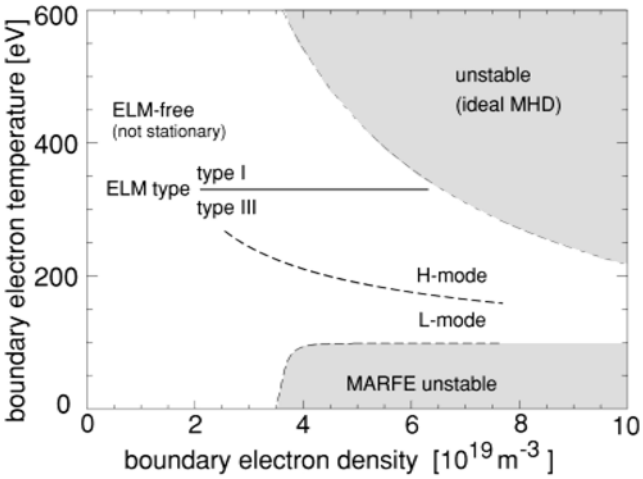

Fig. 9. Edge operational diagram for low triangularity configuration showing regime boundaries. Values T_e and n_e are taken 2 cm inside the separatrix to represent absolute values as well as gradients.

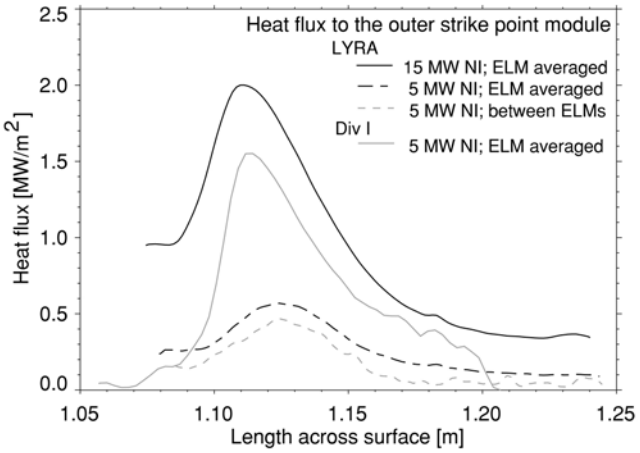

Fig. 10. Heat flux onto the outer divertor strike point module in the lyre-shaped divertor compared to DIV I.

represented by a critical temperature. The type of ELMs changes with increasing pedestal temperature with a small ELM-free region in between.

Type I ELMs are likely to cause an intolerable energy impact on the divertor of next-step fusion experiments. A favorable operational point in this diagram was found with the occurrence of type III ELMs near the ideal pressure limit at high densities and high power flux using feedback-controlled impurity seeding (completely detached H-mode). At higher triangularities, the confinement with type I ELMs is superior to type III ELM scenarios. Mitigating the type I ELM heat flux without significant loss of plasma confinement is essential. This is investigated by triggering frequent ELMs, which expel particles and energy from the plasma edge through pellets.

A second operational window that avoids type I ELMs but keeps the good confinement, also at high density, is the H-mode regime with type II ELMs, which was obtained at somewhat elevated q_{95} and an averaged triangularity of $\delta > 0.35$. As in the high β_N discharges, the magnetic configuration has to be close to double null to increase the magnetic shear. For these conditions, steady-state type II H-modes without any type I ELM were observed, limited only by the length of the plasma-current flattop phase. The energy confinement is close to that of type I ELMy H-mode, and the target load is quasi steady state without temporal variations.

III.F. Divertor Physics

A principal purpose of ASDEX Upgrade is to test concepts for power and particle exhaust. ASDEX Upgrade started with an open divertor configuration, DIV I, characterized by flat horizontal divertor plates made from fine-grain graphite. It was replaced later by the fairly closed lyre-shaped divertor, DIV II, to test the physics underlying the proposed ITER divertor. The geometry was optimized to increase the ionization of hydrogen neutrals around the separatrix and reduce the target heat flux (Fig. 10), especially close to the separatrix. The observed reduction of the ELM-averaged power flow by a factor of 2, compared to the open DIV I divertor, results from an increased radiative power loss in the divertor region. With DIV II, ~45% of the input power is radiated below the X-point, and most of the divertor radiation is concentrated in a small emission zone along the separatrix as predicted by theoretical modeling. The enhanced divertor radiation is due to an increased radiation efficiency of carbon and hydrogen in the divertor plasma. Carbon cools the scrape-off layer plasma down to the 5-eV region, where the hydrogen losses become significant.

DIV II was also optimized for particle compression, which is of particular interest because it determines the pumping efficiency and the degree of particle control. Hydrogen and helium compression is much larger in DIV II than in the open divertor DIV I, as predicted by modeling. The resulting ratio of helium/energy replacement times, which has to be below 10 to 15 for a burning plasma not to be extinguished by the helium ash, is between 4 and 6.

III.G. Plasma-Wall Interaction and First-Wall Material

The use of carbon as a first-wall material in ITER may be impossible due to the chemical erosion and the tritium enrichment in deposited layers. A candidate material is tungsten, which exhibits much more favorable properties with respect to erosion at low-impact energies and other physical properties than carbon. The qualification of tungsten as first-wall material is investigated in

a multistep program toward a carbon-free machine. In the first step, the fine-grain graphite plates of the open divertor DIV I were coated with tungsten. More than 90% of the investigated discharges show tungsten concentrations below the critical concentration for a burning plasma of 2×10^{-5}. A few discharges showed tungsten accumulation due to a comparatively strong inward drift.

In the next step, in 1999, ASDEX Upgrade started with a program to replace the inner vessel carbon tiles by tungsten (Fig. 4). In four steps, the inner heat protection shield and the baffle of the divertor at the high-field side as well as parts of the wall at the low-field side were covered by tungsten so that the total tungsten covered surface is at present ~15 m^2. Again, the tungsten concentration was below the critical concentration. For high core confinement discharges with peaked density profiles that are sensitive to impurity accumulation, a scenario with central ECRH or ICRH was developed to control tungsten accumulation by reducing the impurity inward transport. This is possible due to the relation between heat and particle transport as discussed in Sec. III.B and Chap. 7.

In parallel to the tungsten program, the carbon migration and the mechanism for the buildup of carbon layers below the divertor structure were investigated spectroscopically and with electrical and deposition probes. The existence of a parasitic plasma below the divertor structure was detected.

IV. OUTLINE

This issue is organized as a review of ASDEX Upgrade results and its technical basis. The topics are organized into chapters, written by different authors. The authors have summarized our results, to which other team members have also significantly contributed.

The issue starts with a technical chapter about the machine design and the different heating systems installed at ASDEX Upgrade. The available auxiliary heating power of 30 MW, supplied by three different heating systems, allows the power deposition to be varied and species heated over a large range. Three heating systems—neutral beam, ion cyclotron, and electron cyclotron heating—are presented in detail in Chap. 2. That chapter also includes a description of the pellet refueling system, which is successfully used for density control, as discussed later.

Machine protection and active control of plasma position and plasma shape is essential for the successful operation of ASDEX Upgrade. The reactor-relevant set of distant poloidal field coils makes possible the simultaneous control of a subset of shape parameters to a multivariable problem. The components of these control systems as well as the tools for supervision and machine protection are presented in Chap. 3. That chapter also presents the means for advanced plasma performance control acting on particle fueling and auxiliary heating power systems with single-value feedback controllers.

The technical chapters are followed by a presentation of results from the physics program. This does not include diagnostics and their development.

Advanced tokamak investigations are designed to improve confinement and maximize β to achieve a higher efficiency at a given reactor size. Four scenarios are discussed in Chap. 4:

1. the formation and perpetuation of internal transport barriers for both ions and electrons in reversed magnetic shear discharges with $q_{(min)} \sim 2$
2. full noninductive steady-state current drive scenarios at lower plasma currents and high β_{pol}
3. improved confinement H-modes in weak magnetic shear discharges with $q_{(axis)}$ close to 1
4. integrated high β_N high-triangularity discharges with moderate type II ELMs.

The transport of heat in the core plasma studied by dedicated steady-state and modulated electron cyclotron heating experiments is discussed in Chap. 5. In particular, the mechanism resulting in stiff temperature profiles is reported. These stiff profiles couple the plasma edge with the core plasma. Their understanding and active control are essential for core plasma performance as discussed in this chapter.

The presence of a transport barrier at the plasma edge is a prerequisite for the high-confinement mode (H-mode) and an essential part of the main operation scenarios at ASDEX Upgrade. In Chap. 6, the findings of the H-mode threshold scaling with local and dimensionless parameters, transport barrier properties, and limiting instabilities are presented. Chapter 6 also includes a discussion of ELM types in relation to edge parameters.

Operation at high densities without loss of plasma performance is required for ITER operation. Results of high-density H-mode operation are presented in Chap. 7. In particular, the H-mode density limit, density profile peaking, and pedestal density behavior are discussed. The relation between density and the heat flux profile is investigated and modeled.

A main purpose of ASDEX Upgrade is to test concepts for power and particle exhaust. Energy and particle transport in the scrape-off layer and the different divertor configurations of ASDEX Upgrade are presented in Chap. 8. The radiation capability, heat flux deposition patterns, and the temporal heat flux evolution during ELMs in the divertor are discussed and compared to results of computer modeling. Steep gradients of plasma parameters, such as density, electron, and ion temperature profiles at the plasma edge require adequate diagnostics capable of resolving spatial structures of a few millimetres. The double structure of the observed profiles is described by radial transport governed by critical

gradients near the separatrix and rapid diffusion or even outward drift in the cold scrape-off layer wing.

Magnetohydrodynamic instabilities are performance limiting for high-confinement plasmas. Chapter 9 presents the experimental database of ASDEX Upgrade in the light of theoretical models for rise and control of magnetic islands together with experiments for active control of the size of magnetic islands by modulated and nonmodulated electron cyclotron current drive. Furthermore, instabilities driven by suprathermal particles and the effect of MHD instabilities on advanced scenarios are discussed.

One of the most important design issues for ITER is the choice of plasma facing materials, in particular for the divertor components. In most of the present-day tokamaks, carbon is used as a divertor material due to the good heat flux handling capacity combined with the relatively low Z. However, it has disadvantages, which might be unacceptable in a future fusion device so that it has to be replaced by a reactor-capable material. Studies of carbon erosion and migration, as well as experiments with tungsten as a plasma facing material, are presented in Chap. 10.

Understanding and active control of impurity transport and accumulation is essential to achieving a burning plasma. Dedicated experiments were performed to investigate impurity migration. In combination with transport simulations in terms of anomalous and neoclassical transport, the transport mechanism could be revealed, and the transport coefficient for different impurity species was extracted. The results of core and edge impurity transport investigations are discussed in Chap. 11.

Tokamak plasma discharges can be disrupted by major instabilities, which lead to a fast and irreversible loss of thermal confinement and cause electromagnetic forces that the vessel structure will be designed to withstand. Studies of disruptions seek to understand the physical mechanism, the effect on the machine, and the development of mitigation strategies. Results are presented in Chap. 12.

Advanced tokamak scenarios require a control of the plasma parameters and their profiles. The current profile is especially influenced by dedicated heating scenarios or by externally driven noninductive plasma currents. Experiments with advanced scenarios based on the current drive capability of ASDEX Upgrade are presented in Chap. 13.

V. BIBLIOGRAPHY

Confinement and Core Transport Studies

1. F. RYTER et al., "Confinement and Transport Studies of Conventional Scenarios in ASDEX Upgrade," *Nucl. Fusion*, **41**, 537 (2001).

2. A. G. PEETERS et al., "Transport Analysis of ITB Discharges," *Proc. 18th IAEA Conf. Fusion Energy*, Sorrento, Italy, October 2000 (CD-ROM).

Density Profiles and Fueling

1. J. STOBER et al., "Optimization of Confinement, Stability and Power Exhaust of the ELMy H-Mode in ASDEX Upgrade," *Plasma Physics Contr. Fusion*, **43**, A39 (2001).

2. P. LANG et al., "High Density Operation in H Mode Discharges by Inboard Launch Pellet Refuelling," *Nucl. Fusion*, **40**, 245 (2000).

Advanced Tokamak Discharges and Internal Transport Barrier

1. O. GRUBER et al., "Stationary H-Mode Discharges with Internal Transport Barrier on ASDEX Upgrade," *Phys. Rev. Lett.*, **83**, 1787 (1999).

2. R. WOLF et al., "Performance Heating and Current Drive Scenarios of ASDEX Upgrade Advanced Tokamak Discharges," *Nucl. Fusion*, **41**, 1259 (2001).

3. A. C. C. SIPS et al., "Steady State Advanced Scenarios at ASDEX Upgrade," *Plasma Phys. Contr. Fusion*, **44**, B69 (2002).

Active MHD-Mode Stabilization

1. H. ZOHM et al., "The Physics of Neoclassical Tearing Modes and Their Stabilisation by ECCD in ASDEX Upgrade," *Nucl. Fusion*, **41**, 197 (2001).

2. S. GÜNTER et al., "High-Confinement Regime at High β_N Values Due to a Changed Behaviour of the Neoclassical Tearing Modes," *Phys. Rev. Lett.*, **87**, 275001 (2001).

Divertor Physics and ELM Mitigation

1. O. GRUBER et al., "Observation of Continuous Divertor Detachment in H-Mode Discharges in ASDEX Upgrade," *Phys. Rev. Lett.*, **74**, 4217 (1995).

2. A. HERRMANN, "Overview on Stationary and Transient Divertor Heat Loads," *Plasma Physics Contr. Fusion*, **44**, 883 (2002).

3. J. NEUHAUSER et al., "Transport into and Across the Scrape-Off Layer in the ASDEX Upgrade Divertor Tokamak," *Plasma Physics Contr. Fusion*, **44**, 855 (2002).

Plasma Performance with Tungsten Covered Surfaces

1. R. NEU et al., "The Tungsten Divertor Experiment at ASDEX Upgrade," *Plasma Phys. Contr. Fusion*, **38**, A165 (1996).

2. V. ROHDE et al., "Operation of ASDEX Upgrade with High-Z Wall Coatings," *Proc. 18th IAEA Conf. Fusion Energy*, Sorrento, Italy, October 2000, IAEA-CN-77/EXP74/24 (2001).

➜ H. Meyer et al.: Overview of physics studies on ASDEX Upgrade, in: Nuclear Fusion, 2019

JET

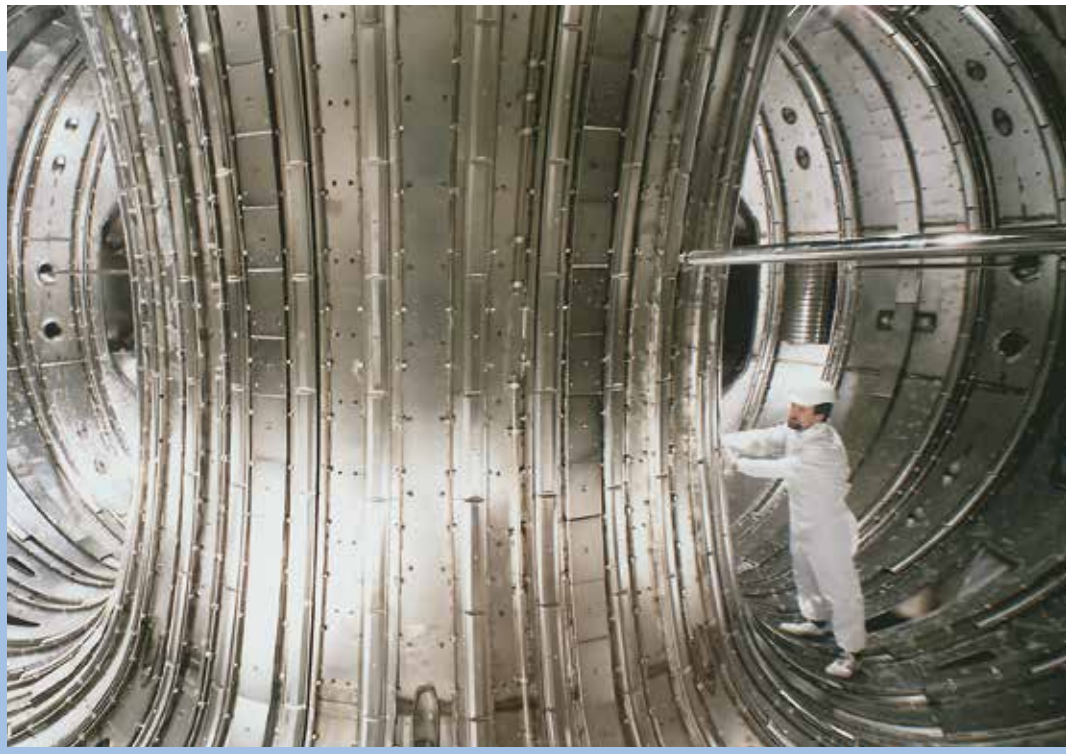

Der Joint European Torus (JET), hier das Plasmagefäß, ging 1983 in Betrieb.

Foto: JET Joint Undertaking

Future Programme

Introduction

In 1978, the original objectives of JET were set out in the JET Design Proposal, EUR JET-R5, as follows:

'The essential objective of JET is to obtain and study a plasma in conditions and dimensions approaching those needed in a thermo-nuclear reactor. These studies will be aimed at defining the parameters, the size and the working conditions of a Tokamak reactor. The realisation of this objective involves four main areas of work:

i) the scaling of plasma behaviour as parameters approach the reactor range;

ii) the plasma-wall interaction in these conditions;

iii) the study of plasma heating; and

iv) the study of alpha-particle production, confinement and consequent plasma heating.

The problems of plasma-wall interaction and of heating the plasma must, in any case, be solved in order to approach the conditions of interest.

An important part of the experimental programme will be to use JET to extend to a reactor-like plasma, results obtained and innovations made in smaller apparatus as a part of the general tokamak programme. These would include: various additional heating methods, first wall materials, the control of the plasma profiles and plasma formation.'

Objectives of JET

The essential objective of JET is to obtain and study plasma in conditions and with dimensions approaching those needed in a thermonuclear reactor. These studies will be aimed at:

1. *Scaling of plasma behaviour as parameters approach the reactor range;*
2. *Plasma-wall interactions in these conditions;*
3. *Plasma heating; and*
4. *Alpha-particle production, confinement and consequent plasma heating.*

At the start of 1992, the Project had almost completed its planned Phase III - Full Power Optimisation Studies. The general objectives of the experimental programme were to optimise performance and to explore the domain of high performance plasmas, studying aspects of plasma physics and engineering including: profile and heating effects; exhaust phenomena; and divertor edge physics. Priority was given to study of the power and energy handling capability of newly installed plasma facing components in regimes relevant to the Next Step and to the New Phase of JET.

Extensive studies had been made in the first and third areas of work of JET's objectives: reactor relevant temperatures (up to 30keV), densities (up to $4x10^{20}m^3$) and energy confinement times (up to 1.8s) had been achieved in separate discharges. The second area of work had been well covered in the limiter configuration for which JET was originally designed. However, the highest performance JET discharges had been obtained with a 'magnetic limiter', (or X-point configuration). The duration of the high performance phase of these discharges exceeded 1.5s; this was achieved by careful design of the targets and specific operation techniques, but is limited, ultimately, by an unacceptably high influx of impurities, characterised by a rapid increase in electron density, effective ionic discharge and radiated power (referred to as the 'bloom').

The fourth area of work had been started by earlier studies of energetic particles produced as fusion products or by ion cyclotron resonance heating (ICRH). It was addressed further during 1991 by the first tokamak plasma experiments in deuterium-tritium mixtures. The high performance achieved in deuterium discharges, together with the experience gained in making substantial modifications to JET in a beryllium environment and with significant vessel activation, gave confidence that an experiment with about 10% tritium in the plasma could be performed and would provide data that could be used to plan an effective campaign of deuterium-tritium experiments in 1996.

During 1991, the JET Council had approved the policy of a stepwise approach to the introduction of tritium in advance of the full D-T phase of JET operations. As a first such step, after having obtained all necessary regulatory approvals, JET successfully carried out a preliminary tritium experiment (PTE-1) in November 1991 (as already described). A release of fusion energy in the megawatt range in a controlled fusion device had been achieved for the first time in the world.

The most recent experiments on JET achieved plasma parameters close to breakeven values for about a second, resulting in large bursts of neutrons. However, in spite of the pulse continuing for many seconds after reaching peak plasma values, the neutron count fell away rapidly as impurities entered the plasma and lowered its performance. This limitation on the time for which near-breakeven conditions could be maintained is due to poisoning of the plasma by impurities (the "bloom"). This has further emphasised the need to provide a scheme of impurity control suitable for a Next Step device.

At its meeting on 19 December 1991, the Council of Ministers adopted Decisions concerning the Euratom Fusion Programme in the period to the end of 1994 and a modification to the Statutes of JET, which prolonged its statutory lifetime by four years until 31

December 1996. The extension will allow JET to implement the new Pumped Divertor Phase of operation, the objective of which is to establish the effective control of plasma impurities in operating conditions close to those of the Next Step. This programme of studies will be pursued before the final phase of full D-T operations in JET.

During 1992, a large proportion of JETs effort was devoted to shutdown work for the new pumped divertor phase of operations. The first stage of the shutdown in 1992 involved removal of components and replacement of faulty toroidal magnetic field (TF) coils. The second stage involves assembly of the four divertor coils and casings inside the vacuum vessel and this was in progress at the end of the year. It is believed to be the first time that full manufacture and assembly of coils has been undertaken in such a confined space, and the work is being done to demanding standards to ensure the highest reliability during subsequent operations. Intensive design and procurement activities for the pumped divertor components to be installed in the third stage of the shutdown have continued.

JET Strategy

Present achievements show that the main objectives of JET are being actively addressed and substantial progress is being made. The overall aim for JET can be summarised as a strategy "to optimise the fusion product ($n_i T_i \tau_E$)". For the energy confinement time, τ_E, this involves maintaining, with full additional heating, the values that have already been reached. For the density and ion temperature, it means increasing their central values $n_i(0)$ and $T_i(0)$ to such an extent that D-T operation would produce alpha-particles in sufficient quantities to be able to analyse their effects on the plasma.

The enhancements to JET aim to build up a high density and high temperature plasma in the centre of the discharge (with minimum impurity levels) where alpha-particles could be observed, while maintaining an acceptably high global energy confinement time τ_E. The mechanisms involved are to decouple the temperature profile from the current density profile through the use of lower hybrid current drive and neutral beam injection to ensure that, at higher central temperatures, the current density in the centre does not reach the critical value that causes sawteeth oscillations.

This involves the following:

a) Increasing the Central Deuterium Density, $n_D(0)$, by:
   - injecting deuterium pellets and high energy deuterium beams to fuel the plasma centre and dilute impurities;
   - injecting pellets to control the influx of edge material;
   - stabilising the m=2, n=1 magnetic oscillations present at the onset of a disruption with magnetic perturbations produced

from a set of internal saddle coils which will be feedback controlled;

b) Increasing the Central Ion Temperature, $T_i(0)$, by:
   - trying to lengthen the sawtooth period;
   - controlling the current profile (by lower hybrid current drive in the outer regions, and by counter neutral beam injection near the centre) to flatten the profile;
   - on-axis heating using the full NB and ICRF additional heating power (24 MW, ICRH, and 20MW, NB);

c) Increasing the Energy Confinement time, τ_E, by:
   - increasing to 6MA the plasma current in full power, H-mode operation in the X-point configuration;

d) Reducing the impurity content, by:
   - using low Z first-wall material (such as beryllium) to decrease the impurity content;
   - controlling new edge material by using the pumped divertor configuration.

In parallel, preparations for the full D-T phase of operations have continued. In particular, JET has completed installation of all the main components of the active gas handling system and commissioning is underway. At the end of the shutdown, JET will be in a position to begin its programme of operations to demonstrate effective methods of power exhaust and impurity control in operational conditions close to those envisaged for ITER before the final phase of full D-T operations. ITER relevant studies will provide stimulation to JET and JET's results will make an important contribution to the development of the ITER design. The following sections describe such studies underway on advanced divertor systems.

Advanced Divertor Studies

Introduction and Overview

The present pumped divertor programme consists of two phases. In the first (Mark I), inertially-cooled target blocks of carbon fibre composite (CFC) or beryllium are mounted on a water-cooled support structure to speed cooling between discharges. The second version, for installation in 1995, was based upon actively-cooled copper elements to which thin beryllium plates were brazed ("Hypervapotrons") to permit thermally steady state operation at high powers.

During 1992, an ad hoc Advanced Divertor Study Group was set up to study the question of possible improvements to the pumped divertor, for the purpose of optimising its performance and reliability. At that time, the Mark I design was nearly finished, but the Mark II design was only partly completed.

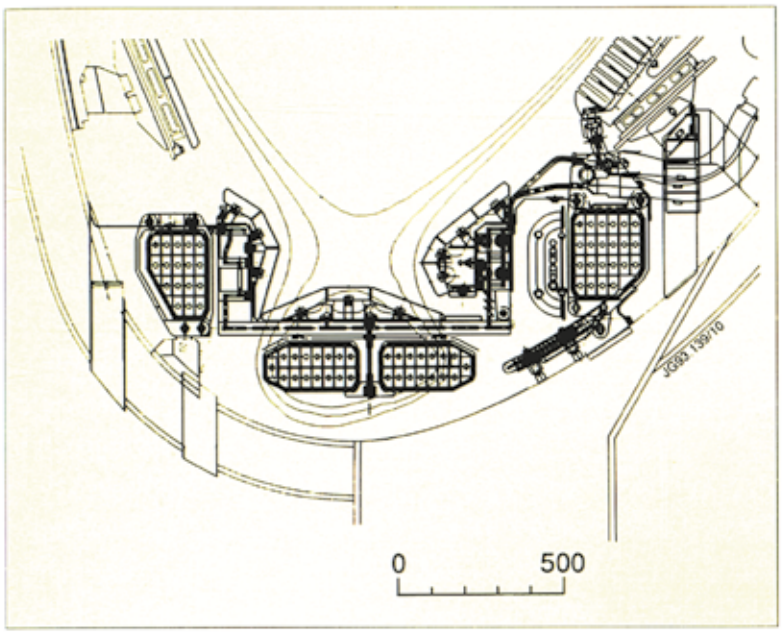

Fig.52: Cross-section of the inertial Mark IIA divertor

The study was motivated by two factors:

(a) it was generally accepted recently that "conventional" divertors, wherein the SOL power flows directly to the target plates, would lead to unacceptably high heat loads in Next Step devices. The exhaust power should be distributed over a much larger divertor surface area than can be obtained by simply tilting the plates, and radiation and charge-exchange processes were the leading candidates for accomplishing this. The Mark I divertor geometry, which was to have been taken over directly into the hypervapotron-based Mark II phase, is not well suited to achieving such divertor conditions, principally because it is too "open";

(b) there was continuing concern about the reliability of brazing beryllium plates to copper hypervapotrons, and the severe risk to the programme, especially in the D-T phase, which a failed braze would imply.

The Study Group was detailed to study both the physics and engineering of various divertor designs, within the constraints imposed by the JET schedule.

The three main functions which a divertor should perform can be summarised as:

- handle the heat load (power exhaust) at acceptable erosion rates;
- control impurity content in the main plasma by reducing sources and retaining impurities in the divertor;
- remove helium ash.

The divertor plasma parameters (n_e, n_i, T_e, T_i, ..) depend most sensitively on two quantities, the power crossing the separatrix (P_{sol}) and the mid-plane separatrix density (n_b). For fixed power, divertor

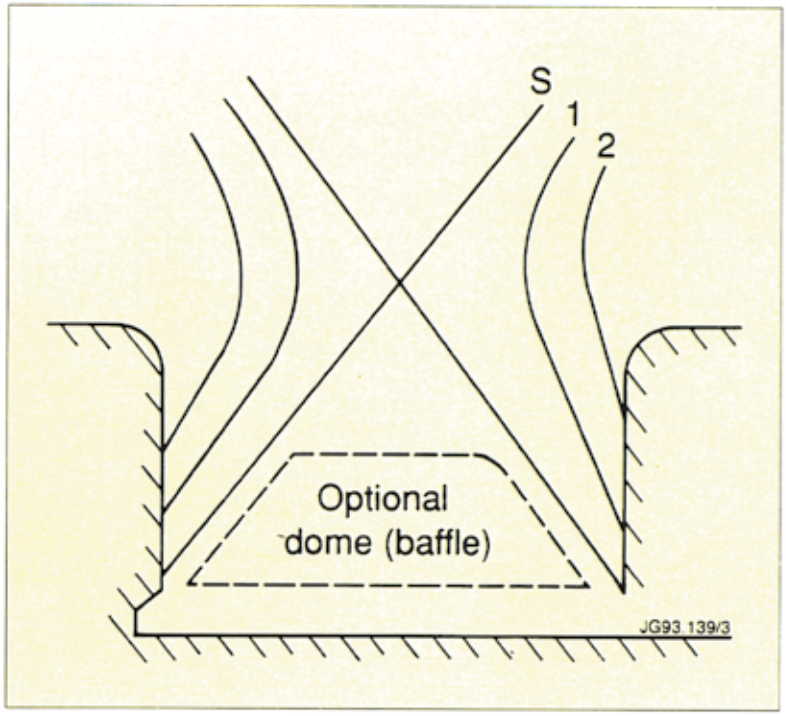

Fig.53: Vertical target divertor with optional baffle

performance improves dramatically as the midplane density is raised. However, when both variables are fixed, the divertor geometry itself can play a major role. Generally speaking, the more "closed" the divertor, the higher its plasma density and the lower its temperature, contributing to improved performance.

The effects of divertor geometry can be divided into two categories. Firstly, there is the purely geometric effect of increasing the wetted area, upon which the conducted power falls, by tilting the plates relative to the poloidal flux surfaces. The second effect arises from the fact that by tilting the plates, the recycling neutrals can be directed either towards the private flux region, in "vertical target" designs, or towards the divertor sidewalls, in "domed horizontal target" designs. Examples of these generic target geometries are shown in Figs.52 and 53. In either case, fewer neutrals, respectively, head directly back towards the main plasma than is the case for divertors with targets oriented orthogonally to the poloidal flux surfaces. More importantly, the distribution of ionisation sources in the divertor is dramatically altered by tilting the plates. This can lead to a major redistribution of plasma profiles in the divertor, which in turn can lead to enhanced volumetric losses from radiation and charge exchanges. Pumping performance can also be enhanced, particularly when "pumping baffles" are introduced.

Divertor Geometries

The geometry of Mark I (see Fig.54(a)) (and the original Mark II hypervapotron design) is relatively wide, U-shaped trough with

nearly vertical sides. It was designed to accommodate a large family of equilibria and to permit high amplitude sweeping. Due to the 1cm gaps between narrow (3cm) tiles, and relatively poor alignment tolerances achievable, it has a small toroidal utilisation factor, and sweeping would be required for all but modest power inputs. The geometry is very "open" for most equilibria of interest, which may limit access to the high recycling/atomic physics regime. However, elevated X-point equilibria having their strike zones on the vertical side walls can probably be produced, permitting investigation of "vertical target" divertor geometries at modest powers and currents.

The basic concept of the Mark II proposal is to use a rigid, toroidally continuous, water cooled base structure upon which target/baffle structures of various designs can be mounted. The rigid base allows for good tile alignment and thus permits the sue of large tiles, with small incidence angles, resulting in large wetted areas. The wetted area depends on the particular magnetic equilibrium chosen, but is typically a factor of four or more larger than in Mark I, virtually eliminating the need for sweeping.

The degree to which the divertor geometry can be optimised in JET is restricted by the geometry of the lower part of the vessel, including the divertor coils, which cannot be changed due to time constraints. Specifically, the divertor floor cannot extend below the top of the case around the lower divertor coil pair, so that the divertor "depth", distance from the X-point to the bottom of the divertor plasma channels, is limited by X-point heights.

For this limited X-point to divertor floor distance, a true "deep-slot" design is not possible. The divertor geometry closest to this design, referred to as Mark IIA (see Fig.54(b)), is of the "domed horizontal target" type, shown in Fig.53. Relative to Mark I, the target is tilted upwards in the centre. This serves the dual purpose of increasing the wetted area and redistributing the re-cycled neutrals, which tend to come off the targets perpendicularly. In addition , the side walls are brought in, in this version, to about the 2cm line.

A deeper, "slot-like" divertor can also be envisaged if the magnetic axes of the equilibria are allowed to rise to about 50cm above the midplane. This version of the divertor is referred to as Mark IIB (see Fig.54(c)). In this version, the targets are nearly vertical side walls, and the high "centre dome" is inserted to reflect neutrals back into the lower part of the divertor plasma. It can easily incorporate openings for pumping or gas puffing, either near its base, or higher up, to test various ITER-relevant ideas on enhancing charge-exchange and radiation losses. Using vertical targets, rather than an orthogonal one at the bottom of the slot, increases the wetted area

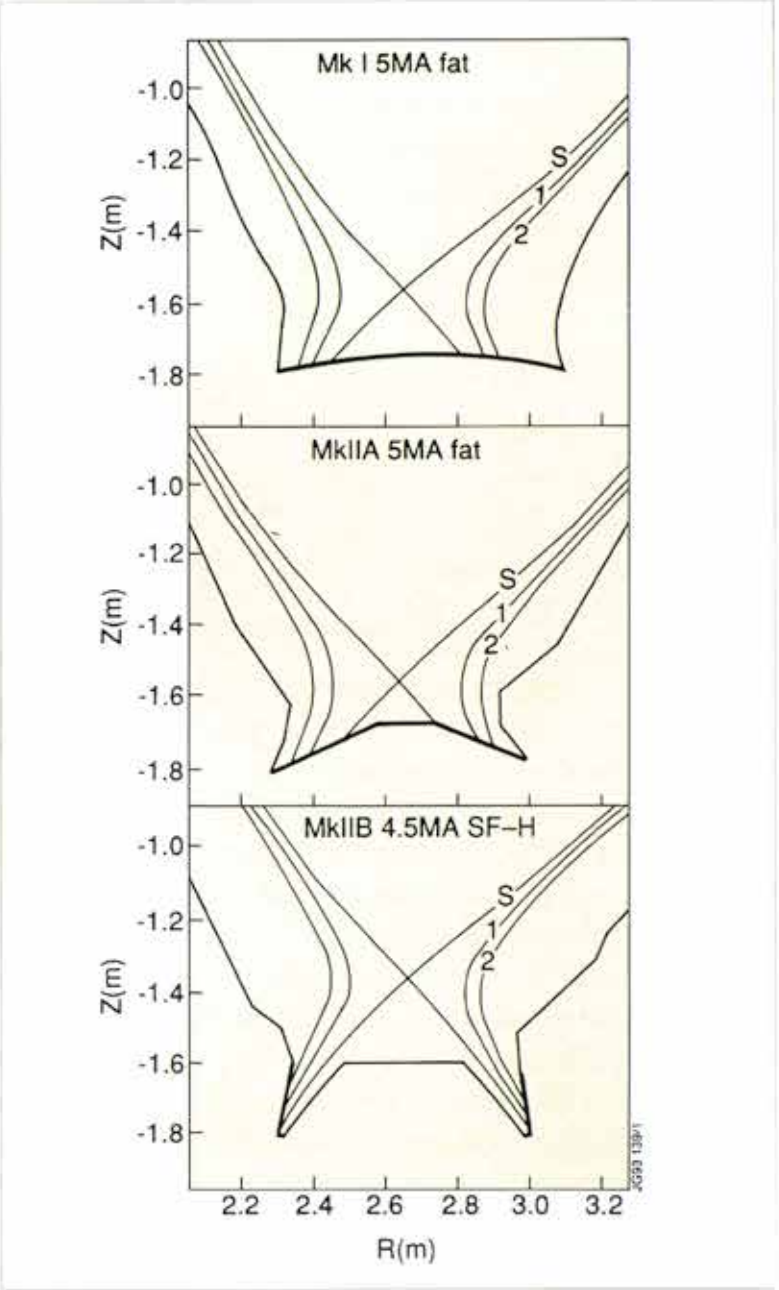

Fig.54: Geometries used for simulations

and thus keeps heat loads to manageable values even for high power, low density pulses, for which it is difficult to radiate large fractions of the SOL power.

Code Predictions of Divertor Performance

The performance of Mark I and versions of Mark II has been simulated using a full 2-D model. The geometries are shown in Fig.54. Mark IIA is a domed horizontal plate design, and Mark IIB is a vertical slot, which fits raised X-point equilibria. The simulations, while preliminary, all tend to confirm that a closed divertor will function more effectively than an open one, which can be deduced from analytical divertor models. Although closing the divertor

means reducing the SOL flow outside the divertor, the gains in power exhaust performance, through entrance into the high recycling/atomic physics regime, and the improved impurity behaviour seem to more than offset the effect of the reduced flow.

The Mark II configurations, while differing from each other in performance, outperformed the more open Mark I in nearly every respect, at fixed input power and SOL midplane density. Mark IIA produced a relatively uniform plasma across a broad target, and is clearly a great improvement over Mark I. It is a relatively conservative design, which will be further optimized by moving the sidewalls closer, and perhaps increasing the height of the centre dome.

Mark IIB is an example of a family of deeper slot geometries which is considered more "ITER relevant". Such geometries can be investigated in JET by raising the X-point. Mark IIB performs well in terms of divertor particle inventory, peak density, radiation per impurity atom, hydrogen radiation, and charge-exchange losses. However, the rather hot, rarefied outer layers of the divertor plasma allow the escape of more impurities than the "outward facing" designs such as Mark IIA.

From the limited number of simulations performed so far with the full multi-species version of the code, it seems that radiation from sputtered impurities will always be small for a high recycling, low temperature divertor. This suggests that injected impurities will be needed.

Divertor optimization is a difficult problem involving many factors. Further work will be undertaken on optimization of the "deep" version of Mark II. This will include investigation of high dome- and unbaffled-vertical target designs, as well as of the effect of puffing and pumping opening in the divertor walls. Simulation of helium transport in the SOL and divertor for the various candidates will also be addressed.

Technical Conceptual Design

A technical conceptual design has been developed. This has a toroidal continuous structure, as shown in cross-section in Fig.52, (with the Mark IIA tile geometry), and could be assembled inside the machine from 48 sections, each compatible with vessel entry. A continuous structure also significantly simplifies the attainment of mechanical stability. Although the forces due to halo currents may be large, the inherent rigidity of a continuous ring enables the support structure to withstand these forces internally. Each module is made up from a 4cm thick baseplate and two 10cm thick fabricated sidewalls. The modules are pre-assembled during manufacture with dowel locations to form a complete ring, which then enables very accurate tile locations. The inherent stiffness of the sidewall struc-

ture allows hinged corner joints, thereby leaving a reasonably large pumping gap open to the cryopump.

A substructure is used to support the tiles according to the chosen divertor geometry. Each tile would be attached by a single spring-loaded central bolt and supported on corner pads. Each module is fitted with its own tile carrier, but adjacent tiles share corner support pads, so that tile-to-tile step accuracy is dependent only on the tolerance of tile thickness. Replacement of a damaged tile is carried out by exchanging a complete carrier, an operation which can be performed by remote handling.

Cooling of the support structure is required to prevent overheating of the divertor coil epoxy. Present designs of the coil and heat shields can withstand radiation from a 350°C surrounding structure, as required for bake-out. The required cooling is modest. The power handling capability of this design has been significantly improved, relative to Mark I, by maximising the total wetted area. The poloidal wetted length is increased by inclining the target plates to the poloidal flux surfaces, while the toroidal length is increased by using carefully aligned large tiles with small inter-tile gaps.

The Mark I, hypervapotron Mark II, and inertially-cooled Mark II can all be swept, with a resultant gain in power handling which is approximately proportional to the field angle of incidence. For a 4° angle, a factor of ~3 gain could be achieved. The Mark I and hypervapotron Mark II were designed to rely upon sweeping, while for most equilibria and plasma powers of interest, inertial Mark II can operate without sweeping. In addition, the inertial Mark II is expected to produce larger volumetric power losses, further increasing its advantage over the older designs.

Conclusions

The Study Group recorded the following conclusions:

- To the extent possible, the divertor should be "closed", (i.e. it should allow as few as possible of the neutrals recycling from the target plate to escape from the "divertor region" below the X-point). Closing the divertor leads to higher density and lower temperature in the divertor. This reduces impurity production, enhances impurity retention, and facilitates access to the "atomic physics" regime where radiation and charge exchange are increased, decreasing the conducted power load to the plates. In addition, the wetted area should be made as large as possible by reducing the angle of incidence of the field line on the target to the limit allowed by target alignment tolerances;
- Only minor changes, specifically with respect to final machining of the target blocks to maximize their effective wetted area, could be made to the Mark I design due to time constraints;

- An inertially cooled version of Mark II, offering high performance (relative to Mark I), flexibility, and minimum risk could be built in about the same time schedule as the hypervapotron-based Mark II. It would allow testing of recent divertor concepts, and could be designed to form the basis for an extended programme.

The inertial Mark II divertor proposed to replace the original hypervapotron design has several innovative features. It is based on a water-cooled, rigid, toroidally continuous floor-and-sidewall structure upon which large tiles can be mounted with a high degree of alignment, permitting small magnetic field line incidence angles with corresponding large wetted area. The design is such that the divertor geometry, which plays a crucial role in divertor performance, can be readily changed by an exchange of tiles and tile holders, requiring only a relatively short machine intervention. Inertial Mark II divertor has a heat handling capacity which meets or exceeds that of the hypervapotron design for pulse lengths of 5-10s at high power, depending on plasma conditions. It can accommodate either beryllium or CFC tiles, allowing investigation of the two leading candidate target materials for Next Step devices.

A technical conceptual design has been developed which has large wetted area to eliminate the need for sweeping. It allows various target plate geometries to be tested, with only a short machine intervention required to change the configuration. This permits the investigation of the effect of geometry on divertor performance, leading to optimization of a Next Step divertor.

Future Plans

The JET Programme is divided into phases governed by the availability of new equipment and fitting within the accepted life time of the Project. Phase I (Ohmic Heating Studies) was completed in September 1984, and Phase II (Additional Heating Studies) in October 1988. Phase III (Full Power Optimization Studies) ended in February 1992. The scientific aims of Phase III were to obtain maximum performance in limiter configuration (currents up to 7MA) and to optimize X-point operation (currents up to 7MA) including a comparison of H-modes in X-point configuration using beryllium (lower X-point) with carbon (upper X-point) dump plates. The programme to 1996 is shown in Fig.55.

JET future plans are dominated by the insertion of a new phase of the Project (Phase IV: Pumped Divertor Configuration and Next-Step Oriented Studies). This phase is subdivided into a Divertor Characterization Plasma and a Full Tritium Compatibility Phase. The final Full Tritium Compatibility Phase, is now scheduled to start in

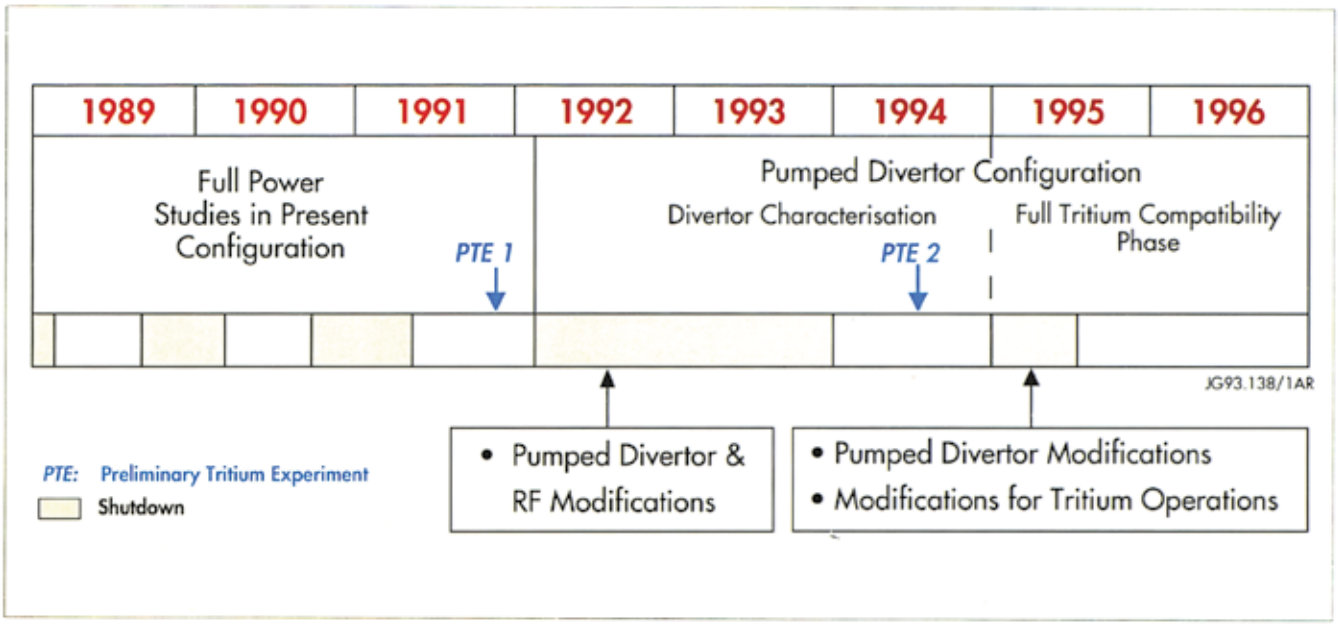

Fig.55: JET Programme Schedule: 1989-1996

1995. This new phase has now been formally approved and has extended the lifetime of the Project by four years to the end of 1996.

The aim of the phase is to demonstrate, prior to the introduction of tritium, effective methods of impurity control in operating conditions close to those of a Next-Step Tokamak with a stationary plasma (10 - 60s) of 'thermonuclear grade' in a single-null axisymmetric pumped divertor configuration. This configuration can only be achieved in JET by using divertor coils internal to the vessel.

Following approval by the JET Council of the stepwise approach to the introduction of tritium in advance of the full Tritium Phase, a first preliminary tritium experiment (PTE-1) was carried out and successfully completed in November 1991. A second tritium experiment (PTE-2) is scheduled for the first half of 1994 at a point, yet to be determined, when divertor operation has been well established, but in time to allow the necessary period of radioactive decay before the following shutdown. The information derived from these preliminary tritium experiments will provide a safer approach to the full tritium phase and will help to optimize the active handling and waste management arrangements.

INTOR/NET

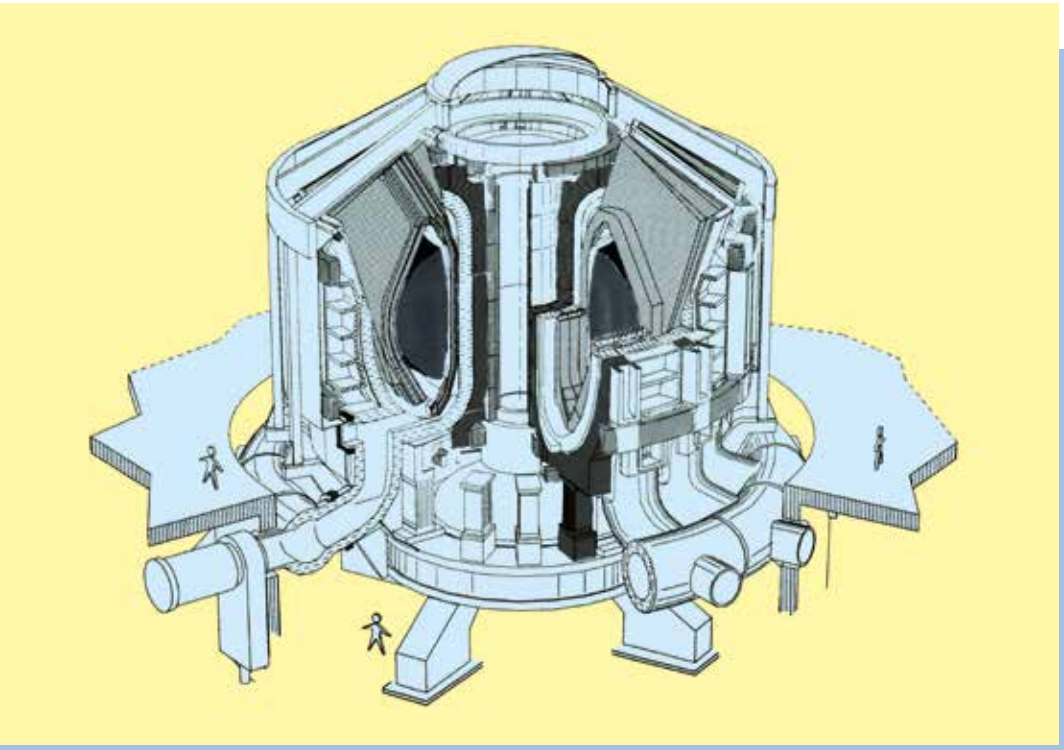

Grafik: NET-Team

Entwurf für NET, den „Next European Torus“

INTOR - A EUROPEAN VIEW

Günter GRIEGER
Max-Planck-Institut für Plasmaphysik
EURATOM Association, D-8046 Garching b. München

ABSTRACT

INTOR is an international cooperative project which started already in 1979. Its task is the demonstration of Tokamak reactor physics and to serve as a test bed for the development of fusion reactor technology. The development of the INTOR concept has reached a rather high degree of self-consistency. The concept is rather conservative in order to achieve sufficient predictability of performance. Particular discussion is devoted to the status of the INTOR physics data base and on the strategy of their generation. It is concluded that INTOR offers a chance to go to the next step within a reasonable time during which the data base will still be improved. The INTOR design concept is also very useful as a reference system for assessing the impact of innovative concepts.

INTRODUCTION

INTOR is an international cooperative project which started already in 1979. At that time the International Fusion Research Council (IFRC) issued clear terms of reference for the INTOR activities which, in essence, led to the following programmatic objectives: INTOR should represent the maximum reasonable step beyond the present generation of experiments (JET, TFTR, JT-60, T-15), it should demonstrate that Tokamak reactor physics is at hand, and should provide a test bed for the development of DEMO technology. Studies of the INTOR Workshop on the state of the art of fusion physics and technology on the one hand and on the DEMO requirements on the other hand have then led to the conclusion that one well-placed step in between DEMO and the present experiments might be sufficient. INTOR is conceived to be this step, and during its definition care was taken that INTOR will address all significant questions. The step width was derived from cost risk benefit considerations involving both steps, the one towards INTOR and the other one from INTOR to DEMO. It should be stressed that this strategy also assumes that all those points not requiring an INTOR-like device for their treatment would be studied in parallel with the help of specialized and dedicated devices. Otherwise, the INTOR task catalogue would be heavily overloaded.

The obvious objection usually encountered by this strategy is that the details of DEMO and even the optimum concept of DEMO are not yet known so that the detailed tasks for INTOR were difficult to define. Deeper studies, however, show that this argument has little bearing on the definition of INTOR since the technologies which will be developed with its help can be applied to a rather wide spectrum of concepts as long as one sticks to toroidal magnetic confinement in general. Or, with other words, whatever the final concept for DEMO will be, it is not so important for developing DEMO-relevant technology to have the identical concept for INTOR. This property allows to select a concept for INTOR for which the data base is largest and which offers the highest predictability of performance. This is of utmost importance because for achieving the INTOR goals, predictable and reliable performance are necessary prerequisites.

INTOR - STATE OF THE ART

On the basis of the above arguments the objectives of INTOR can be clearly defined. The INTOR design concept aims at using reactor relevant technologies to the largest possible extent; but for the basic machine, reliability and predictability are rated even higher. DEMO oriented components not yet meeting the standard for the basic machine are foreseen to be developed and tested in test modules. The INTOR objectives can be expressed in terms of neutron wall load and neutron fluences. A reasonable load of the walls by 14 MeV neutrons is about 1.3 MW/m^2. In terms of neutron fluence three stages of operation can be identified: (i) About 0.2 MWa/m^2 are necessary during stage I in order to fully establish the physics

performance with significant statistics (details will be discussed below). (ii) During stage II about 0.5 MWa/m^2 will be needed for development and testing of DEMO relevant blanket concepts. (iii) Stage III is aiming at testing the long-term performance of components. In this respect the calibration of all simulation methods used to study radiation damage is of particular importance. Table I shows that a neutron fluence of 3 MWa/m^2 might be concidered just sufficient for this purpose. INTOR is conceived to operate in such stages and during stage III to reach the above fluence after about 10 years of operation.

TABLE I: Changes in stainless steel with neutron fluence

Maximum test fluence	Benefit of testing
0-1 MWa/m^2:	Little useful information above existing knowledge.
1-3 MWa/m^2:	Confirmation of low-fluence effects predicted with other sources (e.g. on tensile properties).
3-6 MWa/m^2:	Model verification from observation of microstructure preceding long-term changes in behaviour.
Above 6 MWa/m^2:	Confirmation of performance near end of life (e.g. high swelling).

Progress reports on the INTOR work have been given on several occasions. Fig. 1 should just be a reminder of the Phase IIA-INTOR configuration. Superconducting coils are foreseen

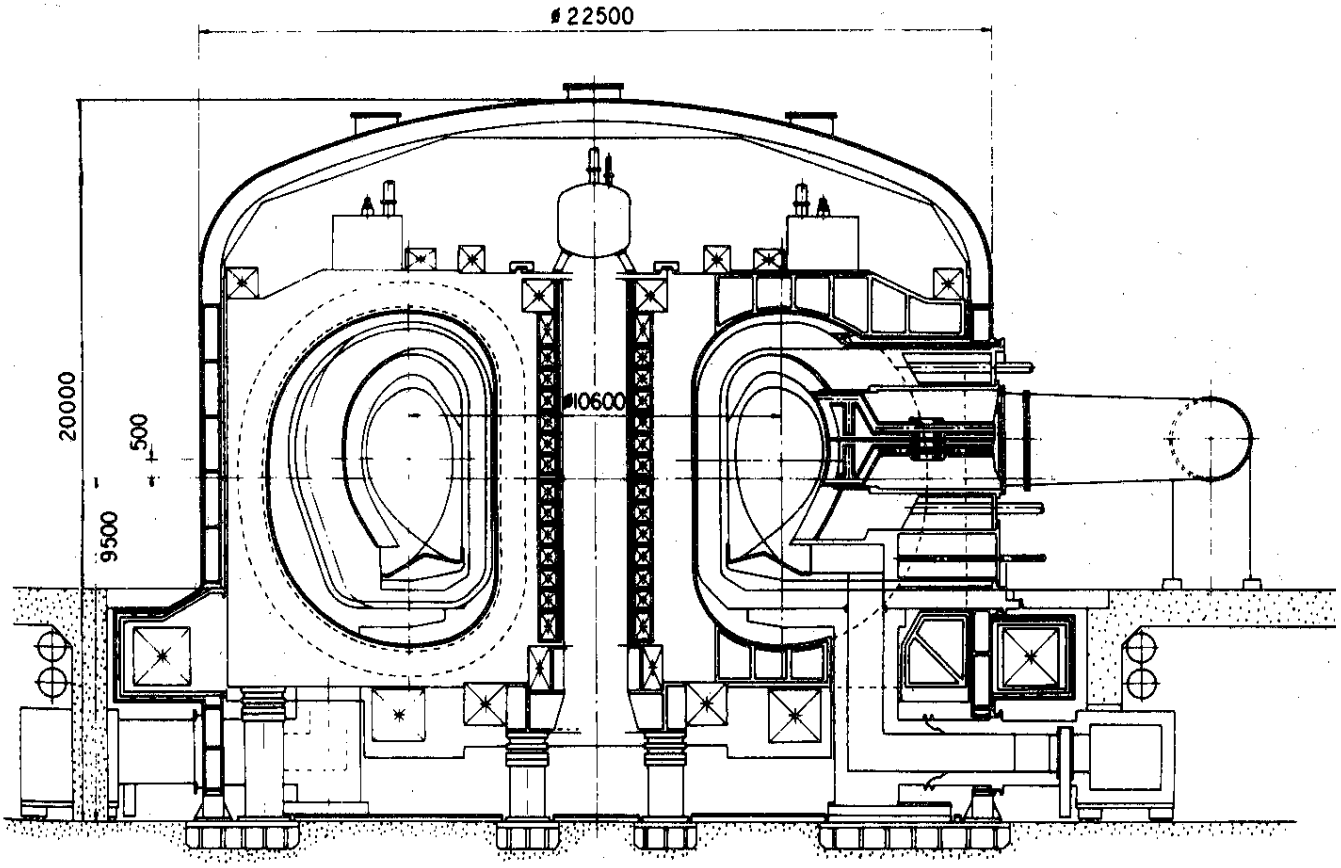

Fig. 1. Elevation view of INTOR phase IIA configuration.

for the toroidal field and for the poloidal one as well. The PF-coils are arranged outside the TF-coils for easier system integration. Their distribution is not yet optimized but selected such that it allows studying of both divertor and limiter configurations simply be changing the coil current ratios. A single null divertor is introduced to control the plasma edge. Compared to earlier intentions neutral particle injection heating is now replaced by ICRH. Lower hybrid current ramp-up and transformer recharging are earmarked for later introduction into the concept but the present data base is not yet considered sufficient to justify this step. Parts of the surface are covered by a blanket in order to reduce the supply demand for tritium.

For most of the details there is consensus among the four INTOR partners. Therefore, the further comments on the present INTOR configuration will be concentrated on such items which are still under intense discussion, and they will elaborate preferentially on the European view.

Divertor vs. Pumped Limiter

For an INTOR-like device it is essential to reduce wall sputtering and thermal load to a tolerable level. Considering the individual development potentials this is more a task for the physicists to establish the proper plasma boundary conditions (high density, low temperature) than for the metallurgists to develop sputtering-resistive materials. Because if one were successful in reducing sputtering significantly, the first wall can be made considerably thinner and thermal cycling becomes much less critical. Intensive studies have led to the conclusion that the desired plasma boundary conditions can be established indeed with the help of a divertor. The INTOR divertor arrangement is illustrated in Fig. 2. The ASDEX-Upgrade experiment at IPP Garching is being built to generate the corresponding data base and is designed such that studying and demonstrating the plasma boundary physics under INTOR relevant conditions becomes possible.

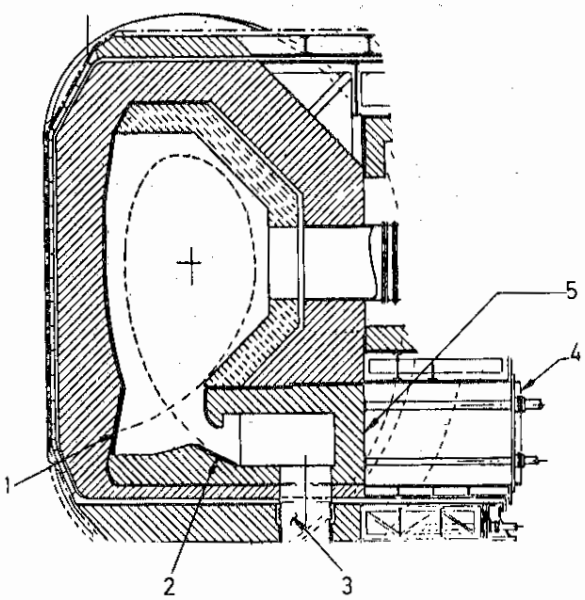

Fig. 2. INTOR divertor configuration (reference design).
1: inner plate, 2: outer plate,
3: vacuum duct, 4: vacuum seal door,
5: divertor module.

As an alternative solution also pumped limiters were studied in the frame of INTOR. Fig. 3 illustrates the INTOR pumped limiter arrangement. It was found that the limiter can be designed to tolerate the heat load expected but concern exists regarding the impurities sputtered from its surface which in case of the limiter are implanted directly on magnetic surfaces still closed. Furthermore, already very small changes of the plasma position would lead to large changes of the power deposition on the limiter surface. Thus, it is the conclusion of the INTOR Workshop that both divertors and pumped limiters have the potential to offer adequate solutions, but divertors have a higher probability of success.

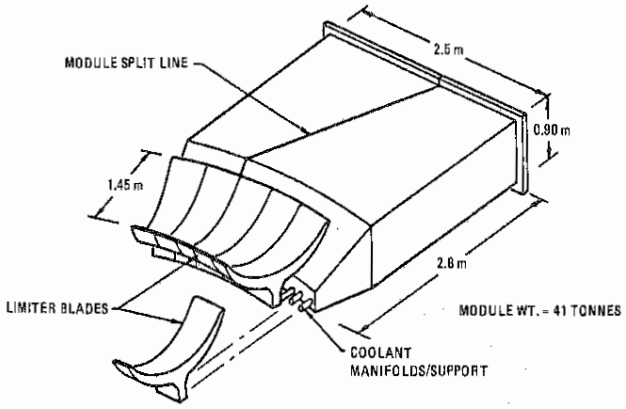

Fig. 3 Shaped, double-edged bottom limiter.

Maintenance Concept

The INTOR maintenance concept is displayed in Fig. 4. Its main feature is that it consists of a semi-permanent frame into which segments can be introduced by straight horizontal motions without moving TF- or PF-coils. This concept requires a not too high number of TF-coils with their outer legs far enough away to provide the free space between the neighbourhood coils needed for segment introduction or removal. This acts against the intention to build a compact machine for which the dimensions of all coils should be minimal.

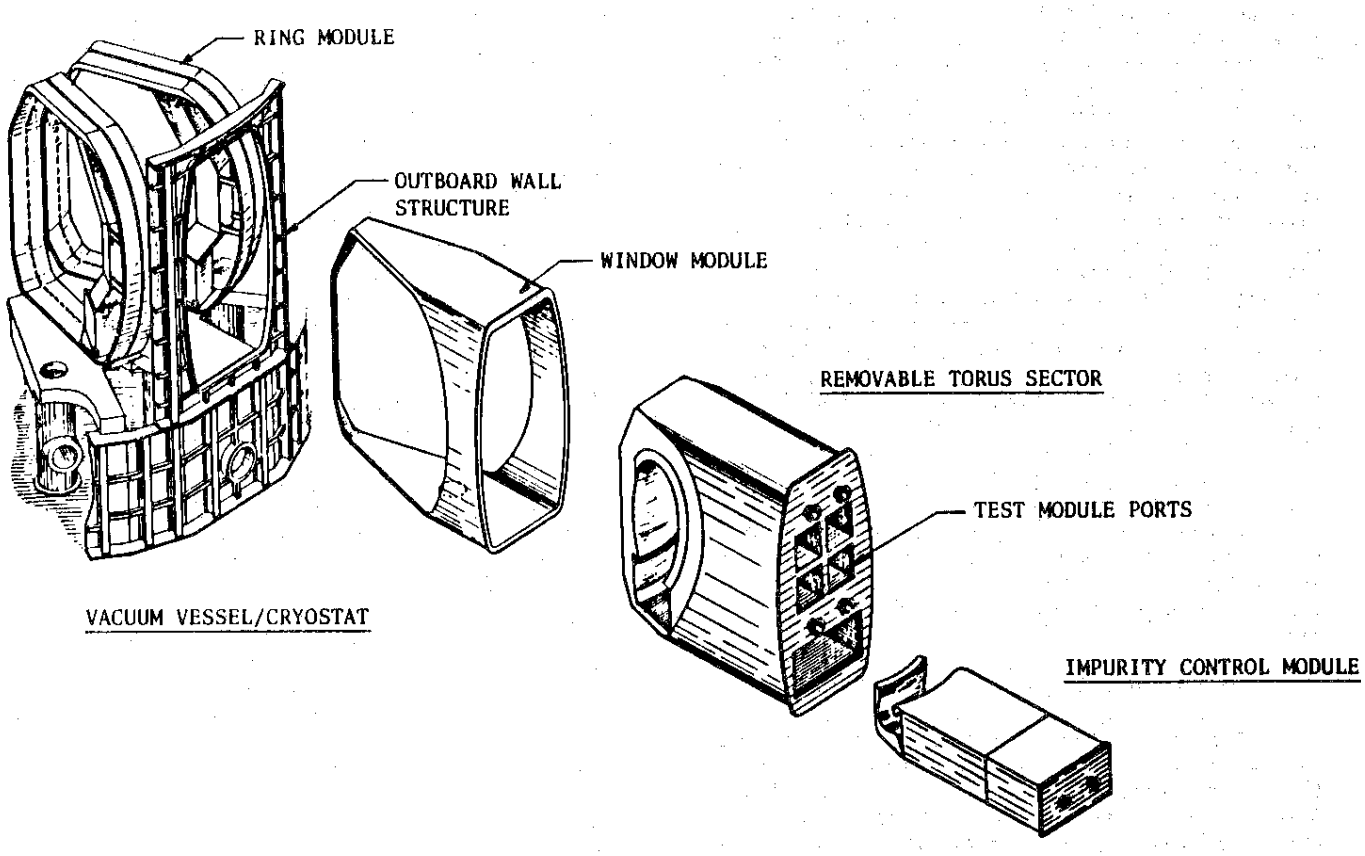

Fig. 4 INTOR maintenance concept.

An alternative solution is favoured by the EC-team which doubles the internal segmentation with respect to the number of TF-coils and removes the segments through vertical ports after some lateral motion in half of the cases. This concept allows (i) a reduction of the TF-coil size to the minimum level but increases the number of TF-coils from 12 to 16 in order to compensate the growth in toroidal field ripple otherwise occurring; (ii) the use of a crane for the removal of segments, and (iii) the introduction of a more efficient PF-coil system. This concept is shown in Fig. 5.

The discussion about the pro's and con's of these two concepts is still alive in the INTOR Workshop.

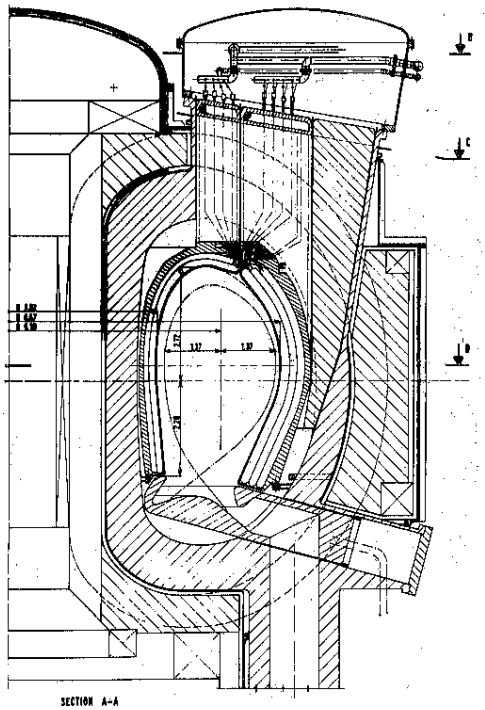

Fig. 5. Alternative maintenance concept. Removal of inner segments through vertical access port.

Tritium Supply Reducing Breeding Blanket

The tritium consumption of INTOR will increase to several kilograms per year once INTOR is moved to stage III operation. This would provide considerable fuel cost. Moreover, it remains questionable whether such large quantities of tritium will be made available to the fusion programme. To reduce these problems to a practicable level already the basic machine of INTOR will be equipped with a blanket capable of breeding at least 60 % of the INTOR tritium consumption. This blanket has to work reliably long before INTOR results can contribute to blanket development so that its design has to be very conservative. The present blanket concept of INTOR is based on Li_2O as breeding material which requires an operating temperature of several hundred degrees and is thus not free of tritium permeation problems.

In Fig. 6 an EC proposal is shown which tries to reduce such problems. All blanket modules are behind a separate, water-cooled vacuum-tight first wall which provides a third containment for the blanket cooling. The breeding is done by liquid $Li_{17}Pb_{83}$ contained in StSt-tubes which can resist the pressure of the cooling water (8 MPa) in case of rupture of the cooling pipes. These helical cooling tubes (water, 250 C) are completely immersed in the liquid breeder which also acts as heat coupler. There are only very few welds per blanket module and no connection between these modules and the vacuum. Moreover, in case difficulties occur, the liquid breeder could be drained out of the blanket or, alternatively, introduced only at later stages of the operational schedule if so desired. It is felt that this additional flexibility will be beneficial for a successful operating programme of INTOR.

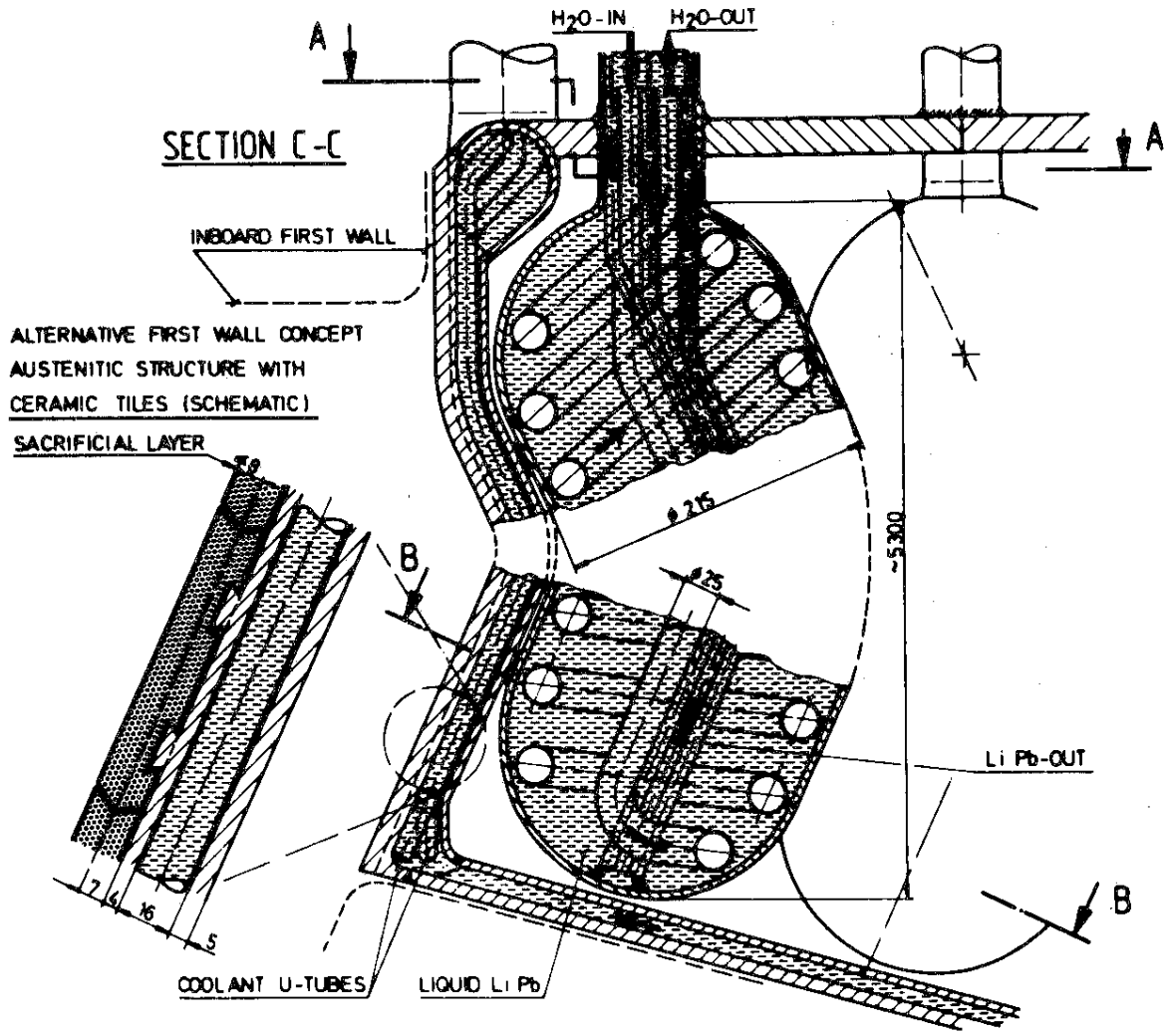

Fig. 6. Alternative first wall and blanket concept.

Status of the INTOR Concept

As mentioned above, the INTOR concept has matured considerably since the initial INTOR phase and reached a rather high degree of self-consistency. The design concept is rather conservative in order to achieve sufficient predictability of performance. There is consensus among the INTOR partners on most of the details. For some critical issues, however, it was found beneficial to perform broader and deeper studies on alternative solutions with the aim to find the optimum one, or to increase the predictability. These studies had a large influence on the fusion programme as a whole in that they have triggered a large number of investigations of direct relevance to reactor questions.

PHYSICS QUESTIONS

Recently, questions came up whether the physics data base for INTOR would develop fast enough and whether it would support the INTOR assumptions, indeed. This is best exemplified by the plasma beta which is a key parameter for reaching the power density needed. The assumed plasma beta is 5.6 % which is significantly above the present theoretical predictions of 4 % or so for INTOR. In this case, INTOR would not achieve its goal. Very probably, such a dramatic question is unique to the physics data base and would probably not come up in the field of INTOR technology because most of the non-physics uncertainties would affect only the degree of performance.

There are two possible reactions in this case. Under DEMO aspects a too low beta would request a considerable increase of the linear dimensions and thus of the cost of DEMO. In this case, the usefulness of the confinement concept chosen could easily become questionable so that simply accepting a much smaller beta value would not be a way out. In this situation the fusion programme has already started to undertake all possible efforts to push up the beta values and, with respect to INTOR, one could wait for the results of these programmes. The INTOR assumption of a beta value of about 5.6 % is a consequence of these considerations.

On the other hand, if one were more concerned about the early availability of an INTOR-like device as a test bed for the development of technology, there would be no need for an extra delay of the INTOR schedule because by some modifications INTOR could be made compatible with the present predictions on beta. This could be achieved by a combination of three or four of the following measures:

- INTOR could still fulfill its objectives if the neutron wall load were reduced from 1.3 to, let's say, 1.0 MW/m^2.
- Within the present assumption on beta (5.6 %) the DT plasma pressure represents only 4.1 %. 1.5 % are foreseen to cover the helium and the impurity pressures. The latter figure may tolerate some reduction.
- A small increase in plasma current may also be tolerable within the available q-limits.
- An increase in vertical elongation would increase the available beta. This measure would also increase the plasma volume and be limited by the increasing difficulty to guarantee positional stability for the plasma.

Such a modified INTOR device would not only satisfy the technology objectives but also provide clear-cut results on the available beta under reactor conditions. These results would be gained already during the initial phase of operation and contribute essential information to the programmes on beta improvement.

In this connection it is essential to remember that the maximum available beta is critically dependent on an optimization of the ohmic heating current profile. It is not at all clear that an alpha-particle power deposition profile will just lead to the temperature and current profiles required. It was for this reason that the burn time for INTOR was chosen between 100 and 200 seconds which is short to the skin time. By this measure it was intended to establish the required ohmic heating current profile during earlier phases of the discharge and to get some help by skin effects to maintain it throughout the full burn pulse. If modifications of the current profile were necessary late in the burn pulse, this would require excessive heating power. Present intentions to increase the burn pulse to 1000 s duration will encounter the above difficulties and need feasible methods to keep the current distribution optimal. It is therefore questionable whether this intention should be followed.

CONSIDERATIONS ON STRATEGY AND CONCLUSIONS

If the physics data base and its expected evolution during the coming years would really be considered too scarce to justify sufficient confidence for INTOR to work, one would start a discussion what physics machine would have the potential to improve the situation. This discussion has to start from the devices already or soon available to the world fusion programmes and their probable contributions to the physics data base. There are the four large Tokamaks TFTR, JET, JT-60 and T-15, and the other toroidal machines concentrated on special issues. Even DT-operation is foreseen with TFTR and JET so that results are expected also for plasmas with significant alpha particle pro

duction. In addition the plasma cross-section of JET is very similar to that of INTOR (see fig. 7) so that the extrapolation to INTOR should only be limited by the differences in aspect ratio and magnetic field strength.

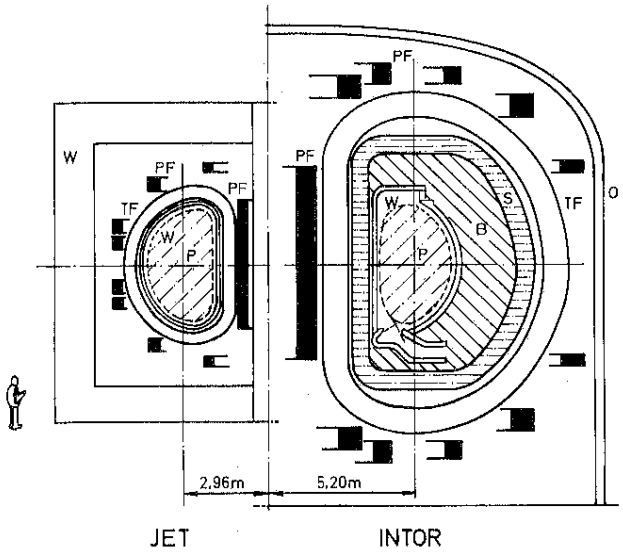

Fig. 7. In-scale comparison between JET and INTOR. Note the similar shape of the plasma cross-sections, but the difference in aspect ratio.

Therefore, if even after a few years of operation of all these devices the additional data base developed by them would still not allow to make with sufficient confidence the predictions on INTOR performance, one would be forced to reduce any extrapolation to a bare minimum. Consequently, such a physics machine had to run at the same global parameters as INTOR including plasma size and parameters, magnetic field, plasma current, aspect ratio and duty cycle, and had to produce a sufficient number of controlled burn pulses of full power and full duration or even longer. This number had to be large enough so that also the statistics on occurence and behaviour of disruptions could be verified under realistic conditions. Thus there would be a need for about 10.000 DT-discharges at full performance or, equivalently, for a neutron fluence of 0.1 to 0.2 MWa/m^2.

Such a device was included as one of the study points of the Cost-Risk-Benefit Analysis done earlier by the INTOR team. This study point is using superconducting coils for the magnetic field circuits because otherwise the superconducting coil development would be shifted too far into the future. On the other hand, it was also clear that some capital cost could be saved by the use of conventional Cu-coils. But the main contribution to the savings would have arisen from the smaller aspect ratio possible with Cu-coils which, however, were violating the above requirement of an aspect ratio equal to that of INTOR. This made the decision to use superconducting coils easier, because the main part of the potential savings could not be used.

In Fig. 8 a comparison is made of rough estimates of the direct capital cost and the operating cost of such a device and of devices designed for total fluences of 2 and 6.6 MWa/m^2 respectively. It is very interesting to note that the direct capital cost of the high fluence devices are not much higher than the cost for a device which has to withstand a neutron fluence of 0.2 MWa/m^2. This is because all the essential elements necessary for operation at high neutron fluxes have already to be present, and that the neutron fluence needed for establishing fully conclusive physics results is already far above being negligible. Moreover, an extensive cost-risk-benefit analysis has shown that a threshold in cost has to be exceeded before a machine capable of answering all the significant physics questions (stage I) can successfully be built. However, the analysis also shows that once the threshold is exceeded, it would provide only little additional cost to make the machine capable of reaching stage III fluence (see Fig. 8).

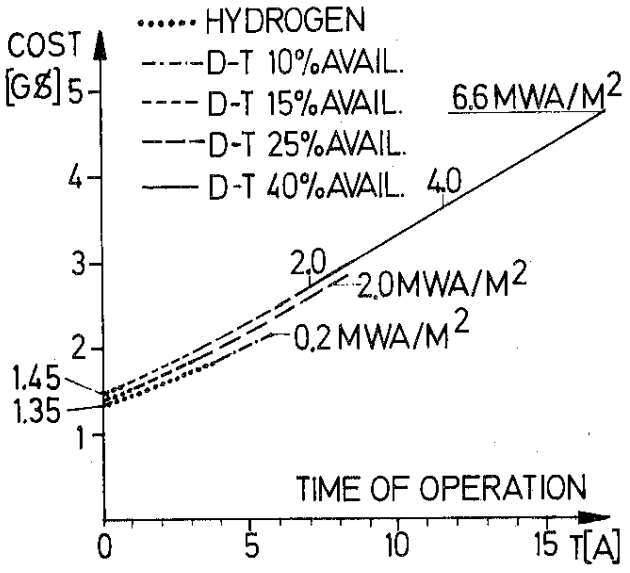

Fig. 8. Accumulation of INTOR operating cost. For three different machines designed for 0.2, 2, and 6.6 MWa/m^2 and staged operation as indicated in the insert. The intersection with the ordinate at T = 0 gives the direct capital cost of these devides.

Under these conditions it still seems to be the best strategy to build an INTOR-like device even if its primary task were only to produce the missing fraction of the physics data base. But one should accept the modest additional capital cost mentioned above to have the chance to go to full fluence if during the initial phase of operation the physics turned out to be right. Alternatively, such a strategy would also allow working on improvements of physics by expanding the initial phase of operation if need be. This possibility arises because high fluence operation is mainly a load on the operating cost and these remain open to later decisions depending on the results then achieved. Variations of this concept are being evaluated at present.

On the basis of all these considerations INTOR provides a realistic chance to go to the next step within a reasonable time determined by the time scale of the present large devices. In parallel, INTOR also offers a rather elaborate reference system for assessing the impact of innovative concepts. If there are some of them demonstrating their potential to lead to large improvements of the INTOR concept, they should be developed with high priority.

This paper is based on the work of scientists and engineers in the EC, Japan, USA and USSR who have contributed to the INTOR Workshop. This international cooperation has proven to be extremely successful.

REFERENCES AND FURTHER INFORMATION

For additional information see:

1. INTOR-Group: International Tokamak Reactor - Zero Phase, IAEA, Vienna 1980, STI/PUB/556

2. INTOR-Group: International Tokamak Reactor - Phase One, IAEA, Vienna 1982, STI/PUB/619

3. INTOR-Group: International Tokamak Reactor - Phase Two A, Part I, IAEA, Vienna 1983, STI/PUB/638

4. G. Grieger, INTOR- Group, "The evolution of the INTOR concept", Plasma Physics and Controlled Nuclear Fusion Research (Proc.10th IAEA Int. Conf. Plasma Physics and Contr. Nucl. Fus. Research, London, 1984), IAEA, Vienna (1985), paper CN-44/G-II-4.

INTOR: CRITICAL ANALYSIS OF INTOR-LIKE DESIGNS

G. GRIEGER[1] and the INTOR GROUP[2]

Abstract

INTOR: CRITICAL ANALYSIS OF INTOR-LIKE DESIGNS.

A critical and comparative analysis of existing INTOR-like designs has been made. The national designs of the four INTOR Partners and the physical and technical constraints on which they are based have been evaluated. The modelling methods used in reactor design have been further developed and compared to test their consistency. Deep insight into the cross-relations between design details and constraints and selected features has been obtained.

1. INTRODUCTION

The original INTOR work plan for the last year (1987) of the INTOR activity originally consisted of an updating of the early (1981) INTOR design concept [1] in order to introduce the results of the studies on critical issues and the evolution of the database. When the discussions on the new ITER activity started, this work plan was changed. The updating of the INTOR design concept was cancelled and replaced by a short and concise list of the changes to be made in the design concept [2], and the time gained in this way was used for a critical analysis of INTOR-like designs. This new work was performed by the INTOR Workshop with the aim of preparing valuable tools and a useful information base for future design work for an engineering test reactor.

2. DESIGNS AVAILABLE

The designs available were FER (Japan), INTOR as of Phase Two A, Part II (International Atomic Energy Agency), NET (European Community), TIBER (United States of America) and OTR (Union of Soviet Socialist Republics). The five designs are characterized by their gross parameters as listed in Table I.

During an INTOR Specialists' meeting [2] on this subject the descriptions of the five designs were converted into a common format in order to make possible a discussion and comparison of the programmatic and technical objectives, the physics and

[1] Permanent address: Max-Planck-Institut für Plasmaphysik, Euratom–IPP Association, D-8046 Garching, Federal Republic of Germany.

[2] The members of the INTOR Group are identified in Paper IAEA-CN-50/F-I-1.

TABLE I. MAJOR PARAMETERS OF INTOR-LIKE DESIGNS

	INTOR	NET	FER	TIBER	OTR
Major radius (m)	5.00	5.18	4.42	3.00	6.30
Minor radius (m)	1.2	1.35	1.25	0.83	1.50
Fusion power (MW)	585	650	406	314	500
Plasma current (MA)	8.0	10.8	8.8	10.0	8.0
Average beta (%)	4.9	5.6	5.3	6.0	3.2
Safety factor, q_I	1.8	2.1	1.8	2.2	2.1
Heating method/power (MW)	ICRH/50	TBD[a]/50	ICRH/50 LH/20	LH/10 NBI/40	ICRH/50
Number of TF coils	12	16	12	16	12
Maximum field at TF coils (T)	11	11.4	12	12	11.7
Volt-seconds	112	181	50	58	210
Neutron wall load peak/ average ($MW \cdot m^{-2}$)	1.6/1.3	1.5/1.0	1.5/1.0	1.6/1.0	1.05/0.8
Tritium inventory (kg)	3.1–4.6	2	2	TBD[a]	3.5–5.0
Test first wall area (m^2)	12	40	9	19	

[a] To be determined.

engineering design constraints, the main features that drive the design concept, and the design specifications. The critical analysis [2] of these designs should reveal the detailed causes for the differences between the designs and yield information on the impact on the design of specific decisions on constraints, features, etc.

For this analysis the designs show rather significant differences in the adopted methods or features and in the resulting parameters. The features provide for:

— Plasma performance: Q = 5 to ignited;
— Current drive method: inductive or non-inductive;
— Pulse length: pulsed (≥ 150 s) to steady state (≥ 1 week);
— Divertor: single null (SN) or double null (DN);
— Tritium breeding capacity (for tritium supply): none to full;
— Plasma heating: various RF schemes, NBI.

The relative span of the parameters covered by the designs is apparent from Fig. 1, and comparison of the horizontal builds in Fig. 2 provides a perhaps even clearer impression.

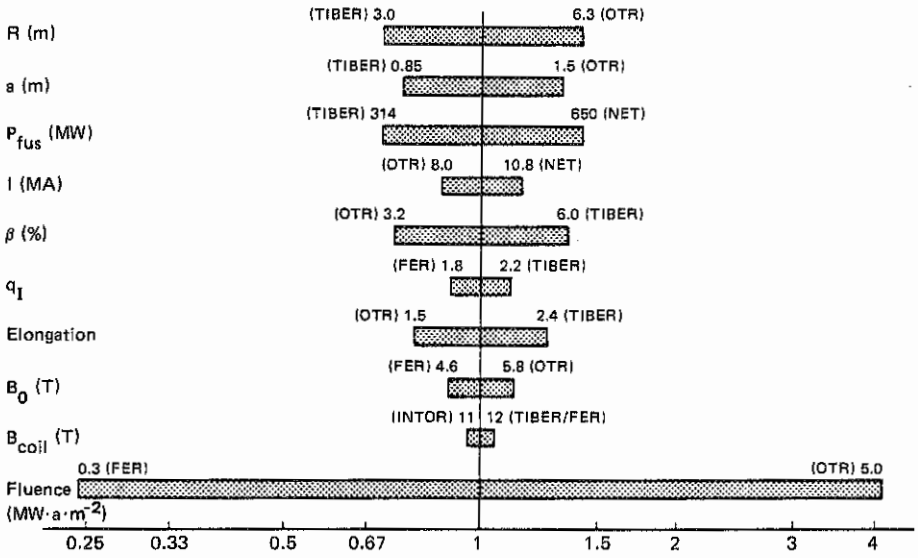

FIG. 1. Relative span of the parameters covered by the designs.

3. CRITICAL ANALYSIS

The analysis is aimed at determining the detailed reasons for the rather large differences between the designs. The reasons might fall into the following categories:

— Objectives,
— Design philosophy,
— Physics assumptions and constraints,
— Engineering design constraints,
— Others.

The results of the study will yield quantitative information on design drivers which have a large impact on the design. For these items a careful assessment of the determining constraints and parameters is important and expansion of the related database by R&D should be particularly rewarding.

Comparison of the objectives as formulated by the leaders of the individual design teams shows that all the designs have in common the purposes of providing an essential step forward, leading to a well balanced point between the present generation of large devices and DEMO, aiming at reactor relevant operating conditions, applying reactor relevant technologies and providing for engineering testing. Differences in the objectives mainly result from strategic considerations and differences in expected budget availability. Thus the differences express themselves mainly as differences in the fluence goal (which also concerns the operating cost) and in the

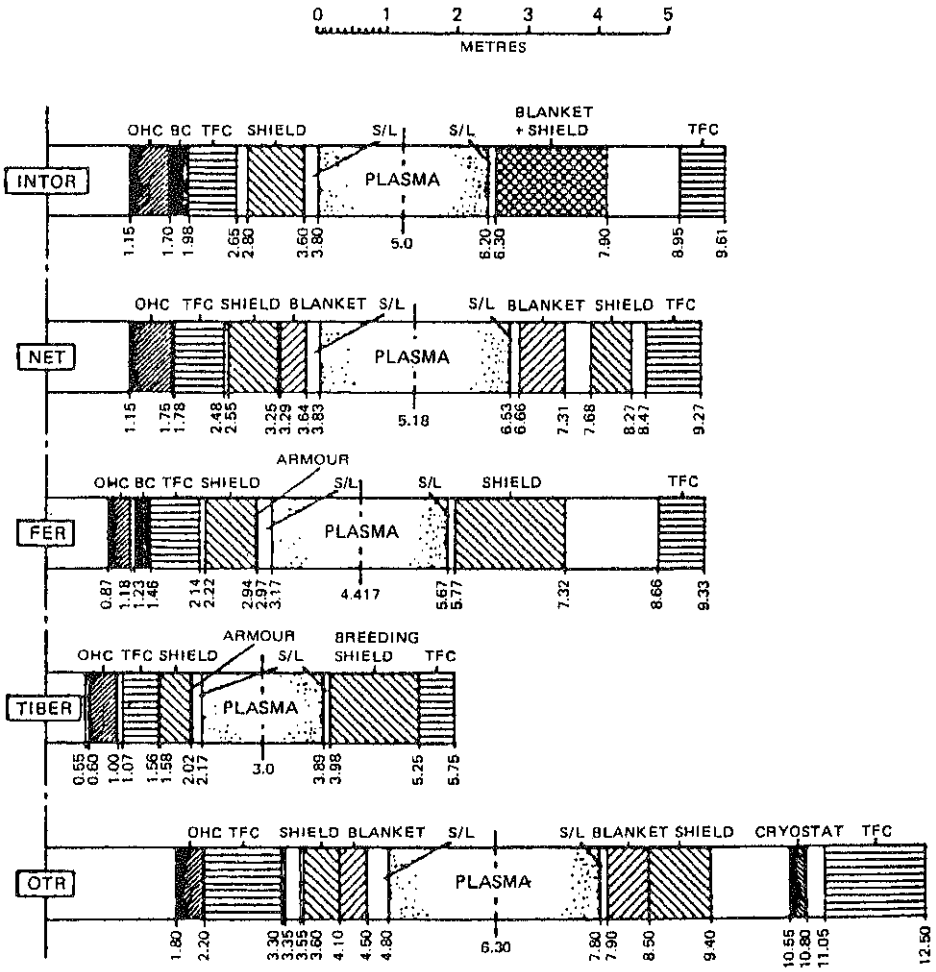

FIG. 2. Comparison of horizontal builds.

intended tritium breeding capability, which is related to the fluence goal. Within the depth of this analysis the fluence target has only a moderate influence on the design and only affects the thickness of the shield. Thus, a difference in objectives is not the prime cause for the differences between the designs.

The other categories require a more detailed analysis. System codes were the tools used for this purpose. Such codes are in use by all INTOR Partners. They are rather elaborate and designed to replicate a design in very great detail. The prevailing design philosophy is a built-in property of these codes. The codes were tested by comparisons between them. This was done by applying them not to their own design but to the design of a Partner, replacing their own input assumptions and constraints

TABLE II. PHYSICS CONSTRAINTS

	INTOR	NET	FER	TIBER	OTR
I_p (MA)	8	10.8	8.74	10	8
K (at 95% of magnetic flux)	1.6	2.05/1.7	1.7	2.4	1.5
$\tau_{E,\ required}$ (s)	1.4	1.9	1.7	0.44	1.7
$\tau_{E,\ ASDEX\text{-}H}/\tau_{E,\ required}$	2.9	3.0	2.3	6.8	3
n (10^{20} m^{-3})	1.6	1.7	1.14	1.06	1.7
Murakami parameter[a] (10^{19} $T^{-1} \cdot m^{-2}$)	19	23	15	8	25
Beta required (%)	4.9	5.6	5.3	6	3.2
Troyon coefficient (%)	4	3.5	3.5	2.8	3.5
Impurity control, divertor type	SN	DN/SN	SN	DN	SN
Pulse length (s)	150	350	800	55	600
Heating	ICRF	TBD[b]	ICRF (LH for ramp-up)	LH + NBI	ICRH

[a] Estimated using line average density.
[b] To be determined.

by those of this Partner and then comparing the result with the Partner's design. After some minor improvements all of the codes were able to replicate the designs of any Partner if the input assumptions were adjusted accordingly. This means that:

— The predictive powers of the system codes of the Partners are very close to each other.
— The design philosophies on which the codes are based are more or less the same.

It thus follows that the differences between the designs are the consequence of the differences in the decisions on the constraints determining the designs and in the selection of design features. It thus becomes possible, by comparing the designs, to directly study the reaction of a design to a variation of the constraints and features. Tables II–IV list the physics constraints, the engineering design constraints and the design features for the five examples.

This study was performed by starting from one design and then replacing successively the physics picture, the engineering picture and the features by those of another design and by checking the outcome. This was done for

TABLE III. MAJOR ENGINEERING DESIGN CONSTRAINTS

	INTOR	NET	FER	TIBER	OTR
Field ripple at edge (%)	1.2	1.5	0.75	0.8	1.0
Impurity control	SN	DN/SN	SN	DN	SN
Plasma elongation (at 95% of magnetic flux)	1.6	2.05/1.7	1.7	2.4	1.5
Maximum radiation to TF coil insulator (rad)	10^9	5×10^8	3×10^9	10^{11}	10^9
Allowable TF coil stress	ASME	600 MPa	600 MPa	600 MPa	600 MPa
Maximum first wall heat flux ($MW \cdot m^{-2}$)	0.4	0.4	0.4	0.3	0.4
Allowable first wall stress	ASME	RCC-MR	ASME	ASME	200 MPa
Directed peak heat flux ($MW \cdot m^{-2}$)	5	5	2	3	5

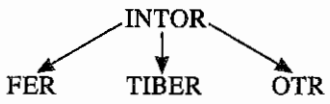

and for

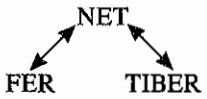

As an example the transition from NET to FER is shown going from top to bottom in Fig. 3. The figure shows the radial build, starting from the axis of rotation on the left, followed by the regions of the OH central coil, the inner leg of the TF coil, the inboard shield, the inboard blanket, the plasma, the outboard blanket, the outboard shield and the outer leg of the TF coil. The figure starts from the NET–DN configuration. The first step, A-1, replaces the NET physics picture by that of FER, but does not yet change the radius of the OH transformer coil. The FER physics is more optimistic than the NET physics and thus leads to a smaller plasma radius and, simultaneously, to a longer burn time. The latter is corrected in step A-2, where the central bore is reduced such that the reduction in volt-seconds corrects for the excess in burn time. This case represents a NET with FER physics. The next step

TABLE IV. MAJOR DESIGN DRIVING FEATURES

	INTOR	NET	FER	TIBER	OTR
Operating mode	Ignited	Ignited	Q > 20–30	Q > 5	Q > 5
Pulse length (s)	150	>200	800	CW	600
Current drive	Inductive	Inductive	Hybrid	Non-inductive	Inductive
Fluence ($MW \cdot a \cdot m^{-2}$)	3.0	0.8	0.3	3.0	5.0
Tritium breeding rate	0.6	0.3	0.0	1.0	1.05
Plasma heating method	ICRH	TBD[a]	TBD[a]	NBI + LH	ICRH
Impurity control	SN	DN/SN	SN	DN	SN
Access for maintenance	Horizontal	Vertical	Horizontal	Horizontal	Horizontal
Weight of largest replaceable component (t)	300	60	250	32	300
Availability/period	25%/10 a	8%/11 a (25%/1a)	7%/6 a	30%/12 a	50%/9 a

[a] To be determined.

introduces the FER engineering: the current density in the TF coils is increased together with the thickness of the outboard shield, which simultaneously leads to the reduction of the field ripple from 1.2 to 0.75%. Then, in step C-1, some of the features are modified. The NET double null divertor is replaced by the FER single null divertor. The elongation is reduced from 2.0 to 1.7 and a bucking cylinder is introduced to support the TF coils, the number of which is reduced from 16 to 12. This change leads to a more circular plasma with a correspondingly larger diameter and requires a larger neutral bore for obtaining the needed volt-seconds. With only 12 TF coils their outer legs have to extend rather far in radius to keep the field ripple down to 0.75%. The final step, C-2, removes the blanket, introduces the low FER fluence target and assumes some RF support in generating and driving the plasma current. A comparison with Fig. 2 demonstrates that the introduction of the FER physics, engineering and features into the NET design leads in fact to the FER design. This means that the impact of the various modifications is understood quantitatively. There is no need for qualitative changes of the system codes. The results can be considered to be rather accurate. They also show that each of the three categories — physics, engineering and features — has considerable influence, although there is some difficulty in defining conclusively what item belongs to which category.

These investigations also allow conclusions to be reached on which items have the highest or the lowest impact on the design. In this connection it is necessary to remember that the impact is the product of the sensitivity times the potential variation

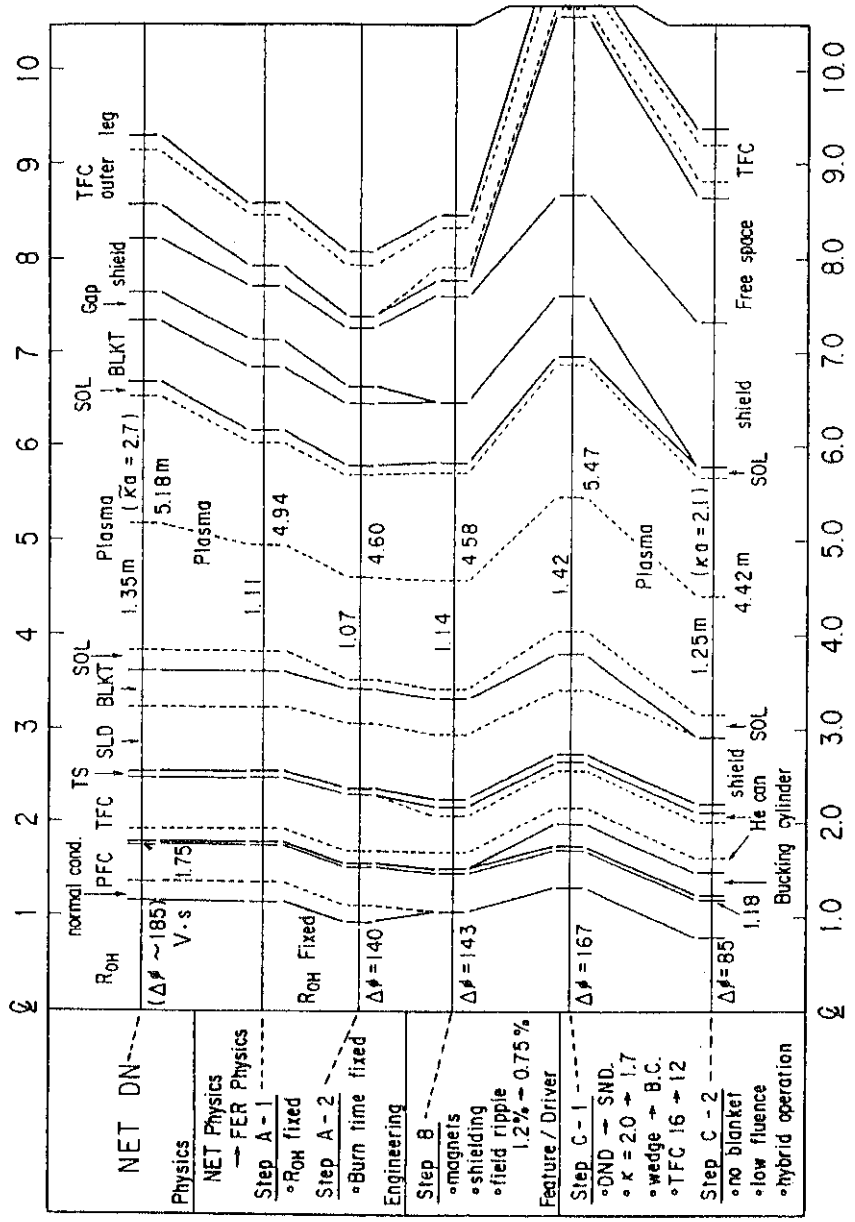

FIG. 3. Radial build. Transition from NET to FER by successive replacement of the NET constraints by the FER constraints.

of the parameter under study. The sensitivity can be deduced from the above studies. The potential variation of the parameter relates to the degree of knowledge and either constitutes a risk for achieving targets or requires the introduction of safety margins which might be expensive. This is related to the quality of the database and the corresponding R&D. On the other hand, considerable uncertainties can be accepted where the sensitivity is low. From the results of such evaluations the following were determined:

141

— Items with the strongest sensitivity to changes:
  Ignition margin or Q [1]
  Safety factor (q)
  Elongation
  Shield attenuation[1]
  Z_{eff} and reactivity[1]
  Neutron wall load
  Beta scaling coefficient (Troyon factor)
  TF coil stress.
— Items with the weakest sensitivity to changes:
  Fluence
  Burn time
  Presence/absence of bucking cylinder[1]
  Presence/absence of inner blanket[1]
  Shield thickness
  Scrape-off layer (inboard)
  Edge ripple[1]
  Plasma inductance[1]
  Plasma profiles
  Volt-seconds
  Radiation dose to insulator[1].

This list is still subject to some scatter between the results obtained by the individual Partners. This is not so much a consequence of the quality of the codes but rather is caused by differences in what is kept constant and what is allowed to change.

4. CONCLUSIONS

Because of the large spread in the parameters of the available INTOR-like designs, a deep insight into the impact of the various design determining properties has been obtained. This was made possible by the utilization of system codes describing the design in rather elaborate detail. These codes have been checked for their

[1] Studied by only one delegation.

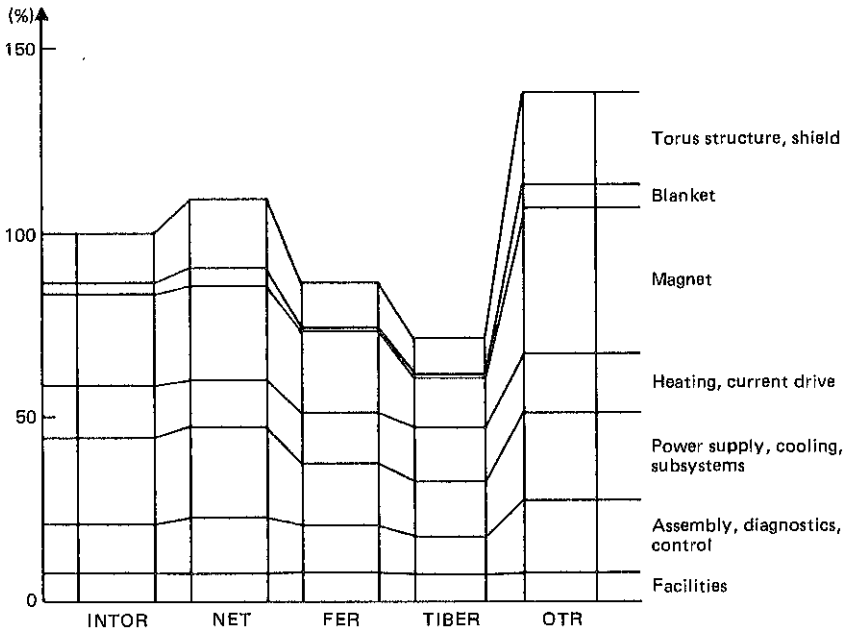

FIG. 4. Comparison of the costs of the individual designs.

predictive power and their degree of accuracy. The results obtained have qualified these codes as fast and reliable aids both for designers and in the definition of R&D programmes. The degree to which the various constraints or features impact the design has been analysed and a list has been established. This list shows items where R&D is particularly rewarding and others with only a small impact on the design. The amount of the potential influence is best demonstrated by a comparison of the direct capital cost of the compared designs, for which calibrated codes also exist. An example is given in Fig. 4, which shows a breakdown of the direct capital costs relative to those of INTOR. These analyses scatter by about 5–15% between the Partners because they also reflect the national traditions with respect to how large projects are organized in their relation to industry. Keeping this in mind one can conclude that in comparison with INTOR the direct capital costs

— Of NET are about the same,
— Of FER are about 10% lower,
— Of TIBER are about 35% lower, and
— Of OTR are about 25% higher.

These are non-negligible factors, indeed.

REFERENCES

[1] INTOR GROUP, International Tokamak Reactor, Phase One (Rep. Int. Workshop Vienna, 1980 and 1981), IAEA, Vienna (1982); summary in Nucl. Fusion **22** (1982) 135.

[2] INTOR GROUP, International Tokamak Reactor, Phase Two A, Part III (Rep. Int. Workshop Vienna, 1985–1987), 2 vols, IAEA, Vienna (1988); summary in Nucl. Fusion **28** (1988) 711.

IAEA-CN-56/F-1-1

NET PREDESIGN OVERVIEW

NET TEAM
(Presented by F. Engelmann)

Max-Planck-Institut für Plasmaphysik,
Garching, Germany

Abstract

NET PREDESIGN OVERVIEW.

NET aims at demonstrating the scientific and technological feasibility of fusion power production in a device based on the tokamak principle. It is designed to achieve controlled ignited burn for a pulse duration of 1000 s and to allow testing of components for a reactor such as systems to exhaust power and particles from the plasma as well as the tritium breeding blanket; it will also demonstrate the availability of technologies essential for a reactor such as superconducting magnets and remote maintenance. Component testing will primarily address functional tests to be done in the basic performance phase of NET, together with the physics experiments. In this phase an average neutron wall load of about 0.8 MW/m^2 will be available for an integral burn time of 2500 h. If considered appropriate, on the basis of the experience gained in this phase, endurance and material tests could be done up to a fluence of about 1 MWa/m^2 in a subsequent, extended performance phase as the device allows 40 000 full performance discharges. Only for the latter phase would a tritium breeding blanket be installed. The NET parameters were derived from the performance requirements. The earlier choice of the values of the plasma current (25 MA), the plasma elongation ($b/a \approx 3$) and the aspect ratio ($R/a \approx 3$) has been confirmed. However, the longer pulse duration of 1000 s now adopted, and the use of more conservative design criteria partly as a result of the outcome of the R&D activities undertaken in the meanwhile, has resulted in an increase of the major radius to 7.3 m. The NET predesign, now completed, and the accompanying R&D programme in physics and technology support launching of the engineering design phase.

1. INTRODUCTION

During the NET predesign phase, the NET design was developed in depth in several critical areas [1], starting from the basis led out in the conceptual design phase [2,3]. The work was supported by a comprehensive R&D programme in physics and technology. In this paper an overview of the results of the NET predesign is given with emphasis on the NET performance characteristics and parameters.

2. TECHNICAL OBJECTIVES AND DESIGN PRINCIPLES

The technical objectives of NET are:

- to demonstrate reactor plasma performance and, in particular, to achieve controlled ignited burn of a DT plasma and to generate long burn pulses;
- to demonstrate the availability of technologies essential for a future reactor, such as superconducting magnets and remote maintenance;
- to test components for a future reactor, such as systems to exhaust power and particles from the plasma, and the tritium breeding blanket.

The guiding principle in the design of NET has been to ensure maximum technical simplicity, to use prudent criteria for the physics basis and for the technologies to be applied, and to give a prominent role to safety and environmental considerations. Only technologies were adopted which are either already in hand or can be demonstrated prior to construction of NET. Areas where reliance on the development potential of tokamak physics is necessary are power and particle exhaust as well as disruption control.

3. PLASMA PERFORMANCE

The operating regime of the plasma in a tokamak reactor is characterized by a low recirculation of power back into the plasma, a long burn pulse length, and a fusion power density as high as the physics constraints allow. Quantitatively, a reactor plasma will be operated at

$$C = P_{\alpha} / P_{tot} > 0.9$$

with P_{α} being the fusion α-particle power and P_{tot} the total heating power of the plasma, i.e., effectively in an ignited mode; the burn pulse length t_{burn} will be at least several thousand seconds, much longer than the time t_{res}

characterizing the resistive diffusion of the profile of the plasma current; and the plasma will be operated not far from the pressure (or equivalently beta) limit, typically at

$$\beta/\beta_{Troyon} > 0.8$$

147

and in the vicinity of the density limit.

From an operational point of view these constraints imply that in a reactor a high-beta plasma burning at $C > 0.9$ must be maintained in steady state conditions with respect to all time-scales characterizing the various dynamical processes appearing in the plasma. These time-scales are related to the power and particle balances as well as to the diffusion of the plasma current profile; in addition, there may be further characteristic time-scales related to the interaction of the plasma with the walls.

NET is conceived to allow demonstration of this reactor plasma performance, minimizing at the same time the extrapolation from presently operating tokamaks as well as the investment cost. This is possible because the physics information that is needed can be obtained without generating discharges having all the features of a reactor plasma simultaneously although an option is maintained for operation with an extended performance closer to the operating regime of the reactor. In fact, it is sufficient to show separately

(i) that the power and particle balance can be controlled in the ignited mode under steady state conditions with respect to the transport processes of energy and particles. For this, a minimum burn time $t_{burn} \approx 30\ \tau_E$ is needed (τ_E being the energy confinement time of the plasma) and operation at $C > 0.9$ is required; and

(ii) that it is possible to operate routinely at high plasma beta ($\beta/\beta_{Troyon} > 0.8$) for at least $t_{burn} \approx 3\ t_{res}$. For this it is permissible to work at lower C, e.g., at $C \geq 0.7$ and, therefore, to use external power for active current profile control, if needed, and for sustaining the power balance at

148

reduced plasma current and/or magnetic field (to increase β/β_{Troyon}).

Typical numbers for the two time-scales τ_E and t_{res}, under reactor conditions as well as in NET, are $\tau_E \approx 3$ s and $t_{res} \approx 300$ s.

NET is, therefore, conceived to achieve operation at $C > 0.9$ for at least 100 s, and in addition it is able to operate for burn pulses of at least 1000 s at $C > 0.7$.

The objective of operation at $C > 0.9$ determines the energy confinement capability required and, effectively, the plasma current needed. The aspect ratio of the NET plasma was taken to be $A = 3$. This choice minimizes the uncertainties in predicting the confinement properties of the plasma as present large tokamaks all have aspect ratios around this value. The option of an appreciably larger aspect ratio and correspondingly lower plasma current does not offer significant advantages in cost or in performance, in particular with respect to the power exhaust conditions.

NET has the capability for driving the plasma current inductively for a pulse length of 1000 s to be able to operate the discharge at the highest possible C and at high plasma density.

High-recycling conditions at the divertor plates can then be established, which is a prerequisite for providing acceptable working conditions for the power and particle exhaust system. While in recent experiments a divertor plasma with a temperature in the eV range has been obtained under such conditions, the demonstration of an operating regime extrapolatable to NET is still outstanding. In particular, there remain uncertainties with respect to the effect of edge localized modes. To ensure a satisfactory lifetime of the plasma-facing components, it is essential that the frequency of occurrence of hard plasma disruptions be reduced with respect to present experiments. The availability of efficient disruption control is therefore assumed.

For attaining a pulse duration of 1000 s, control of the profile of the plasma current is anticipated to be necessary. This requirement drives the need for external

power and, hence, limits the value of C accessible in this regime. However, the external power actually needed for this aim cannot yet be definitely quantified. It appears that a broad current profile must be maintained to keep the sawtooth mixing radius sufficiently small, typically less than one third of the plasma minor radius. Such a profile also makes operation at higher values of the plasma beta possible. For this, about 30%, or more, of the plasma current has to be driven non-inductively by injection of external power and by the bootstrap effect; on this basis a need for an external power of about 70 MW is estimated which, for $P_{fus} \approx 1$ GW, corresponds to $C \approx 0.75$.

4. COMPONENT TESTING AND STAGED OPERATION

The unique feature of NET, as far as component testing is concerned, is that it provides a "fusion reactor environment", namely the appropriate combination of surface loads (heat and particles) and of volume loads (heat, neutrons and electromagnetic forces) as present in a DT burning device. Only NET will therefore offer the possibility to test these interacting aspects of complex components, and it is for this purpose that it will be primarily used.

A reactor will operate without blanket replacement for at least five full power years at a wall loading of 2-4 MW/m^2, corresponding to 10-20 MWa/m^2, i.e. 100-200 dpa in steel at the first wall. However, the average neutron wall load, in a Next Step tokamak, cannot exceed 2 MW/m^2, and its availability, taking into account the down-times imposed by the requirements of the testing programme itself and of maintenance/ replacement of components, is estimated to be only 10-15%. The neutron fluence on the first wall, therefore, accumulates rather slowly (~2 dpa per year) and at high cost (~400 M$ per year).

Under these operating conditions, extrapolation to a reactor, with acceptable risk, of the testing results of components having a weak interaction with plasma and

neutrons, such as superconducting magnets, remote handling, tritium systems, and heating/current drive systems, is possible. However, for the in-vessel components, i.e. the plasma-facing components and blanket, the testing capability is more limited.

150

The performance aspects of these latter components, to be tested, are:

i) Ability of the plasma-facing components to sustain the loads under conditions of long burn at reactor-relevant power flux and in the presence of disruptions;
ii) Ability of the blanket to breed and release tritium, and to satisfy the key requirements of a reactor (e.g., breeding ratio larger than 1, high temperature operation, low tritium inventory);
iii) Ability of the in-vessel components to resist a fluence of 14 MeV neutrons that approaches the reactor level and, at the same time, minimizing inventories of activated materials.

These issues must be addressed in the above order of priority, because only when the in-vessel components have shown that they perform satisfactorily their functions as described in i) and ii), the endurance questions of point (iii) can be tackled. Furthermore, the testing of the functional requirements of the plasma-facing components (mission i)) and of the blanket (mission ii)) are consistent with a limited fluence (about 0.3 MWa/m^2) and availability, while for mission iii) an enhanced wall loading, approaching the reactor level, and improved availability are needed. In addition, only this latter mission necessitates breeding a large part of the tritium needed for operation in the device itself, therefore requiring a driver blanket.

For these reasons, the technical objectives of NET include the functional tests (missions i) and ii)), but mission iii) is left to an optional second phase of operation. Hence, NET operation will be carried out in stages. During the basic performance phase, the functional testing will be performed. This requires 2500 h of integral burn time [1], including the physics investigations for which about 500 h are needed. Only during the basic performance phase, on the basis of the operating experience gained and of the component test

results, will it be decided whether it is appropriate to continue operation into an extended performance phase to do endurance tests up to fluence of about 1 MWa/m^2. For this latter phase, a tritium breeding blanket would be installed. Anyway, for material characterization, an intense 14 MeV neutron source will be required in parallel to NET.

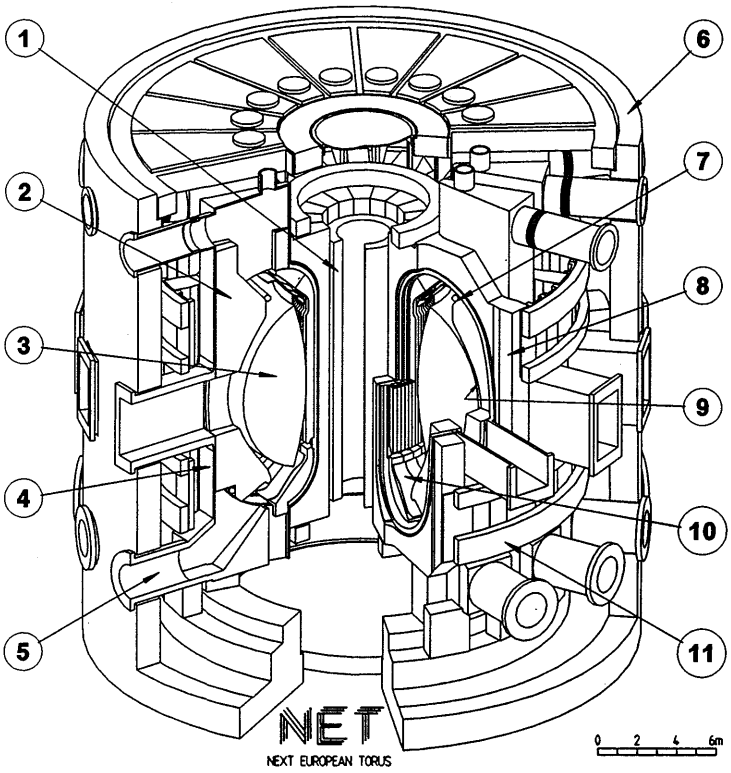

FIG. 1. Three-dimensional view of the NET device.

5. NET MAIN PARAMETERS AND OPERATIONAL CHARACTERISTICS

152

The parameters of NET follow from the requirements to allow operation at $P_\alpha/P_{tot} = 0.9$, to provide a transformer capability for driving the plasma current inductively for 1000 s, and to ensure a lifetime of the basic device of 40000 full performance shots. The choice of the values of the plasma current (25 MA), the plasma elongation (b/a≈2) and the aspect ratio (R/a≈3) as made for NET in 1988 [3] has been confirmed. However, the longer pulse duration now adopted, and the use of more conservative design criteria partly as a result of the R&D activities undertaken, resulted in an increase in major radius of about 15 % over the value given in Ref. [3].

The basic parameters of the NET device (see Fig.1) and its operational characteristics are:

Plasma current, I (MA):	25
Plasma major radius, R (m):	7.3
Plasma minor radius, a (m):	2.43
Aspect ratio, R/a:	3
Elongation, b/a *):	2
Magnetic field on axis, B (T):	5.2
Safety factor, q_ψ *):	3
Fusion power, P_{fus} (GW):	1.2
Average neutron wall load, L_{wall} (MW/m^2):	0.8
Troyon coefficient, g (10^{-2}Tm/MA):	1.5
Average plasma temperature, (<T>) (keV):	10
Average plasma density, <n> (10^{20}m^{-3}):	1
Maximum allowable helium concentration (%):	10
Impurity contamination (effective ion charge), Z_{eff}:	< 2

*) at 95% of the magnetic flux

The confinement properties of the NET plasma have been quantified assuming that NET operates in the H-regime with edge localized modes. In this regime, plasma energy losses are comparatively low and at the same time accumulation of impurities, in present experiments, can be kept within acceptable limits. The confinement scaling developed during the ITER Conceptual Design Phase for this case was adopted [4]. However, as there are still significant uncertainties in the extrapolation of this regime to NET conditions, a nominal margin of more than 2 for reaching the target of $C = 0.9$ was kept when applying the confinement scaling.

The reference plasma equilibrium was selected to be a double null configuration because of the flexibility of this configuration. Slight deviations from up-down symmetry allow to generate asymmetric double null ("semi-double null") as well as single null configurations with a vertical offset of the magnetic axis up to about 0.5 m. The plasma current, for the same value of the safety factor q_ψ at the edge, is only slightly lower in these configurations, by about 5% in the most extreme case. The variety of configurations offering comparable confinement properties thus is larger then in a device designed around a strongly asymmetric single null configuration with a large axis offset. Furthermore, in an up-down symmetric plasma configuration the heat loads and particle fluxes are distributed over four plates (rather than two), and plasma position control is simplified as horizontal and vertical perturbations of the position are only weakly coupled.

For the basic performance phase, an external power, P_{ext}, of 70 MW is foreseen to allow for current profile control. This power also covers the needs for heating to burn conditions ($\approx$ 50 MW), for burn temperature control (about 25 MW), plasma initiation, and soft discharge shutdown. The design of the NET device is compatible with adopting combinations of RF systems (electron cyclotron, lower hybrid, ion cyclotron waves) and high energy neutral beam injection.

154

TABLE I. NET OPERATING POINTS

	Full Current		Reduced Current			β-limit	
	full ignition	burn control	burn control	full ignition	70 MW CD	higher L_{wall}	nominal L_{wall}
I (MA)	25	25	23.8	22.4	20.2	21	19.6
B (T)	5.2	5.2	5.2	5.2	5.2	4.4	4.1
q(ψ=95%)	3	3	3.1	3.3	3.7	3	3
P_{fus} (GW)	1.2	1.2	1.2	1.2	1.2	1.5	1.2
C (=P_α/P_{tot})	1	0.9	0.9	1	0.75	0.8	0.7
L_{wall} (MW/m^2)	0.8	0.8	0.8	0.8	0.8	1	0.8
t_{burn} (s)	1000	800	1000	1400	2100	2000	2500
I_{BS}/ I	0.12	0.11	0.13	0.15	0.2	0.21	0.22
I_{CD}/ I	0	0	0	0	0.12	0.12	0.18
g	1.6	1.6	1.6	1.8	2	2.5	2.6
β (%)	3.2	3.1	3.1	3.1	3.1	4.9	5.1
β_{pol}	0.4	0.39	0.43	0.49	0.6	0.63	0.65
<T> (keV)	11.7	9.6	9.7	10.6	10.3	11.1	10.4
<n> (10^{20}m^{-3})	0.9	1.08	1.07	0.98	1.02	1.05	1.02
Z_{eff}	1.8	1.71	1.71	1.75	1.92	2	2
P_{ext} (MW)	0	27	27	0	70	70	100
P_α (MW)	241	242	241	241	241	294	241
P_{div} (MW)	123	131	131	114	124	139	135
τ_E^{req} (s)	4.7	4.3	4.3	4.8	3.7	3.5	3.4
$\tau_E^{H\text{-}ELM\text{-}90}$ (s)	6.7	6.5	6.3	6.2	5	4.7	4.5
$\tau_E^{req}/\tau_E^{H\text{-}ELM\text{-}90}$	0.7	0.65	0.7	0.75	0.75	0.75	0.75

definitions: I_{BS} - bootstrap current; I_{CD} - current driven by external power; P_α - α-particle power; P_{div} - power exhausted through divertor; τ_E^{req}, $\tau_E^{H\text{-}ELM\text{-}90}$ - required and extrapolated energy confinement times.

Table I shows a selection of operating points of NET. The first four columns exemplify cases in which current profile control is assumed not to be necessary and, hence, no external power is used to drive current. The first and the fourth column refer to ideally ignited cases (C=1); the second and the third column correspond to C = 0.9, allowing for burn temperature control. The last three columns give examples of low C operation using external power for current profile control and for reaching high beta operation. Impurity seeding, to enhance radiation losses, is allowed for in the last three cases. At nominal plasma current (25 MA) there is a large margin with respect to the beta limit. Therefore, operation at appreciably higher wall loading keeping the plasma beta below the permissible limit (e.g., operating at 25 MA and g ≈ 2.5, yielding L_{wall} ≈ 2 MW/m^2 and P_{fus} ≈ 3 GW) would in principle be possible in an enhanced performance phase.

6. DESIGN CHARACTERISTICS

The basic device, consisting of the superconducting (Nb_3Su) magnet systems and the containment structures, has been designed to operate through the basic and extended performance phases.

Vertical rather than horizontal access for maintenance of the blanket segments has been chosen for NET because it allows a better optimization of the affected systems ; in particular the poloidal field coils can be located at positions which permit the plasma equilibria needed to be created more effectively.

The choice of the number of toroidal field coils is the result of a trade-off between toroidal magnetic field ripple considerations and maintenance requirements. Layout studies have led to the choice of 16 coils for NET : a higher number of coils would have made the maintenance procedures of the in-vessel components more difficult, a lower number would have unnecessarily increased the outer radius of the toroidal field coils and, consequently, the magnetic energy of poloidal and toroidal field systems.

156

For the plasma-facing components, which are subject to demanding operation conditions, remote replacement through horizontal ports in a minimum number of operations has been foreseen. For the basic performance phase, cooling by water at low pressure and temperature (< 3.5 MPa, < 150°C in normal operation) has been selected. The first wall structure can be integrated with or separated from the neutron shield. Two basic design concepts have been studied which differ in the way the low Z protective armour is provided. The first concept uses local limiters to take the loads due to fast particles, having tiles made of carbon fibre composites (CFC) brazed to heat sink tubes. These limiters are designed for heat loads of about 5 MW/m^2. The first wall proper, in this concept, would be covered by a low Z coating (B_4C or Be). In a second concept, CFC tiles are mechanically attached to the heat sink and are passively cooled via radiation or conduction. The divertor is made of CFC armour, 1 cm thick, of high thermal conductivity, brazed in "monobloc" geometry around cooling tubes in Mo-alloy or DS Cu. The divertor plates are designed to operate at a static peak divertor heat flux of up to 15 MW/m^2.

The device has been designed for full remote maintenance, with provisions for hands-on maintenance where possible. Three confinement barriers are present during operation to avoid release of radioactive material in case of accident.

Details of the design are documented in Ref. [1].

7. SUMMARY AND CONCLUSIONS

The primary role of NET is to establish a reactor plasma and to assess the basic performance of its components with a view to reactor applications. The guiding principles of the NET design have been a prudent extrapolation from present physics and technology data as well as maximum technical simplicity and safety considerations. The NET predesign has been completed,

supported by a comprehensive R&D programme in physics and technology. From this study the following main conclusions can be drawn:

- The priority chosen for the technical objectives, namely DT plasma ignition, extended burn and functional tests of main components, in the first phase of operation ("basic performance phase") is confirmed. The option of a second phase of extended performance in a more reactor relevant mode of operation should be pursued during the engineering design; the actual implementation of this phase will depend on the results of the basic performance phase.
- The design and the results from the R&D activity support the launching now of the engineering design as it was planned in the formulation of the EC Fusion Programme 1992/94.
- Key issues requiring an intense effort are the industrial fabrication and extensive testing of highly reliable and high performance superconducting magnets, the identification of a configuration of the plasma-facing components and of ways of power exhaust which are able to reduce the present high concentration of heat load on the walls facing the plasma.
- The preliminary safety analysis of the NET predesign indicates that the safety requirement of no disruption in community life in case of accidental release of radioactivity is achievable.

REFERENCES

[1] The NET Team, "NET Predesign Report", Fusion Engineering and Design, to be published.

[2] The NET Team, "The Next European Torus", Fusion Technology **14** (1988) 1 -246.

[3] The NET Team, "The NET Project", Proc. 12th Conf. on Plasma Physics and Contr. Nucl. Fusion Res., Nice, 12-19 October 1988; IAEA, 1989, Vol. 3, p. 285.

[4] Post, D.E., Borrass, K., et al., "ITER Physics", ITER Documentation Series No. **21**, IAEA, Vienna, 1991.

ITER/DEMO

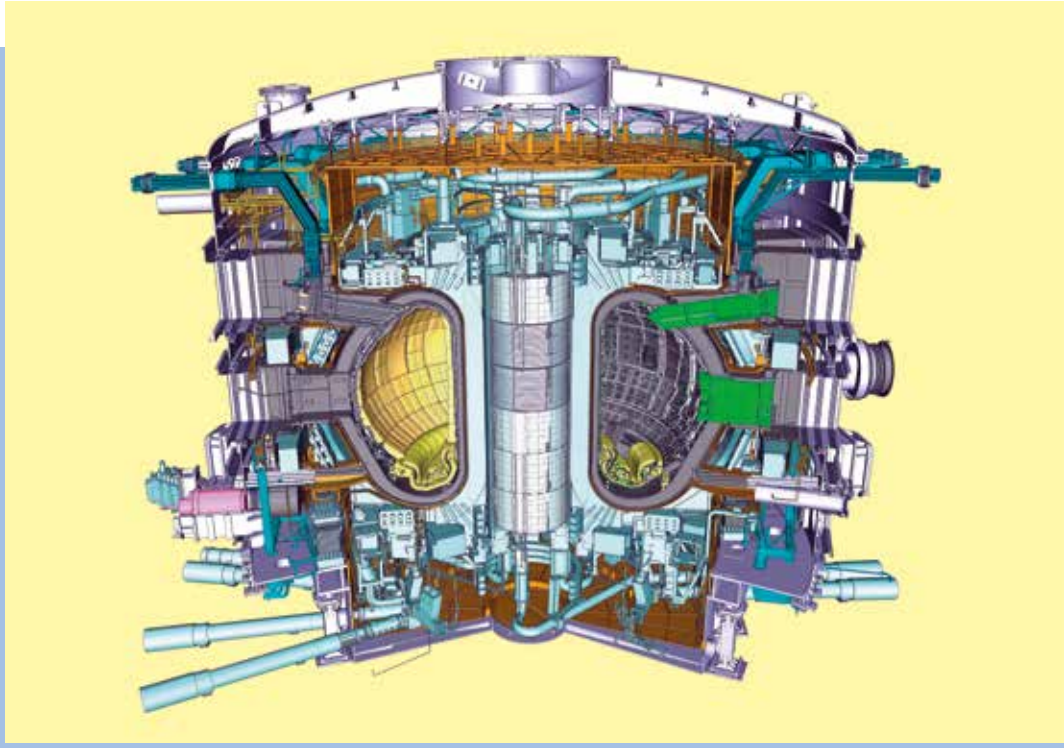

Der internationale Experimentalreaktor ITER im Entwurf

Grafik: ITER-Organisation

➜ B. Bigot: Progress toward ITER's First Plasma, in: Nuclear Fusion, 2019

➜ G. Federici et al.: DEMO design activity in Europe: Progress and updates, in: Fusion Engineering and Design, 2018

3

STELLARATOREN

Der Stellarator Wendelstein 7-AS (1988 – 2002)

Foto: IPP

STELLARATOREN

3.1 EINLEITUNG

Die unter Führung von Klaus Pinkau 1981 formulierten „Aims of IPP“ entwarfen unter anderem ein langfristiges Entwicklungsprogramm für die Stellarator-Linie des Instituts. Damit sorgten sie für einen beträchtlichen Motivationsschub, der letztendlich die Optimierung des Stellarator-Konzepts möglich machte.

Die physikalischen Grundlagen

Für das bessere Verständnis seien zunächst die physikalischen Grundlagen zusammengefasst: Die drei Bedingungen für das Zünden und Brennen des Plasmas in einem Fusionskraftwerk, das Deuterium und Tritium als Brennstoff nutzt, sind gut bekannt. Sie werden im Tripelprodukt $nT\tau$ aus Plasmadichte n, Plasmatemperatur T und Energieeinschlusszeit τ beschrieben. Dabei ist die Energieeinschlusszeit ein Maß für die Wärmeisolation des Plasmas. Sie kennzeichnet die Energieverluste des Plasmas, für die zwei Prozesse verantwortlich sind: Stöße zwischen den Plasmateilchen und Plasmaturbulenz, d. h. kleine Wirbel, welche Teilchen und Energie nach außen befördern können. Im Allgemeinen dominieren turbulente Prozesse diesen Energie- und Teilchentransport. Im Stellarator jedoch, dessen Entwicklung im IPP im Folgenden nachgezeichnet wird, kann dies auch anders sein.

Für die Wärmeisolation des Plasmas gegen die Umgebung sorgen starke Magnete, die Feldstärken von einigen Tesla erzeugen. Die Lorentz-Kraft des Magnetfeldes zwingt die Ionen und Elektronen des Plasmas zu Kreisbewegungen um die Feldlinien. Ihr Radius senkrecht zum Feld, der Larmor-Radius, nimmt dabei die Rolle einer mittleren freien Weglänge ein. Magnetisierte Plasmen verhalten sich anisotrop: Transportvorgänge parallel zu den Feldlinien besitzen eine große mittlere freie Weglänge, senkrecht dazu sind sie durch den Larmor-Radius beschränkt.

Die einfachste Einschlussgeometrie wäre eine geradlinige Anordnung von Magnetfeldspulen. Sie eignet sich wegen der Verluste an den Enden einer solchen Anlage jedoch nicht zum Einschließen von Hochtemperaturplasmen. Zwar wurden bei der Entwicklung sogenannter Spiegelmaschinen kunstvolle Endstücke entwickelt, die als „magnetische Verschlüsse“ lineare Anordnungen abdichten sollten. Die grundlegende Idee ist dabei, das Magnetfeld B an den beiden Enden anzuheben, wodurch ein magnetischer „Spiegel“ entsteht, der einen Teil der zur Öffnung strömenden Plasmateilchen reflektiert – daher die Bezeichnung „Spiegelmaschine“: Ohne Stöße ist die Bewegung eines geladenen Teilchens im nun inhomogenen Magnetfeld durch die Erhaltung des magnetischen Moments $\mu = mv_{\perp}^2/2B$ und die der Gesamtenergie $E = m/2(v_{\perp}^2+v_{//}^2)$ bestimmt. Bei Annäherung an den Endbereich mit erhöhtem Feld erhöht sich auch die zum Feld senkrechte Geschwindigkeitskomponente $v_{\perp}$, was zu Lasten der parallelen Geschwindigkeit $v_{//}$ geht. Diese kann im Extremfall zu Null werden: Das Teilchen wird reflektiert und bleibt eingeschlossen. Für den Teilcheneinschluss kommt es also auf das Verhältnis von $v_{\perp}$ zu $v_{//}$ an. Teilchen mit kleinem $v_{\perp}/v_{//}$ können dabei trotz der Endspiegel verloren gehen. Weil diese Gruppe ständig durch Stöße mit neuen Teilchen aufgefüllt wird, kommt es trotz der Spiegel zu einer endlichen Teilchen- und Energieeinschlusszeit. (Die Einschlussphysik ist jedoch noch etwas komplexer. Elektronen werden nämlich häufiger in diese Teilchengruppe gestreut als Ionen. Es bilden sich daher Raumladungen aus, deren elektrische Felder den Einschluss ebenfalls beeinflussen. Die Folge aus all dem: Wegen insgesamt zu hoher Verluste wurde das Spiegelmaschinen-Programm in den USA vollständig und in Russland bis auf Spezialanwendungen eingestellt.

Die Endverluste in linearen Anordnungen lassen sich in ringförmig geschlossenen, d.h. toroidalen Geometrien vermeiden, bei denen die Spulen im Kreis aufgestellt sind. In diesem Fall ist das Magnetfeld axial-symmetrisch, jedoch inhomogen, weil die Feldstärke zum Zentrum des Ringes hin ansteigt. Dies bringt ähnliche Effekte wie bei der Spiegelmaschine ins Spiel: Der Feldgradient ∇B übt auf ein Teilchen mit magnetischem Moment μ eine Kraft $-\mu\nabla B$ aus, die zu einer senkrecht zu Feld und Feldgradient stehenden vertikalen Drift führt. Ähnlich wie bei der Spiegelmaschine kommt es zu Teilchen- und Energieverlusten. Es bildet sich ein elektrisches Feld, so dass sich kein Kräftegleichgewicht einstellen kann. Die Lösung für dieses Problem wurde in den 1950er Jahren gefunden: Die Magnetfeldlinien dürfen nicht axial im Einschlussvolumen umlaufen, sondern spiralförmig, also helikal. Neben dem ringförmigen Feld, dem Toroidalfeld, um das es bisher ging, ist eine zweite, dazu senkrecht stehende Feldkomponente notwendig, das Poloidalfeld. Diese Feldanordnung führt zur Driftkompensation, weil die vertikale Drift auch in das Zentrum des toroidalen Einschlussvolumens führen kann. Ohne Stöße zwischen den Teilchen gäbe es auf diese Weise keine Verluste.

Zwei verschiedene Einschlusskonzepte beruhen auf diesem Grundgedanken zweier überlagerter Feldkomponenten, die in ihrer Summe eine Verdrillung der Feldlinien bewirken – der Tokamak und der Stellarator. Wie in Kapitel 2 beschrieben, erzeugt in Anlagen vom Typ Tokamak ein ringförmiger Strom im Plasma, der im einfachsten Fall induktiv erzeugt wird, das Poloidalfeld. In diesem Fall setzt der Plasmaeinschluss die Existenz des Plasmas bereits voraus. Es braucht gute elektrische Leitfähigkeit, damit ein ausreichend hoher Plasmastrom induziert werden kann. Dafür reicht die Stromheizung zunächst aus. Für Plasmen nahe den Zielwerten für ein Kraftwerk sind jedoch zusätzliche Heiztechniken von mehreren zehn Megawatt Leistung notwendig. Weil das Tokamak-Plasma selbst einen Teil des einschließenden Magnetfeldes erzeugt, spricht man hier von internem Einschluss.

Dagegen baut der Stellarator auf externen Einschluss: Das gesamte Magnetfeld wird allein durch äußere Spulen erzeugt; das Vakuumfeld besitzt auch ohne Plasma einschließende Eigenschaften. Lyman Spitzer von der Universität Princeton konnte 1951 zeigen, dass eine Anordnung aus helikalen Magnetwicklungen, die sich in verdrillter Multipolanordnung außen um das Plasmagefäß herumschrauben, eine poloidale Feldkomponente erzeugen kann. Die Spulen schließen sich nach einigen toroidalen und poloidalen Umläufen und erzeugen einen Magnetfeldkäfig mit einer endlichen Zahl toroidaler Perioden.

Auf diese Weise lassen sich unterschiedliche Konzepte verwirklichen. In Torsatrons – bzw. Heliotrons, wie sie in Japan genannt werden – fließen in den helikalen Leitern alle Ströme in dieselbe Richtung. In Stellaratoren fließen die Ströme wechselseitig in unterschiedliche Richtungen, der Gesamtstrom durch eine poloidale Ebene ist also Null. Ein anderer wichtiger Parameter für den Aufbau des magnetischen Systems ist die Zahl der helikalen Leiter. Ein sogenannter l=3-Stellarator mit drei helikalen Leiterpaaren erzeugt ein einschließendes Vakuumfeld, das zu einem dreieckigem Plasmaquerschnitt führt. Entsprechend hat das Plasma eines l=2-Stellarators einen elliptischen Querschnitt, der sich schraubenförmig entlang der zentralen magnetischen Achse dreht.

Die ersten IPP-Stellaratoren

In den 1960er Jahren begann das IPP unter der Führung von Günter Grieger mit der Entwicklung der Stellaratoren der „Wendelstein"-Linie. Dieser Name war der europäische Reflex auf das „Projekt Matterhorn" des US-Stellarator-Programms, wobei die Namenswahl im IPP dem Wesen des helikalen Einschlusses näherkam. Heute werden helikale Systeme in Spanien, den USA und Japan betrieben. Neben dem optimierten Stellarator Wendelstein 7-X im IPP in Greifswald ist die „Large Helical Device" (LHD) in Japan, ein Heliotron, das wichtigste Experiment.

Die ersten IPP-Stellaratoren Wendelstein 1-A und 1-B waren nach dem Vorbild des Model-C-Stellarators in Princeton als „Rennbahn" – englisch „racetrack" – konzipiert. Es waren also keine rein kreisförmigen Anordnungen, sondern es lagen gerade Strecken zwischen den beiden Bögen. Diese

Anlagen, wiewohl lediglich in der Größe von Tischanordnungen, lieferten bereits wichtige Erkenntnisse: Die poloidale l=2-Periodizität ist der l=3-Konfiguration vorzuziehen; die geraden Teile einer Rennbahn führen zu Feldstörungen, die den Einschluss verschlechtern. Die Nachfolgeexperimente Wendelstein 2-A und 2-B bauten auf diesen Erkenntnissen auf.

Ende der 1960er Jahre geriet die Stellarator-Forschung in eine ernsthafte Krise: Die mit dem C-Stellarator in Princeton erreichten Plasmawerte waren den Ergebnissen des aus Russland kommenden Tokamak weit unterlegen. Dieses „Sputnik-Erlebnis“ der US-Fusionsforschung führte zum raschen Umbau des C-Stellarators hin zum ST-Tokamak. „S“ steht hierbei für „symmetric“ und weist damit auf einen wichtigen Aspekt für guten magnetischen Einschluss hin.

Auch im IPP wurde der Fortgang der Stellarator-Forschung diskutiert. Die Schlussfolgerung war hier jedoch nicht, die Linie aufzugeben, sondern vielmehr das Forschungsfeld um den Tokamak zu erweitern. Ein Grund für das Festhalten am Stellarator waren die guten Ergebnisse von Wendelstein 2-B, die man in Princeton damals etwas ungläubig das „Munich Mystery“ nannte.

Anfang der 1970er Jahre beschloss man also, zwei größere Anlagen zu bauen, den Tokamak Pulsator und den Stellarator Wendelstein 7-A. Sie gingen 1973 und 1975 in Betrieb. Wendelstein 7-A wurde mit leistungsfähigen Heizapparaturen ausgestattet, so dass weltweit erstmalig der reine Stellarator-Betrieb möglich wurde – der Betrieb ohne einen im Plasma induzierten Strom. Insgesamt entwickelte sich diese zweigleisige Strategie zu einem Alleinstellungsmerkmal des IPP mit weitreichenden wissenschaftlichen und, wie sich später zeigen sollte, auch politischen und gesellschaftlichen Folgen.

Stellarator und Tokamak parallel zu untersuchen, brachte große wissenschaftliche Vorteile: Man konnte die zwei komplementären Konzepte des äußeren und inneren Einschlusses untersuchen, dabei aber die gleichen Techniken für den Bau, den Betrieb, die Heizung und die Diagnostik der Anlagen nutzen, was den Mehraufwand in Grenzen hielt. Vorzüge des Tokamak waren der rotationssymmetrische Aufbau, der sicherstellte, dass auch die im inneren Magnetfeldspiegel reflektierten Plasmateilchen eingeschlossen bleiben. Hinzu kam der einfache magnetische Aufbau, die simple Strom-Heizung, mit der ein Grundplasma erzeugt werden konnte, sowie schließlich eine breite internationale Datenbasis. Vorzug des Stellarators war, dass bereits das Vakuum-Magnetfeld einschließenden Charakter besaß. Dadurch eignet sich der Stellarator grundsätzlich für den Langpuls- und Dauerbetrieb. Zudem ist ein Stellarator-Plasma stabiler gegen die Ausbildung magnetohydrodynamischer Instabilitäten, was das Arbeiten an den angezielten Betriebsgrenzen für Dichte und Plasmadruck möglich machen sollte.

Wie in Kapitel II.1 im Detail beschrieben, verlangt ein Fusionskraftwerk die Steuerung der Energie- und Teilchenflüsse aus dem Plasma und der daraus folgenden Plasma-Wand-Wechselwirkung. Bei Tokamaks wird das hierfür nötige Divertor-Feld durch spezielle Magnetspulen aufgebaut. In Stellaratoren bildet sich die magnetische Begrenzung des Plasmas günstigerweise durch eine natürliche „Separatrix“, die sich über eine Kette magnetischer Inseln am Plasmarand ergibt. Die komplementäre Zukunftsaufgabe des IPP-Fusionsprogramms war es also, den Poloidalfeld-Divertor für den Tokamak und den Insel-Divertor für den Stellarator zu entwickeln.

Dem Stellartor hafteten jedoch zwei fundamentale Probleme an – ein technisches und ein physikalisches. Eine große technische Herausforderung bei einem Stellarator-Kraftwerk ist der Bau großer supraleitender helikaler Spulen sowie die starke Verkopplung von helikalen und toroidalen Spulen, die kaum Platz bieten würden für den fernbedienten Zugang zum Inneren des Kraftwerks. Dieses Problem wurde konzeptionell durch die sogenannten Rehker-Wobig-Spulen gelöst. Die Stromwege in den helikalen und toroidalen Spulen lassen sich beim l=2-Stellarator durch modulare, nicht-ebene Einzelspulen nachbilden. Auf diese Weise kommt man wie beim Tokamak zu Einzelspulen handhabbarer Größe, die industriell gefertigt und ausgeliefert werden können. Diese Spulen sind jedoch nicht mehr flach, sondern dreidimensional verwunden. Mit Hilfe dieser modularen Spulen können

unterschiedliche Eigenschaften helikaler Systeme kombiniert werden, etwa verschiedene Helizitäten. So lässt sich der gesamte Konfigurationsraum, den helikale Systeme anbieten, technisch umsetzen.

Das physikalische Problem des Stellarators ist grundsätzlicher Natur: Der äußere Einschluss erlaubt keine Feldanordnung mit kontinuierlicher Symmetrie; das einschließende Magnetfeld und das daraus resultierende Plasma sind dreidimensional verwunden. Beim Tokamak dagegen sorgt die Axialsymmetrie dafür, dass die toroidale Winkelkoordinate eine ignorable Koordinate ist. Neben den sogenannten freien Teilchen sind daher auch die im Magnetfeldspiegel der toroidalen Anordnung gefangenen Teilchen eingeschlossen. Im Stellarator dagegen gibt es neben dem toroidalen auch einen helikalen Spiegel und deshalb treten drei Klassen von Teilchen auf – freie Teilchen sowie im toroidalen Spiegel und im helikalen Spiegel gefangene Teilchen. Sowohl im Tokamak wie im Stellarator führen die gespiegelten Teilchen, deren Bahnen durch die Inhomogenität des Magnetfeldes weit von den Flussflächen wegführen, zu sogenannten neo-klassischen Verlusten. Auf die im helikalen Spiegel gefangenen Teilchen des Stellarators wirkt jedoch nicht wie beim Tokamak die Driftkompensation, weshalb sie wie bei der Spiegelmaschine das einschließende Feldvolumen verlassen. Bei Plasmen mit Kraftwerkswerten bestimmen diese Verluste den Einschluss – und er wäre nicht ausreichend. Dem Stellarator drohte damit das Schicksal der Spiegelmaschine. Der Entschluss zur Fortsetzung des Stellarator-Programms war deshalb zugleich der Auftrag an die Stellarator-Theorie des IPP, einen Weg zur Optimierung des Stellartorkonzepts zu finden.

Aims of IPP

Die von Klaus Pinkau 1981 initiierte Programmdiskussion mündete in die Formulierung der „Aims of IPP". Auf der Stellarator-Seite sah diese Zukunftsplanung die Weiterführung von Wendelstein 7-A vor sowie die theoretische und experimentelle Entwicklung „fortgeschrittener" Stellaratoren. Dabei baute man auf einem dreifachen Fundament auf:

- auf den Erfolgen von Wendelstein 7-A[1)], insbesondere auf dem Beweis, dass netto-stromfreie Stellarator-Plasmen die gleiche Einschlussqualität wie vergleichbare Tokamaks zeigen,
- auf den Rehker-Wobig-Spulen für den Bau künftiger Stellaratoren und
- auf den ersten Erkenntnissen zur Optimierung des Stellarators.

Die experimentelle Entwicklung wurde in zwei Schritten geplant: Zunächst vorgesehen war der Bau des kleinen „Advanced Stellarator" Wendelstein 7-AS mit modularen Spulen aus Kupfer[2)]. Im Erfolgsfall sollte dann der Bau des größeren Wendelstein 7-X folgen, ein vollständig optimierter Stellarator mit modularen supraleitenden Spulen, der die Fähigkeit zum Dauerbetrieb nachweisen sollte.

Wendelstein 7-AS ging 1988 nach dreijähriger Bauzeit mit der in den „Aims of IPP" geplanten Ausstattung in Betrieb und wurde bis 2002 genutzt. 1981 hatte man als Ziele für die Anlage formuliert,

- den quasi-stationären Betrieb zu demonstrieren,
- den Transport von Plasma- und Verunreinigungsteilchen zu untersuchen,
- druckgetriebene innere Ströme (Pfirsch-Schlüter-Gleichgewichtsströme, Bootstrap-Strom) und extern von Heizverfahren erzeugte Ströme zu analysieren,
- Gleichgewicht und Stabilität des Plasmas bei hohem Druck zu untersuchen und
- unterschiedliche Heizverfahren zu testen.

Von besonderer Bedeutung für die Entwicklung des optimierten Stellarators sind die an Wendelstein 7-AS erbrachten Nachweise,

- dass mit modularen Spulen ein Feldsystem, das sich aus unterschiedlichen Multipolanteilen (vor allem l=2 und l=3) zusammensetzt, mit guten Flussflächen für den Plasmaeinschluss erzeugt werden kann,
- dass die Reduktion der Pfirsch-Schlüter-Ströme zu einem stabilen Plasmagleichgewicht führt,
- und dass sich der von Druckunterschieden getriebene Bootstrap-Strom quantitativ verstehen lässt.

[1)] siehe Seite 195 ff.: G. Grieger et al.: Confinement of stellarator plasmas with neutral beam and RF heating in W VII-A, in: Plasma Phys. Control. Fusion 28 (1986)
[2)] siehe Seite 207 ff.: Application for Preferential Support, Phase I, for Wendelstein VII-AS. Part I, Executive Summary, Dezember 1981)

In wichtigen Einzelstudien an Wendelstein 7-AS wurde gezeigt

- wie das radiale elektrische Feld im Plasma den dominanten Verlustkanal durch binäre Stöße (Elektronen- oder Ionenwurzel) festlegt,
- dass die Teiloptimierung von Wendelstein 7-AS zu beachtlichen Beta-Werten von 3,4 Prozent führt – im Vergleich zu niedrigen 0,7 Prozent bei dem klassischen l=2-Stellarator Wendelstein 7-A (wobei der Beta-Wert für das Verhältnis von Plasmadruck zu Magnetfelddruck steht),
- und dass sich das im Tokamak ASDEX entdeckte High-Confinement Regime, oder kurz H-Regime, auch im Stellarator realisieren lässt, was die Universalität der zugrunde liegenden Einschlussphysik belegt[3)].

Zunächst nicht geplant, aber sehr wichtig für Wendelstein 7-X war es, dass mit Wendelstein 7-AS der Insel-Divertor verwirklicht und modellmäßig beschrieben werden konnte. Für Technik wie Modellierung war die Dreidimensionalität von Plasma-Randschicht und Divertor eine große Herausforderung. Eine Weiterentwicklung des dazu für Wendelstein 7-AS eingesetzten EMC-3-Codes erlaubte später eine zielgenaue Auslegung des Insel-Divertors von Wendelstein 7-X. Die Ergebnisse von Wendelstein 7-AS sind in der Arbeit von Hirsch et al.[4)] ausführlich zusammengefasst. Sie waren eine wichtige Grundlage für die europäische Genehmigung des Nachfolgers Wendelstein 7-X.

Der Stellarator Wendelstein 7-X

1993 stellte das IPP-Stellarator-Team das neue Projekt in einer Rundreise zu insgesamt 34 Stationen allen Mitgliedern des europäischen Fusionsprogramms vor[5)]. 1994 und 1996 folgten in zwei Schritten die europäischen Finanzierungszusagen für Wendelstein 7-X. Die wissenschaftliche Attraktivität des optimierten Stellarators war dabei ein wichtiger Grund dafür, Wendelstein 7-X in das europäische Fusionsforschungsprogramm aufzunehmen. Die Optimierung, die einst Arnulf Schlüter begonnen hatte, wurde nach der Formulierung der „Aims of IPP“ von der Gruppe um Jürgen Nührenberg energisch vorangetrieben. Sie orientierte sich an sieben Zielen:

(1) Bau eines Magnetfeldkäfigs mit ineinander geschachtelten Flussflächen bei großem Plasmaquerschnitt. Gefordert war eine Magnetfeldtopologie ohne magnetische Störungen in Form großer magnetischer Inseln im Plasmainneren, die die Einschlussqualität beeinträchtigt hätten.

(2) Ein Plasmagleichgewicht bei Beta-Werten bis zu 5 Prozent. Dies bezieht sich auf die Stärke druckgetriebener Ströme – Pfirsch-Schlüter- sowie Bootstrap-Strom. Beide lassen sich minimieren, wie Wendelstein 7-AS indirekt nachwies durch die Analyse des Plasmagleichgewichts bei hohen Beta-Werten. Nur wenn diese Ströme klein genug sind, bleibt die Qualität des optimierten Vakuumfeldes auch bei hohem Plasmadruck – und den daraus resultierenden Plasmaströmen – erhalten.

(3) Plasmastabilität bis zu Beta-Grenzwerten von 5 Prozent, eine Bedingung für die druck- und stromgetriebenen Instabilitäten. Die Minimierung der Pfirsch-Schlüter-Ströme verbessert auch die Stabilitätseigenschaften des Plasmas.

(4) Ein kleiner Bootstrap-Strom, um die Einschlussqualität des Vakuumfeldes, d.h. den externen Einschluss, nicht zu stören. An diesem wichtigen Parameter zeigen sich die Vorteile der in den „Aims of IPP“ gewählten zweigleisigen Forschungsstrategie. Während beim Tokamak der Bootstrap-Strom möglichst groß werden soll, um mit geringerem technischem Aufwand den nicht-induktiven Plasmastrom aufrecht zu erhalten, muss er beim optimierten Stellarator möglichst klein werden. Die IPP-Experimente ASDEX Upgrade und Wendelstein 7-AS konnten zeigen, dass der Bootstrap-Strom für beide Konfigurationen und alle relevanten Szenarien sicher vorhersagbar ist.

(5) Vernachlässigbare Driftverluste bei kraftwerksähnlichen Plasmawerten. Diese Forderung adressiert direkt die konzeptionelle Schwachstelle des Stellarators, nämlich die aus der Dreidimensionalität folgenden Driftverluste. Sie steigen mit hoher Potenz der Plasmatemperatur T (Flüsse ~ $T^{9/2}$) derart an, dass ein konventioneller Stellarator für ein Kraftwerk letztlich nicht in Frage kommt.

[3)] F. Wagner et al., W7AS – One step of the Wendelstein stellarator line, in: Phys. Plasmas 12 (2005)
[4)] siehe Seite 213 ff.: M. Hirsch et al.: Major results from the stellarator Wendelstein 7-AS. In: Plasma Phys. Control. Fusion 50 (2008) (Ausschnitt)
[5)] siehe Seite 232 ff.: Wendelstein Project Group: Wendelstein 7-X, Application for Preferential Support, Phase I, (Preface, Executive Summary, part I (Seite 1-7) August 1990

(6) Guter Einschluss der Helium-Teilchen in einem späteren Kraftwerk, also eine ausreichende Selbstheizung des gezündeten Plasmas: Zum einen soll der Anteil der Helium-Ionen, die mit einem ungünstigen $v_\perp/v_{//}$-Verhältnis aus dem Fusionsprozess hervorgehen – die sogenannten prompten Verluste – gering sein. Zum anderen sollen die Teilchen so lange im Plasma verbleiben, bis sie ihre Energie dort abgegeben haben. Wie gut dies gelingt, kann in heutigen Anlagen nur in verkleinertem Maßstab untersucht werden: Wendelstein 7-X ist kein Kraftwerk und wird insbesondere nicht mit Tritium betrieben. Helium-Ionen werden daher nicht erzeugt. Skaliert auf das Magnetfeld von Wendelstein 7-X von 2,5 Tesla kann das Verhalten von Helium-Ionen jedoch durch andere energiereiche Ionen simuliert werden. Solche Teilchen mit Energien um die 60 Kiloelektronenvolt lassen sich mit der Plasmaheizung von Wendelstein 7-X erzeugen, so dass erste günstige Befunde bereits vorliegen.

(7) Bildung einer magnetischen Inselkette am Plasmarand: Mit ihrer Hilfe sollen die Energie- und Teilchenflüsse aus dem Plasma und ihre Wechselwirkung mit der Gefäßwand kontrolliert werden. Wie schon Wendelstein 7-AS zeigte, können „natürliche“ Inseln, die sich aufgrund der toroidalen Periodizität des dreidimensionalen Plasmas am Plasmarand bilden, die Plasmaflüsse effektiv in separate Divertorkammern ableiten.

Diese sieben gewünschten Plasmaeigenschaften müssen sich aus einer geeigneten, „optimierten“ Geometrie des magnetischen Feldes ergeben. Diese Geometrie wird jedoch von vielen Parametern bestimmt – dem Verhältnis von großem und kleinen Plasmaradius, der Zahl der toroidalen Perioden, der Mischung der poloidalen Feldkomponenten, der Rotationstransformation und anderen mehr. Eine analytische Problembehandlung ist angesichts dieser Komplexität nicht mehr möglich. Verlangt ist vielmehr eine numerisch gestützte Optimierungsstrategie. Unter anderem für diese Aufgabe betrieb das IPP seit 1979 einen leistungsfähigen Cray-Rechner – weltweit der erste seiner Art für die Forschung – und hat seine Rechner- und Datenanalyse-Kapazitäten systematisch ausgebaut. Daraus entstand letztlich das Rechenzentrum der Max-Planck-Gesellschaft in Garching.

Obwohl die Optimierung des Stellarators ohne Rechnerunterstützung nicht zustande gekommen wäre, ist Wendelstein 7-X dennoch nicht das Produkt der Numerik alleine. Eine physikalische Richtschnur, die von J. Nührenberg entwickelt wurde, war das Konzept der quasi-isodynamischen Systeme[6]: Unter Symmetriebedingungen lassen sich Einschlusskonzepte definieren, die keine radialen Flüsse und Ströme aufweisen, sog. isodynamische Systeme. Sie lassen sich jedoch in toroidalen Geometrien nicht realisieren. Dagegen kann in quasi-isodynamischen Systemen die Feldstärke |B|, die für den Teilcheneinschluss verantwortlich ist[7], in dreidimensionalen helikalen Systemen zweidimensional gestaltet werden.

Die den Ingenieur betreffenden Forderungen beim Bau der Maschine waren, modulare Spulen zu entwerfen, die eine Flussflächengeometrie in Form eines Pentagons liefern (m=5). Das Magnetfeld war in den Ecken des Pentagons, also den Bereichen mit Feldkrümmungen, zu erhöhen. Auf diese Weise wurde der von den Spiegelmaschinen her bekannte Effekt genutzt, Teilchen mit hohem Verhältnis $v_\perp/v_{//}$, die für radiale Verluste anfällig sind, aus den kritischen Zonen auszusperren. Die wesentlichen poloidalen Feldanteile sind l = 1, 2 und 3 und führen zu einer starken räumlichen Verformung der Flussflächen. Ferner sollte die magnetische Achse des verschachtelten Flussflächensystems bereits helikal verdreht sein und so aus der Geometrie heraus eine hohe Rotationstransformation erlauben (iota=1).

Während sich der europäische Genehmigungsprozess von Wendelstein 7-X weitgehend auf wissenschaftliche, technische und forschungsstrategische Aspekte konzentrierte, war der nationale Prozess von politischen Entscheidungen und regionalen Interessen überlagert. Bis Frühjahr 1993 gab es keine ministerielle Zustimmung zu Wendelstein 7-X. Es war offensichtlich schwer möglich, neben dem Forschungsreaktor FRM-II ein weiteres Großexperiment nach Bayern zu vergeben. Erst im Dialog mit dem neuem Forschungsminister Dr. Paul Krüger änderte sich die Perspektive. Er hatte Interesse an Projekten, die rasch in den neuen Bundesländern anzusiedeln wären und zum Aufbau der dortigen Forschungsinfrastruktur beitragen könnten. Als Standort für Wendelstein 7-X bot sich

[6] J. Nührenberg, R. Zille: Quasi-Helically Symmetric Toroidal Stellarators, in: Phys. Lett. A 129, Seite 115-117 (1986), https://doi.org/10.1016/0375-9601(86)90539-6
[7] A. H. Boozer: Transport and isomorphic equilibria, in: Phys. Fluids 26 (1983) Seite 496-499

die Hansestadt Greifswald an mit ihrer traditionsreichen Universität, deren mathematisch-naturwissenschaftliche Fakultät einen Forschungsschwerpunkt Plasmaphysik aufwies.

Viele Institutionen waren für die Genehmigung des neuen Projekts am neuen Ort zuständig und mussten dafür gewonnen werden – der Bund sowie die Länder Mecklenburg-Vorpommern und Bayern als Geldgeber, die Max-Planck-Gesellschaft, die Stadt Greifswald sowie die Universität. Die Entscheidung der Wissenschaftlichen Leitung des IPP unter Führung Klaus Pinkaus fiel sehr früh zu Gunsten von Greifswald. Der Genehmigungsprozess war zum Ende der Legislaturperiode jedoch nicht abgeschlossen. In die Forschungsinfrastruktur-Liste aufgenommen, wurde Wendelstein 7-X jedoch Teil der Koalitionsvereinbarung von CDU und FDP. 1996 schließlich konnte eine Verwaltungsvereinbarung zwischen dem Bund und den Ländern Mecklenburg-Vorpommern und Bayern unterzeichnet werden.

Aufgabe des IPP war es nun nicht mehr, wie ursprünglich geplant, ein Großexperiment in vertrauter Umgebung zu realisieren. Stattdessen war ein Institut auf der grünen Wiese zu errichten. Daneben galt es, über einen Sozialplan möglichst viele Erfahrungsträger aus Technik und Physik von Garching für Greifwald zu gewinnen. 1997 konnte der Grundstein für das Teilinstitut des IPP gelegt werden; im Juli 2000 wurde der Neubau eröffnet.

Im Jahr 2015 schließlich, 34 Jahre nach der Erwähnung in den „Aims of IPP“, ging Wendelstein 7-X in Betrieb. Obwohl die Plasmaheizungen noch nicht vollständig zur Verfügung standen und die Wasserkühlung für Wand und Divertor erst später eingeplant war, brachten bereits die ersten Experimentierphasen entscheidende Erkenntnisse bei relevanten Plasmawerten[8]:

- Die gemessene Flussflächentopologie kann rechnerisch nur nachempfunden werden, wenn man annimmt, dass die störenden Ausgleichsströme reduziert sind – so wie es die Optimierung vorgesehen hatte. Die Untersuchungen sollen nahe der erwarteten Beta-Grenze weitergeführt werden, sobald mehr Heizleistung zur Verfügung stehen wird.
- Das Magnetfeldsystem von Wendelstein 7-X ist flexibel genug, um optimierte ebenso wie nichtoptimierte, eher klassische Stellarator-Konfigurationen verwirklichen zu können. In diesem Vergleich wurde der bootstrap-Strom untersucht, wobei sich der Strom im Plasma voll entwickeln konnte. Gute qualitative Übereinstimmung zwischen den Messergebnissen und den entsprechenden neo-klassischen Rechnungen konnte erzielt werden[9].
- Wichtig für die prinzipielle Kraftwerkseignung des Stellarators ist es nachzuweisen, dass die neoklassischen Verluste durch die Optimierung abgesenkt werden. Schon bei den moderaten Heizleistungen, die bislang zur Verfügung standen, konnten Plasmawerte erzielt werden, zum Beispiel Elektronentemperaturen von 3 Kiloelektronenvolt, die wegen zu hoher neo-klassischer Verluste ohne Optimierung nicht hätten erreicht werden können[10].
- Im driftoptimierten Plasma von Wendelstein 7-X mit niedrigen neo-klassischen Verlusten überwiegen – wie beim Tokamak – die Verluste durch turbulenten Transport und bestimmen die Einschlusszeit. In beiden Konfigurationen – in ASDEX Upgrade und Wendelstein 7-X – zeigt sich, dass die von Ionengradienten getriebene Turbulenz den Einschluss der Ionen begrenzt, wie in einer kürzlichen vergleichenden Studie nachgewiesen wurde[11]. Diese Instabilitäten lassen sich durch Veränderung der Dichteprofile stabilisieren. Das Verfahren funktioniert sowohl bei Tokamaks als auch bei Stellartoren mit optimiertem neo-klassischen Transport. In solchen Szenarien wurden für helikale Systeme die höchsten Werte für das Tripelprodukt $nT\tau$ nachgewiesen.
- Die Entwicklung des Insel-Divertors wurde mit Wendelstein 7-X erfolgreich fortgesetzt. Dank der Eignung des Stellarators zum Betrieb bei hohen Dichten konnten Zustände geschaffen werden, bei denen nahezu 100 Prozent der ins Plasma eingebrachten Leistung in Randschicht und Divertor als Strahlung großflächig abgegeben wird. Solche Plasmen sind in der Fachsprache „abgelöst“ vom Plasma-Wand-Kontakt in den Divertorkammern, wodurch thermische Überlastung vermieden wird.

---

[8] siehe Seite ... ff: T. Klinger et al.: Overview of first Wendelstein 7-X high-performance operation, in: 2019, Nucl. Fusion 59, 112004

[9] Dinklage, A., Beidler, C.D., Helander, P. et al.: Magnetic configuration effects on the Wendelstein 7-X stellarator, Nature Phys. 14 (2018) 855–860, https://doi.org/10.1038/s41567-018-0141-9

[10] siehe Seite ... ff: Beidler, C.D., Smith, H.M., Alonso, A., et al.: Demonstration of reduced neoclassical energy transport in Wendelstein 7-X, Nature, 596 (2021) 221–226, https://doi.org/10.1038/s41586-021-03687-w

[11] M.N.A. Beurskens et al.: Confinement in electron heated plasmas in Wendelstein 7-X and ASDEX Upgrade; the necessity to control turbulent transport, in: Nuclear Fusion (2021), im Druck, https://doi.org/10.1088/1741-4326/ac36f1

Die Prinzipien der Quasi-Symmetrie lassen sich für die in Frage kommenden toroidalen Symmetrien – axial, helikal oder poloidal (im Rahmen quasi-isodynamischer Felder wie bei Wendelstein 7-X) verwirklichen. In den USA und Japan wurden solche Systeme mit den Anlagen HSX (Helically Symmetric Experiment) der Universität von Wisconsin-Madison und Heliotron J an der Universität von Kyoto gebaut und erfolgreich betrieben. Die Grundlagen für diese Konzepte wurden weiterentwickelt. So hat man im IPP Konfigurationen gefunden, welche die Helium-Teilchen eines Kraftwerks bereits im Vakuumfeld einschließen würden. In Princeton wurden Konzepte entwickelt, bei denen die Abweichungen von der Quasi-Symmetrie sehr gering sind, etwa in der Stärke des Erdmagnetfeldes. Die Arbeiten beweisen zwar nicht, dass man Quasi-Symmetrie vollständig realisieren kann, wohl aber, dass man ihr für praktische Anwendung ausreichend nahekommen kann.

Für ein Stellarator-Kraftwerk kommt nur ein optimiertes helikales System in Frage. Im IPP wird entlang der Wendelstein-Linie das HELIAS-Kraftwerkskonzept entwickelt. Wichtige technische Fragen wurden abgeklärt – der Bau großer modularer Spulen, das Abstützungskonzept für diese Spulen, der Einbau sogenannter Blankets für das Erzeugen von Tritium und die Kosten für das Kraftwerk. Ob es zum Bau einer solchen Anlage kommen wird, hängt auch vom Erfolg des Tokamaks ITER ab. Viele technische Entwicklungen von ITER können auf den Stellarator übertragen werden. Die Strategie der Europäischen Fusionsforschung sieht vor, nach ITER einen DEMO-Tokamak zu bauen und parallel dazu einen HELIAS-ITER zu realisieren. Mit welchen Gewichtungen nach einem erfolgreichen ITER-Betrieb Tokamak- und Stellartorkonzepte möglicherweise parallel weiterverfolgt werden, wird von der weltweiten Energieversorgung einer dann auf nahezu zehn Milliarden Menschen gewachsenen Erdbevölkerung abhängen.

Zusammenfassung

Unter der Führung von Klaus Pinkau wurden 1981 die „Aims of IPP“ formuliert, die unter anderem ein langfristiges Entwicklungsprogramm für die Stellarator-Linie des IPP entwarfen – ein beträchtlicher Motivationsschub, der die Optimierung des Stellarator-Konzepts möglich machte. Es wurde geplant, die physikalischen Grundlagen und technischen Voraussetzungen für optimierte Stellaratoren in zwei experimentellen Schritten zu überprüfen – im ersten Schritt mit dem kleinen, teilweise optimierten Stellarator Wendelstein 7-AS. Im Erfolgsfalle sollte eine große, vollständig optimierte Anlage mit supraleitenden Spulen folgen: Wendelstein 7-X. Dank der Erfolge von Theorie und Experiment konnten die nationale und internationale Fusionsforschung, die Max-Planck-Gesellschaft und die Zuwendungsgeber von dieser Strategie überzeugt werden. 2015 begannen die Experimente an Wendelstein 7-X, jedoch nicht im bayerischen Garching, sondern – als größtes Forschungsprojekt in den neuen Bundesländern – in Greifswald in Mecklenburg-Vorpommern.

Heute ist Wendelstein 7-X ein wichtiges Experiment des europäischen Fusionsforschungskonsortiums EUROfusion, das die Anlage mitfinanziert. Forscherinnen und Forscher aus der ganzen Welt arbeiten an Wendelstein 7-X. Der Weg der Forschung ist vorgezeichnet und bietet eine Perspektive für weitere 10 bis 15 Jahre bedeutsamer Untersuchungen. So gesehen, wurde im Frühjahr 1981 ein Programm entworfen, das für fünfzig Jahre einzigartige Forschungsperspektiven eröffnete.

2.1
EINLEITUNG
TOKAMAKS
KARL LACKNER
SEITE 8

Friedrich Wagner,
emeritiertes Wissenschaftliches Mitglied des Max-Planck-Instituts für Plasmaphysik

Plasma Physics and Controlled Fusion Vol.28, No.1A pp.43-53, 1986 0741-3335/86$3.00+ .00
Printed in Great Britain Institute of Physics and Pergamon Press Ltd.

CONFINEMENT OF STELLARATOR PLASMAS WITH NEUTRAL BEAM AND RF HEATING IN W VII-A

G. Grieger and W VII-A Team*,
NI-Team**, ECRH Group***, Pellet Injection Group (K. Büchl)

Max-Planck-Institut für Plasmaphysik
EURATOM-Association, D-8046 Garching, FRG

* G. Cattanei, D. Dorst, A. Elsner, V. Erckmann, G. Grieger, P. Grigull, H. Hacker, H.J. Hartfuß, H. Jäckel, R. Jaenicke, J. Junker, M. Kick, H. Kroiss, G. Kuehner, H. Maaßberg, C. Mahn, S. Marlier, G. Müller, W. Ohlendorf, F. Rau, H. Renner, H. Ringler, F. Sardei, M. Tutter, A. Weller, H. Wobig, E. Würsching, M. Zippe

** K. Freudenberger, W. Ott, F.-P. Penningsfeld, E. Speth

*** W. Kasparek, G. Müller, P.G. Schüller, K. Schwörer, M. Thumm, R. Wilhelm (Inst.f.Plasmaforschung, Univ. Stuttgart)

ABSTRACT

WENDELSTEIN VII-A has been operated for ten years. It is a low-shear, high-aspect-ratio device. The confinement properties have been thoroughly studied for both ohmically heated and net-current free plasmas. For the latter case, NBI- and ECF-maintained plasmas were of particular importance. It was found that under optimized conditions the core of high-pressure, net-current free plasmas is mainly governed by collisional effects. The experiment will now be shut down for upgrading it into the Advanced Stellarator WENDELSTEIN VII-AS.

KEY WORDS

Stellarator, WENDELSTEIN VII-A, Confinement, Radial electric fields, Net-current free operation, NBI, ECF-heating, Resonances.

INTRODUCTION

WENDELSTEIN VII-A started operation ten years ago. Towards the end of 1985 the machine will be shut down for upgrading it into the Advanced Stellarator WENDELSTEIN VII-AS. It is thus justified to start with a short summary of the main results obtained during the ten years of operation of W VII-A before concentrating on the main subject of this paper.

The definition of W VII-A, 15 years ago, was based on the results of the worldwide Stellarator programme which included race-track machines, like the C-Stellarator and URAGAN, HELIOTRONS, etc., together with the favourable results of the WENDELSTEIN I and II series operated with thermal cesium and barium plasmas. Whereas the plasma confinement in the other machines seemed to be more or less governed by Bohm diffusion, the results obtained by Berkl and others (1966) with cesium or barium plasmas in W I-B and W II-A clearly showed that collisional diffusion can be reached. These experiments also exhibited the effects of resonances in the twist number iota /2/ for $\iota = m/n$ as shown by Grieger and co-workers (1971) (see Fig. 1).

For these reasons, W VII-A was designed with the smallest possible deviation from axisymmetry: no race-track, TF-ripple $\leq 10^{-4}$ over the plasma cross-section, and even the helical ripple could be kept below $\varepsilon_h \leq 2$ %. In addition, the shear of the magnetic field, $\Delta\iota/\iota$, was arranged below 2 % in order to be able to exclude major resonances of the twist number from the confinement region. For stability, the configuration was provided with an average magnetic well. In order to achieve highest flexibility, the twist was introduced into the configuration by the field of an l = 2, m = 5 helix superimposed upon a purely toroidal

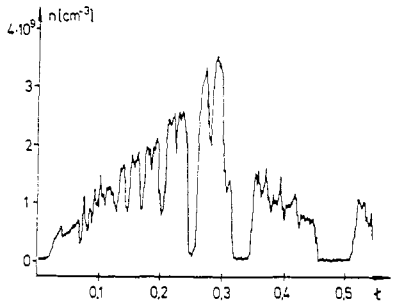

Fig. 1. Confinement vs. twist number ι for a barium plasma in the shearless Stellarator W II-A. For constant input flux of barium plasma the resulting density is a direct measure of the confinement time.

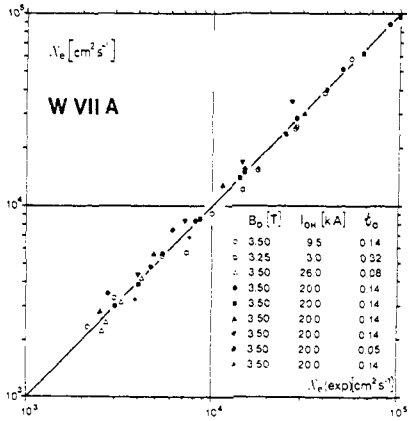

Fig. 2 Electron heat conduction for OH-plasmas in W VII-A for regions free of tearing modes and sawteeth.
$\chi_{e,OH} = 3.8 \cdot 10^{18} \cdot 1/n_e T_e^{2/3}$ is compared with experimental results.

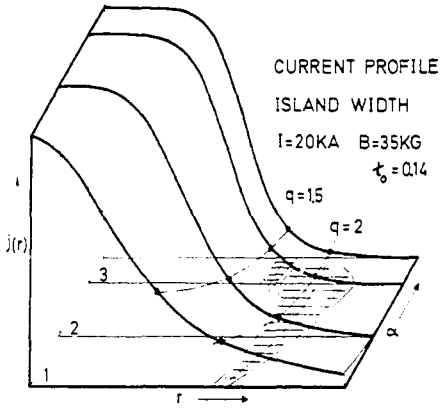

Fig. 3. Expected width of magnetic islands (hatched region) for various profiles of the OH-current distribution as they may result from the power deposition profile of NBI.

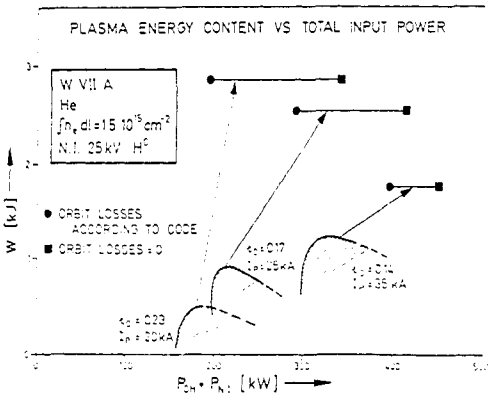

Fig. 4 Increase in plasma energy by NBI heating of OH target plasmas (hatched region). In all cases the curves indicate that the confinement time increases with the application of NBI.

main magnetic field. The major parameters of W VII-A are R = 2 m, $\bar{a} \approx 0.1$ m (depending on iota), $B \leq 4$ T, $t \leq 0.6$ at B = 3 T. For plasma heating, the machine was equipped with an air-core transformer for ohmic heating and later amended by 1.2 MW near-perpendicular neutral particle injection, 200 kW ECH with a frequency of 28 GHz first and 70 GHz later, and with about 500 kW ICH.

MAIN RESULTS

Ohmic Discharges

Already the first experiments with ohmic discharges (W VII-A Team, 1977) clearly showed that current disruptions could be fully stabilized by the Stellarator helical field whenever its contribution to the twist exceeded $t_0 = 0.14$ or so. Under such conditions tearing mode evolution and island generation could be analysed even far into the regime which would be subject to disruptions under pure Tokamak operation (W VII-A Team, 1979). χ_e, the electron heat conduction coefficient was measured locally in such regions of the profile as were free of low order tearing modes and sawtooth oscillations, and yielded (see Fig. 2)

$$\chi_{e,OH} = 3.8 \cdot 10^{18} \frac{1}{n_e T_e^{2/3}} \text{ cm}^2 \text{ s}^{-1} \qquad (1)$$

with $[n] = \text{cm}^{-3}$ and $[T] = \text{eV}$. This relation was found for all the accessible parameter ranges. There was no explicit dependence on the plasma current except where tearing modes occurred. There the transport was certainly larger. For these measurements B was 3.5 T. From later experiments at lower magnetic fields there are indications that the coefficient of proportionality shows some decrease with decreasing magnetic field.

Ohmic Discharges With Additional Heating

Care has to be taken when applying high power neutral injection to an ohmic discharge. The differences in the power deposition profile can easily lead to a change in the electron temperature profile, thus to a change in the OH-current distribution and to an onset of one of the critical tearing modes (e.g. m = 2) in turn (Fig. 3). With the help of the externally produced iota the resonant surfaces can be shifted in radius and as long as the most critical ones (low m and n) can be kept out of the regions of steep gradients of current density the above effects can be avoided. Under such conditions high power neutral beam injection heating is found to be efficient, to lead to steep temperature gradients in the plasma edge region, and not to exhibit confinement deteriorations (Fig. 4), (W VII-A Team and others, 1981).

In Figure 5, 120 kW of 70 GHz ECH power were applied to an OH discharge and the parameters of the OH and the EC heated discharge compared. One observes a significant increase in electron temperature combined with an only slight increase in electron density. Since the total heating power, 160 instead of 130 kW, stays nearly constant, a strong increase in electron energy confinement results. The observed effect is in rather good agreement with the electron heat conduction of equation (1), which for the plasma parameters reached in this experiment still yields the major contribution to χ_e.

Transition from Ohmic to Net-Current Free Discharges

With sufficient neutral injection power, the discharge can be maintained by neutral particle injection alone and the initial ohmic current needed for the production of a target plasma be ramped down to zero. At the same time the current in the helical windings was increased so as to keep the total twist constant. Such net current-free plasmas are very quiescent in that all MHD fluctuations die out, and the global energy confinement time shows a corresponding improvement. Figure 6 shows also a remarkable reduction of the H_α-signal when the net-current free conditions are reached. Such signals can be observed at all observation ports around the torus, and when normalizing them by the increasing electron density, they indicate a substantial increase in particle confinement (W VII-A Team and others, 1983 a). The particle confinement time reaches values of 0.1 s or more. Figure 7 shows the effect of a pellet injected into such a current-free discharge. Although density and temperature show strong variations, there is no instantaneous change in the total plasma energy, since the

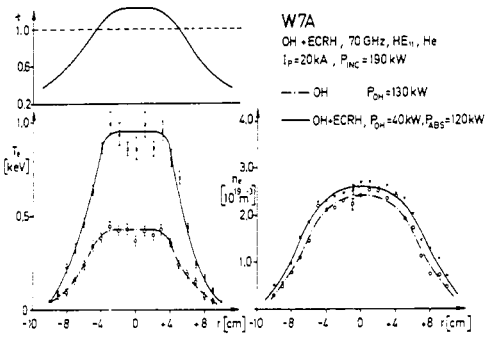

Fig. 5. Comparison of an OH-plasma without and with additional ECRH. The increase in plasma energy indicates a substantial increase of the confinement time for ECRH.

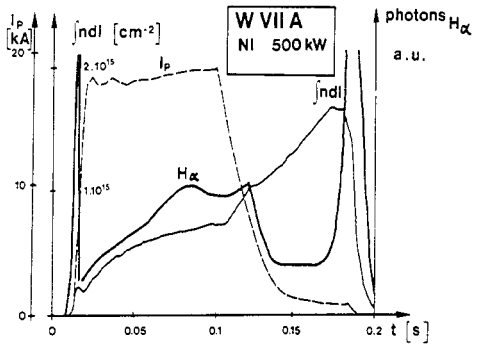

Fig. 6 Transition to net-current free, NBI-maintained operation. The decreasing H_α-signal, inspite of the strongly increasing density, indicates an increase of the particle confinement by about a factor of five at t = 0.17 s.

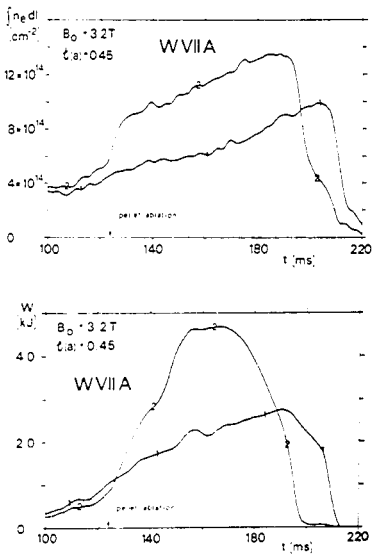

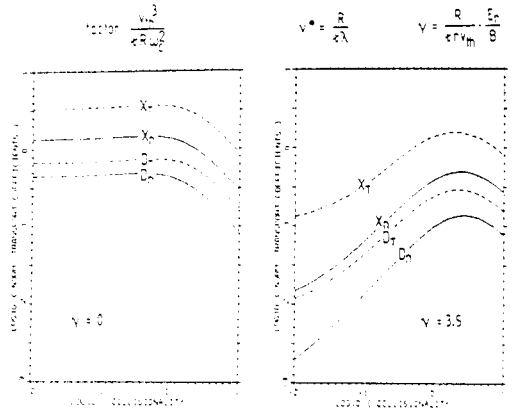

Fig. 8 Calculated transport coefficients vs. collisionality for two values of γ, which is proportional to the electric field, γ = 0 and γ = 3.5. The discharge mentioned in the text correspond to collisionality of 0.1. For this typical case γ = 3.5 corresponds to $E_r \approx 500$ V/cm.

Fig. 7 Pellet injection into an NBI-maintained discharge. Two discharges with and without pellet injection are compared. The top figure demonstrates that the pellet adds its amount of particles to the plasma density without appreciable loss during the course of the discharge. The continuous increase of n is caused by absorption from NBI. The bottom figure shows that there is no instantaneous change of the plasma energy when the pellet is launched. The steeper increase of W is caused by better NBI absorption with higher target density. The earlier decrease of W is caused by higher radiation with higher n.

ionization energy can be neglected. The density jump agrees with the number of the injected particles. The larger rate of increase of the plasma energy after pellet injection reflects the increased absorption of injection power due to the higher plasma density. The density trace indicates that nearly all injected particles remain within the discharge during its full duration which is consistent with a particle confinement time of 0.1-0.2 s or so. Similar particle confinement times were obtained for laser-ablated aluminum the dynamics of which is largely consistent with neo-classical confinement theory except for some regions in space and time where the transport is larger (W VII-A Team and others, 1985 a). There are indications that these deviations may result from the transient formation of magnetic islands or ergodic regions.

In this connection it is immediately obvious that the long confinement times achieved for all particle species in net-current free discharges provide problems with the impurity concentrations piling up during the period of the particle containment time (W VII-A Team and others, 1983 b). Particularly with the high particle densities reached by NBI-maintained discharges radiation mainly by oxygen lines - its ionization states being determined also by charge exchange recombination - becomes the dominant power loss at the end of the discharge. With a plasma radius of only 0.1 m and the high plasma densities reached in W VII-A it is not surprising that the impurities show the observed influence.

RADIAL ELECTRIC FIELD AND CONFINEMENT

Cross-field transport in net-current free Stellarator plasmas is strongly influenced by the formation of radial electric fields. It is well known that such electric fields modify the particle orbits. In particular, the excursion of passing particles from the magnetic surfaces becomes strongly reduced once the ExB-velocity becomes large compared to the poloidal component of the particle's parallel velocity, $v_{\parallel} \iota r/R$. Trapped particles might become untrapped by the same mechanism and then experience the same effect. Transport, being proportional to the square of the step size, will be affected in turn.

Neo-classical theory, within its range of validity, considers the effect of the electric field and takes it into account by requiring ambipolarity of the diffusion fluxes

$$\Gamma_e - \sum_i z_i \cdot \Gamma_i = 0 \qquad (2)$$

From the above arguments and $v_{\parallel,e} \gg v_{\parallel,i}$ it is clear that the radial electric field mainly changes the radial transport of the ions whereas that of the electrons remains nearly unaffected. In the theoretical analyses, when determining the electric field via eq.(2) it is customary to assume that the distribution functions f_e and f_i are both Maxwellian and that the dimensions of the plasma are large compared to all essential scale lengths. In strongly heated real laboratory plasmas these assumptions are easily violated.

Caused by the geometric conditions, high power neutral particle injection (28 keV, $\leq$ 500 kW absorbed power) into W VII-A is nearly perpendicular (6° off normal) so that a considerable fraction of the injected neutrals will be born as ions on or scattered into orbits intersecting the wall if there were only the "thermal ambipolar" electric field. If the electron confinement is good, there were no change in electron flux to compensate the higher ion losses and to maintain ambipolarity. Thus for the reason of the corresponding high energy tail in the ion distribution function and of the plasma dimensions allowing the formation of a loss cone, a radial electric field will spring up so as to reduce the ion losses again to those of the electrons by acting on the ion orbits. The same effect might occur with any other heating scheme like ICH or even with ECH where it is observed that the waves interacting with the edge plasma lead to high ion energy tails.

Such electric fields have been found in W VII-A. They were deduced from the measured Doppler shift of impurity lines. Outside about half the plasma radius the measurements yield typical polodial rotational velocities between 10 and 30 km/s corresponding to radial electric fields of 0.3 to 1.0 kV/cm. Under these conditions the E=0-poloidal macroscopic motion of the radiating ions was negligibly small so that no correction needed to be applied. Also the toroidal plasma rotation, measured by the same technique, was typically only of the same order of magnitude as the poloidal one and thus negligible in this connection.

Figure 8 displays the transport coefficients for two values of the radial electric field, $E_r = 0$ and $E_r \simeq 500$ V/cm, as they are obtained by analytical computations. The coefficients

are defined by the following two equations for particle and power transport respectively

$$\Gamma = - n[D_n \cdot (n'/n + z\phi'/T) + D_T \cdot T'/T] \quad (4)$$

$$Q = - nT[\chi_n(n'/n + z\phi'/T) + \chi_T \cdot T'/T] \quad (5)$$

The parameters of a typical discharge: ($n_e = 7.5 \cdot 10^{13}$ cm^{-3}, $T_i = 0.85$ keV, $T_e \approx 0.5$ keV, $B = 3$ T, $\iota \approx 0.5$) correspond to a collisionality of 0.1 in Fig. 8.
The discovery of these electric fields has three main and essential consequences: (i) The heating efficiency of the nearly perpendicular neutral beam injection increased by factors of up to three (or even more for counter-injection) by trapping a considerable fraction of the orbits lost otherwise. Thus the absorbed NBI power could reach values of up to 500 kW. (ii) According to Fig. 8, the ion particle confinement time should increase considerably. Since the resulting times are longer than the duration of the discharge, they are not accessible to direct measurement. The results displayed in Fig. 7 strongly indicate that the particle confinement time is very long indeed. (iii) As apparent from Fig. 8, also the ion heat conductivity, $\chi_{i,T}$, experiences a drastic reduction with E_r due to the reduced step width in the collisional transport. This effect is supported by the experimental results because without this reduction there was no chance to satisfy the power balance of the electrons and ions without violating laws resulting from basic collisional effects. It also predicts that in NBI heated plasmas the ions stay at higher temperature than the electrons which agrees with the observations.

Collisional slowing down of the high-energy ions resulting from neutral injection was verified from the measured charge exchange spectra and from the time-dependent neutron emission when using DD plasmas, (W VII-A Team and others, 1984).

Thus the occurrence and the influence of the radial electric field are basically understood. They result from classical effects and geometrical limitations only. The connected influence on particle orbits and transport is large and supported by experimental results.

ELECTRON CYCLOTRON FREQUENCY PLASMAS

Electron cyclotron frequency (ECF) plasmas could be generated in W VII-A without any special means for pre-ionisation and without using OH currents. 200 kW RF power were available for this purpose, with a frequency of 28 GHz in the earlier experiments and 70 GHz later. These plasmas are highly interesting for two reasons: (i) to serve as a target plasma for further heating by more intense heating sources like NBI or ICF, and (ii) to preferentially study the transport properties of the electron component of the plasma.

As far as case (i) is concerned, only plasmas generated by using the 70 GHz frequency have a chance to reach interesting parameters since the low cut-off density connected with 28 GHz only allows plasmas to be established with densities not exceeding 10^{13} cm^{-3}. Fig. 9 shows an example of an ECF generated plasma ($n_{eo} = 2 \cdot 10^{13}$ cm^{-3}, $T_{eo} = 1.4$ keV) further heated and maintained by NBI. It reaches densities of $n_{eo} = 1.1 \cdot 10^{14}$ cm^{-3} and temperatures of $T_{e,o} = 350$ eV so that this method of plasma generation is experimentally proven and available. Densities of up to $5 \cdot 10^{13}$ cm^{-3} are accessible by ECF (70 GHz) application alone. The cut-off density is $6 \cdot 10^{13}$ cm^{-3}.

First information on electron transport was obtained by using the 28 GHz gyrotron. The plasma parameters achieved are plotted in Fig. 10 (label 28 GHz). Taking the density profile from the measurement the various contributions to the heat conduction are calculated and shown in Fig. 11a. The axisymmetric part, $\chi_{e,HH}$, is taken from Hinton-Hazeltine (1976), the ripple contribution, $\chi_{e,ripple}$, from Shaing and others (1984). The anomalous part is given by eq. (1) of this paper but the coefficient reduced to $1.5 \cdot 10^{18}$ (for $B = 1$ T) to obtain best agreement with the experiment. The sum of the three contributions very well agrees with the values of χ_e derived from the local temperature gradients and the assumption of central power deposition. Contributions by radiation are small under these conditions (10-30 kW).

Also in Fig. 10 the data for a 70 GHz discharge at $B = 2.5$ T are shown. The results clearly exhibit a considerable increase in density and temperature for about the same ECF power applied as before, indicating a large increase of confinement as qualitatively expected from neo-classical theory. Fig.11(b), however, shows that in the region of the steepest gradients the neo-classical effects have already become smaller than $\chi_{e,OH}$ so that a clear-cut verifi-

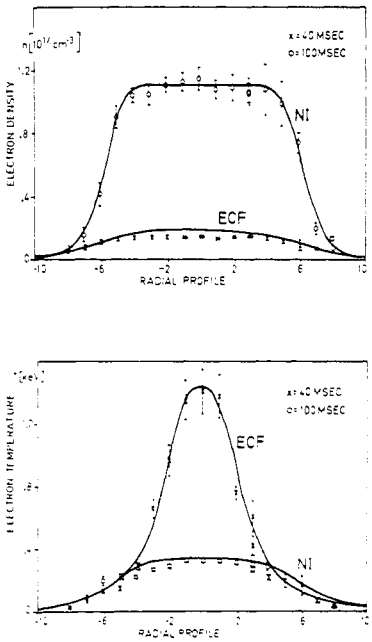

Fig. 9 A target plasma produced from the gas phase by 100 kW absorbed ECF-power is "taken over" by NBI with three injectors (220 kW absorbed power).

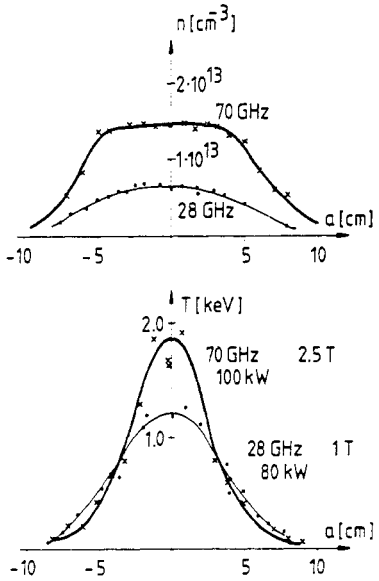

Fig. 10 ECF produced net-current free discharges for two cases: 28 GHz at 1 T and 70 GHz at 2.5 T. One immediately observes the difference in gradients. Please note that the particle source is at the edge but the power source at the plasma center.

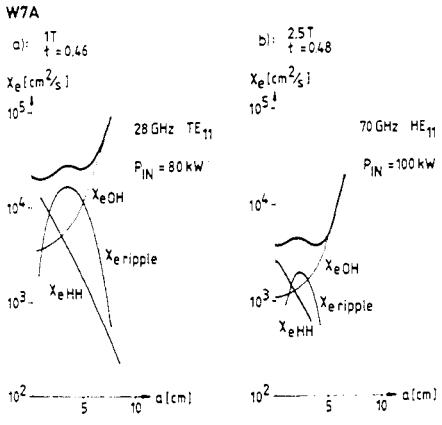

Fig. 11: Electron heat transport coefficients for the two discharges shown in Fig. 10. The bold trace is the sum of the three contributions:
$\chi_{e,HH}$, $\chi_{e,ripple}$ and $\chi_{e,OH}$ (see text).

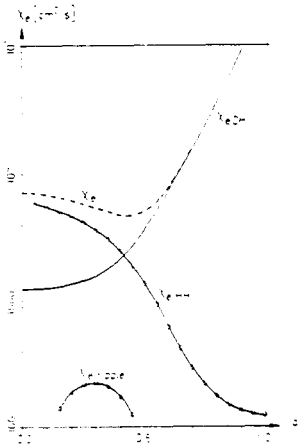

Fig. 12 Calculated transport coefficients for a discharge with $\iota(o) = 0.1$, $\iota(a) = 0.35$, $T_e(o) = 0.87$ keV, $n_e(o) = 2.2 \cdot 10^{13}$ cm^{-3}, $B = 2.5$ T and $\chi_{e,OH} = 2.5 \times 10^{18}/nT^{2/3}$.

cation of their variation with B is difficult.

The essential result of these experiments is that in cases where n and T are high enough for the anomalous contribution of eq. (1) to become small against the neo-classical transport coefficients the latter ones determine the discharge. Since the neo-classical transport coefficients for the electron channel strongly increase with temperature whereas the opposite behaviour is found (at least for all the plasma parameters accessible) for $\chi_{e,OH}$ of eq. (1) one should be able to conclude that the influence of $\chi_{e,OH}$ becomes more and more restricted to the plasma edge the higher the plasma parameters grow. Since this is an important point it is useful to add information about a discharge produced by 70-GHz RF power but with a small plasma current superimposed to reduce the twist value mainly at the plasma center and thus to increase the neo-classical transport coefficients as compared to the OH ones. Fig. 12 shows that the bulk plasma region of this discharge is governed by neo-classical effects indeed. Ripple effects are not expected to contribute. With these coefficients the temperature profile has been calculated and compared with the measurements in Fig. 13. The agreement is very satisfactory. Please note that there is no normalization factor for the peak temperature, thus the comparison is on absolute terms.

The determination of the electron heat transport will remain an essential element of future experimental work. In this connection, the method of modulating part of the gyrotron power in an on-off fashion of a few hundred cycles per second has proven to be a powerful method. Figure 14 shows the results of such an experiment. Assuming that the main RF power is deposited around the plasma center, one clearly observes the time delay of the arriving heat wave and its effect on the local (magnetic surface) plasma energy.

CONFIGURATIONAL EFFECTS

When describing the main results obtained with W VII-A it was implicitly assumed that the magnetic configuration was adjusted for optimum confinement conditions and the minima seen already in Fig. 1 avoided by proper choice of iota and its variation over the plasma cross-section. It should be understood, however, that major resonances in iota ($\iota = m/n$, with m and n not too large integers), wherever they occur in the plasma, have strong effects on confinement for all the plasmas investigated in W VII-A. These effects are basically understood but the details prevailing in a particular discharge are often difficult to analyse.

At rational values of iota the basic concept of simple nested magnetic surfaces is violated. Under such conditions, the configuration is sensitive either to formation of magnetic islands or ergodic regions by small error fields so that parallel heat transport can "short-circuit" certain confinement regions, or to the creation of convective cells also leading to enhanced transport. Thus, the confinement properties of a particular plasma in a particular configuration are governed by the actual values of iota, its resonances, and the amount of shear. The determining factors for the individual configurations are threefold: (i) the vacuum configuration including all error fields, (ii) any iota and shear produced by j(r) either deliberately introduced by a small loop voltage or resulting from the particular conditions of plasma heating, and (iii) any iota and shear resulting from the finite plasma pressure as given by Kisslinger and Wobig (1985) which reduces |B| by the diamagnetic effect and causes pressure driven currents (bootstrap current?). All these effects are interrelated by the transport conditions depending on them, (W VII-A Team and others, 1985 b).

With the aim to separate these effects, very low beta plasmas were investigated in W VII-A where pressure effects should still be negligible. Fig. 15 shows that for vanishing plasma current a deep minimum occurs at $\iota = 0.5$ accompanied by maxima at both sides. The shear produced by a plasma current of 2 kA already shows some influence on the confinement properties. At I = 4 kA the shear is large enough but not yet too large (see later) to drastically improve the situation for $\iota(a) = 0.5$ and to reach the maxima, but now for all values of iota around $\iota = 0.5$. Under these conditions iota is about 0.7 in the plasma center. The contribution of the plasma current to plasma heating is still negligibly small ($\lesssim 2$ kW).

In Fig. 16 the results of similar experiments are described but for higher plasma pressures. In this case pressure driven currents contribute to the variation of iota over the cross-section. The optimum confinement is achieved for a plasma current of $I \approx 2$ kA for which the loop voltage is just zero. Higher or lower plasma currents require positive or negative loop voltages to be applied. The same measure is necessary if the pressure driven current varies as a consequence of the confinement (and thus pressure) variation with iota. For a plasma

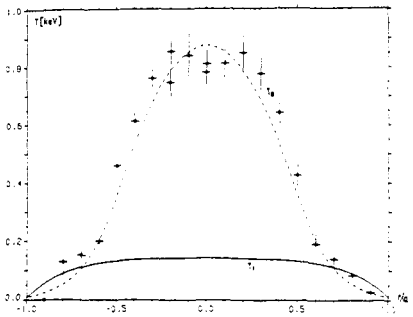

Fig. 13 Comparison of the calculated T_e-profile with the experimental data points. The calculated ion temperature is also given.

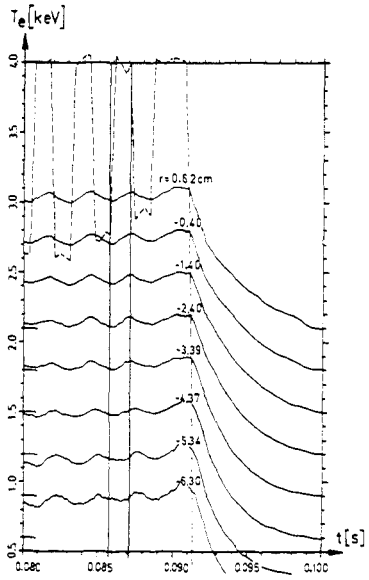

Fig. 14 Time variation of ECE measured electron temperature for different plasma radii. As indicated by the dashed line at the top of the figure, a fraction of the 70 GHz gyrotron power is pulsed in an on-off fashion. The two vertical lines, for the times of switching on or off the gyrotron power, allow the detection of the corresponding heat wave travelling from the inside to the edge of the plasma. Please note from the right-hand end of the traces that the individual traces have been displaced in vertical direction to make relative comparison easier.

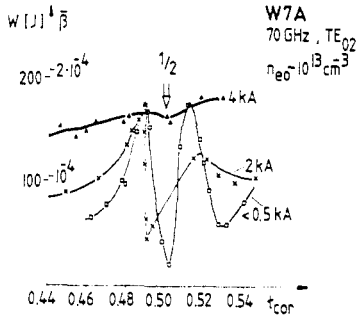

Fig. 15 Achieved plasma energy vs. $t(a)$ for constant gyrotron power aiming at low beta. Shear is varied by small plasma currents. The values indicated are adjusted by proper selection of small loop voltages.

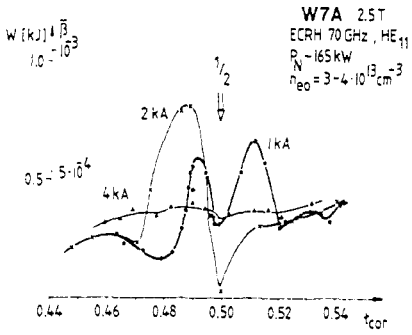

Fig. 16 The same as Fig. 15, but for higher beta values. In this case, also pressure driven currents contribute to the details of the magnetic configuration.

current of 4 kA the confinement parameters become rather independent of iota (except for the general trend to increase with iota). This is similar to the conditions of Fig. 15 but now the maxima of the 2 kA-case are not reached anymore. With the expected distribution of the pressure driven current this result may be explained by the fact that for I = 4 kA and high enough pressure the local shear has become too large to be able to keep the regions of steepest pressure gradients free of low order resonances.

The obvious conclusion from these experiments is that some shear has a positive effect on confinement indeed. Its magnitude has to be limited, however, to avoid the occurrence of major resonances at those regions where the steepest pressure gradients are expected. The vacuum magnetic configuration selected has to consider the contributions by pressure driven currents. As indicated by Fig. 16 it can be chosen such that for the self-adjusting pressure driven current optimum confinement conditions are reached. With the available heating power the maximum beta values achieved in W VII-A ($\beta_o \lesssim 1\%$, $\bar{\beta} = 0.3\%$) were a factor of four higher than those of Fig. 16 without any indication of a limitation in $\bar{\beta}$ being reached already, as pointed out by the W VII-A Team and others (1984).

SUMMARY AND CONCLUSIONS

WENDELSTEIN VII-A is a low-shear, high-aspect-ratio Stellarator. It has now been operated for 10 years. Its main results were:

Ohmically heated discharges were found to be sensitive to tearing modes. Already with a small external contribution to the twist of the magnetic lines, $\iota_o \gtrsim 0.14$, the disruptions could be stabilized and the tearing modes studied in a quasi-stationary fashion. Regions free of tearing modes and sawtooth oscillations exhibited anomalous electron heat transport $\chi_{e,OH} \sim n_e^{-1} T_e^{-2/3}$, independent of plasma current. It is very satisfactory to note that at reactor plasma densities and temperatures this formula leads to values by orders of magnitude smaller than the neo-classical contributions to χ_e.

Ohmically heated Stellarator plasmas, further heated either by NBI or ECF, do not show degradation in confinement if care is taken in avoiding major resonances in the confinement region. Typically, the discharge follows the above law as long as it yields the major contribution to χ_e according to the plasma parameters reached.

Net-current free discharges could be maintained by NBI or ECF application. These discharges show no MHD-fluctuations anymore and show the corresponding improvements of confinement. Particle confinement is very long and also the dynamics of laser-ablated impurities (aluminum) seems to be largely consistent with neo-classical confinement theory except for some regions in space and time where the transient formation of magnetic islands or ergodic regions tend to increase the transport.

The self-formation of radial electric fields was found to strongly increase the confinement properties by acting on the ion particle orbits. These fields originate from high energy ions born on orbits intersecting the wall and the condition of ambipolarity. They increase the heating efficiency of NBI and reduce the ion heat conduction. A necessary prerequisite for their occurrence is good electron confinement. ECF-heated plasmas allow the conclusion that for the body of the plasma ($r/a < 2/3$) electron transport is close to neo-classical values including ripple effects which, however, are small for W VII-A.
Confinement in W VII-A is very dependent on the extent to which major resonances in the configuration can be avoided. Some shear is helpful in broadening the maxima of confinement but too much shear does not allow avoiding major resonances in the confinement region around which the transport is increased. Plasma currents driven by the plasma pressure and by the particular heating scheme used are contributing to the details of the magnetic configuration and have thus to be considered carefully. The above results have been obtained for optimized confinement conditions, where the plasma energy has maxima with respect to the value of iota.

WENDELSTEIN VII-A will now be shut down for upgrading it into the Advanced Stellarator WENDELSTEIN VII-AS. By making proper use of the non-axisymmetry of Stellarators, this concept promises to reduce the secondary currents and thus the Shafranov shift, and also to lead to further improvements of the particle confinement, as reported by Brossmann and others (1983). W VII-AS also has a larger plasma radius than W VII-A, thus reducing wall effects accordingly. Together with the increased capacity of the available heating schemes, this should also allow further increase of the plasma parameters.

REFERENCES

Berkl, E., D. Eckhartt, G. von Gierke, and G. Grieger (1966). Resistive diffusion of cesium plasma in a Stellarator. Phys. Rev. Letters, 17, 906.

Brossmann, U., W. Dommaschk, F. Herrnegger, G. Grieger, J. Kißlinger, W. Lotz, J. Nührenberg, F. Rau, H. Renner, H. Ringler, J. Sapper, A. Schlüter, and H. Wobig (1982). Plasma Physics and Controlled Nuclear Fusion Research 1983, (Proc. 9th Int. Conf. Baltimore), Vol. III. IAEA Vienna. p. 141.

Grieger, G., W. Ohlendorf, H.D. Pacher, H. Wobig, and G.H. Wolf (1971). Particle-confinement minima in the Wendelstein II-a-Stellarator. Plasma Physics and Controlled Nuclear Fusion Research 1971, (Proc. of 4th Int. Conf. Madison/USA), Vol.III. IAEA Vienna. pp 37-48.

Hinton, F. L. and W.N.G. Hazeltine (1976).Theory of plasma transport in toroidal confinement systems. Rev. Mod. Phys., 48. p. 239.

Kißlinger, J., and H. Wobig (1985). Stellarator Equilibrium by low-beta-expansion. To be published in Europhysics Conference Abstracts 11th EPS Conference on Controlled Fusion and Plasma Physics, Budapest, 1985. Paper No. 144.

Shaing, K.C., R.H. Fowler, D.E. Hastings, W.A. Houlberg, E.F. Jaeger, J.F. Lyon, J.A. Rome, J.S. Tolliver, and J.D. Callen (1984). The radial electric field in a non-axisymmetric torus. Plasma Physics and Controlled Nuclear Fusion Research.Vol. 2. IAEA Vienna. p. 189.

W VII-A Team (1977). Ohmic heating in the W VII-A Stellarator. Plasma Physics and Controlled Nuclear Fusion Research 1977, (Proc. 6th Int. Conf. Berchtesgaden 1976), Vol.II. IAEA Vienna. p.81.

W VII-A Team (1979). Investigation of the m = 2 mode at q-values around 2 in the W VII-A. Plasma Physics and Controlled Nuclear Fusion Research 1979, (Proc. 7th Int. Conf. Innsbruck 1978), Vol. II. p. 277.

W VII-A Team and NI Group (1981). Neutral injection in the Wendelstein VII-A Stellarator with reduced ohmic current. Plasma Physics and Controlled Nuclear Fusion Research 1981, (8th Int. Conf. Brüssel 1980). Vol. I. IAEA Vienna, p. 185.

W VII-A Team and NI Group (1983 a). Energy and particle confinement in currentless W VII-A Discharges. In S. Methfessel (Ed.),Europhysics Conference Abstracts 11th EPS Conference on Controlled Fusion and Plasma Physics, Aachen, 1983 a, Vol. 7D, Part 1, European Physical Society, Geneva. pp. 191-194.

W VII-A Team and NI Group (1983 b). Neutral injection heating in the Wendelstein VII-A Stellarator. Plasma Physics and Controlled Nuclear Fusion Research 1983, (Proc. 9th Int. Conf. Baltimore 1982), Vol. II. IAEA Vienna. p. 241.

W VII-A Team and NI Group (1984). Plasma confinement and the effect of the rotational transform. Plasma Physics and Controlled Nuclear Fusion Research 1984, (Proc. 10th Int. Conf. London 1984), Vol.2. IAEA Vienna. p. 371.

W VII-A Team and NI Group (1985 a). Impurity transport in the Wendelstein VII-A Stellarator. Accepted for publication in Nuclear Fusion. IAEA Vienna.

W VII-A Team, NI Team, and ECRH Group (1985 b). Influence of the Magnetic Configuration on Plasma Behaviour in the Wendelstein VII-A Stellarator. To be published in Europhysics Conference Abstracts 11th EPS Conference on Controlled Fusion and Plasma Physics, Budapest, 1985. Paper No. 146.

WENDELSTEIN 7-AS

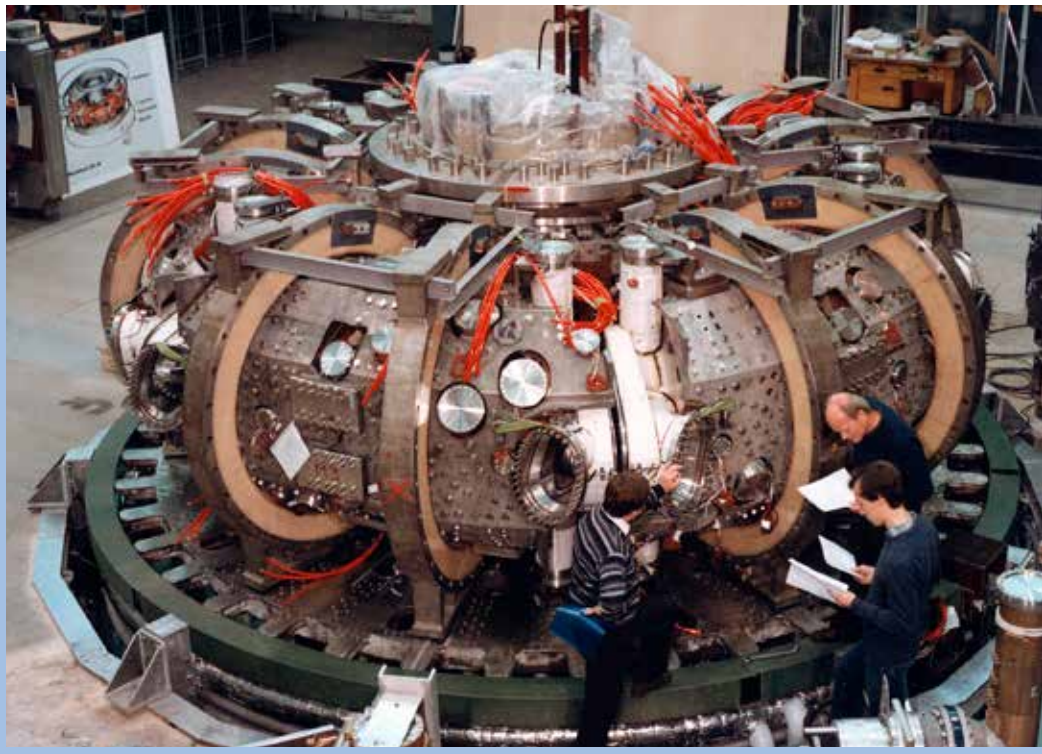

Der Stellarator Wendelstein 7-AS (1988 - 2002) während des Aufbaus

Foto: IPP, Thomas Henningsen

APPLICATION FOR PREFERENTIAL SUPPORT
PHASE I
for
WENDELSTEIN VII-AS

Part I
Executive Summary
December 1981

TABLE OF CONTENTS

I. INTRODUCTION

This summary presents the principle and rationale for the modular Advanced Stellarator W VII-AS which is an upgraded version of the W VII-A stellarator at Garching. The first part describes the aims of the project, its basic properties, its correlation to other stellarator experiments, time schedule, and first cost estimates. In the second part, the physical and technical components are described in detail.

The justification of fusion research on the Stellarator line is based mainly on two facts: the reactor potential of the stellarator and the encouraging results of stellarator experiments. A recent review paper [1] and a new reactor study (Los Alamos LA 8976 . MS) present an extensive data collection on this subject. In accordance with the problems and tasks identified in these papers, W VII-AS (AS means Advanced Stellarator) will investigate those physical phenomena which are of importance for a stellarator reactor of the advanced type. It also will incorporate technical aspects of the stellarator reactor, in particular the modular coil system.

A new property of the W VII-AS configuration is the optimized structure of the magnetic field, different from the simple $l = 2$ configuration in W VII-A. This concept of optimized magnetic fields also differs from HELIOTRON E and URAGAN 3. In these two competing devices equipped with helical windings high rotational transform is needed for plasma equilibrium and high shear for MHD stability.

In W VII-A, however, the plasma equilibrium is optimized at a moderate rotational transform and MHD stability is ensured by a magnetic well.

The basic ideas for optimization of stellarator equilibria have been developed by A. Schlüter and his co-workers, the W VII-AS proposal has been worked out in close cooperation with this group.

References

[1] Joint U3-EURATOM Steering Committee on Stellarators, Report IPP 2/254

II. AIMS OF THE W VII-AS EXPERIMENT

The aims of the W VII-AS experiment are:

- to investigate plasma behaviour in an optimized magnetic field configuration for which theory predicts improved plasma equilibrium and smaller neoclassical transport losses compared to classical $l = 2$ configurations, like W VII-A;
- to investigate a plasma without ohmic heating currents which drive instabilities and cause anomalous losses;
- to make use of a modular set of poloidally closed coils instead of the conventional helix/TF coil system;
- to improve access to various heating methods with higher power as compared with W VII-A including their use for plasma generation without any OH current;
- to increase the plasma radius to twice the radius of W VII-A for getting better screening of impurities from the plasma centre and better separation between plasma core and wall.

The modification of the experiment requires the construction of the following components:

- the modular coil system
- the vacuum tube
- the pumping system
- the mechanical structure of the modular coil system
- modification of the W VII-A coils.

No changes are needed for the structure of the TF-coil system, the OH-transformer, the vertical field system, cooling system and power supply, etc.. Further developments of diagnostic methods and heating methods are required.

The W VII-AS experiment is a necessary step in order to investigate optimized plasma configurations. In W VII-X, a larger device succeeding W VII-AS, maximum plasma beta will be the basic aim. Also, the technological aspects of W VII-X will be oriented towards the requirements of a future stellarator reactor.

III. RATIONALE OF THE W VII-AS EXPERIMENT

1) Reactor Aspects

The favourite reactor properties of the stellarator are now widely recognized. The steady-state magnetic field alleviates the problem of cyclic thermal stresses, fatigue on the coils and eddy currents. Plasma start-up occurs on existing magnetic surfaces, disruptive instabilities are absent. There is neither a need for an ohmic heating transformer nor for an electric energy storage system. A moderate aspect ratio provides for good access for maintenance.

For a stellarator reactor, key topics to be addressed are:

1) maximum plasma beta
2) plasma confinement
3) effects of impurities
4) effective heating schemes

5) the complexity of the modular magnetic system (forces, stresses, maintenance)
6) blanket problems.

Satisfactory answers to all of these problems have to be found for reaching the goal of a stellarator reactor.

The single modular coil system selected for W VII-AS replaces the two systems, helix and TF-coils, used so far, and thus removes one of the major obstacles for building larger stellarator devices or even stellarator reactors. In principle, also W VII-AS could be built with helical windings and separate TF-coils, but its magnetic field configuration, which can be understood as a superposition of conventional $l = 0, 1, 2, 3$ fields, would require a rather complicated helical coil system. Therefore, already for the still moderate size of W VII-AS, the modular solution is simpler than the helix/TF system. For these reasons and for its reactor relevance, the modular coil system has been incorporated into the W VII-AS device. Thus, also point 5) of the problem list is tackled, and basic know-how and experience will be gained from constructing this device.

Whether such a modular stellarator can be extrapolated to full reactor size depends on the forces acting on these coils. This can best be evaluated by comparison with a tokamak.
(i) For the same value of the toroidal magnetic field, the total current in the modular stellarator coils would be identical to the current in the TF-coils of a tokamak. Therefore, also the magnetic pressure and the centripetal forces are of the same order. These forces do not provide severe problems with tokamaks.
(ii) All other forces have to be compared with the effects of the vertical fields needed for equilibrium in tokamaks. There they introduce a rather large torque on the whole TF-coil system. In stellarators, it is essential to note that these forces balance already within one field period. If such a period is taken as one module, then there occur no forces at all from one module to the next which is an essential advantage for any reactor design.

The technique of constructing non-planar reactor size coils is being developed already in mirror machine research. There remains the problem of sufficient space for the blanket between the plasma and the magnet system. The space available very much depends on the configuration chosen. If it were not for the low theoretical value of the limiting ß, W VII-AS could simply be scaled up to reactor size (R = 20 m). Under these conditions, the space for a blanket is sufficient (1.5 m) but not ample. This means that later configurations have not only to be optimized for ß but also for sufficient blanket space, at the same time.

2) Relation to W VII-A

The proposed W VII-AS will be a modification of the existing W VII-A. This device has been in operation successfully during the period 1976-81.

a) General description of W VII-A

For plasma production and heating, ohmic heating and neutral beam injection have been applied. For the next period before the dismantling of the W VII-A device, r.f. heating will be studied. Especially, ion cyclotron resonance heating ICRH ($P_{rf} \sim 500$ kW) and electron cyclotron resonance heating ECRH will be used to gain experience for establishing clean plasmas at higher power in W VII-AS.

W VII-A	W VII-AS
Conventional stellarator	Modular coil stellarator
$l = 2$, $m = 5$	$m = 5$
$0 < \iota < 0.55$	$\iota_0 = 0.38$
external transform, low shear	low shear
$B_0 \leq 3.5$ T	$B_0 = 3$ T
Main field	Toroidal field $\pm$ 1 T varies shear and transform
R = 2 m, a ~ 0.1 m	R = 2.1 m, a ~ 0.2 m

b) Results of W VII-A

Promising results have been obtained by W VII-A. It has been demonstrated that MHD effects related to the net plasma current lead to significant deterioration of stability and confinement:

- The internal sawtooth mechanism restricts the current density to $j(0) \sim B/R\ (1- \iota_0)$ and therefore the heating power density.
- The behaviour of MHD tearing modes localized at resonant surfaces depends on the current density distribution. Thus, for the external transform $\iota_0 > 0.14$, the dangerous (2,1) mode and disruptive instability are prevented during the ohmic heating phase. But with stronger heating by neutral beams, even at $\iota_0 > 0.4$ soft disruptions related to the (3,2) mode have been observed.
- The anomalous electron heat conduction χ_e is similar to tokamaks and seems to be related to the plasma current. In addition, at high current and plasma density, extended island formation contributes to the losses. [I].

The transition to “currentless” stellarator operation has been a major step for W VII-A. It has been achieved by neutral injection at significant plasma parameters. Starting with a target plasma produced by ohmic heating, the plasma current had to be reduced during the neutral injection phase [2]. This method, however, implies several constraints:

- For sufficient beam absorption across the small plasma diameter (a = 0.2 m), high densities $n > 10^{14}$ cm^{-3} are mandatory.
- Fast current reduction is only possible by control of the temperature and current density profiles to avoid instabilities during the change of the rotational transform profile: from a current carrying “tokamak-like” configuration to a shearless stellarator one. Therefore, a careful adjustment of the density increase and of the increase of the helical current with the condition $\iota_0 + \iota_p \sim 0.5$ is necessary.
- At high density, strong radiative losses must be tolerated. Most probably, impurity ions contaminating the beam are unfavourably deposited in the plasma core and are responsible for the increase of the impurity concentration [3]. A long particle confinement time seems to support the density and impurity increase during the injection phase of a currentless plasma.
- Operation is possible only at rather high collisionality (Pfirsch-Schlüter regime) and in the plateau regime.

Nevertheless, remarkable improvement of the “currentless” plasma could be demonstrated:

- High plasma pressure

$n_e \geq 1.5\ 10^{14}$ cm^{-3}
$T_e, T_i \sim 400$ eV
$ß(0) \sim 0.6$ % at 3 T

could be maintained without indication of MHD instabilities.
- The energy confinement and particle confinement are significantly improved compared to ohmically sustained discharges. With an energy confinement time of $\tau_E > 20$ ms, neoclassical ion heat conduction becomes the important channel. The dramatic reduction of electron heat conduction losses seems to be supported by the observation of a significant reduction of the fluctuations.
- The heating efficiency of neutral beam injection seems to exceed the predictions of the ODIN code. The uncertainty of the power deposition profiles prevents a detailed description of the energy balance transport. But the indicated reduction of orbit losses may be explained by the effect of radial electric fields which improves the confinement of high energetic ions.

c) Modification of W VII-A to W VII-AS

For the continuation of the experiments in W VII-A, several guidelines must be considered. The configuration of the proposed W VII-AS will be similar to that of W VII-A with respect to the main field, rotational transform ι_0, and magnetic well. The shear will be low, therefore it is possible to avoid critical resonant surfaces within the confinement region.

Additionally, the constraints of W VII-A will be reduced. The improvements are:

- Better access to currentless operation due to plasma build-up and heating by non-ohmic methods.

- More effective heating due to improved access for neutral injection and RF heating.
- Operation at lower density ($n < 5 \cdot 10^3$ cm^{-3}) will allow the study of transport conditions in the long mean free path region.
- Screening of the plasma core from atomic processes at the boundary due to the larger plasma radius. Better control of the impurity flow into the plasma. Increase of $\int$ ndl.
- Sufficient power to achieve high temperature (T_e, $T_i > 1$ keV) and high plasma pressure ß > 1 % which will allow the study of ß-limitations

The plasma parameters envisaged for W VII-AS are within reasonable extrapolations from W VII-A results so that the proof of the advantages of the new AS-configuration seems to be possible.

3) Relation to Other Stellarator Experiments

Competing devices are listed in Table I, indicating their main parameters and heating equipment applied. Only a few of them, HELIOTRON E and URAGAN 3, will be operational at the time of completion of W VII-AS. Possibly, the conversion of the ISX tokamak into a system with additional helical windings may lead to a continuation of the investigations of ohmically heated Stellarators. The final design of the planning group at Oak Ridge, USA, may become available in the course of the next year.

Plans for new Stellarators are existing in Moscow (L-3) and Madison (WISTOR-U). All these devices follow the conventional line, building $l = 2$, $l = 3$ configurations and are not of the advanced type. In this respect, W VII-AS holds a singular position.

With the concept of low transform, low shear, magnetic well, and reduced secondary currents, W VII-AS is an alternative to HELIOTRON E. The otherwise equivalent capabilities of both machines may allow checks of the effects of shear and magnetic well in a similar parameter range.

References

[1] W VII-A Team, Bull. Am. Phys. Soc., 26, 7 (1981), paper 2U 12, page 892
[2] W VII-A Team and Neutral Injection Team, Neutral Injection in the Wendelstein VII-A Stellarator with Reduced Ohmic Current, Proc. IAEA 8th Int. Conf. on Plasma Physics and Contr. Nucl. Fus. Res., Brussels 1980, IAEA-CN-38/H-2-2
[3] IPP Neutral Injection Team and W VII-A Team, Neutral Injectors for the Wendelstein VII-A Stellarator: Reliability, Impurities, Proc. Third Neutral Beam Heating Workshop, Gatlinburg, Tennessee (USA), 1981

TABLE I

HELIOTRON E (Kyoto, Japan) 1980

Main toroidal field	$B_0 = 2$ T
Helical symmetry	$l = 2$
Number of field periods	m = 19
Rotational transform	$\iota_0 \rightarrow 2$, high shear
Plasma radius	a = 0.2 m
Heating:	
Electron cyclotron heating at 60 GHz (1982)	
Neutral beam heating at 2.6 MW (1981)	

URAGAN 3 (Kharkov, USSR) 1981

Main toroidal field	$B_0 = 3$ T
Helical symmetry	$l = 3$
Number of field periods	$m = 9$
Rotational transform	$\iota_0 \rightarrow 0.8$, high shear, separatrix
Plasma radius	$a = 1.5$ m
Heating:	
Alfven wave heating, 2 MW (1982)	
Neutral beam heating, > 1.5 MW (1983)	

IV. THE PRINCIPLES OF OPTIMIZATION

Conventional stellarators are dominated by one single helical field (traditionally $l = 2$ or $l = 3$) and have equilibrium- and stability-ß limits which are probably too low for practical application ([1-3], and refs. cited therein); moreover, near the $ß_e$-limit, $j_\parallel$ is comparable to that of a tokamak with the same twist of the magnetic field so that the preferable situation of small parallel current density is not realized.

Therefore, studies of vacuum field configurations were made to reduce the ratio $j_\parallel / j_\perp$ with the constraint of an average magnetic well which guarantees low-ß stability. For small twist number per period the parallel current density is governed by the variation on magnetic surfaces of

$$Q = \int dl/B$$

where the integral is performed along a field line over one field period. Reducing the variation of Q should therefore increase the obtainable value of $ß_e$ by reducing the Shafranov-shift and simultaneously reduce transport in the collisional and plateau regimes because the deviation of the drift surfaces of circulating particles from magnetic surfaces is reduced. These predictions were verified with 3D MHD codes [4, 5, 6, 7] and Monte-Carlo-simulations of transport [8, 7].

A significant reduction of $j_\parallel/j_\perp$ over all of the plasma cross-section can only be achieved if the effect of toroidal curvature is overcome with the help of $l = 1$ helical field components which increase the local curvature and, unavoidably, also the population of localized particles. These particles can, however, be chosen to be situated in a region of small curvature, so that their drift velocity is small. In the resulting stellarator, which could also be described as toroidally linked mirrors, trapped particle transport is not essentially larger than in a classical stellarator.

These requirements, together with the choice of the number of periods $m = 5$ and an upper bound on the aspect ratio ($A \sim 10$), led to the magnetic field configuration W VII-AS.

(Ende des Ausschnitts)

References

[1] Lortz, D., Nührenberg, J., Plasma Physics and Controlled Nucl. Fusion Research 1978 (Proc.7th Int. Conf., Innsbruck, 1978), Vol. II, IAEA, Vienna (1979) 309

[2] Chodura, R., Schlüter, A., Kaufmann, M., Lotz, W., Plasma Physics and Contr. Nucl. Fusion Research 1978 (Proc.7th Int. Conf., Innsbruck, 1978), Vol. II, IAEA, Vienna (1979) 335

[3] Fielding, P.J., Hitchon, W.N.G., J. Plasma Physics 24 (1980) 453

[4] Chodura, R., Dommaschk, W., Lotz, W., Nührenberg, J., Schlüter, A., Plasma Physics and Contr. Nucl. Fus. Res. 1980, (Proc.3th Int. Conf., Brussels 1980), Vol. I, IAEA, Vienna (1981) 807

[5] Chodura, R., Dommaschk, W., Herrnegger, F., Lotz, W., Nührenberg, J., Schlüter, A., Stellarators, Joint US-EURATOM Report (1981), Report IPP 2/254, Sec.V.2

[6] Chodura, R. , Dommaschk, W., Herrnegger, F., Lotz, W., Nührenberg, J., Schlüter, A., IEEE Transactions of Plasma Science, December 1981

[7] Chodura, R., Dommaschk, W., Herrnegger, F., Lotz, W., Nührenberg, J., Schlüter, A., US-JAPAN Theory Workshop on 3-D MHD Studies for Toroidal Devices, Oct.19-21, 1981, Oak Ridge, Tennessee

[8] Lotz, W., Nührenberg, J., Proc. of the Annual Meeting on Theoretical Aspects of Contr. Thermonucl. Res., Austin 1981, paper 3B41

➜ M. Hirsch, et al.: Major results from the stellarator Wendelstein 7-AS (Review Article), in: Plasma Physics and Controlled Fusion, 2008, Seiten 1-9, 181-184

WENDELSTEIN 7-X

Foto: IPP, Jan Michael Hosan

Der Stellarator Wendelstein 7-X ging 2015 in Betrieb.

3.4 WENDELSTEIN 7-X

WENDELSTEIN VII-X
Application for Preferential Support

WENDELSTEIN Project Group
IPP-EURATOM Association
AUGUST 1990

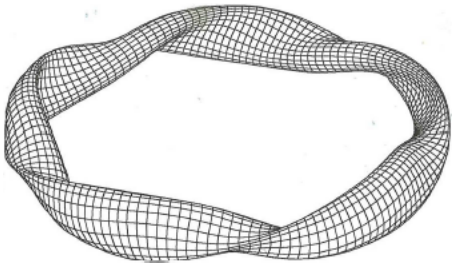

Application for Preferential Support consisting of the following parts:

Preface
Executive Summary
Part 1: Wendelstein VII-X -Device
Phase I Application
Part 2: Stage I Plasma Heating
Phase I Application
Part 3: Stage II Plasma Heating
Phase I Application
Part 4: Preparatory Engineering R & D
Phase I and II Application *

* This part of the proposal was already submitted in May 1990. It is repeated here for completeness.

Preface

IPP is submitting herewith the proposal for the next major stellarator of the WENDELSTEIN line. This proposal is of particular importance because it aims at probing the viability of the Wendelstein Advanced Stellarator (Helias) as a desirable fusion reactor concept.

The stellarator confines toroidal plasmas with magnetic fields generated by currents in coils that are external to the plasma. It shares many features of toroidal confinement with the tokamak, but unlike the tokamak, no net plasma current is required. Thus, there is no need for systems to maintain such a plasma current, steady state operation is an inherent property, and plasma disruptions driven by a net plasma current are not possible. These properties are of major importance for fusion reactors. In addition, the absence of a net plasma current makes the stellarator the confinement system with the smallest free energy that is available for driving instabilities.

The WENDELSTEIN VII-X experiment, which we are proposing, will be an integrated concept test which is needed for producing convincing predictions on the properties of ignited plasmas in Advanced Stellarators. DT operation of W VII-X is neither foreseen nor necessary for this purpose. Essential details of the concept have been developed at IPP and the according optimization has led to a number of distinguishing features of the proposed experiment: The magnetic axis is

helical, which gives improved equilibrium, stability, drift orbits, and transport properties as compared to those of circular axis stellarators. But, at the same time, the helicity is small enough to avoid complications in the construction. With a major and minor radius of 5.5 m and 0.53 m, respectively, and a magnetic field strength of 3 T, the experiment will be just large enough in size to establish the physics data base that is required for the design of a stellarator device for DT-ignition. The plasma parameters that we hope to achieve in Wendelstein VII-X for this purpose are ion and electron temperatures of a few keV, densities of more than 10^{20} m^{-3}, confinement times of a few tenth of a second, and volume-averaged ß values of up to 5 %.

Present and future WENDELSTEIN stellarators are modular in their design characteristics. Modularity greatly eases construction assembly, and the servicing, and will thus be of particular importance in later radioactive devices. Therefore, the development of modular coil systems for stellarators and their successful operation is an important step in the demonstration of stellarator technology. The magnet of W VII-X will be made of modular, superconducting coils. A convincing concept has been developed for the W VII-X magnet by utilization of the experience gathered by the construction of W VII-AS. It allows the construction, assembly, and separate testing of sectors consisting of one field period each before delivery to the institute.

The W VII-X experiment is a natural progression from the existing W VII-AS. W VII-X embodies, however, a much higher degree of optimization. Nevertheless, already W VII-AS is optimized to the degree which demonstrates that the theoretically predicted properties of Advanced Stellarators can be realized in experiments. The reduction of the Shafranov shift demonstrated in the experiment is one example. W VII-AS has further produced a great number of essential results, all of them being important for the lay-out of W VII-X. The largest electron temperatures achieved in any stellarator so far, nearly 3 keV peak, have been reached by ECRH with moderate heating power (less than 1 MW). Also, the highest densities achieved in any stellarator so far, $\langle n \rangle = 2 \times 10^{20}$ m^{-3}, have been produced and maintained by 1.5 MW NBI after carbonization of the device. The corresponding gross confinement time is about 20 ms and the volume average ß above 0.6 %. Also, the concept of positive but limited shear is fully supported. A reduced sensitivity to resonances and ß effects is thus expected in W VII-X.

The technology and physics of stellarators and tokamaks have much in common. Both concepts supplement and support each other's development. For example, the clearest evidence that the bootstrap current behaves as expected from neoclassical theory comes from the experiments on the W VII-AS and ATF stellarators. Stellarators are also important in the development of an understanding of toroidal transport in general. This comes from both the wider range of magnetic configurations in stellarators and from less constraints (e.g. as the link between toroidal current and electron temperature profiles in case of tokamaks).

The IPP is the only laboratory in the world that has large experimental programmes on both, stellarators and tokamaks, and is, therefore, uniquely positioned to profit from the strong interactions between the two programmes. Indeed, with the present termination of the ASDEX programme, a significant part of the ASDEX team is joining the W VII-AS division whose lead is already taken over by F. Wagner, the former head of ASDEX. This allows the other part of the IPP stellarator team under G. Grieger to fully concentrate on WENDELSTEIN VII-X.

There is intensive cooperation with the Spanish stellarator team which is concentrating its work on basic stellarator questions. There is further cooperation of similar intensity with the two other major stellarator groups outside of the EC, namely of Japan and of the USA. In Japan (Toki), the Large Helical Device (LHD) is approved and is in the design stage. It has similar objectives as W VII-X but is of the torsatron type. In the US (Oak Ridge), there is no immediate plan to proceed from the ATF to a next step device but there are studies on a tight aspect ratio stellarator. All this work is complementary to our activities which makes collaboration with these partners particularly fruitful.

In order to give full information on the WENDELSTEIN VII-X project as a whole and, at the same time, to allow for a staged procedure in the later submission of the related Phase-II applications for preferential support, this Application on WENDELSTEIN VII-X is divided into four parts, the confinement device, two stages of heating, and preparatory engineering R & D. This is further explained at the end of the introduction of the Executive Summary.

Executive Summary

1. Introduction

1) The stellarator is a concept for confining toroidal plasmas with magnetic fields generated by currents exclusively outside the plasma region. It shares with the tokamak the basic concept of nested magnetic surfaces for achieving confinement. However, a net toroidal plasma current, as needed in tokamaks, is not required in stellarators. Thus, stellarators without this current can be operated in steady state, without disruptions, without request for an external current drive system, and without need for more than one single coil system for generating the confining magnetic field. These properties are of major importance for fusion reactors. After ignition, a stellarator reactor would work continuously on refuelling and exhaust alone. Since a net toroidal current provides free magnetic energy to drive instabilities in particular of disruptive nature, this reservoir is minimum in stellarators. The stellarator is the toroidal confinement system with the smallest free energy.

2) The stellarator concept was invented by Lyman Spitzer at Princeton in the early 1950s. IPP's interest in this concept started only a few years after this date, and from then on stellarators at IPP have played a major role in achieving goals that have been essential for the viability of this toroidal confinement approach. Unfortunately, world stellarator research suffered a severe setback, when the C-stellarator in the United States showed disastrous confinement in the early sixties. At that time, the tokamak took the lead in the empirical understanding of confinement. On the other hand, continued research at IPP in the sixties validated the basic stellarator confinement principle and demonstrated the importance of the exact value of field line twist. In the seventies, significant confinement of a hot plasma in W IIb and particularly in W VII-A refuted the disastrous confinement results of the C-stellarator. This was supported also by the experimental results from Heliotron-E (Kyoto) and L-2 (Moscow). In 1980, for the first time, significant confinement had been demonstrated in W VII-A in stellarator operation proper, i.e. without net toroidal plasma current. In order to become a candidate for a reactor working in steady state, it was however

- necessary to develop the "classical" configuration, like that of W VII-A, whose viability was endangered by strong classical physics arguments, into the reactor relevant "Advanced" Stellarator concept, and to demonstrate sufficient confinement and plasma pressure (β) in such a configuration, and
- important to "modularize" the stellarator technically.

This has become possible, because during the last decade theorists have made large progress in understanding classical stellarator physics and have been able to overcome the associated criticisms.

A two-step procedure had been adopted for the development of Advanced Stellarators and supported by both of the Beckurts Review Panels: first, to upgrade the W VII-A device into the W VII-AS with the aim to demonstrate the feasibility of the modular coil approach and to verify some essential properties of the new, Advanced Stellarator concept,

and now, in a second step, to demonstrate the reactor capability with a new and larger device, Wendelstein VII-X, which takes full advantage of the theoretical progress.

3) The general progress of the stellarator programme at the IPP has also profited from the close collaboration with the tokamak department. This will be continued between ASDEX-Upgrade and W VII-AS, and will later be extended to Wendelstein VII-X. This collaboration will be intensified by the fact that about 1/4 of the scientists working presently on ASDEX will join the W VII-AS team this summer along with their technical support. Thereby, intimate knowledge of relevant tokamak physics (particularly in the areas of confinement, impurity control, auxiliary heating, refuelling and plasma stability) gained by the research on ASDEX will become available within the W VII-AS team. In addition, the experience of these physicists and the technicians, who come with them, in the design of divertor (or pumped limiter) structures along with their knowledge in edge diagnostics and experience in analyzing and modelling tools will be of extreme benefit. On the other hand, also the tokamak line will profit from the foreseen close collaboration. The stellarator will contribute with detailed studies on transport issues which can be of importance for the tokamak line too but which are not possible there like the effect of trapped particles on transport (in Wendelstein VII-X trapped particles can be localized in the weak curvature regions), the role of shear or that of the plasma current (which is of utmost importance for tokamak confinement, stability and its operational limit). Long pulse operation up to quasi-continuous operation can more easily be achieved in stellarators while they might turn out to be indispensible for predictions on plasma wall interaction under reactor conditions. For this purpose, comparative studies will be done between the tokamak and the stellarator program in the IPP; the details of a common fluctuation program are presently under discussion.

The in-depth comparison between the properties of divertor tokamaks and advanced stellarators should then make it possible to assess quality and potential of future stellarators beyond.

4) A Project Group on the preparation of Wendelstein VII-X was established at IPP already in 1983. Its work and the general experimental and theoretical progress in the field of Advanced Stellarators, mentioned above, has now reached a state which allows the transition to the next-step device in the stellarator line, Wendelstein VII-X. In order to give full information on the Wendelstein VII-X project as a whole and, at the same time, to allow for a staged procedure in submitting the later Phase II-applications for preferential Support, the Application on Wendelstein VII-X is divided into four parts, and preceded by a Preface and an Executive Summary. Part 1 contains the Phase I application on the confinement device, the Wendelstein VII-X proper. Part 1 also contains the full physics argumentation on the foreseen plasma heating. Plasma heating is intended to be provided in two successive stages with Stage I being needed when the experiment starts operation and Stage II being added somewhat later for exploring high-power heating and ß limits.

Parts 2 and 3 of the Application provide Phase I related technical information on these two heating stages. Finally, Part 4, which has been already submitted in May 1990 and is repeated here for completeness, is a combined Phase I and Phase II application on the fabrication of a modular coil and a sector of the cryostat because it is an urgent task to demonstrate the engineering of these most essential components. Figure 1 illustrates the intended schedule and interrelation between this procedure and the later Phase II proposals.

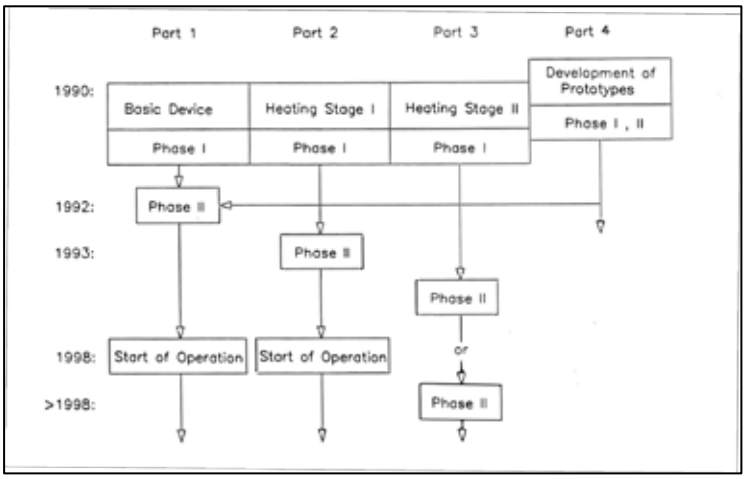

Fig. 1: Wendelstein VII-X, general schedule

2. Basis for Wendelstein VII-X and Selection of its Magnetic Configuration

5) The definition of Wendelstein VII-X is based on: i) Achievements in optimizing stellarator configurations (the Helias concept); these result from theoretical activities in IPP which continued in parallel to the construction and initial operation of W VII-AS. ii) Results from successful construction and operation of W VII-AS and from other stellarators of the world programme.

2.1 The Helias concept

6) The configuration selected for Wendelstein VII-X will be of the Helias type (HELical Advanced Stellarator) which is a toroidal plasma equilibrium with appropriately optimized properties. This optimization of stellarator configurations was carried out with respect to the following set of criteria:

- high quality of vacuum-field magnetic surfaces (regular boundary, avoidance of simple values of twist (or rotational transform) ι, ("resonances") adjustment of the shear, sufficiently small thickness of islands)
- good finite-β equlibrium properties (small shift of the magnetic axis [Shafranov shift], small change of ι with ß at fixed external currents)
- good MHD stability properties (stability with respect to local resistive interchanges and ideal ballooning at $\langle\beta\rangle \gtrsim 0.05$)
    - small neoclassical transport in the l/n-regime (equivalent ripple $\delta_e \lesssim 0.02$)
    - small bootstrap current in the lmfp-regime (ratio of bootstrap current in a stellarator to the bootstrap current in a tokamak with same aspect ratio and rotational transform, $J_{BS,stel} \lesssim 0.1\, J_{BS,tok}$)
- good collisionless α-particle containment at operational values of ß (fractional prompt loss < 0.1)
- good modular coil feasibility (sufficiently large distance between coils and plasma and a sufficiently small coil curvature)

7) The small axis shift and the small change of rotational transform and shear with increasing plasma pressure are a consequence of the achieved small parallel current density. A comparison of a convenient measure of the plasma currents, $(j_{\|}^2 / j_{\perp}^2)$, between WV VII-AS and a Helias configuration shows a reduction (partly due to an increase of ι) by one order of magnitude. More generally, compatibility and simultaneous achievement of all of the above criteria has been proven. The nature of the optimization result can be characterized as follows:

The simultaneous achievement of the above set of criteria essentially determines the structure of the magnetic field strength distribution of the configuration and its geometrical shape is then a consequence of this structure.

8) While the optimization only takes into consideration classical physics goals it also results in very interesting and desirable perspectives as far as anomalous transport is concerned: most of the discussed mechanisms for exciting anomalous transport (stochasticity in vacuum and finite-β fields, trapped orbits, instabilities such as ballooning, tearing and trapped-particle drift modes) are reduced substantially. In addition, the observed potential of stable operating a stellarator at unusually high densities, with the confinement time found to increase with density, is another route to increase confinement.

2.2 Results from Wendelstein VII-AS

9) W VII-AS is the first Advanced Stellarator. It has started plasma operation about one and a half years ago. In W VII-AS, properties of the Advanced Stellarator concept could be introduced only to a limited extent. This is for two reasons: firstly, the state of knowledge reached at the time, when the design of W VII -AS was frozen in, was limited, i.e. the large increase in knowledge reached since could not influence the W VII-AS concept anymore. Secondly, since W VII-AS is an upgrade of W VII-A, geometrical constraints set by the support structure of W VII-A had to be observed. Nevertheless, this procedure allowed the installation of a magnetic configuration promising a reduction of the axis shift by a factor of 2. This quantity is a convenient measure for the equilibrium physics because it is determined in an integral fashion by the internal currents (Pfirsch-Schlüter currents) needed to balance the toroidal effect. A reduction of a factor of 2

in the axis shift was and is still considered to be significant for demonstrating the basic physics of Advanced Stellarators in general and to be easily accessible to experimental verification at the same time.

10) Experimental results obtained from W VII-AS already support the following conclusions which are of basic importance for the physics and technology picture underlying Wendelstein VII-X:

- A modular coil system is technically feasible and cost-effective in construction.
- Its technical accuracy is as high as required, was cost-effective in its achievement and led to excellent agreement between the measured magnetic surfaces and the designed ones.
- The importance of configurational effects is confirmed: major resonances have to be avoided in the confinement region. Shear has to be maximized within these constraints. These effects are less drastic in a configuration bound by a separatrix of the magnetic field as compared to a configuration bound by a material limiter.
- The reduction by a factor of about 2 of the axis shift occurring with increasing ß could be demonstrated and so verifies the equilibrium concept of the Advanced Stellarator.
- The measured bootstrap current agrees rather well with the calculated one. ECR current drive was verified and successfully applied for compensation of other currents. Plasma operation of up to 1.5 s has been established exhibiting internal plasma time constants (e.g. time variations of internal currents) of about this duration.
- By ECRH (0.2 – 0.8 MW) plasmas could be generated at B = 2.5 T and maintained with peak electron temperatures of 2.5 keV, densities of 5 x 10^{19} m^{-3}, which is close to the cut-off density, energy confinement times of up to 20 ms, and χ_e at 2/3 of the plasma radius well below 1 $m^2 s^{-1}$, not all of these parameters in the same discharge though. Two consistent sets of parameters for ECRH plasmas (see Fig. 3) with a = 0.17 m are:
  (1) $P_{rf} = 700$ kW, $n_{e,0} = 3.5\ 10^{19}$ m^{-3}, $T_{e,o} = 2.4$ keV, $T_{i,0} = 0.8$ keV, $\tau_E = 8.5$ ms,
  χ_e (2/3 a) = 0.7 m^2 s^{-1}
  (2) $P_{rf} = 350$ kW, $n_{e,0} = 4.2\ 10^{19}$ m^{-3}, $T_{e,o} = 1.7$ keV, $T_{i,0} = 0.4$ keV, $\tau_E = 17$ ms,
  χ_e (2/3 a) = 0.35 m^2 s^{-1}

  The low ion temperature observed with ECRH plasmas is of course in accordance with the low power transfer from the electrons to the ions under the conditions of these experiments.

- Two consistent sets of parameters for NBI plasmas (see Fig. 3) obtained after carbonization of the device (for a ≈ 0.17 m and ι ≈ 0.34) are
  (3) $P_{NBI} = 1.3$ MW, $\langle n \rangle = 2.1 \cdot 10^{20}$ m^{-3} (!), $T_{e,o} = 0.65$ keV, $\tau_E = 22$ ms, $\langle \beta \rangle = 0.61$ %
  (4) $P_{NBI} = 650$ kW, $\langle n \rangle = 1.4 \cdot 10^{20}$ m^{-3}, $T_{e,o} = 0.6$ keV, $\tau_E = 28$ ms, $\langle \beta \rangle = 0.40$ %
  At these high densities with nearly box-type density profiles an accurate determination of the central ion temperature is above the capability of all the installed diagnostics, but there is little doubt that the ion temperature will be very close to the electron temperature for which values of up to 0.7 keV have been measured.

2.3 Transport behaviour

11) The confinement quality plays – of course – the same crucial role in a stellarator as in a tokamak. Transport analysis on W VII-AS indicates that the electron heat diffusivity χ_e approaches the neoclassical limit in the plasma core; χ_e in the periphery, however, is governed by anomalous processes. Because of the strong T_e-dependence of the neoclassical χ_e ($\propto T_e^{7/2}$) its reduction to acceptable reactor values is mandatory. This has been achieved in the present Wendelstein VII-X concept as described above. However, with this steep temperature dependence, neoclassical losses should be completely negligible for all cases with $T_e << T_{e,\,reactor}$ rendering the confinement, to anomalous processes. For their contribution to transport – like in tokamaks – statistical procedures would be useful to assess the confinement time to be expected in a W VII-X type of configuration; unlike the situation for tokamaks, however, the databasis of stellarator confinement results is limited and diverse – a consequence of the only few relevant stellarators in operation, which, in addition show systematic differences in their configurations. As argued in 8) means introduced in the Wendelstein VII-X configuration for reducing neoclassical losses are expected also to reduce anomalous losses.

Stellarator experiments display a confinement time which degrades with heating power – a feature as it is known for tokamaks both for L- and H-mode confinement. The power scaling obtained is similar, typically $\tau_E \propto P^{-0.6}$. The power variation of τ_E is an important feature of the LHS-scaling for stellarators. The similarity of this scaling to the tokamak

L-mode scaling is born out by a good representation of both tokamak and stellarator confinement data by the more rigorous plateau scaling which is – unlike empirical scaling laws – footed on a concept for anomalous transport.

In addition to similarities in scaling, transport and confinement properties of currentless stellarator plasmas reveal their kinship to the tokamak in a variety of other aspects: the anomalous electron transport increases at the plasma edge; particle and energy transport are closely linked with $D/\chi_e \sim 0.1 - 0.3$; an inward velocity can lead to impurity accumulation; attempts to explain the edge transport by electrostatic turbulence with a similar structure of the density fluctuations have been made.

It cannot be decided at present, whether the intrinsic advantages of stellarators (DC-operations, no disruptions, single coil configuration) can be obtained without enhanced anomalous transport. Therefore, in the stellarator too, favourable prospects will rely on the development of regimes with sufficiently good confinement. As the power degradation of τ_E is rather universally observed, the conditions which determine the prefactor in the relation $\tau_E \propto P^{-0.6}$ are of extreme importance. Prerequisites for H-mode-like edge conditions (separatrix, recycling and impurity control) can be realised in Wendelstein VII-X. The experience on H-mode operations – as gained on ASDEX – will be available on W VII-AS with the increase of its team by ASDEX scientists. In addition, the characteristics of Wendelstein VII-X, listed in 8), not only reduce neoclassical transport but are also expected to be a means to reduce anomalous losses.

In summary, the similarities in tokamak and stellarator transport features together with the optimization characteristics of Wendelstein VII-X yield favourable prospects for the confinement properties of Advanced Stellarators. Part 1 of the Application for Wendelstein VII-X will contain a detailed assessment of the confinement as it can be expected for Wendelstein VII-X.

3. Objectives of Wendelstein VII-X

12) The overall goal of Wendelstein VII-X is progress in the understanding of physics and engineering relevant to stellarator reactor-grade fusion plasmas, in particular relevant to Advanced Stellarators, continuing and augmenting W VII-AS experience and knowledge. Generally, stellarators are considered the leading alternative to tokamaks when recalling the four obvious inherent potential physics advantages: stationarity since the equilibrium does not rely on a net toroidal plasma current, no danger of disruptions, for the same reason, smaller excursions per bounce period of all trapped particles and less free energy because of the external generation of the entire confining field. Added to this are potential engineering advantages resulting from the possibility for only one single coil system for generating the entire confining magnetic field. Furthermore, experimentation with Wendelstein VII-X and comparison of the results with those of tokamaks will allow investigations on the influence on transport of net toroidal plasma currents and of the different behaviour of trapped particle orbits so that Wendelstein VII-X may foster deeper understanding of toroidal magnetic confinement in general. Thus, the programmatic objectives of Wendelstein VII-X are:

- Achievement of adequate confinement and investigation of plasma transport under reactor relevant conditions, including the confinement properties of fast particles
- Application of effective non-ohmic heating methods to generate the plasma and to reach plasma temperatures of several keV
- Investigation of impurity transport and development of means for impurity control
- Achievement of $\langle\beta\rangle$-values of 0.04 to 0.05 and analysis of the β-limit
- Long-term and quasi-stationary operation
- Study of plasma refuelling, exhaust and plasma wall interaction under steady state conditions
- Developments of means for proper control of the plasma edge conditions

13) The planning activities and theoretical studies over several years have now resulted in the completion of the conceptual design of Wendelstein VII-X, the second step of the chain of experiments described in the introduction. It will employ the full potential of the Helias concept described above, and will utilize a modular coil system. Its dimensions will be considerably increased as compared to W VII-AS in order to provide access to plasma parameter regimes adequate to allow conclusions about the reactor properties of Advanced Stellarators. These considerations have led to the following technical objectives for Wendelstein VII-X:

- A steady state magnetic field of 3 T on axis
- Powerful heating systems for plasma generation and heating (ECRH) and for further heating by NBI and ICRH
- Optimum access for neutral beam injection
- Maximum distance between plasma and first wall
- Flexibility in the magnetic field structure (variation of rotational transform and mirror ratio, position control)

4. Description of Wendelstein VII-X

14) Wendelstein VII-X is a modular Advanced Stellarator realizing a 5-period Helias configuration.

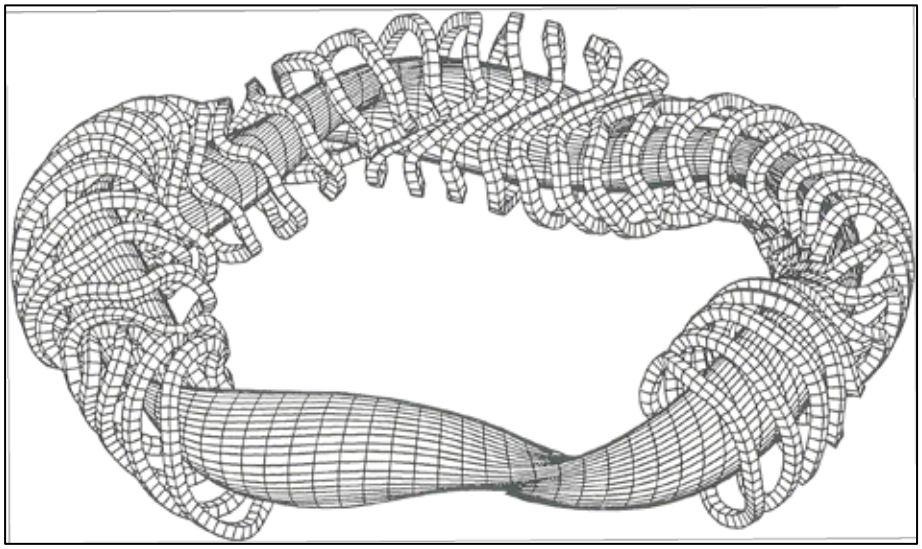

Fig. 2 *Sketch of Wendelstein VII-X basic configuration. The lines on the plasma surface indicate the magnetic field lines and meridional sections, respectively.*

In the standard configuration iota on axis is 0.84 and on the boundary 1.0, thus providing larger shear than in W VII-AS but still small enough to avoid major resonances in the confinement region. The equilibrium properties are characterized by strongly reduced Pfirsch-Schlüter currents with the balancing currents less than 0.75 (!) of the diamagnetic currents. MHD stability at $\langle\beta\rangle = 0.043$ is achieved by providing a vacuum field magnetic well and small Pfirsch-Schlüter currents rather than by magnetic shear. Neoclassical transport is strongly reduced and characterized by an equivalent ripple $\delta_e \lesssim 0.015$. The residual bootstrap current is small. In the boundary region, a separatrix bounded by magnetic islands of corresponding topology could be arranged so that the desired divertor action of this region can be investigated and the appropriate means be developed. Experimental flexibility with respect to resonance as well as trapped-particle physics manifests itself in the possibility for variation of the rotational transform by ± 0.2, of the shear by ± 0.1, and of the amplitude of the mirror field along the magnetic field up to 0.1. A sketch of the configuration is displayed in Fig. 2. Major design data can be found in Tables 1 and 2.

Table 1: Characteristic Nondimensional Data of the Experiment Wendelstein VII-X

Rotational transform, ι, on axis/boundary	0.84/0.99
Variation of ι	± 0.2
Variation of shear	± 0.1
Variation of mirror field	0.1
Pfirsch-Schlüter currents, $\langle j_\parallel^2/j_\perp^2\rangle$	0.5
Magnetic well depth	0.01
MHD stability limit, $\langle\beta\rangle_{st}$	0.043

Equivalent ripple, δ_e	0.015
Ratio of bootstrap currents, $J_{BS,stel}$ / $J_{BS,tok}$	$\lesssim 0.1$

Table 2: Characteristic Dimensional Data of the Experiment Wendelstein VII-X

Average major radius, R_0	5.5 m
Average plasma radius, r_a	0.53 m
Average coil radius, r_c	1.14 m
Min. distance plasma - coils, Δ_{pc}	0.29 m
Min. distance plasma - wall, Δ_{pw}	0.12 m
Induction on axis, B_0	3.0 T
Max. induction at coils, B_m	6.1 T
Total magnetic energy, W_m	600 MJ
Max. net force (one coil), F_{res}	3.6 MN

5. Performance targets and plasma heating

15) The objectives of the experiment as stated above require the achievable plasma parameters to be in the following ranges:

Central temperatures, $T_i(0)$, $T_e(0)$	2 - 5 keV
Central electron density, $n_e(0)$	0.1 - 2 x 10^{20} m^{-3}
Energy confinement time, τ_E	0.1 - 0.5 s
Average beta value, $\langle\beta\rangle$	≤ 0.05

(Ende des Ausschnitts)

➜ T. Klinger et al.: Overview of first Wendelstein 7-X high-performance operation, in: Nuclear Fusion, 2019

➜ C. D. Beidler, H. M. Smith, A. Alonso et al.: Demonstration of reduced neoclassical energy transport in Wendelstein 7-X, in: Nature, 2021

4

ANHANG

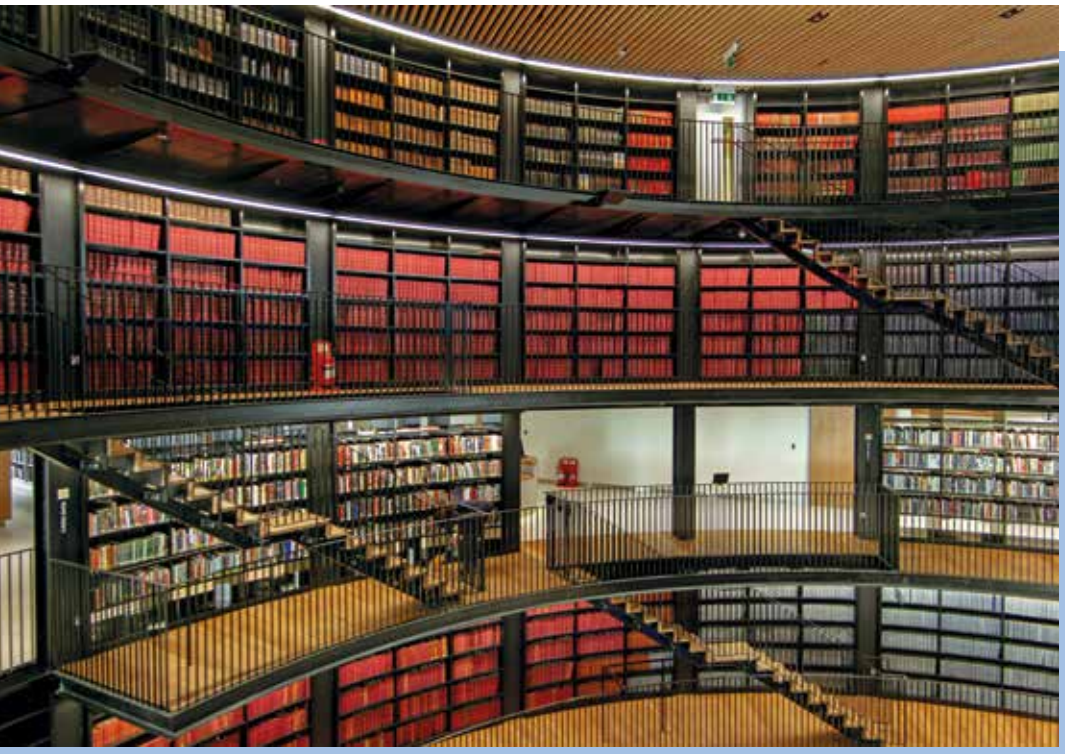

Foto: pexels-olga-lioncat-7244563

ANHANG

4.1 BIBLIOGRAPHIE KLAUS PINKAU

K. Pinkau: The Conversion Length of High Energy Photons. Nuovo Cimento, 3, 1156, 1956

K. Pinkau: Observations on Electromagnetic Cascades in Nuclear Emulsions. Nuovo Cimento, 3, 1285, 1956

K. Pinkau: Energy Determination of Electromagnetic Cascades in Nuclear Emulsions.
Phil. Mag., 2, No.23,1389, 1957

B. Edwards, J. Losty, D.H. Perkins, K. Pinkau and J. Reynolds: Analysis of Nuclear Interactions of Energies between 1000 and 100 000 BeV. Phil. Mag., 3, No.27, 237, 1958

P.H. Fowler, D.H. Perkins and K. Pinkau: Observation of the Suppression Effect on Bremsstrahlung.
Phil. Mag., 4, No.45, 1030, 1959

J. Duthie, C.M. Fisher, P.H. Fowler, A. Kaddoura, D.H. Perkins and K. Pinkau: Spectrum of g-Rays and Nuclear-Active Component of Air Showers at 11.000 Meters, Part II. Proc. Moscow Cosmic Ray Conf.,
Part I, p. 30; Part II, p. 35, I, 1960

P.H. Fowler, D.H. Perkins and K. Pinkau: Energy Determination of Electromagnetic Cascades.
Proc. Moscow Cosmic Ray Conf., II, p. 48, 1960

J.G. Duthie, C.M. Fisher, P.H. Fowler, A. Kaddoura, D.H. Perkins and K. Pinkau:
The Study of High-Energy g-Rays Produced by Cosmic Radiation at 40 000 Feet. Part I: Experimental Disposition, and Determination of Energy and Nature of Electromagnetic Cascades. Phil. Mag., 6, 89, 1961

J.G. Duthie, C.M. Fisher, P.H. Fowler, A. Kaddoura, D.H. Perkins, K. Pinkau and W. Wolter: The Study of High-Energy g-Rays Produced by Cosmic Radiation at 40 000 Feet. Part II: The Energy Spectrum of Cascades and its Interpretation. Phil. Mag., 6, 113, 1961.

K. Pinkau: The Development of Cascades Initiated by Nuclear Interaction. Phil. Mag., 6, No. 65, 657, 1961

M. Bowler, J. Duthie, P.H. Fowler, A. Kaddoura, D.H. Perkins, K. Pinkau and W. Wolter:
High Energy Gamma-Rays and Jet Showers. J. Phys. Soc. Japan, 17, Suppl. A-III, 424, 1962

K. Pinkau: The Three-Dimensional Development of Nucleonic Cascades.
J. Phys. Soc. Japan, 17, Suppl. A-III, 446, 1962

J. Duthie, P.H. Fowler, A. Kaddoura, D.H. Perkins and K. Pinkau: The Flux of g-Rays at High Altitudes, and Comparison with the Muon Flux at Sea-Level. Nuovo Cimento, 24, 122, 1962

K. Pinkau and H. Selk: Radiosonde zur genauen Messung des Luftdruckes und verschiedener Temperaturwerte. Atomkernenergie, 10, 365, 1963

ICEF Collaboration: High-Energy Nuclear Interaction from the International Co-operative Emulsion Flight. Supplemento Al, Nuovo Cimento, I, 1039, 1963

K. Pinkau: Über die Bedeutung einiger Meßergebnisse der Ultrastrahlungsphysik für die Kernphysik.
Fortschritte der Physik, 12, 139, 1964

K. Pinkau, U. Pollvolgt and C. Reppin: Spark-Emulsion Chamber for Balloonflights.
Proc. Jaipur Cosmic Ray Conf., 5-57, 548, 1964

E. Heidbreder and K. Pinkau: The Production-Spectrum of Particles in Interactions above 1000 GeV Energy.
Proc. Jaipur Cosmic Ray Conf., 5-24, 227, 1964.

D. Köhn, K. Pinkau and G. Wibberenz: Gamma-Ray Spectrometer for Balloonflights.
Proc. Jaipur Cosmic Ray Conf., 3-31, 203, 1964

K. Pinkau: Limitations to Methods of Energy Determination of Electromagnetic Cascades.
Nuovo Cimento, 33, 221, 1964

K. Pinkau: Errors in Electromagnetic Cascade Measurements Due to the Transition Effect.
Phys. Rev., 139, 6B 1548, Sept. 1965

K. Pinkau: Multiplicity of High Energy Interactions. Proc. London Cosmic Ray Conf., 2, 895, 1965

K. Pinkau, U. Pollvogt, W. Schmidt and R.W. Huggett: Balloon Experiment Using Spark Chambers and an Ionization Spectrometer. Proc. London Cosmic Ray Conf., 2, 821, 1965

K. Pinkau and K.V. Thompson: Design Calculations for Ionization Spectrometers: Cascade Development. Rev. Sci. Instr., 37, No. 3, 302, 1966

D. Köhn, K. Pinkau und G. Wibberenz: Messung des sekundären Gammaspektrums von 0,2 bis 2 GeV in der oberen Atmosphäre. Zeitschr. f. Phys., 193, 443, 1966

K. Pinkau: Molière's Theory of Multiple Scattering Applied to the Spark Chamber. Zeitschr. f. Phys., 196, 163, 1966

K. Pinkau: Die Messung solarer und atmosphärischer Neutronen. Zeitschr. f. Naturforschg., 21a, Heft 12, 2100, 1966

K. Pinkau: Kosmische Gammastrahlung. Mitt. Max-Planck-Gesellschaft, 6, 328, 1966

K. Pinkau, C. Reppin und V. Schönfelder: Bestimmung des Schwerpunkts von Teilchenschauern mit Hilfe der Doppelkeilmethode. Nucl. Instr. and Meth., 49, 13, 1967

K. Pinkau: The Measurement of Multiple Scattering, of Track Direction and Position in Spark Chambers. Nucl. Instr. and Meth., 48, 173, 1967.

R. Lüst und K. Pinkau: Theoretical Aspects of Celestial Gamma Rays. Electromagnetic Radiation in Space, J.G. Emming (Ed.), D. Reidel, Dordrecht, p. 231, 1967

L. Haser und K. Pinkau: Über Forschungsaufgaben des Instituts für extraterrestrische Physik am Max-Planck-Institut für Physik und Astrophysik. Sciences et Industries Spatiales, No. 5/6, 2, 1967

R. Holynski, V. Jones and K. Pinkau: Lateral and Angular Structure of Electromagnetic Cascades. Canadian J. of Physl., 46, 278, 1968

E. Heidbreder und K. Pinkau: Production Spectrum of Gamma Rays in High Energy Interactions and High Energy Gamma Ray Intensity at 2900 m. Zeitschr. f. Phys., 211, 51, 1968.

R. Holynski, W.V. Jones and K. Pinkau: Experimental Tests of Cascade Theory at High Energies. MPI-PAE/Extraterr. 9/68, 1968

R. Holynski, W.V. Jones and K. Pinkau: Experimental Tests of Cascade Theory at High Energies. Phys. Rev., 176, No. 5, 1661, 1968

K. Pinkau: Proposal for an Experiment to Measure Solar and Atmospheric Neutrons. MPI-PAE/Extraterr. 3/68, 1968.

K. Pinkau: Investigation of Spark Chamber Systems with Respect to Power of Resolution in Energy, Position, and Direction. MPI-PAE/Extraterr. 5/68, 1968

C.J. Crannell, H. Crannell, C.R. Gillespie, K. Pinkau and R.R. Whitney: Experimental Determination of the Transition Effect in Electromagnetic Cascade Showers. Bull. Am. Phys. Soc., 13, HEPL 587, 694, 1968 (Abstract)

K. Pinkau: Gamma-Astronomie-Experiment mit Hilfe eines Scout Satelliten. MPI-PAE/Extraterr. 10/68, 1968

H. Göllnitz, R. Gorenflo, E. Heidbreder, K. Pinkau, C. Reppin and V. Schönfelder: Design of a Neutron Scattering Chamber Using Monte Carlo Calculations. MPI-PAE/Extraterr. 14/68, 1968

K. Pinkau: Probleme der Röntgen- und Gamma-Astronomie. Mitt. Astron. Ges., 25, 37, 1968; Die Sterne, 45, 81, 1969

W.V. Jones, K. Pinkau, U. Pollvogt, W.K.H. Schmidt and R.W. Huggett: A Study of the Properties of an Ionization Spectrometer with 10, 20,5 and 28 GeV/c Incident Protons. MPI-PAE/Extraterr. 23, 1969., Nucl. Instr. & Meth., 72, 173, 1969.

W.K.H. Schmidt, K. Pinkau, U. Pollvogt and R.W. Huggett: Measurement of the Primary Cosmic-Ray Proton Spectrum between 40 and 400 GeV. MPI-PAE/Extraterr. 24, 1969., Phys. Rev., 184, No. 5, 1279, 1969

E.R. Goza, R.W. Huggett, S. Krzywdzinski, E. Stafford, W.V. Jones, K. Pinkau, U. Pollvogt and W.K.H. Schmidt: Balloon Experiment Using an Ionization Spectrometer in Conjunction with an Emulsion Stack and Spark Chambers to Study High-Energy Cosmic Rays and Particle Physics. Bull. Am. Phys. Soc., 14, 90, 1969

W.V. Jones, K. Pinkau, U. Pollvogt and W.K.H. Schmidt: Calibration of an Ionization Calorimeter with Incident Protons of 10, 20,5 and 28 GeV/c. Bull. Am. Phys. Soc., 14, 91, 1969

C.J. Crannell, H. Crannell, C.R. Gillespie, K. Pinkau and R.R. Whitney: Experimental Determination of the Transition Effect in Electromagnetic Cascade Showers. Phys. Rev., 182, No. 5, 1435, 1969

K. Pinkau, U. Pollvogt, W.K.H. Schmidt and R.W. Huggett: Measurement of the Primary Cosmic Ray Proton and Alpha-Particle Spectra above 10 GeV/Nucl. Mitt. Astron. Ges., 27, 143, 1969., Acta Physica Academiae Scient. Hungar., Suppl. 1, 29, 291, 1970

E. Heidbreder, K. Pinkau, C. Reppin and V. Schönfelder: Measurement of the Distribution in Energy and Angle of High -Energy Albedo Neutrons and Determination of an Upper Limit for the Solar Neutron Flux. J. Geophys. Res. Lett., 75, No. 31, 6347, 1970.

E. Heidbreder, K. Pinkau, C. Reppin und V. Schönfelder: A Balloon Borne Detector to Determine High Energy Neutrons in Energy and Direction. Nucl. Instr. & Meth., 88, 137, 1970

K. Pinkau: Pulsars and the Distribution of Celestial Gamma Rays. Phys. Rev. Lett., 25, No. 9, 603, 1970

K. Pinkau: Objectives of Future Gamma-Ray Missions. Open Questions relating to Observations of Celestial Gamma Rays. Proc. ESRO Coll. Noordwijk, ESRO SP-58, S. 33, 1970

W.V. Jones, K. Pinkau, U. Pollvogt, W.K.H. Schmidt and R.W. Huggett: Properties of an Ionization Spectrometer exposed to 10, 20,5, and 28 GeV/c Machine accelerated Protons.
Acta Phys. Acad. Hung., 29, Suppl. 4, 521, 1970

H. Coxell, C.R. Gillespie, R.W. Huggett, D.R. Humphreys, K. Pinkau and P.K. MacKeown: Studies of Hadron Interactions at Energies around 10 TeV using an Ionization Spectrometer-Emulsion Chamber Combination.
Acta Phys. Acad. Hung., 29, Suppl. 4, 497, 1970

K. Pinkau: Ursprung der kosmischen Strahlung. Sterne und Weltraum, 9, Nr. 11, 280, 1970. Physik und Kosmologie, Colloquium Verlag Berlin, S. 29, 1971.

H.C. van de Hulst, A. Scheepmaker, B.N. Swanenburg, H.A. Mayer-Hasselwander, E. Pfeffermann, K. Pinkau, H. Rothermel, H. Schneider, W. Voges, J. Labeyrie, P. Keirle, J. Paul, G. Bellomo, G. Bignami, G. Boella, L. Scarsi, G.W. Hutchinson, A.J. Pearce, D. Ramsden, R.D. Wills, and P.J. Wright: Spectral Analysis of Gamma Rays with the COS-B satellite. The Caravane Collaboration. New Techniques in Space Astronomy, IAU Symposium No. 41, eds. F. Labuhn and R. Lüst, D. Reidel, Dordrecht, S. 37, 1971

H.A. Mayer-Hasselwander, K. Pinkau, K.H. Schenkl, W. Voges, and H.J. Schneider: Investigation of the Power of Resolution of a Spark Chamber for Gamma-Ray Astronomy. New Techniques in Space Astronomy, IAU Symposium No. 41, eds. F. Labuhn and R. Lüst, D. Reidel, Dordrecht, S. 72, 1971

E. Heidbreder, K. Pinkau, C. Reppin, and V. Schönfelder: Measurements of the Distribution in Energy and Angle of High-Energy Neutrons in the Lower Atmosphere, J. Geophys. Res., 76, No. 13, 2905, 1971

J.F. Ormes, V.K. Balasubrahmanyan, T. Bowen, R.W. Huggett, T.A. Parnell, and K. Pinkau: Composition and Spectra of High Energy Cosmic Rays. A Proposal for an Orbiting Laboratory for the HEAO. Goddard Space Flight Center, Greenbelt, Md. X-661-71-1, 1971

K. Pinkau: Kosmische Röntgen- und Gammastrahlung. Sterne und Weltraum, 10, Nr. 8/9, 221, 1971

K. Pinkau: Analysis Procedure of Gamma Ray Astronomy Spark Chamber Data. MPI/PAE-Extraterr. 56, 1971

U. Pollvogt, K. Pinkau, W.K.H. Schmidt, and R.W. Huggett: Energy Calibration of an Ionization Spectrometer for Alpha-Particles. Bull. Am. Phys. Soc., 16, 656, 1971

G. Kettenring, H.A. Mayer-Hasselwander, E. Pfeffermann, K. Pinkau, H. Rothermel, and M. Sommer:
Investigation of Gamma Radiation from the Crab Pulsar.
Proc. 12th Intern. Conf. on Cosmic Rays, Hobart, Tasmania, 1, 57, 1971

C. Reppin, V. Schönfelder, G. Kanbach und K. Pinkau: Energy Spectrum and Angular Distribution of Atmospheric Albedo Neutrons. Proc. 12th Intern. Conf. on Cosmic Rays, Hobart, Tasmania, 2, 834, 1971

H. Billing und K. Pinkau: Discussion of the spectrum of Low Energy Cosmic Rays in Interstelllar Space, (Diskussion des Spektrums der niederenergetischen kosmischen Strahlung im interstellaren Raum.) Verhandlungen DPG, 8, 512, 1971

W.V. Jones, K. Pinkau, U. Pollvogt, and W.K.H. Schmidt: Some Properties of Nuclear Interaction Obtained with an Ionization Spectrometer at Proton Energies from 10 to 28 GeV. Nuovo Cimento, 8A, 8, No. 3, 575, 1972

K. Pinkau: High Energy Astrophysics Research at the Max-Planck-Institute. Atomkernenergie, 19, 133, 1972

H.A. Mayer-Hasselwander, E. Pfeffermann, K. Pinkau, H. Rothermel and M. Sommer:
Observation of the Diffuse Cosmic Gamma Radiation in the 30-50 MeV Region.
MPI-PAE/Extraterr. 64, 1972., Astrophys. J., 175, No. 1, L23, 1972

K. Pinkau: Analysis Procedure of Gamma Ray Astronomy Spark Chamber Data. Nucl. Instr. & Meth., 104, 517, 1972

K. Pinkau, H.M. Kappler, and D. Hovestandt: Activities in Space Research at the Max-Planck-Institut für extraterrestrische Physik, Garching bei München (F.R.G.). Industries Atomique & Spatiales, 6, 54, 1972

K. Pinkau: Kosmische Gammastrahlen. MPI-PAE/Extraterr. 83, 1973

K. Pinkau: Report to the Goddard Workshop on Gamma Ray Astronomy Results obtained in Europe since the IAU-Symposium No. 55. “Gamma Ray Astrophysics”, NASA SP-339, Washington, 1973

K. Herterich, K. Pinkau, H. Rothermel, and M. Sommer: On the Measurement of the Diffuse Cosmic Gamma Radiation in the 30-50 MeV Range. 13th Intern. Cosmic Ray Conf., Denver, Colorado, Conf. Papers, 1, 21, 1973

W. Voges, K. Pinkau, Y. Koechlin, J.P. Leray, G. Boella, G. Sironi, and M. Turner: First Results on Gamma Ray Observation from the ESRO TD-1A Satellite.
13th Intern. Cosmic Ray Conf., Denver, Colorado, Conf. Papers, 1, 293, 1973

K. Pinkau: Merkwürdige Objekte der Röntgen- und Gamma-Astronomie. Physik 1973, Plenarvorträge, 10, 33, Physik Verlag, Weinheim, 1973

K. Pinkau: X-Rays and Gamma Rays.
13th Intern. Cosmic Ray Conf., Denver, Colorado, Conf. Papers, 5, 3501, 1973

K. Pinkau (Hrsg): Interstellar Medium. Proc. NATO Advanced Study Institutes Series. C. Mathematical and Physical Sciences 6, D. Reidel, Dordrecht, 1974.

W. Voges and K. Pinkau: The Observation of a Gamma -Ray Burst from the ESRO TD-1A Satellite.
Proc. Conf. on Transient Cosmic Gamma- and X-Ray Sources, Los Alamos, 49, 1974

K. Pinkau: Wie sterben die Sterne? Mitt. Alexander von Humboldt-Stiftung, 29, S. 18, 1974

K. Pinkau: Merkwürdige Objekte der Röntgen- und Gammaastronomie. Jahrbuch 1973 der DGLR, Köln, 1974

K. Pinkau: Gamma-Ray Observations of the Sky from the TD-1 Satellite.
Proc. 9th ESLAB Symp. Frascati, ESRO SP-106, 1974

K. Pinkau: Wie sterben die Sterne? Sterne und Weltraum, 1, S. 4, 1975

K. Pinkau: Observation of Celestial Gamma Rays. Origin of Cosmic Rays, J.L. Osborne and A.W. Wolfendale (Eds.), D. Reidel, Dordrecht, S. 335, 1975

K. Pinkau: Cosmic Rays and the Dynamics of the Galaxy. Proc. ESRO Workshop, Frascati, ESRP SP-109, 1975

K. Pinkau: Gamma Ray Astronomy (0.1-1000 MeV). COSPAR Space Research XV, Akademie-Verlag, Berlin 1975

Empfehlungen des Gutachterausschusses „Großinvestitionen in der Grundlagenforschung“, 1975

K. Pinkau: Der Einsatz des Spacelab für naturwissenschaftliche Grundlagenforschung.
Vulkan-Verlag, Essen, 365, S. 27, 1976

K. Pinkau: Kosmische Partikelstrahlung. Physik und Didaktik, Bayer. Schulbuch-Verlag, München, S. 167, 1976

K. Pinkau: Progress in Extraterrestrial Research through Shuttle and Spacelab. Utilization of Space Shuttle and Spacelab. DGLR-AAS, Bonn, S. 519, 1976

K. Pinkau: Gamma-Astronomie. Mitt. Astron. Ges., 40, 59, 1976

K. Pinkau: Die Entstehung der Elemente im Kosmos. Die BASF, 1, 1977 UNIVERSITAS, 12, 1265, 1977

K. Pinkau: Gamma Ray Astronomy. MPI-PAE/Extraterr. 137, 1977, Proc. 15th Intern. Cosmic Ray Conf., Plovdiv, 10, 149, 1977

K. Pinkau: Status of High Energy Gamma Ray Astronomy. Bull. Am. Phys. Soc., 23, No. 4, 590, 1978

Recommendations of the Science Advisory Committee on the Development of Space Science in the 1980s, ESA Science Advisory Committee (SAC), 1978.

K. Pinkau: Forschungsplanung in einem Institut der Max-Planck-Gesellschaft am Beispiel des Instituts für extraterrestrische Physik in Garching. Konstanzer Blätter für Hochschulfragen,
Universitäts-Verlag, Konstanz, 58, Jhg. XVI, 73, 1978

Space Science in Europe, European Science Foundation, 1979

K. Pinkau: Present Status of g-ray Astronomy. Nature, 277, No. 5691, 17, 1979

K. Pinkau: The Sky in the Light of Gamma Rays. (COSPAR) X-Ray Astronomy, Eds. W.A. Baity and L.E. Peterson, Pergamon Press, Oxford and New York, S. 523, 1979

B. Aschenbach and K. Pinkau (Eds.): X-Ray and Gamma-Ray Astronomy in the 1980s

K. Pinkau: Compton-Scattering Model for the g-Ray Emission of NGC 4151. Proc. 16th Intern. Cosmic Ray Conf., Kyoto, 1, 165, 1979. MPI-PAE/Extraterr. 159, 1979

K. Pinkau: Die Bedeutung der langfristigen Planung bei der ESA für die Weltraumforschung in der Bundesrepublik Deutschland. Verhandlungen DPG (VI), 14, 1076, 1979

K. Pinkau: Weltall - Der Aufbau des Kosmos. Forum heute. Bibl. Inst. Mannheim, Bd. 2, S. 185, 1979

J.M. Ryan, E.L. Chupp, D.J. Forrest, M.L. Cherry, I.U. Gleske, E. Rieger, G. Kanbach, K. Pinkau, C. Reppin, G. Share, R.L. Kinzer, W.N. Johnson, J.D. Kurfess: The Gamma-Ray Spectrometer for the Solar Maximum Mission. In: Proc. 16th International Cosmic Ray Conf., Kyoto, Japan, Vol. SP, p. 3 - 1, August 1979

Empfehlungen zur Forschung und zum Mitteleinsatz in den Hochschulen, Wissenschaftsrat, 1979

Empfehlungen zur Errichtung eines Polarforschungsinstitutes

Empfehlungen zur Forschung und zum Mitteleinsatz in den Hochschulen

E.B. Hughes, R. Hofstadter, A. Johansson, J. Rolfe, D.L Bertsch, W.J. Cruickshank, C.H. Ehrmann, C.E. Fichtel, R.C. Hartman, D.A. Kniffen, R.W. Ross, D.J. Thompson, K. Pinkau, H. Rothermel, M. Sommer, H.A. Mayer-Hasselwander, A. Favale, and E.J. Schneid: Characteristics of the Telescope for High Energy g-Ray Astronomy Selected for Definition Studies on the Gamma Ray Observatory.
NASA Technical Memorandum 80590, October 1979., Trans. Nucl. Sci. NS-27, 364, 1980

K. Pinkau: Die Bedeutung der langfristigen Planung bei der ESA für die Weltraumforschung in der Bundesrepublik. Mitt. Astron. Ges. 47, 219, 1980

K. Pinkau: Compton-Scattering Model for the g- Ray Emission of NGC 4151. Astron. Astrophys. 87, 192, 1980

K. Pinkau: Localized Sources of High-Energy Gamma Rays. Ninth Texas Symposium on Relativistic Astrophysics. Eds. J. Ehlers, J.J. Perry, M. Walker, Annals of the New York Academy of Sciences, 336, 234, 1980

H.A. Mayer-Hasselwander, K. Bennett, G.F. Bignami, R. Buccheri, N. D´Amico, W. Hermsen, G. Kanbach, F. Lebrun, G.G. Lichti, J.L. Masnou, J.A. Paul, K. Pinkau, L. Scarsi, B.N. Swanenburg, and R.D. Wills:
COS-B Observation of the Milky Way in High-Energy Gamma Rays. Ninth Texas Symposium on Relativistic Astrophysics, Eds. J. Ehlers, J.J. Perry, M. Walker, Annals of the New York Academy of Sciences, 336, 211, 1980

D.J. Forrest, E.L. Chupp, J.M. Ryan, M.L. Cherry, I.U. Gleske, C. Reppin, K. Pinkau, E. Rieger, G. Kanbach, R.L. Kinzer, G. Share, W.N. Johnson, J.D. Kurfess: The Gamma Ray Spectrometer for the Solar Maximum Mission. Solar Physics, 65, 15, 1980., D. Reidel Bib l. Dordrecht

K. Pinkau: Gamma Ray Astronomy. 7th Europ. Cosmic Ray Symp., Leningrad, Sept. 1980.
“Cosmic Rays” at V.A. Dargachev and D.B. Kocharov. Academy of Sciences of the USSR, Leningrad, 80, S. 158

D.J. Forrest, E.L. Chupp, J.M. Ryan, C. Reppin, E. Rieger, G. Kanbach, K. Pinkau, G. Share, G. Kinzer:
Evidence for Impulsive Ion Acceleration During the 0312 UT Flare of 1980 June 7., Proc. of the 17th Intern. Cosmic Ray Conf., Paris, 10, 5, 1981

J.M. Ryan, D.J. Forrest, E.L. Chupp, M.L. Cherry, C. Reppin, E. Rieger, K. Pinkau, G. Kanbach, G.H. Share, R.L. Kinzer, M.S. Strickman, W.N. Johnson, J.D. Kurfess: Observations with the SMM Gamma-Ray Spectrometer: The impulsive solar flares of 1980, March 29., Astrophys. J. Lett. Vol. 244, L175, 1981, March 15

E.L. Chupp, D.J. Forrest, J.M. Ryan, M.L. Cherry, C. Reppin, G. Kanbach, E. Rieger, K. Pinkau, G.H. Share, R.L. Kinzer, M.S. Strickman, W.N. Johnson, J.D. Kurfess: Observation of the 2.223 MeV Gamma-Ray Line on the SMM Satellite - The Event of 1980, June 7., The Astrophys. J., 244: L171-L174, 1981, March 15

Empfehlungen des Gutachterausschusses „Großprojekte der Grundlagenforschung“, (Berufen vom Bundesminister für Forschung und Technologie, 1981)

H.A. Mayer-Hasselwander, K. Bennett, G.F. Bignami, R. Buccheri, P.A. Caraveo, W. Hermsen, G. Kanbach, F. Lebrun, G.G. Lichti, J.L. Masnou, J.A. Paul, K. Pinkau, B. Sacco, L. Scarsi, B.N. Swanenburg, R.D. Wills:
Large-Scale Distribution of Galactic Gamma Radiation Observed by COS-B. Astron.
Astrophys. 105, 164-175, 1982, May 15, 1982

K. Pinkau, U. Schumacher: Fusionsforschung mit magnetischem Plasmaeinschluß.
Atomwirtschaft-Atomtechnik, 27, 131, 1982

E.L. Chupp, D.J. Forrest, J.M. Ryan, J. Heslin, C. Reppin, K. Pinkau, G. Kanbach, E. Rieger, G.H. Share:
A Direct Observation of Solar Neutrons Following the 0118 UT Flare on 1980, June 21.,
Astrophys. J. Lett., Vol. 263, No. 2, Part 2, L95, 1982

K. Pinkau: Vorschlag einer Neutronendiagnostik für Fusionsplasmen. Z. f. Naturforsch., 37a, 741-743, 1982

K. Pinkau, U. Schumacher: Kernfusion mit magnetisch eingeschlossenen Plasmen.
Phys. in unserer Zeit, Vol. 13, Heft 5, 1982

K. Pinkau: Stand und Aussichten der Kernfusion. Gesellschaft Deutscher Naturforscher und Ärzte, 1982

C.E. Fichtel, D.L. Bertsch, R.C. Hartman, D.A. Kniffen, D.J. Thompson, R. Hofstadter, E.B. Hughes, K. Pinkau, G. Kanbach, H.A. Mayer-Hasselwander, H. Rothermel, M. Sommer:
The Energetic Gamma Ray Experiment Telescope (EGRET) on the Gamma Ray Observatory.
Spring Meeting of the American Phys. Soc., April 18-21, 1983.

C.E. Fichtel, D.L. Bertsch, R.C. Hartman, D.A. Kniffen, D.J. Thompson, R. Hofstadter, E.B. Hughes, L.E. Campbell-Finman, K. Pinkau, H.A. Mayer-Hasselwander, G. Kanbach, H. Rothermel, M. Sommer: EGRET: The high Energy Gamma Ray Telescope for NASA´s Gamma Ray Observatory, Paper Code No. T1-10, 1983

K. Pinkau: Verantwortlichkeit identifizierbar machen! Phys. Bl. 39, Nr. 3, 1983

Empfehlungen des Gutachterausschusses „Weltraumforschung/Weltraumtechnik“, 1984.

K. Pinkau: Stand und Aussichten der Kernfusion mit magnetischem Einschluß.
Westdeutscher Verlag 1984, N 327

K. Pinkau: Kontrollierte Kernfusion - Stand und Aussichten. FOCUS MHL, 2. Jahrgang, Heft 3, S. 180, Juli 1985

K. Pinkau: Setting Priorities in Big Science. Proceeding of the ESRC/NSF Symposium “Rise and Fall of a Priority Field”, Paris, 1985

K. Pinkau: Co-operation and Competition in Science and Advanced Technology. 6th Parliamentary and Scientific Conference, Tokyo/Tsukuba, 3-6 June 1985., Doc. 5450 Annex, S. 219, October 1985

Denkschrift für die Gründung einer Akademie der Wissenschaften zu Berlin, 1985

D.J. Thompson, D.L. Bertsch, A. Favale, C.E. Fichtel, R.C. Hartman, R. Hofstadter, E.B. Hughes, S.D. Hunter, B.W. Hughlock, G. Kanbach, D.A. Kniffen, Y.C. Lin, J.R. Mattox, H.A. Mayer-Hasselwander, P.L. Nolan, K. Pinkau, H. Rothermel, E.J. Schneid, M. Sommer, and A.H. Walker: Calibration of the EGRET High-Energy Gamma-Ray Telescope in the 20-10,000 MEV with a Tunable Beam of Quasi-Monoenergetic Gamma-Rays at SLAC, presented at the IEEE 1986 Nuclear Science Symposium, Washington, D.C. (86-018), 1986

Empfehlungen des Sachverständigenkreises für „Neutronenquellen für die Forschung in der Bundesrepublik Deutschland“, 1986

K. Pinkau: Kann die Kernfusion langfristig ein Ausweg sein? Bankhaus Reuschel & Co. München, 18. März 1987

K. Pinkau: Technologiefolgenabschätzung - Auftrag und Probleme. Siemens, 5/1987

K. Pinkau: Was erwarten die Wissenschaftler von den Politikern und der Öffentlichkeit?
Pharm. Ind., Band 49, 8/1987

K. Pinkau: Nunmehr gibt es sie, die Akademie der Wissenschaften zu Berlin.
Jahrbuch der Berliner Wissenschaftlichen Gesellschaft 1987

Ansprache anläßlich der Übergabe der Denkschrift für die Gründung einer Akademie der Wissenschaften zu Berlin,
Jahrbuch Akademie der Wissenschaften 1987, S. 193-199

G. Kanbach, D.L. Bertsch, A. Favale, C.E. Fichtel, R.C. Hartman, R. Hofstadter, E.B. Hughes, S.D. Hunter, B.W. Hughlock, D.A. Kniffen, Y.C. Lin, H.A. Mayer-Hasselwander, P.L. Nolan, K. Pinkau, H. Rothermel, E.J. Schneid, M. Sommer, D.J. Thompson: The Project EGRET (Energetic Gamma-Ray Experiment Telescope) on NASA´s Gamma-Ray Observatory GRO. Proceedings of the Workshop "Actual Problems of Gamma Ray Astronomy in the Light of the Planned Experiments". Odessa, May 4-8, 1987., Space Science Reviews March 12, 1988

K. Pinkau: Der entfesselte Prometheus? Wissenschaft und Technik im Spannungsfeld von Politik und Öffentlichkeit.
Allgemeine Vermessungsnachrichten, 1/1988.

K. Pinkau: Technology Assessment in Perspective. Siemens, Vol. 55, 1/1988

K. Pinkau: Evaluación de las consecuencias de la tecnología: Objetivos y problemas, Siemens, 2/1988

K. Pinkau: Ansprache anläßlich der Übergabe der Denkschrift für die Gründung einer Akademie der Wissenschaften zu Berlin. Jahrbuch der Akademie der Wissenschaften zu Berlin 1987.,
Walter de Gruyter Berlin - New York, 1988

K. Pinkau: Kernfusion – Grundlagenforschung im Spannungsfeld gesellschaftlicher Erwartungen.
Tagesdokumentation der AGF-Jahrestagung 1988, 27, 1988

G. Kanbach, D.L. Bertsch, A. Favale, C.E. Fichtel, R.C. Hartman, R. Hofstadter, E.B. Hughes, S.D. Hunter, B.W. Hughlock, D.A. Kniffen, Y.C. Lin, H.A. Mayer-Hasselwander, P.L. Nolan, K. Pinkau, H. Rothermel, E.J. Schneid, M. Sommer, D.J. Thompson: The Project EGRET (Energetic Gamma-Ray Experiment Telescope) on NASA's Gamma-Ray Observatory GRO. Space Science Review 49, 69 – 84, 1988.

Space Science in the Twenty-First Century: Imperatives for the Decades 1995 to 2015. Overview,
ISBN 0-309-03838-3. Astronomy and Astrophysics, ISBN 0-309-03875-8 National Academy Press, 1988

K. Pinkau: Technologiefolgenabschätzung - Auftrag und Probleme. Jahrbuch Elektrotechnik 1989,
Band 8. vde-Verlag 33, 1988

K. Pinkau, U. Schumacher und G.H. Wolf: Fortschritte der Fusionsforschung mit magnetischem Plasmaeinschluß.
Phys. Bl. 45 Nr. 2, 41-68, 1989

G. Kanbach, D.L. Bertsch, A. Favale, C.E. Fichtel, R.C. Hartman, R. Hofstadter, E.B. Hughes, S.D. Hunter, B.W. Hughlock, D.A. Kniffen, Y.C. Lin, J.R. Mattox, H.A. Mayer-Hasselwander, C. von Montigny, P.L. Nolan, K. Pinkau, H. Rothermel, E.J. Schneid, M. Sommer, D.J. Thompson, A.H. Walker: The EGRET Instrument. Gamma Ray Observatory Science Workshop, 10 - 12 April, 1989

C.E. Fichtel, D.L. Bertsch, R.C. Hartman, R. Hofstadter, E.B. Hughes, B.W. Hughlock, S.D. Hunter, G. Kanbach, D.A. Kniffen, Y.C. Lin, H.A. Mayer-Hasselwander, P.L. Nolan, K. Pinkau, H. Rothermel, E.J. Schneid, M. Sommer, D.J. Thompson, and C. von Montigny: High Energy Gamma Ray Astrophysics and what EGRET might contritbute. Proceedings GRO-Workshop, GSFC, April 1989

D.L. Bertsch, C.E. Fichtel, R.C. Hartman, R. Hofstadter, E.B. Hughes, B.W. Hughlock, S.D. Hunter, G. Kanbach, D.A. Kniffen, N. Laubenthal, J.R. Mattox, H.A. Mayer-Hasselwander, C. von Montigny, K. Pinkau, P.L. Nolan, E.J. Schneid, D.J. Thompson, Y.C. Lin: The EGRET Data Analysis System, 1989

K. Pinkau et al.: Memorandum eines vom Bundesminister für Forschung und Technologie berufenen Sachverständigenausschusses zu „Grundsatzfragen und Programmperspektiven der Technikfolgenabschätzung", Juni 1989

K. Pinkau: Kernfusion - Grundlagenforschung im Spannungsfeld gesellschaftlicher Erwartungen
Festvortrag, gehalten am 30.11.1988, anläßlich der Jahresversammlung der Arbeitsgemeinschaft der Großforschungseinrichtungen in München, „Leben ohne Risiko?".
Verlag TÜV Rheinland GmbH, ISBN 3-88585-674-3, Köln 1989

K. Pinkau: Folgenabschätzung der Technik. Technik und Bildung, Königsteiner Forum, E.J.M. Kroker, B. Dechamps, Frankfurter Allgemeine Zeitung GmbH, Wirtschaftsbücher, ISBN 3-924875-43-X, S. 153, 1989

K. Pinkau: Present Status of Fusion Research and Large International Facilities. Proceedings of the IV EPS Seminar on International Research Facilities, March 17 - 19, 1989, Zagreb, Yugoslavia, European Physical Society, Ruder Boskovic Institute, Institute of Research and Development of Safety, Zagreb, S. 275, 1989

K. Pinkau: Science and Politics. XIIIth International Congress of History of Science. Hamburg-Munich, 1989, Sudhoffs Archiv Beihefte 30

G. Zankl, K. Pinkau: Auf dem Weg zum Fusionsreaktor (1990): In: Wissenschaft und Technik in Europa (Scientific Europe), Foundation Scientific Europe (Hrsg.),
Spektrum der Wissenschaft Verlagsgesellschaft mbH, Heidelberg, S. 230, 1991

K. Pinkau: Jahresbericht Studienstiftung 1991, S. 41

K. Pinkau: Energie ist die Währung der Zukunft. Essener Hochschulblätter, Universität-Gesamthochschule Essen, 1991

K. Pinkau: Wissenschaft und Politik: Umweltstandards als spezieller Fall der Technikfolgenabschätzung. Einheit der Wissenschaften, Internationales Kolloquium der Akademie der Wissenschaften zu Berlin, Bonn, 25. - 27. Juni 1990, S. 429-440, 1991

K. Pinkau: Wissensfolgenabschätzung - wie genau können oder dürfen wir unsere Zukunft planen? Festvortrag anläßlich der Jahrestagung der Fraunhofer-Gesellschaft, 1991

K. Pinkau: Wissenschaft und Politik: Umweltstandards als spezieller Fall der Technikfolgenabschätzung. Einheit der Wissenschaften, Akademie der Wissenschaften zu Berlin, Forschungsbericht 4, 429, 1991

E.J. Schneid, D.L. Bertsch, C.E. Fichtel, R.C. Hartman, S.D. Hunter, G. Kanbach, D.A. Kniffen, P.W. Kwok, Y.C. Lin, J.R. Mattox, H.A. Mayer-Hasselwander, P.F. Michelson, C. von Montigny, P.L. Nolan, K. Pinkau, H. Rothermel, M. Sommer, P. Sreekumar, and D.J. Thompson: EGRET Detection of High Energy Gamma Rays from the 1991 May 3, Gamma Ray Burst, A&A, 5.12.1991

J. Diekmann, A. Gierer, H.-J. Krupp, K. Pinkau, H.-J. Queisser, F.P. Schäfer, H. Schaefer, K. Stephan, D. Weiß, H.T. Witt: Sonnenenergie, Akademie der Wissenschaften zu Berlin, Forschungsbericht 1, 1992

K. Pinkau: Fusionsforschung - Stand der Forschung und Perspektiven.
RWE Energie, Tagungsbericht, ISBN 3-89355-060-7, 91, 1992

K. Pinkau, K. Decker, C.F. Gethmann, H.W. Levi, J. Mittelstraß, S. Peyerimhoff, G. zu Putlitz, A. Randelzhofer, O. Renn, C. Streffer, F.E. Weinert: Umweltstandards - Grundlagen, Tatsachen und Bewertungen am Beispiel des Strahlenrisikos. Akademie der Wissenschaften zu Berlin, Forschungsbericht 2, 1992

S.D. Hunter, G. Kanbach, D.A. Kniffen, P.W. Kwok, Y.C. Lin, J.R. Mattox, H.A. Mayer-Hasselwander, P.L. Nolan, K. Pinkau, H. Rothermel, E.J. Schneid, M. Sommer, P. Sreekumar, D.J. Thompson, C. von Montigny: Search for periodic gamma-ray emission from Cygnus X-3 by the EGRET telescope on the Compton Gamma-Ray Observatory. In: Ap. J., 401, pp. 724-727, 1992

D.A. Kniffen, D.L. Bertsch, C.E. Fichtel, R.C. Hartman, S.D. Hunter, J.R. Mattox, D.J. Thompson, K.T.S. Brazier, G. Kanbach, H.A. Mayer-Hasselwander, C. von Montigny, K. Pinkau, J. Chiang, J.M. Fierro, Y.C. Lin, P.F. Michelson, P.L. Nolan, E.J. Schneid, H.I. Nel, J. Taylor, M. Bailes, S. Johnston, R.N. Manchester, A.G. Lyne, N. d´Amico, and L. Nicastro: EGRET Observations of Pulsars. In: AIP Press 280, New York, 177, 1992

D.J. Thompson, D.L. Bertsch, C.E. Fichtel, J.M. Fierro, R.C. Hartman, S.D. Hunter, G. Kanbach, D.A. Kniffen, Y.C. Lin, J.R. Mattox, H.A. Mayer-Hasselwander, P.F. Michelson, C. von Montigny, H.I. Nel, P.L. Nolan, K. Pinkau, H. Rothermel, E.J. Schneid, M. Sommer, P. Sreekumar, and Timing Analysis of EGRET/CGRO Data David J. Thompson: Preliminary EGRET High Energy Gamma Ray Obervations of the Crab Pulsar. 92-014 Proceedings of Workshop on Physics of Isolated Pulsars

C.E. Fichtel, D.L. Bertsch, B.L. Dingus, R.C. Hartman, S.D. Hunter, P.W. Kwok, J.R. Mattox, P. Sreekumar, D.J. Thompson, D.A. Kniffen, Y.C. Lin, P.L. Nolan, P.F. Michelson, G. Kanbach, H.A. Mayer-Hasselwander, C. von Montigny, K. Pinkau, H. Rothermel, M. Sommer, and E.J. Schneid: ENERGETIC GAMMA RAY EXPERIMENT TELESCOPE CONTRIUBUTIONS TO THE COMPTON OBSERVATORY SYMPOSIUM, by EGRET Gamma Ray Observatory, In: AIP 93-14

R.C. Hartman, D.L. Bertsch, C.E. Fichtel, S.D. Hunter, G. Kanbach, D.A. Kniffen, P.W. Kwok, Y.C. Lin, J.R. Mattox, H.A. Mayer-Hasselwander, P.F. Michelson, H.I. Nel, P.L. Nolan, K. Pinkau, H. Rothermel, E.J. Schneid, M. Sommer, P. Sreekumar, D.J. Thompson, and C. von Montigny: Detection of High-Energy Gamma Radiation from Quasar 3C 279 by the EGRET Telescope on the Gamma Ray Observatory. In: ApJ Letters, 385, L1-L4, 1992

D.L. Bertsch, K.T.S. Brazier, C.E. Fichtel, R.C. Hartman, S.D. Hunter, G. Kanbach, D.A. Kniffen, P.W. Kwok, Y.C. Lin, J.R. Mattox, H.A. Mayer-Hasselwander, C. von Montigny, P.F. Michelson, P.L. Nolan, K. Pinkau, H. Rothermel, E.J. Schneid, M. Sommer, P. Sreekumar, and D.J. Thompson: Pulsed High-energy g-radiation from Geminga (1E0630+178). Nature, Vol. 357, 306, 1992

D.J. Thompson, Z. Arzoumanian, D.L. Bertsch, K.T.S. Brazier, N. D'Amico, C.E. Fichtel, J.M. Fierro, R.C. Hartman, S.D. Hunter, S. Johnston, G. Kanbach, V.M. Kaspi, D.A. Kniffen, Y.C. Lin, A.G. Lyne, R.N. Manchester, J.R. Mattox, H.A. Mayer-Hasselwander, P.F. Michelson, C. von Montigny, H.I. Nel, D. Nice, P.L. Nolan, K. Pinkau, H. Rothermel, E.J. Schneid, M. Sommer, P. Sreekumar, and J.H. Taylor: Pulsed High Energy g-rays from the radio pulsar PSR 1706-44 (2CG342-02), Nature, 359, 615, 1992

P.L. Nolan, D.L. Bertsch, C.E. Fichtel, R.C. Hartman, R. Hofstadter, E.B. Hughes, S.D. Hunter, G. Kanbach, D.A. Kniffen, Y.C. Lin, J.R. Mattox, H.A. Mayer-Hasselwander, P.F. Michelson, C. von Montigny, K. Pinkau, H. Rothermel, E.J. Schneid, M. Sommer, P. Sreekumar, and D.J. Thompson: Performance of the EGRET Astronomical Gamma Ray Telescope. 1992. IEEE Transactions Nucl. Sci., 39, 993-996

P. Sreekumar, D.L. Bertsch, C.E. Fichtel, R.C. Hartman, S.D. Hunter, G. Kanbach, D.A. Kniffen, P.W. Kwok, Y.C. Lin, J.R. Mattox, H.A. Mayer-Hasselwander, P.F. Michelson, C. von Montigny, P.L. Nolan, K. Pinkau, H. Rothermel, E.J. Schneid, M. Sommer, D.J. Thompson: Observations of the Large Magellanic Cloud in High-Energy Gamma Rays. 1992. ApJ Letters, 400, L67-L70

P.F. Michelson, D.L. Bertsch, J. Chiang, C.E. Fichtel, R.C. Hartman, S.D. Hunter, G. Kanbach, D.A. Kniffen, P.W. Kwok, Y.C. Lin, J.R. Mattox, H.A. Mayer-Hasselwander, P.L. Nolan, K. Pinkau, H. Rothermel, E.J. Schneid, M. Sommer, P. Sreekumar, and D.J. Thompson: Search for Periodic Gamma-Ray Emission from Cygnus X-3 by the EGRET Telescope on the Compton Gamma-Ray Observatory. 1992. ApJ, 401, 724-747

Y.C. Lin, D.L. Bertsch, J. Chiang, C.E. Fichtel, R.C. Hartman, S.D. Hunter, G. Kanbach, D.A. Kniffen, P.W. Kwok, J.R. Mattox, H.A. Mayer-Hasselwander, P.F. Michelson, C. von Montigny, P.L. Nolan, K. Pinkau, H. Rothermel, E.J. Schneid, P. Sreekumar, and D.J. Thompson: Detection of High Energy Gamma Ray Emission from the BL Lac Object MKN 421 by the EGRET Telescope on the Compton Observatory. 1992, ApJ, 401, L61-L64

J.R. Mattox, D.L. Bertsch, B.L. Dingus, C.E. Fichtel, R.C. Hartman, S.D. Hunter, P. Sreekumar, D.J. Thompson, P.W. Kwok, K.T.S. Brazier, T. Halaczek, G. Kanbach, H.A. Mayer-Hasselwander, C. von Montigny, K. Pinkau, H.D. Radecke, H. Rothermel, M. Sommer, J.M. Fierro, Y.C. Lin, P.F. Michelson, P.L. Nolan, J. Chiang, D.A. Kniffen, and E.J. Schneid: EGRET Observation of the Constellation of Cygnus. In: AIP Press 280, New York, 365, 1993

C.E. Fichtel, D.L. Bertsch, B.L. Dingus, R.C. Hartman, S.D. Hunter, G. Kanbach, D.A. Kniffen, P.W. Kwok, Y.C. Lin, J.R. Mattox, H.A. Mayer-Hasselwander, P.F. Michelson, C. von Montigny, P.L. Nolan, K. Pinkau, H. Rothermel, E.J. Schneid, M. Sommer, P. Sreekumar, and D.J. Thompson: High Energy Gamma-Ray Emission from Active Galactic Nuclei Observed by the Energetic Gamma-Ray Telescope Experiment (EGRET).
In: AIP Press 280, New York, 461, 1993

C.E. Fichtel, D.L. Bertsch, B.L. Dingus, R.C. Hartman, S.D. Hunter, P.W. Kwok, J.R. Mattox, P. Sreekumar, D.J. Thompson, D.A. Kniffen, Y.C. Lin, P.L. Nolan, P.F. Michelson, G. Kanbach, H.A. Mayer-Hasselwander, C. von Montigny, K. Pinkau, H. Rothermel, M. Sommer, and E.J. Schneid: Preliminary EGRET Source Catalog.
In: AIP Press 280, New York, 1194, 1993

K. Pinkau: Energie war die Währung der Vergangenheit, Energie ist die Währung der Zukunft - was können und wollen wir uns dafür kaufen? - In: Fortschritt und Gesellschaft. Hrsg.: E.-L. Winnacker,
Stuttgart: Hinzel 1993, S. 71 (Ed. Universitas)

K. Pinkau: Fusionsforschung: Stand der Forschung und Perspektiven. In: Freib. Univ. bl. 120, S. 69-82, 1993

C.E. Fichtel, D.L. Bertsch, B.L. Dingus, R.C. Hartman, S.D. Hunter, G. Kanbach, D.A. Kniffen, P.W. Kwok, Y.C. Lin, J.R. Mattox, H.A. Mayer-Hasselwander, P.F. Michelson, C. von Montigny, P.L. Nolan, K. Pinkau, H. Rothermel, E.J. Schneid, M. Sommer, P. Sreekumar, D.J. Thompson: Results from the Energetic Gamma-Ray Experiment Telescope (EGRET) on the Compton Observatory. 1993. Adv. Space Res., Vol. 13, No. 12, 637-646

P. Sreekumar, D.L. Bertsch, B.L. Dingus, C.E. Fichtel, R.C. Hartman, S.D. Hunter, G. Kanbach, D.A. Kniffen, Y.C. Lin, J.R. Mattox, H.A. Mayer-Hasselwander, P.F. Michelson, C. von Montigny, P.L. Nolan, K. Pinkau, E.J. Schneid, and D.J. Thompson: Constraints on the Cosmic Rays in the Small Magellanic Cloud. 1993.
Physical Review Letters, Vol. 70, No. 2, 127

D.L. Bertsch, B.L. Dingus, C.E. Fichtel, R.C. Hartman, S.D. Hunter, G. Kanbach, D.A. Kniffen, Y.C. Lin, J.R. Mattox, H.A. Mayer-Hasselwander, P.F. Michelson, C. von Montigny, P.L. Nolan, K. Pinkau, E.J. Schneid, P. Sreekumar, and D.J. Thompson: Detection of Gamma Ray Emission from the Quasar PKS 0208-512. 1993, ApJ, 405, L-21-L24

C.E. Fichtel, D.L. Bertsch, R.C. Hartman, S.D. Hunter, G. Kanbach, D.A. Kniffen, P.W. Kwok, Y.C. Lin, J.R. Mattox, H.A. Mayer-Hasselwander, P.F. Michelson, C. von Montigny, P.L. Nolan, K. Pinkau, H. Rothermel, E.J. Schneid, M. Sommer, P. Sreekumar, D.J. Thompson: Overview of First Results from EGRET. 1993.
A&A Suppl., Ser. 97, 13-16, 1993

C. von Montigny, D.L. Bertsch, C.E. Fichtel, R.C. Hartman, S.D. Hunter, G. Kanbach, D.A. Kniffen, P.W. Kwok, Y.C. Lin, J.R. Mattox, H.A. Mayer-Hasselwander, P.F. Michelson, P.L. Nolan, K. Pinkau, H. Rothermel, E.J. Schneid, M. Sommer, P. Sreekumar, and D.J. Thompson: EGRET observations of 3C 273. 1993, A&A Suppl., Ser 97, 101-103

G. Kanbach, D.L. Bertsch, C.E. Fichtel, R.C. Hartman, S.D. Hunter, D.A. Kniffen, P.W. Kwok, Y.C. Lin, J.R. Mattox, H.A. Mayer-Hasselwander, P.F. Michelson, C. von Montigny, P.L. Nolan, K. Pinkau, H. Rothermel, E.J. Schneid, M. Sommer, P. Sreekumar, and D.J. Thompson: Detection of a long-duration solar gamma-ray flare on June 11, 1991 with EGRET on COMPTON-GRO. 1993, A&A Suppl., 349-353, 1993

R.C. Hartman, D.L. Bertsch, B.L. Dingus, C.E. Fichtel, S.D. Hunter, G. Kanbach, D.A. Kniffen, Y.C. Lin, J.R. Mattox, H.A. Mayer-Hasselwander, P.F. Michelson, C. von Montigny, P.L. Nolan, B.G. Piner, E.J. Schneid, P. Sreekumar, and D.J. Thompson: EGRET Detection of High-Energy Gamma Radiation from the OVV Quasar 3C 454.3, 1993, ApJ, 407, L41-L44

S.D. Hunter, D.L. Bertsch, B.L. Dingus, C.E. Fichtel, R.C. Hartman, G. Kanbach, D.A. Kniffen, P.W. Kwok, Y.C. Lin, J.R. Mattox, H.A. Mayer-Hasselwander, P.F. Michelson, P. Moller, C. von Montigny, P.L. Nolan, K. Pinkau, H.-D. Radecke, H. Rothermel, P. Shaver, E.J. Schneid, M. Sommer, P. Sreekumar, and D.J. Thompson: Detection of High-Energy Gamma Rays from Quasar PKS 0528+134 by EGRET on the Compton Gamma Ray Observatory. 1993, ApJ, 409, 134-138

H.A. Mayer-Hasselwander, D.L. Bertsch, K.T.S. Brazier, J. Chiang, C.E. Fichtel, J.M. Fierro, R.C. Hartman, S.D. Hunter, G. Kanbach, P.W. Kwok, D.A. Kniffen, Y.C. Lin, J.R. Mattox, P.F. Michelson, C. von Montigny, P.L. Nolan, K. Pinkau, H. Rothermel, E.J. Schneid, M. Sommer, P. Sreekumar, D.J. Thompson: High-Energy Gamma-Radiation from Geminga observed by EGRET MPE-Preprint 265, September 1993

P.L. Nolan, Z. Arzoumainian, D.L. Bertsch, J. Chiang, C.E. Fichtel, J.M. Fierro, R.C. Hartman, S.D. Hunter, G. Kanbach, D.A. Kniffen, P.W. Kwok, Y.C. Lin, J.R. Mattox, H.A. Mayer-Hasselwander, P.F. Michelson, C. von Montigny, H.I. Nel, D. Nice, K. Pinkau, H. Rothermel, E.J. Schneid, M. Sommer, P. Sreekumar, and D.J. Thompson: Observations of the Crab Pulsar and Nebula by the EGRET Telescope on the Compton Gamma Ray Observatory. 1993, ApJ, 409, 697-704

D.J. Thompson, D.L. Bertsch, C.E. Fichtel, R.C. Hartman, R. Hofstadter, E.B. Hughes, S.D. Hunter, B.W. Hughlock, G. Kanbach, D.A. Kniffen, Y.C. Lin, J.R. Mattox, H.A. Mayer-Hasselwander, C. von Montigny, P.L. Nolan, K. Pinkau, H. Rothermel, E.J. Schneid, M. Sommer, P. Sreekumar, D. Tieger, and A.H. Walker: Calibration of the Energetic Gamma-Ray Experiment Telescope (EGRET) for the Compton Gamma Ray Observatory. 1993,
ApJ suppl Ser. 86, 629-656

D.J. Thompson, D.L. Bertsch, C.E. Fichtel, R.C. Hartman, S.D. Hunter, G. Kanbach, D.A. Kniffen, P.W. Kwok, Y.C. Lin, J.R. Mattox, H.A. Mayer-Hasselwander, P.F. Michelson, C. von Montigny, P.L. Nolan, K. Pinkau, E.J. Schneid, P. Sreekumar: Gamma Radiation from Blazar PKS 0537-441., 1993, ApJ, 410, 87-89

S.D. Hunter, D.L. Bertsch, B.L. Dingus, C.E. Fichtel, R.C. Hartman, G. Kanbach, D.A. Kniffen, P.W. Kwok, Y.C. Lin, J.R. Mattox, H.A. Mayer-Hasselwander, P.F. Michelson, C. von Montigny, P.L. Nolan, E.J. Schneid, P. Sreekumar, and D.J. Thompson: Detection of high energy gamma rays from BL Lac PKS 0235+164 by the EGRET telescope on the Compton observatory. 1993, A&A, 272, 59-62

J.R. Mattox, D.L. Bertsch, J. Chiang, B.L. Dingus, C.E. Fichtel, R.C. Hartman, S.D. Hunter, G. Kanbach, D.A. Kniffen, P.W. Kwok, Y.C. Lin, H.A. Mayer-Hasselwander, P.F. Michelson, C. von Montigny, P.L. Nolan, K. Pinkau, E.J. Schneid, P. Sreekumar, and D.J. Thompson: The EGRET Detection of Quasar 1633+382., 1993,
ApJ, 410, 609-614

D.A. Kniffen, D.L. Bertsch, C.E. Fichtel, R.C. Hartman, S.D. Hunter, G. Kanbach, P.W. Kwok, Y.C. Lin, J.R. Mattox, H.A. Mayer-Hasselwander, P.F. Michelson, C. von Montigny, P.L. Nolan, K. Pinkau, E.J. Schneid, P. Sreekumar, D.J. Thompson: Time Variability in the Gamma-Ray Emission of 3C 279. 1993, ApJ, 411, 133-136

J.M. Fierro, D.L. Bertsch, K.T.S. Brazier, J. Chiang, N. D'Amico, C.E. Fichtel, R.C. Hartman, S.D. Hunter, S. Johnston, G. Kanbach, V.M. Kaspi, D.A. Kniffen, Y.C. Lin, A.G. Lyne, R.N. Manchester, J.R. Mattox, H.A. Mayer-Hasselwander, P.F. Michelson, C. von Montigny, P.L. Nolan, E.J. Schneid, D.J. Thompson: Pulsed High-Energy Gamma rays from PSR 1055-52. 1993, ApJ, 413, L27-L30

C.E. Fichtel, D.L. Bertsch, J. Chiang, B.L. Dingus, J.A. Esposito, J.M. Fierro, R.C. Hartman, S.D. Hunter, G. Kanbach, D.A. Kniffen, P.W. Kwok, Y.C. Lin, J.R. Mattox, H.A. Mayer-Hasselwander, L. McDonald, P.F. Michelson, C. von Montigny, P.L. Nolan, K. Pinkau, H. Rothermel, P. Sreekumar, M. Sommer, E.J. Schneid, D.J. Thompson, and T. Willis: The First Energetic Gamma-Ray Experiment Telescope (EGRET) Source Catalog. NASA, Goddard Space Flight Center, Greenbelt, Maryland 20771. Accepted for publication in Astrophysical Journal Supplement.

K. Pinkau: Vorbehalte gegenüber der Technik? zur Debatte, Themen der Katholischen Akademie in Bayern, 23. Jahrgang, Nummer 6, B 215 75F München November/Dezember 1993

K. Pinkau: Experimente mit dem Sternenfeuer: Option für die Energieversorgung von morgen.
AGF-Forschungsthemen 7, 9 -11, 1994

K. Pinkau: Fusionsforschung - Stand der Forschung und Perspektiven, In: Spannungsfeld Energie - Probleme und Perspektiven, Hans Mohr (Hrsg.), 121-151, Rombach GmbH Druck- und Verlagshaus, 1995

K. Pinkau: Welche Ziele soll sich die Forschung stecken, und welche Wege soll sie beschreiten, um sich angemessene Freiräume zu sichern? - Der schrumpfende Freiraum der Forschung, Symposium der Max-Planck-Gesellschaft, Schloß Ringberg, Berichte und Mitteilungen Heft 1/1995, ISSN 0341-7778

K. Pinkau: The role of the Associations in the European fusion programs - Reprinted from Fusion Engineering and Design 30 (1995), Elsevier Science B.V. Amsterdam, The Netherlands

K. Pinkau: Forschungsfreiheit und Forschungspflicht - Experimente mit der Natur: Wissenschaft und Verantwortung: Interdisziplinäres Forum/Ernst-Ludwig Winnacker, Herg. und eingel. von Venanz Schubert (Wissenschaft und Philosophie: Bd. 11) ISBN 3-88096-361-4, 1995

K. Pinkau: The early days of gamma-ray astronomy, Astronomy & Astrophysics Supplement Series, Special Issue, Third Compton Symposium, Vol. 120, No. 4, December III, 1996 p.43, ISSN 0365-0138

K. Pinkau: Berlin Brandenburgische Akademie der Wissenschaften. Jahrbuch 1995, Akademie-Verlag

K. Pinkau: Das Energieproblem – Eine unbewältigte Gefahr (Akademievorlesung am 18. Mai 1995)
Berlin-Brandenburgische Akademie der Wissenschaften, Berichte und Abhandlungen,
Akademie-Verlag Band 2, 285 -308, 1996, ISBN 3-05-002958-7

K. Pinkau: Erkenntnis und Fortschritt für den Forscher und für das Gemeinwesen (Vortrag 20.11.1995, Konferenz der Deutschen Akademien der Wissenschaften, Hrsg. Nordrhein-Westfälische Akademie der Wissenschaften) Sonderdruck, Verlag Philipp von Zabern, ISBN 3-8053-1885-5

K. Pinkau, Ch. Stahlberg: Technologiepolitik in demokratischen Gesellschaften, Eine Publikation der Karl Heinz Beckurts-Stiftung, Edition UNIVERSITAS, S. Hirzel, Wissenschaftliche Verlagsgesellschaft Stuttgart,
ISBN 3-8047-1473-0

K. Pinkau: Energie aus Kernfusion, atw 42. Jg. (1997) Heft 3, Internationale Zeitschrift für Kernenergie, 3/1997,
ISSN 143-5254AWAKAG:42(3)145-216

K. Pinkau: Internationale Großprojekte, ihre Begründung, Entstehung, Arbeitsweise und ihre Auswirkungen, Symposium der Max-Planck-Gesellschaft, Schloß Ringberg/Tegernsee, Berichte und Mitteilungen MPG 1/1997

K. Pinkau: Stand und Perspektiven der Fusionsforschung, Verhandlungen der Gesellschaft Deutscher Naturforscher und Ärzte, 119. Versammlung, 21. bis 24. September 1996 Regensburg, Koordinaten der menschlichen Zukunft: Energie - Materie - Information - Zeit, S. 125 -139,
Wissenschaftliche Verlagsgesellschaft mbH, Stuttgart, ISBN 3-80471525-7

K. Pinkau: Stand und Perspektiven der Fusionsforschung. 60. Physiker-Tagung in Jena, Energie und Zukunft, Zukunftsweisende Methoden der Energienutzung vom Passivhaus bis zur Fusion, Hrsg. W. Nahm und K. Schultze, Deutsche Physikalische Gesellschaft, DPG-GmbH, 183-227, 1996

K. Pinkau: Die offene Gesellschaft und ihre Wissenschaft. Wissenschaft - Staat - Gesellschaft, Festkolloquium am 21.02.1997 anläßlich der Verabschiedung von Herrn Dr. Ernst-Joachim Meusel,
Herausgegeben von: Max-Planck-Institut für Plasmaphysik, 85748 Garching, 41-49, 1997

K. Pinkau: Von internationalen Forschungszentren (CERN, ILL, JET) zu multinationalen Einrichtungen. Wünsche an das künftige Wissenschaftssystem, Kolloquium für Dr. jur. Ernst-Joachim Meusel auf Schloß Ringberg vom 26. - 28. Juni 1997,
Herausgegeben von: Max-Planck-Institut für Plasmaphysik, 85748 Garching, 36-41, 1997

K. Pinkau: Neue Energiequellen: Mit Hilfe von Fusionsforschung aus Meerwasser Strom gewinnen.
Impressum: Position 03 Wege im Wandel: Eine Initiative der deutschen Industrie. Juni 1997,
Herausgeber: BDI, Bundesverband der Deutschen Industrie 03, 10-11, 1997

K. Pinkau: Freiheit der Forschung bei den Zukunftstechnologien. Globalisierung und informationelle Rechtskultur in Europa, Informationelle Teilhabe und weltweite Solidarität, Herausgeber:
Siegfried Lamnek/Marie-Theres Tinnefeld, 1. Auflage Baden-Baden, Nomos Verlags-Gesellschaft, 1998

K. Pinkau, O. Renn: Environmental Standards. Scientific Foundations and Rational Procedures of Regulation with Emphasis on Radiological Risk Management. Published by Kluwer Academic Publishers, Dordrecht, Netherland, 1998

K. Pinkau: Silhouettes: rhetoric and science, European Review, Vol. 6, No. 3, 327-332, 1998, Cambridge University Press

K. Pinkau: The ESA Science Programme – A View from Germany, Proceedings of an International Symposium, The History of the European Space Agency, 135-148, SP-436, June 1999, Co-sponsored by European Space Agency (ESA) and The Science Museum, London

K. Pinkau, Ch. Stahlberg: Wie finden Innovationsprozesse statt? Forschung im freien Staat.
Eine Publikation der Karl Heinz Beckurts-Stiftung, Edition UNIVERSITAS, S. Hirzel,
Wissenschaftliche Verlagsgesellschaft Stuttgart, S. 5, 43-53, 1999

K. Pinkau, D. Sadowski (Hrsg.), „Entrepreneurial Spirits“, Horst Albach zum 70. Geburtstag.
Die Akademie der Wissenschaften zu Berlin, Verlag Dr. Th. Gabler, Wiesbaden 2001, S. 29 1- 305

K. Pinkau: Sicherheit und Verläßlichkeit in der Energietechnik. Technikkultur. Von der Wechselwirkung der Technik mit Wissenschaft, Wirtschaft und Politik, Stiftung Brandenburger Tor der Bankgesellschaft Berlin 2000/2001, S. 128-140

K. Pinkau: History of gamma-ray telescopes and astronomy. Experimental Astronomy, 25 (1-3), 157-171, 2009

K. Pinkau: History of gamma-ray telescopes and astronomy. In B.R. Brandl, R. Stuik, & K.-M. J. K. (Eds.),
400 Years of Astronomical Telescopes. A Review of History, Science and Technology, 155-169,
New York, NY: Springer, 2010

4.2 QUELLENNACHWEISE

Wir danken den Verlagen und Herausgebern für die freundlichen Genehmigungen zum Nachdruck:

2.2.1 F. Wagner: Regime of Improved Confinement and High Beta in Neutral-Beam-Heated Divertor Discharges of the ASDEX Tokamak, in: Physical Review Letters 49, Nr. 19 (1982) S. 1408 ff.

2.2.3 Y. Shimomura et al.: Characteristics of the Divertor Plasma in Neutral-Beam-Heated ASDEX Discharges, in: Nuclear Fusion 23 (1983) S. 869ff.

2.2.4 F. Wagner: The history of research into improved confinement regimes, in: The European Physical Journal H, 43 (2018) S. 523-549, DOI: 10.1140/epjh/e2016-70064-9

2.3.1 ASDEX-Upgrade Design Team and Tokamak Theory Group: ASDEX Upgrade – Definition of a tokamak experiment with a reactor compatible poloidal divertor, März 1982 (Ausschnitt)

2.3.2 A. Herrmann, O. Gruber: Chapter 1: ASDEX Upgrade - Introduction and Overview, in: Fusion Science and Technology (2003) 44:3, S. 569-577, DOI: 10.13182/FST03- A399

2.3.3 H. Meyer et al.: Overview of physics studies on ASDEX Upgrade, in: Nuclear Fusion 59 (2019) S. 112014 ff., DOI 10.1088/1741-4326/ab18b8

2.4.1 JET Joint Undertaking: Annual Report 1992, Mai 1993, S. 85-96

2.5.1 G. Grieger: INTOR - A European View, in: Fusion Technology 8 (1985) S. 206 ff.

2.5.2 G. Grieger & INTOR-Group: INTOR: Critical Analysis of INTOR-Like Designs, in: Plasma Physics and Controlled Nuclear Fusion Research 3 (1988) Twelfth Conference Proceedings, Nice, 12-19 October 1988, S. 203 – 2013, IAEA-CN-50/F-I-2, © und freundliche Genehmigung zum Nachdruck: IAEA, Wien

2.5.3 F. Engelmann & NET Team: NET Predesign Overview, in: Plasma Physics and Controlled Nuclear Fusion 3 (1992), Fourteenth Conference Proceedings, Würzburg, Germany, 30.09. - 07.10.1992, S. 229 - 242, IAEA-CN-56/F-1-1, © und freundliche Genehmigung zum Nachdruck: IAEA, Wien

2.6.1 B. Bigot: Progress toward ITER's First Plasma, in: Nuclear Fusion 59 (2019), S. 112001 ff., DOI: 10.1088/1741-4326/ab0f84

2.6.2 G. Federici et al.: DEMO design activity in Europe: Progress and updates, in: Fusion Engineering and Design 136, (2018) S.729-741

3.2.1 G. Grieger et al.: Confinement of stellarator plasmas with neutral beam and RF heating in W VII-A, in: Plasma Physics and Controlled Fusion 28 (1986) S. 43-53

3.3.1 Application for Preferential Support, Phase I, for WENDELSTEIN VII-AS. Part I. Executive Summary, 1981

3.3.2 M. Hirsch, et al.: Major results from the stellarator Wendelstein 7-AS (Review Article), in: Plasma Physics and Controlled Fusion 50 (2008) S. 053001 ff., DOI:10.1088/0741-3335/50/5/053001

3.4.1 Wendelstein Project Group: Wendelstein 7-X. Application for Preferential Support, Executive Summary (Ausschnitt), 1990

3.4.2 T. Klinger et al.: Overview of first Wendelstein 7-X high-performance operation, in: Nuclear Fusion 59 (2019) S. 112004 ff., DOI: 10.1088/1741-4326/ab03a7

3.4.3 C. D. Beidler, H. M. Smith, A. Alonso et al.: Demonstration of reduced neoclassical energy transport in Wendelstein 7-X, in: Nature 596 (2021) S. 221–226, DOI: 10.1038/s41586-021-03687-w

Impressum
Herausgeber: Max-Planck-Institut für Plasmaphysik, Garching / Greifswald, 2021
Redaktion: Isabella Milch
Gestaltung: Graphisches Atelier Fenke, München
ISBN 978-3-00-071044-5